Cellular mechanisms involved in the regulation of voltage gated potassium channels in rat small pulmonary vasculature

Firth, Amy

Award date:
2006

Awarding institution:
University of Bath

CELLULAR MECHANISMS INVOLVED IN THE REGULATION OF VOLTAGE GATED POTASSIUM CHANNELS IN RAT SMALL PULMONARY VASCULATURE

Submitted by Amy Firth

For the degree of PhD of the University of Bath 2006

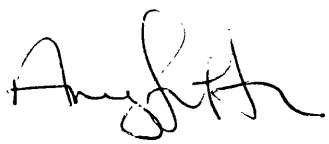

ProQuest LLC
789 East Eisenhower Parkway
P.O. Box 1346
Ann Arbor, MI 48106-1346

All truths are easy to understand once they are discovered;
the point is to discover them

Galileo Galilei
(1564 – 1642)

Acknowledgements

The processes involved in the discovery of science are not through the work of one individual, but through building on the knowledge and framework created by others: Furthermore, successful research is not a solitary achievement, support and discussions play a crucial part in aiding the discovery process. Throughout the course of this PhD I have been fortunate to have benefited from a number of individuals to whom I am indebted.

I would like to express my gratitude to my supervisor Sergey Smirnov for his guidance and wisdom throughout the research and his photographic expertise at my wedding. The help of Dr Kathyrn Yuill must also be acknowledged for her contribution to the confocal microscopy experiments and to the whole cell patching data with rotenone, for both of which she completed about two thirds of the experiments. I would also like to thank her for her invaluable support and friendship. Thanks also to Dr. Kim Dora and Prof. Chris Garland for their generosity in allowing me extensive use of their confocal microscope and wire myograph.

Scientific research is not confined to the laboratory and, as such, this thesis could not have been accomplished without the support of my husband, Rich, and my family whom I love dearly.

Abstract

Objectives: Inhibition of voltage-gated K^+ (Kv) channels in pulmonary arterial smooth muscle cells (PASMCs) contributes to the development of hypoxic pulmonary vasoconstriction (HPV). Mitochondria have been proposed as the major oxygen sensing organelles in PASMCs. Although a role for mitochondrial-dependent cellular redox state changes that modulate Kv channels has been proposed, the precise mechanism of the interaction between Kv channels and mitochondria remains unclear. To understand these mechanisms the effect of various mitochondrial inhibitors on Kv channel currents (I_{Kv}) were investigated in rat PASMCs and PAs. Comparisons were drawn to the mesenteric circulation.

Methods: Patch-clamp technique under different intracellular conditions and in the presence of a variety of pharmacological tools. Three key parameters of I_{Kv} were assessed; activation, inactivation and I_{Kv} block. Additionally, Mg^{2+} and Ca^{2+} fluorescent measurements were performed and whole vessel contractility was assessed using a Mulvany–Halpern myograph.

Results: The mitochondrial uncoupler CCCP, and mitochondrial electron transport chain (mETC) inhibitors, rotenone, myxothiazol, antimycin and cyanide, induced similar significant changes in all three I_{Kv} parameters. Antimycin-induced effects, as the most pronounced were studied in detail. It was found that these effects 1) cannot be entirely explained by changes in cellular redox state, 2) are mimicked by the ATP synthase inhibitor oligomycin, 3) were significantly inhibited by cell dialysis with 5 mM Na_2ATP, EDTA or with 5 (instead of 0.5) mM $MgCl_2$, whereas intracellular MgATP partially reversed the effect, 4) both CCCP and antimycin caused a significant increase in intracellular Mg^{2+} (Mg^{2+}_i) and 5) hypoxia caused an increase in Mg^{2+}_i and a leftward shift in I_{Kv} activation, mimicking the effect of mitochondrial inhibitors .

Additionally, the involvement of the Na^+-Mg^{2+} (NME), alongside the Na^+-Ca^{2+} (NCE) and Na^+-H^+ (NHE) exchangers on I_{Kv} activation and block was evaluated using various extracellular and intracellular conditions. 1) Na^+_o removal (to block the exchangers) caused i) a leftward in I_{Kv} activation, ii) a significant increase in the slope of the dependency and iii) a decrease in the maximal whole-cell conductance. 2) Removal of

external Mg^{2+}, intracellular EDTA and 100 μM amiloride, a putative NME inhibitor, all significantly attenuated Na^{+}_{o}-dependent effects on I_{Kv}. 3) The effects on I_{Kv} activation were significantly attenuated by 3 μM KB-R7943 (a reverse mode inhibitor of the NCE) and extracellular alkalanisation by 0.6 pH unit (the conditions facilitating accumulation of intracellular Na^{+}), but not by elevated $[Ca^{2+}]_i$, intracellular BAPTA, extracellular acidification or by the NHE inhibitor 5-(N-methyl-N-isobutyl) amiloride.

Significant differences between pulmonary and mesenteric circulation were found, suggesting specificity of the observed mechanism to the pulmonary circulation.

Conclusions: Collectively, these findings suggest the presence of a novel mitochondrial-mediated Mg^{2+}_{i}-dependent mechanism in the regulation of Kv channels in PASMCs, which could be involved in HPV. It also suggests that Kv channel activity at physiological membrane potentials in PASMCs chiefly depends on Mg^{2+}_{i} concentration determined by the balance between the extracellular Mg^{2+} influx and release and its extrusion by the NME, thus representing a novel regulatory mechanism for Kv channels in PASMCs. Despite some similarities the same overall mechanism was not present in MASMCs.

Abbreviations and symbols

2PK	two pore K^+ channels
4-AP	4-aminopyridine
AA	arachidonic acid
AMP	adenosine monophosphate
AMPK	AMP-activated protein kinase
ATP	adenosine 3,5-trisphosphate
BK_{Ca}	large conductance Ca^{2+} -activated K^+ channel
$[Ca^{2+}]_I$	intracellular calcium concentration
cADP-ribose	cyclic adenoside diphosphate- ribose
$Ca\dot{M}$	Ca^{2+}-calmodilin complex
cAMP	3'5'–adenosine monophosphate
CCE	capacitative calcium exchange
cGMP	3'5'–guanosine monophosphate
CH	chronic hypoxia
ChTx	charybdotoxin
CICR	calcium induced calcium release
C_m	cell capacitance
CO	carbon monoxide
COPD	chronic obstructive pulmonary disease
DAG	diacylglycerol
DMEM	Dulbeccos' modified eagles' medium
DMSO	dimethylsulphoxide
DPI	diphenyleneiodonium sulphate
DTT	dithiorethrol
E-C coupling	electromechanical cell coupling
EETs	epoxyeicosatrienoic acids
EGTA	ethylene glycol-bis (β-aminoethyl ether)-N, N, N', N'-tetra-acetic acid
E_K	K^+ equilibrium potential given by Nernst equation
E_m	cell resting membrane potential
ERG	ether-à-go-go-related genes
ET-1	Endothelin -1

ET_A, ET_B	Endothelin-1 receptor subtype A or B
FCS	fetal calf serum
G_{max}	peak I_{Kv} conductance
HEPES	N-2-hydroxyethylpaperazine-N-2-ethanesulphonic acid
H_2O_2	hydrogen peroxide
hPASMC	human pulmonary artery smooth muscle cells
HPV	hypoxic pulmonary vasoconstriction
k_a	slope factor of I_{Kv} activation
K_{ATP}	ATP sensitive K^+ channel
K_{Ca}	calcium activated K^+ channel
KCNQ	Kv long QT or Kv7 channels
K_{ir}	inwardly rectifier K^+ channel
k_h	slope factor of I_{Kv} inactivation
K_{NDP}	nucleotide diphosphate regulated ATP sensitive K^+ channel
K_v	voltage-gated K^+ channel
IbTx	iberiotoxin
IP_3	inositol 1,4,5-triphosphate
IP_4	inositol-1,3,4,5 tetrakisphosphate
I_K	potassium current
I_{Kv}	voltage gated K^+ current in VSMCs
I_{Kv1}	Kv1 type of K^+ current in rat conduit PASMCs
I_{Kv2}	Kv2 type K^+ current in rat conduit PASMCs
I_{KN}	non-inactivating current
I_{leak}	leak current
I_{norm}	normalised current
I_{SOC}	store operated channel current
I-V	current – voltage relationship
KO	knock out
LQT	long QT syndrome
MASMC	mesenteric artery smooth muscle cell
mETC	mitochondrial electron transport chain
MLCK	myosin light chain kinase
mRNA	messenger ribonucleic acid
NADPH	nicotinamide adenine dinucleotide phosphate-oxidase

NCE	sodium-calcium exchanger
NCKX	potassium dependent sodium-calcium exchanger
NHE	sodium-hydrogen exchanger
NME	sodium-magnesium exchanger
NMDG	N-methyl-D-glucamine
NO	nitric oxide
NSCC	non-selective cation channel
PAH	pulmonary arterial hypertension
PASMC	pulmonary artery smooth muscle cell
PH	pulmonary hypertension
PBS	phosphate buffered saline
PKA	protein kinase A
PKC	protein kinase C
PKG	protein kinase G
PIP_2	phosphatidyl inositol di-phosphate
PLC	phospholipase C
P-Loop	pore forming loop
P_{O2}	partial oxygen pressure
PP	perforated patch
PSS	physiological salt solution
R	regression coefficient
ROCC	receptor operated cation channel
ROK	Rho kinase
ROS	reactive oxygen species
RT-PCR	reverse transcription polymerase chain reaction
RyR	ryanodine receptor
SERCA	sarcoplasmic-endoplasmic Ca^{2+} ATPase
s.e.m.	standard error of the mean
siRNA	small interfering ribonucleic acid
SMC	smooth muscle cell
SOC	store operated channel
SO^-	superoxide ion
SR	sarcoplasmic reticulum
SUR2B	sulphonyl urea receptor subunit 2B

TASK	TWIK related Acid Sensitive K^+ channel
TEA	tetraethylammonium
TM	transmembrane
TRP	transient receptor potential channels
TRPC	classical or canonical TRP channels
TRPM	melastatin related TRP channels
TRPV	vanilloid TRP channels
TTX	tetrodotoxin
TWIK	twin pore weakly inwardly rectifying potassium channel
TXA_2	thromboxane A_2
V_a	half-activation potential
V_h	half inactivation potential
ΔV_a	relative change in V_a
ΔV_h	relative change in V_h
V_m	membrane potential
VOCC	voltage operated calcium channel
VSMC	vascular smooth muscle cell
v/v	volume by volume
w/v	weight by volume
$\Delta\Psi_m$	change in mitochondrial membrane potential

Contents

2. METHODS

3. MITOCHONDRIA IN THE REGULATION OF Kv CHANNELS

4. HYPOXIA AND THE REGULATION OF I_{Kv} ACTIVATION AND $Mg^{2+}{}_i$ IN PASMCs

5. MITOCHONDRIAL DEPENDENT REGULATION OF I_{Kv} IN MASMCs

6. FUNCTIONAL IMPLICATIONS OF THE MITOCHONDRIAL DEPENDENT REGULATION OF IKv

7. Na^+-Mg^{2+} EXCHANGER AND INVOLVEMENT OF Na^+ DEPENDENT MECHANISMS IN I_{Kv} REGULATION

Figures

Tables

Equations

Chapter 1

INTRODUCTION

1.1 Vascular smooth muscle

Understanding vascular-related pathophysiological disease states requires extensive knowledge of the complex vessel structure and functional organisation in the cardiovascular system (Pugsley & Tabrizchi, 2000). Despite variation in different vascular beds, a common histological level of blood vessels is shared. Blood vessels contain elastic tissue laid in concentric layers (highly extensible) interspersed with collagen (reinforcing stiffness) and circumferentially arranged smooth muscle cells (SMCs). Three distinct regions (*tunicas*) have been described: *tunica intima, tunica media* and *tunica adventitia*. The major vessels in mammals consist mainly of *tunica media*, primarily composed of SMCs and elastin fibres. There is variation in the number of smooth muscle layers, the larger more muscular arteries, such as the aorta, have many highly organised layers separated by an elastic lamella, whereas less muscular arterioles have only one smooth muscle layer.

1.2 *Pulmonary circulation and its structural organisation*

The pulmonary circulation is a high flow, low pressure system. Its vascular bed resembles that of the systemic circulation though the walls of larger pulmonary arteries are only 30% of the thickness of those in the aorta and the smaller arteries have relatively little smooth muscle. Pulmonary circulation is essential to the maintenance of circulating O_2 levels and when O_2 levels are compromised (partial pressure of oxygen (P_{O2}) below 60 mmHg) it responds uniquely by constricting and diverting blood flow to the well ventilated areas (ventilation-perfusion matching), a phenomenon known as hypoxic pulmonary vasoconstriction (HPV), (Dumas *et al.*, 1999). Conversely, the systemic circulation responds to low P_{O2} by dilating to provide a better O_2 supply to target organs (Wadsworth, 1994). Features of the pulmonary vasculature in the rat are similar to that in humans, thus making the rat a suitable model to study pulmonary related diseases (Hislop & Reid, 1978).

1.2.1 Pulmonary structural organisation

The main trunk of the pulmonary artery leaves the right ventricle and divides into two, the left and right pulmonary arteries. These arteries have a similar muscular media to the main trunk but contain three, instead of four, central laminae, the right supplies the four right lobes of the lung and the left a single lobe. The axial artery inside the lung looses one more layer of central laminae and as the arteries branch from this towards the periphery the central laminae continues to decrease as the wall thickness decreases (Hislop & Reid, 1978). A typical structure of a segment of the pulmonary arterial tree is shown in Fig. 1.1 A. There are three different models that have previously been used to label the arteries in the complex pulmonary artery tree. These are the Weibel model, the Strahler model, and the Diameter-Defined Strahler's system (Fig. 1.1).

The Weibel model (Fig. 1.1 B) labels the largest vessel as generation one and assumes a symmetrical dichotomy exists whereby at each bifurcation the generation increases by one. In humans this model predicts 28 orders of the PA tree (Weibel, 1963). The Strahler/Horsfield system (Fig 1.1 C) labels the smallest non-capillary blood vessel as order 1 and at the point where two vessels of order 1 meet an order 2 vessel forms and this pattern repeats (Singhal *et al.*, 1973; Yen *et al.*, 1984). The Diameter-Defined Strahler's system (Fig. 1.1 D) has an addition to the original Strahler model (Jiang *et al.*, 1994): when a vessel of order n with diameter D_n meets another vessel of order n, the vessel formed is called a vessel of order $n + 1$ only if its diameter is larger than $D_n + (S_n + S_{n+1}) / 2$, S_n and S_{n+1} represent the standard deviations for diameters of orders n and $n + 1$. Using this model there are a total of 15 orders of the human (Huang *et al.*, 1996) and 11 orders of the rat PA tree (Jiang *et al.*, 1994). The Weibel model is the one most often referred to and possibly the simplest; it was therefore the preferred choice for labelling arteries throughout this thesis.

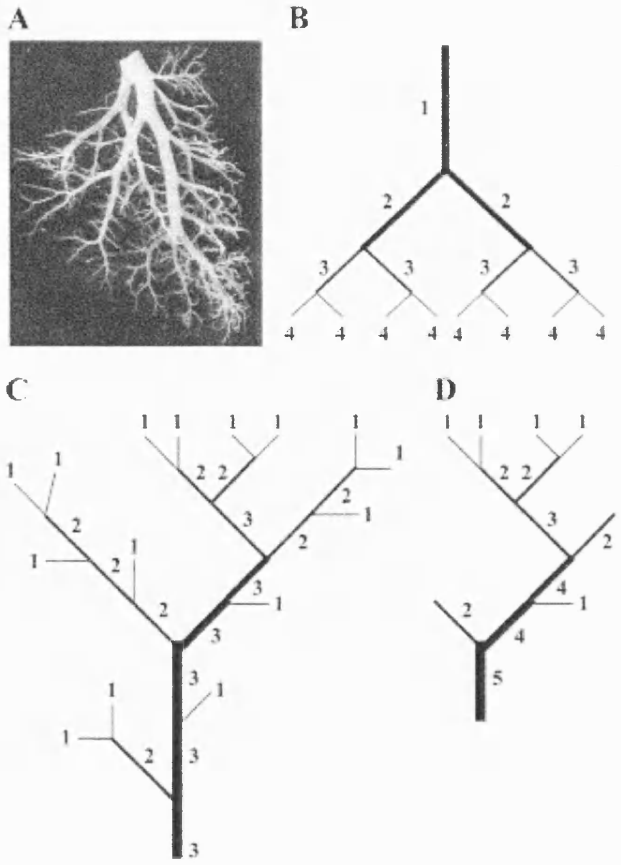

Figure 1.1. Structural organisation of the pulmonary vascular tree. (A) The structure of a typical segment of the arterial tree. (B), (C) and (D) show the Weibel Model' the 'Strahler model' and the 'Diameter-defined Strahler's system' schemes, respectively, for labelling the complex artery structure. Reproduced from Mandegar *et al.* (2004).

1.3 Regulation of intracellular calcium concentration

The main function of pulmonary arteries is to regulate blood flow by changing vessel diameter. The contractility of smooth muscle is reliant upon the intracellular calcium concentration ($[Ca^{2+}]_i$). At rest $[Ca^{2+}]_i$ is low (~100nM) creating a gradient greater than 10000 fold with the extracellular level (~1.6mM, Himpens *et al.*, 1992). The fundamental systems co-ordinating to control $[Ca^{2+}]_i$ are: 1) extracellular Ca^{2+} entry via voltage operated calcium channels (VOCCs); 2) receptor operated cation channels (ROCCs); 3) Ca^{2+} release and sequestration from and into the sarcoplasmic reticulum (SR); 4) store-operated channels (SOCs) activated by depletion of the SR; 5) Ca^{2+}-

ATPase and Na^+-Ca^{2+} exchanger (NCE) responsible for plasmalemmal Ca^{2+} efflux and 6) mitochondrial Ca^{2+} release and sequestration.

Ca^{2+} entry can be activated by changes in membrane potential, known as excitation-contraction coupling (E-C coupling), (Bauer & Sanders, 1985) or by neurotransmitter or hormonal stimulation of receptors, known as pharmacomechanical coupling (Somlyo & Somlyo, 1968). In E-C coupling VOCCs are activated when depolarisation surpasses a threshold, just a few millivolts is sufficient to open VOCCs and allow Ca^{2+} influx, causing contraction (Brayden & Nelson, 1992). In different vascular beds this threshold varies, possibly due to the voltage dependence and density of VOCCs and the type and density of K^+ channels expressed in SMCs. Ionic concentration gradients determine the membrane potential in vascular SMCs (VSMCs). Activity of electrogenic ion exchangers, such as the NCE or the Na^+-K^+ ATPase, also affects membrane potential; for example, activation of the NCE hyperpolarises the membrane (Bolton, 1979). Neurotransmitters increase the permeability to Ca^{2+} via voltage independent ROCCs and may stimulate Ca^{2+} entry either directly by causing depolarisation and VOCC activation, or via the release of an intracellular messenger. The nature of the messenger coupled receptor activation to Ca^{2+} entry has not yet been fully elucidated, however the involvement of 3'5'–adenosine monophosphate (cAMP), 3'5'–guanosine monophosphate (cGMP), diacylglycerol (DAG) and protein kinase C (PKC) have been proposed in the activation of VOCCs, and ROCCs may open either directly or via second messengers such as inositol-1,4,5 trisphosphate (IP_3) or inositol-1,3,4,5 tetrakisphosphate (IP_4) (van Breemen & Saida, 1989).

The SR is the major store of intracellular calcium ions ($Ca^{2+}{}_i$) and its effective permeability is determined by the relative rate of influx and efflux mechanisms. The sarcoplasmic/endoplasmic reticulum Ca^{2+} ATPase (SERCA) serves to sequester Ca^{2+} by removing it from the cytoplasm and refilling the internal Ca^{2+} stores; SERCA is also sensitive to thapsigargin (Treiman *et al.*, 1998). The levels of $Ca^{2+}{}_i$ present are reflective of the filling state of the internal Ca^{2+} stores (Rueda *et al.*, 2002). It has been suggested that an active SERCA pump is essential to obtain optimal Ca^{2+} release in SMCs (Gomez-Viquez *et al.*, 2003). The predominant mechanism by which the SR can be stimulated to release Ca^{2+} is by IP_3 acting upon IP_3 receptors. IP_3 is increased after agonist receptor activation causing phospholipase C (PLC) induced hydrolysis of

phosphatidylinositol bisphosphate (PIP_2) to yield IP_3 and DAG (Tasker *et al.*, 1999). When Ca^{2+} entry via ROCCs and VOCCs increases in $[Ca^{2+}]_i$ to μM concentrations further Ca^{2+} release can be induced from the SR via interaction with ryanodine receptors (RyRs), a phenomenon known as calcium induced calcium release (CICR) (Lesh *et al.*, 1998). SOCs can also be activated to increase Ca^{2+} entry, the mechanism by which this happens is predominantly dependent on depletion of the intracellular Ca^{2+} stores (Brueggemann *et al.*, 2006).

Additionally, the mitochondria are emerging as regulators of $Ca^{2+}{}_i$, having a capacity to effectively store/buffer sub-plasmalemmal Ca^{2+} (Parekh, 2003; Malli *et al.*, 2003). It is, therefore, suggested that mitochondrial Ca^{2+} uptake occurs alongside Ca^{2+} release via the mitochondrial NCE to contribute to ER Ca^{2+} refilling (Malli *et al.*, 2003). Additionally, SR release of Ca^{2+}, via RyR or IP_3 mediated mechanisms, increases mitochondrial Ca^{2+} in PASMCs (Drummond & Tuft, 1999). It is currently unknown to what extent the mitochondria are involved in ER refilling and Ca^{2+} homeostasis, though it is considered to be important (Ward *et al.*, 2004). It is also possible that mitochondrial regulation of Ca^{2+} may have an important role in HPV, hypoxia has indeed been shown to inhibit mitochondrial uptake of Ca^{2+} (Kang *et al.*, 2002).

1.4 Membrane dependent ion transport mechanisms in the regulation of EC coupling in VSMCs.

Spanning the membrane of VSMCs are several types of ion channels, exchangers and antiporters, all interacting to control vascular contractility via the regulation of $[Ca^{2+}]_i$. Such channels include voltage-gated sodium and calcium channels, voltage independent calcium and non-selective cation channels, chloride channels and voltage- and ligand-gated K^+ channels. Plasmalemmal Ca^{2+} and Na^+-K^+ ATPase are also present, alongside an array of exchangers: the NCE (Nabel *et al.*, 1988), Na^+-H^+ (NHE), (Yun *et al.*, 1995) and Na^+-Mg^{2+} (NME), (Gunther, 1993). The development of cell isolation and electrophysiological (mainly patch clamp) techniques has enabled these channels to be studied comprehensively under normal and pathophysiological conditions (Jackson *et al.*, 1997). The following sections will characterise briefly each of these ion transport mechanisms in PASMCs, with a more extensive discussion on the role of K^+ channels and particularly Kv channels, reflecting the main interest of this work.

1.4.1 Sodium channels

Okabe *et al.* (1988) were the first to describe a rapidly activating and inactivating inward current (I_{in}) in rabbit PASMCs that was dependent upon extracellular Na^+. This current was also found to be present in other vascular tissues including; cultured human pulmonary (Platoshyn *et al.*, 2005), human aortic (Cox *et al.*, 1998), mesenteric (Berra-Romani *et al.*, 2005) and cultured human, rabbit and pig coronary (Choby *et al.*, 2000) SMCs. Na^+ channels consist of four internally homologous subunits each containing six TM domains, the S5-S6 TM domains fold to create an internal pore. These subunits form a single principle subunit: the structural basis of this pore determines the selectivity and conductance properties of the channel and is described in detail (Marban *et al.*, 1998). The functional role of Na^+ channels in the PA is not clear. Tetrodotoxin, a specific Na^+ channel inhibitor, has no effect upon membrane potential, $Ca^{2+}{}_i$ release or proliferation in PAs and, therefore, they are generally regarded as unimportant in the control of the normal function of these vessels (Platoshyn *et al.*, 2005). It is noteworthy that the occurrence of I_{Na} in mesenteric SMCs was found to be dependent upon the enzymatic isolation conditions and this may account for discrepancies in the observations of I_{Na} in VSMCs (Berra-Romani *et al.*, 2005).

1.4.2 Voltage operated calcium channels (VOCCs)

As mentioned above, VOCCs are integral to the maintenance of vascular tone and are ubiquitously expressed in VSMCs. VOCCs are formed as a complex of several different subunits: α1, α2, β, γ, and δ. Similar to Na^+ channels, they consist of four domains each containing six TM regions. The α1 subunit is essential for channel functioning, it forms the Ca^{2+} selective pore and contains the voltage sensor. Generally, six subtypes of VOCC have been identified (L-, N-, P-, Q-, R-and T-), of these the dihydropyridine-sensitive, high voltage-activated slowly inactivating L-type and the low voltage-activated rapidly inactivating T-type have predominantly been characterised in VSMCs. It has been proposed that R-type channels may be present in VSMC; recently R-type currents were up regulated in cerebral arteries during subarachnoid haemorrhage enhancing constriction (Ishiguro *et al.*, 2005). However, they are yet to be fully characterised using electrophysiological techniques. L-Type channels have a predominant role in the regulation of vascular tone; they are regulated by membrane

potential in VSMCs and are activated by depolarisation of the cell membrane. Additionally, vasoconstrictors also act, in part, by opening the L-type channels again through membrane depolarization or second messenger activation (Nelson *et al.*, 1990). Only the L-type have been substantially characterised in PASMCs and are thought to be important in elevating Ca^{2+}_i during hypoxia. Differences in Ca^{2+} channel density and oxygen sensitivity were also observed along the PA tree in studies using specific VOCC inhibitors and direct measurement of VOCC currents (Franco-Obregón & López-Barneo, 1996; McMurtry *et al.*, 1976; Leach *et al.*, 1994). Recent studies also suggest that the T-type are important in the proliferation of human PASMC (Rodman *et al.*, 2005).

1.4.3 Transient receptor potential channels (TRP): Molecular correlates for SOC?

TRP channels belong to the superfamily of cation channels due to their 6TM structure enclosed by N and C termini, with each subunit contributing to the channel pore (Hofmann *et al.*, 2002). The main TRP channel subtypes are: classical or canonical TRP (TRPC), vanilloid receptor related TRP (TRPV) and melastatin related TRP (TRPM) (Clapham *et al.*, 2001). In VSMCs more than 10 TRP isoforms have been detected; TRPC1 and 6 are ubiquitously expressed, TRPC4 is widely expressed and TRPC3, 5 and 7 are also detected following injury (Beech, 2005). Briefly, TRP channel activity is suggested to be important in modulating vessel contractility, regulation of Ca^{2+}_i, osmotic stress, Mg^{2+} homeostasis and in the response to vascular injury (Beech, 2005). Additionally, VSMC proliferation and remodelling are likely to influence the expression of TRPC isoforms and thus may alter their function (Golovina *et al.*, 2001). Published data on TRPM and TRPV subtypes is scarce; TRPM 2-4 and 7-8 and TRPV 1-4 have been detected using RT-PCR in both de-endothelialised rat aorta and PA (Inoue *et al.*, 2006). For an in-depth discussion of the properties and functional significance of TRP channels in the vasculature please refer to Dietrich *et al.* (2006).

SOCs are activated by the depletion of intracellular Ca^{2+} stores and, due to varied experimental conditions, there is discrepancy over the involvement of capacitative calcium entry (CCE) in SOC currents (I_{SOC}) (Brueggemann *et al.*, 2005). Using the A7r5 cell line and freshly isolated MASMCs Brueggemann *et al.* (2005) showed, by measuring cytosolic Ca^{2+} using fura-2 fluorescence and electrophysiological techniques,

that store depletion of Ca^{2+} activated CCE which corresponded to I_{SOC} suggesting an I_{SOC}/CCE pathway. Using small interfering RNA (siRNA) and infecting cells with an adenovirus expressing an anti-sense nucleotide sequence it has been proposed that the molecular correlate for this channel was likely to be TRPC1, an isoform of the TRP family of non-selective cation channels (Brueggemann *et al.*, 2006). I_{SOC} also associates to TRPC1 expression in cerebral arteries and internal mammary arteries (Bergdahl *et al.*, 2005). Expression of TRP1, a TRP gene proposed to encode the channels responsible for CCE and I_{SOC}, was also up regulated in proliferating PASMC. Moreover, Sweeney *et al.* (2002) demonstrated that TRPC1 resembled I_{SOC} and, by regulating CCE, had a crucial role in PASMC proliferation and regulating $Ca^{2+}{}_i$.

1.4.4 ATP dependent transporters

Ca^{2+} ATPase

In addition to the SERCA described in section 1.3, a plasmalemmal Ca^{2+}-ATPase (PMCA) which functions to remove Ca^{2+} from cells exists in VSMCs (Pande *et al.*, 2006) and prevents overloading of the cytoplasm with Ca^{2+} (Guerini *et al.*, 2005). The PMCA is encoded by four genes (PMCA 1-4) of which the vascular smooth muscle expresses PMCA-4 and, to a lesser extent, the PMCA-1 (Pande *et al.*, 2006). The PMCAs contain 10 TM domains, with C and N regions in the cytosol. The key regulatory domain is within the C- tail and contains a calmodulin-binding domain and the sites of phosphorylation by PKC and PKA (Guerini *et al.*, 2005). Functionally, the pump itself has not been studied in any great detail though, interestingly, PMCA activity has been shown to increase in the presence of H_2O_2 (1 mM) and matrix metalloprotease 2 (MMP-2) in PASMCs (Mandal *et al.*, 2003).

Na^+-K^+ ATPase

The Na^+-K^+ ATPase is the chief mechanism for Na^+ extrusion, transporting both Na^+ and K^+ against their concentration gradients. It is a heterodimer formed from a catalytic α subunit and a glycosylated β subunit (Koster *et al.*, 1995). The α subunit is functionally important conferring the binding sites for the physiological ligands (namely Na^+, K^+, Mg^{2+} and ATP) and for ouabain, a specific inhibitor which displays tissue

specific affinity for the pump (Juhaszova & Blaustein, 1997). The Na^+-K^+ ATPase utilises energy derived from ATP hydrolysis to undergo conformational changes to enable binding and release of Na^+ and K^+ (Skou & Esmann, 1992). The pump may also be regulated by phosphorylation, PKA and PKC are postulates to phosphorylate the α subunit (Blanco *et al.*, 1998), and its structure and function is comprehensively reviewed in Skou (2004).

1.4.5 Sodium dependent exchangers

While Na^+-K^+ ATPase is mainly responsible for Na^+ extrusion, Na^+ could potentially enter the cell via several Na^+-dependent transport mechanisms, including the NCE, a potassium dependent NCX (NCKX), NHE and NME, such Na^+ dependent mechanisms are functionally important in the vasculature as they have essential roles in both excitation contraction coupling and pH/ion homeostasis. All of these exchangers are important in the homeostasis of intracellular ions such as Ca^{2+}, Na^+, K^+ and Mg^{2+}, which could potentially affect the Kv channel activity. The physiological and pharmacological characteristics of these exchangers will be discussed in depth in Chapter 7, where their role in Kv channel regulation will be described.

1.4.6 Potassium channels

Potassium channels are the key regulators of cellular excitability and are fundamentally involved in the regulation of cellular resting membrane potential. The membrane topologies of the main classes of potassium channels (voltage-dependent K^+ channels (Kv), large conductance Ca^{2+} activated K^+ channels (BK_{Ca}), ATP dependent K^+ channels (K_{ATP}) and two pore domain K^+ channels (2PK)) are found in Fig. 1.2. Briefly, Kv channels are tetrameric 6TM spanning proteins formed from symmetrically arranged potassium channel subunits, either in a homo or hetero multimeric combination (see Table 1.2), surrounding a central pore highly selective to the transportation of K^+ ions across the cell membrane (MacKinnon, 1991a) (Fig. 1.2 A). In the voltage-gated potassium channels the S4 TM domain contains four Arg residues which are essential for depolarisation dependent opening of the channel (Aggarwal & MacKinnon, 1996). Selectivity to potassium ions is energetically favoured through a flexible pore lined by a backbone of carbonyl groups, a sequence highly conserved

between different K^+ channels (Noskov & Roux, 2006; Noskov *et al.*, 2004). BK_{Ca} channels also form tetramers which consist of 4 α and 4 β subunits. The α subunit has 7 TM domains and features extracellular N- and intracellular C- termini (Fig. 1.2 B) (Wallner *et al.*, 1996). The channel is regulated by the β subunit which comprises of two membrane-spanning domains separated by an extracellular loop. As in Kv channels, the S4 region contains positively charged residues and confers voltage sensitivity of the channel. K_{ATP} channels consist of an octameric complex of four pore-forming inward rectifier K^+ (K_{ir}) channel subunits (K_{ir} 6.1 or 6.2) (Fig. 1.2 C) and four sulphonyl urea receptors (SURs) (Aguilar-Bryan & Bryan, 1999). 2PK channels have four TM segments (denoted M1-M4), two pore forming domains (P1 and P2), a short cytoplasmic N-terminal and a long cytoplasmic C-terminal. In addition, an extracellular loop exists between the M1 and P1 regions (Lesage & Lazdunski, 2000) (Fig. 1.2 D). It is believed that two α subunits of 2PK are necessary to form functionally active channels.

1.4.6.1 Role of K^+ channels in VSMCs

Being expressed in all arteriolar SMC membranes, K^+ channels are important in the regulation of cell membrane potential (V_m) (Yuan, 1995; Nelson & Quayle, 1995). In SMC the driving force for K^+ ions is out of the cell, thus opening of K^+ channels precedes K^+ efflux and hyperpolarisation of the membrane. Closure or inhibition of K^+ channels conversely instigates membrane depolarisation and subsequent opening of voltage-gated L-Type Ca^{2+} channels, increasing Ca^{2+}_i. Elevated Ca^{2+}_i, in turn, causes CICR from the SR further increasing Ca^{2+}_i concentration. Ca^{2+} activates the contractile apparatus by binding calmodulin. The Ca^{2+}-calmodulin complex (CaM) binds the CaM dependent myosin light chain kinase (MLCK), phosphorylates the myosin light chains (LC_{20}), increases the activity of myosin ATPase and, ultimately, increases cross bridge cycling causing contraction (Horowitz *et al.*, 1996).

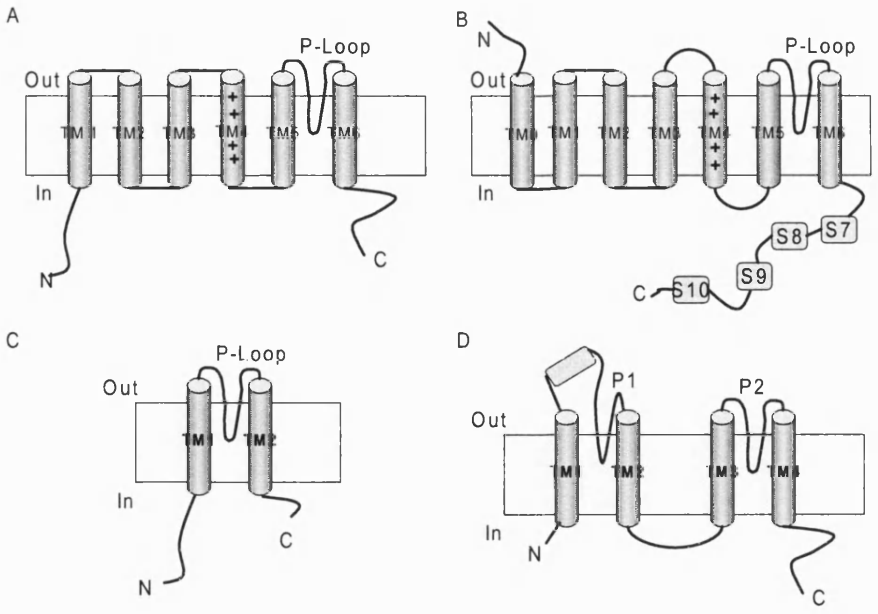

Figure 1.2. Putative topology of K^+ channel subunits in VSMCs (a planar view). (A) Kv channel α subunit, (B) BK_{Ca} channel α subunit, (C) K_{ir} subunit of K_{ATP} channels and (D) 2PK channels. The pore forming loops are defined as P-Loops in A-C and P1 and P2 in D. The transmembrane (TM) domains are indicated in each subunit.

Functional K^+ channels expressed in VSMCs are listed in Table 1.1 and include: Kv, BK_{Ca}, K_{ATP}, K_{ir} and TASK channels. A basic overview of the key functional properties (activation, inactivation and exogenous blockers) of these channels in vascular smooth muscle are summarised in Table 1.2.

K^+ channels, therefore, play a pivotal role in the regulation of vascular smooth muscle tone (Mandegar & Yuan, 2002; Mandegar *et al.*, 2002). Decreased Kv channel activity and the subsequent rise in $[Ca^{2+}]_i$ has been implicated in stimulating PASMC proliferation and could potentially be involved in pulmonary vascular medial hypertrophy in patients with pulmonary hypertension (Platoshyn *et al.*, 2000). High circulating glucose levels associated with diabetes mellitus are shown to increase reactive oxygen species (ROS) by inducing super oxide (SO^-) production which impairs Kv channel activity (Liu *et al.*, 2001; Liu & Gutterman, 2002b); although ROS may also decrease or leave Kv channels unaffected depending upon the oxidant species (Gutterman *et al.*, 2005). BK_{Ca} channels have also been linked to coronary atherosclerosis (Bolotina *et al.*, 1991). Vascular remodelling is now associated with both promotion of SMC proliferation and attenuation of cell apoptosis where K^+ efflux

also inhibits cytoplasmic caspases (Remillard & Yuan, 2004). This is well documented for altered K^+ channel activity in the pulmonary vasculature in conditions where chronic hypoxia is prevalent (such as living at high altitude), (Remillard & Yuan, 2005), resulting in increased medial hypertrophy of the arterial walls and the ensuing pulmonary hypertension (PH). Consequentially, dysfunctional potassium channel regulation in blood vessels is thought to contribute to the development of major cardiovascular diseases and attention is being drawn to them as potential therapeutic drug targets (Mandegar & Yuan, 2002; Mandegar *et al.*, 2002; Sobey, 2001).

Table 1.1. Functional K^+ channels expressed in VSMCs.

	K^+ Channel					
Tissue	**Kv**	**BK_{Ca}**	**K_{ATP}**	**K_{ir}**	**TASK**	**KCNQ**
Pulmonary	Yuan, 1995; Peng *et al.*, 1996	Peng *et al.*, 1996; Barman *et al.*, 2003	Clapp & Gurney, 1992		Gurney *et al.*, 2002; Gardener *et al.*, 2004	Joshi *et al.*, 2006
Cerebral	Robertson & Nelson, 1994	Robertson *et al.*, 1993		Zaritsky *et al.*, 2000		
Mesenteric	Xu *et al.*, 1999	Sansom & Stockand, 1994	Quayle *et al.*, 1995		Gardener *et al.*, 2004	
Coronary	Remillard & Leblanc, 1996	Tanaka *et al.*, 1997	Gollasch *et al.*, 1996	Quayle *et al.*, 1996		
Portal vein	Edwards *et al.*, 1993	Miller *et al.*, 1993	Hart *et al.*, 1992			Ohya *et al.*, 2003
Aortic	Tammaro *et al.*, 2004	Tammaro *et al.*, 2004				

The functional characteristics and physiological roles of K^+ channels in VSMCs have been extensively investigated over the past decade and a complete discussion is beyond the scope of this thesis. For a comprehensive overview of the role of potassium channels in the regulation of VSMC function refer to recent reviews (Sobey, 2001; Cox & Rusch, 2002; Korovkina & England, 2002; Jackson, 2000b). The structure and function of BK_{Ca}, K_{ATP}, Kv, KCNQ and TASK channels will be discussed further in relation to pulmonary circulation, focusing on Kv channels that are of specific interest to this study.

Table 1.2. Properties of potassium channels in vascular smooth muscle (with particular focus on pulmonary circulation).

K^+ Channel	*Subtype*	*Accessory subunits*	*Activated by ....*	*Inhibited by...*	*Antagonists*
BK_{Ca}	***Slo1* or KCNMA1** (Orio *et al.*, 2002)	**β1**(Brenner *et al.*, 2000; Cox & Aldrich, 2000; Orio *et al.*, 2002), **β2, β 3, β4** (Platoshyn *et al.*, 2004[1])	**PKG** (Barman *et al.*, 2003[1]), **NO** (Bolotina *et al.*, 1994; Brakemeier *et al.*, 2003), **PKA** (Carl *et al.*, 1991, **EETs** (Zhang *et al.*, 2001; Archer *et al.*, 2003), **CO** (Xi *et al.*, 2004; Wang *et al.*, 1997), **AA** (Lu *et al.*, 2005), **Depolarisation inc $[Ca^{2+}]_i$** (Jackson, 2000	**PKC** (Barman *et al.*, 2004[1]; Minami *et al.*, 1993), **ROS** (Tang *et al.*, 2004), **dec pH_i** (Schubert *et al.*, 2001), **Hyperpolarisation inc $[Ca^{2+}]_i$** (Nelson & Quayle, 1995), **c-Src** (Alioua *et al.*, 2002)	**IbTX** (Gao & Garcia, 2003; Giangiacomo *et al.*, 1992), **ChTX** (Gao & Garcia, 2003), **Paxilline** (DeFarias *et al.*, 1996; Tammaro *et al.*, 2004), **1mM TEA** (Li & Aldrich, 2004),
Kv	**Kv 1.1-1.7&1.10, Kv2.1, Kv3.1b, 3.3&3.4, Kv4.1&4.1, Kv5.1 , Kv 6.1-3, Kv9.1&3, Kv10.1, v11.1** (Archer *et al.*, 1998[1]; Smirnov, 2002 8666 /id}[1]; Coppock, 2001 8997 /id}[1]; Platoshyn, 2004 10664 /id}[1])	**Kv β1, Kv β2, Kv β3** (Accili *et al.*, 1997; Platoshyn *et al.*, 2004[1])	**Depolarisation** (Nelson & Quayle, 1995[1]), **PKA** (Aiello *et al.*, 1995; Son *et al.*, 2006), **dec pH_i** (Berger *et al.*, 1998[1])	**Hyperpolarisation** (Nelson & Quayle, 1995[1]), **PKC** (Aiello *et al.*, 1996), **inc $[Ca^{2+}]_i$** (Cox & Petrou, 1999), **Rho kinase** (Cachero *et al.*, 1998)	**4-AP** (Osipenko *et al.*, 1997[1]), **cyt P450 inhibitors (clotrimazole)** (Yuan *et al.*, 1995[1]), **correolide** (Cheong *et al.*, 2001)

KCNQ	**KCNQ1** (Ohya *et al.*, 2003; Joshi *et al.*, 2006[1]; Yeung & Greenwood, 2005)	**None yet identified** (Yeung & Greenwood, 2005), **ERG1?** (Ohya *et al.*, 2002)	**Depolarisation** ((Nelson & Quayle, 1995[1])	**Hyperpolarisation** (Nelson & Quayle, 1995[1])	**Linopirdine** (Joshi *et al.*, 2006[1]; Ohya *et al.*, 2003), **XE991** (Joshi *et al.*, 2006[1]; Yeung & Greenwood, 2005), **Ba^{2+}** (Gibor *et al.*, 2004)
K_{ATP}	**K_{ir} 6.1** (Cui *et al.*, 2002[1]; Teramoto, 2006), **K_{ir} 6.2** (Isomoto *et al.*, 1996)	**SUR2B** (Cui *et al.*, 2002[1];Isomoto *et al.*, 1996)	**PKA** (Sun *et al.*, 2006), **CGRP** (Wellman *et al.*, 1998), **decreased ATP** (Clapp & Gurney, 1992), **PKG** (Nelson & Quayle, 1995[1]), **pinacidil** (Quayle *et al.*, 1997)	**Increased ATP** (Glavind-Kristensen *et al.*, 2004; Wilson *et al.*, 2000), **Ca^{2+} activated PP2B** (Wilson *et al.*, 2000), **PKC** (Chrissobolis & Sobey, 2002)	**Glybenclamide** (Jackson, 1993), **Tolbutamide** (Nelson & Quayle, 1995[1])
2 pore domain K^+ channels	**TASK-1&2**, THIK-1, TRAAK, TREK-1&2, TWIK-1&2 (Gurney *et al.*, 2003[1]; Gardener *et al.*, 2004[1])		**Depolarisation and inc pH_o** (Gardener *et al.*, 2004[1]), **PKA** (Olschewski *et al.*, 2006[1])	**Hyperpolarisation and dec pH_o** (Gardener *et al.*, 2004[1])	**Zn^{2+}** (Gurney *et al.*, 2003[1]), **Anandamide** (Gurney *et al.*, 2003[1])

[1] Pulmonary circulation

Arachidonic acid (**AA**); Carbon monoxide (**CO**); calcitonin gene related peptide (**CGRP**); Charybdotoxin (**ChTX**); epoxyeicosatrienoic acids (**EETs**); nitric oxide (**NO**); iberiotoxin (**IbTX**); Protein kinase A/C/G (**PKA/C/G**); protein phosphatase 2B (**PP2B**).

1.5 Hypoxic pulmonary vasoconstriction (HPV)

The pulmonary circulation responds uniquely to hypoxia by contracting and thus diverting blood flow from poorly ventilated regions to those with better oxygen supply and matching ventilation to perfusion, this phenomenon is widely known as hypoxic pulmonary vasoconstriction or HPV. Conversely, systemic circulation responds by dilating and maximising blood flow and oxygen supply to cells around the body. Exposure to acute hypoxia may result in HPV. If hypoxia is sustained vascular remodelling occurs and the more serious condition of pulmonary arterial hypertension (PAH) develops (Dumas *et al.*, 1999). Despite extensive research the mechanisms of HPV are still to be fully elucidated. How O_2 levels are detected in PASMCs, what interim signalling is involved and which components act as effectors remain debated.

1.5.1 Multiple mechanisms involved in HPV

There are many components proposed to be involved in the mechanism of HPV and currently there is no single mechanism that can entirely explain the phenomena (Weissmann *et al.*, 2006b; Aaronson *et al.*, 2006). Specific pathways will be discussed in detail later. It is currently well accepted that elevated $[Ca^{2+}]_i$ is crucial to the development of HPV. One of the mechanisms proposed supports Ca^{2+} entry via L-Type Ca^{2+} channels (McMurtry *et al.*, 1976), subsequent to inhibition of Kv channels and membrane depolarisation. Kv channel inhibition is controversially thought to involve ROS mediated by a decrease in H_2O_2, this is due to a reduction of SO^- production by the mETC resultant of the decreased O_2 supply (Weir & Archer, 1995; Archer & Michelakis, 2002). Alternatively, others have shown data supporting an increase in ROS (Waypa & Schumacker, 2006) and no significant role for Ca^{2+} entry via L-type channels (Robertson *et al.*, 2000b). Ca^{2+} from intracellular stores triggering SOCC, the opening of Ca^{2+}-permeable cation channels and sensitisation of the contractile apparatus to Ca^{2+} involving Rho-kinase (ROK) are now increasingly postulated to be involved HPV (Robertson *et al.*, 2000b). Furthermore, other groups dispute Kv channels being the key regulator of membrane potential and provide evidence for TASK being the initial trigger for depolarisation in PASMC in response to hypoxia (Gurney & Joshi, 2006).

In isolated arteries HPV exhibits a biphasic profile (Fig. 1.3). An initial transient contraction, proposed to be predominantly due to SOC (Robertson *et al.*, 2003) and a progressively increasing contractile response dependent upon the presence of an endothelium. Interestingly, the removal of the endothelium does not suppress the rise in $[Ca^{2+}]_i$ during phase 2 further supporting an involvement of Ca^{2+} sensitisation in the SMCs.

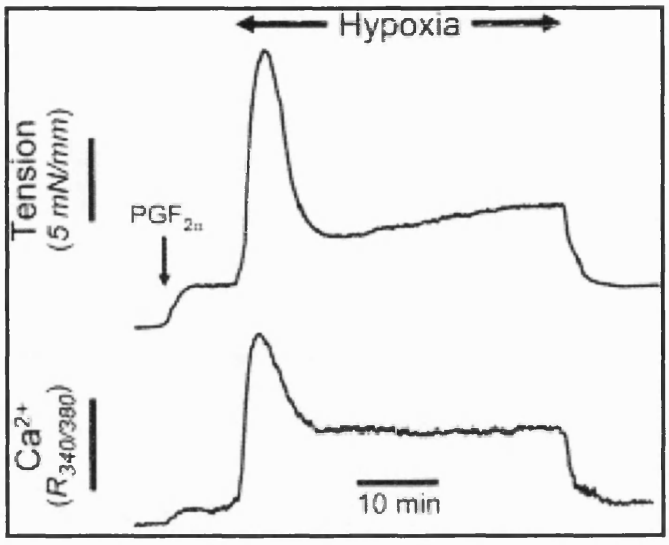

Figure 1.3. Two phase response of PA to acute hypoxia. Above is the change in vessel tension and below changes in Ca^{2+} concentration. Reproduced with kind permission from Ward *et al.*, (2004).

1.6. O_2 sensors and mechanisms of O_2 sensing

Currently there is little consensus over the mechanisms by which cells sense changes in oxygen tension despite it being a key function of tissues such as the carotid body and pulmonary vasculature. Mitochondria, being the major consumers of oxygen, have emerged at the forefront of current research into mechanisms of oxygen sensing in the pulmonary vasculature. Detection of anoxia would appear to be simple – oxidative phosphorylation (OXPHOS) would cease to take place, though detection of changes in oxygen tension within a physiological range is much more complex. NADPH oxidase could be another candidate and will be discussed first.

1.6.1 Nicotinamide Adenine Dinucleotide Phosphate (NADPH) oxidase

The presence of a unique cytochrome b-245 containing NADPH oxidase in calf PASMCs was demonstrated to increase production of effector superoxide ($SO^{\cdot}$) in response to hypoxia, a process inhibited by NADPH inhibitor diphenyleneiodonium (DPI), but not mETC inhibitor myxothiazol (Marshall *et al.*, 1996). However, when wild type and $gp91^{phox}$ knock out (KO) mice were exposed to hypoxia, HPV still occurred in whole lung preparations despite an attenuation of $SO^{\cdot}$ production (Archer *et al.*, 1999). However, in support of a role for NADPH oxidase, Weissmann *et al.* (2006c) found that $p47^{phox}$ KO mice did display a reduced acute hypoxic response, though CH-induced changes were maintained. Essentially this group supported an acute role for NADPH oxidase, but favoured a more prominent mechanism involving the mitochondria. Archer *et al.* (1999) concluded that NADPH does not have a prominent role in oxygen sensing leading to Kv channel inhibition and HPV, and postulated that, as inhibition of mETC complex I mimics hypoxia, inhibits I_K, reduces ROS production and causes vasoconstriction, the mitochondria might be involved in O_2 sensing.

1.6.2 Mitochondria

The notion that redox status is involved in pulmonary vascular tone was first proposed by Weir *et al.* (1985) and then Archer *et al.* (1986) reinforced this concept. Surmounting evidence now postulates mitochondria as one of the most important O_2 sensors in the pulmonary vasculature. Due to the large O_2 consumption by the mitochondria it makes sense that they also act as cellular oxygen sensors. In intact lungs and PASMCs, proximal mETC inhibitors are proven to prevent a rise in PA pressure and block contraction in response to hypoxia, thus attenuating HPV, whereas distal inhibitor antimycin itself caused constriction and did not abrogate HPV; pinpointing a functional significance of the mETC in the mechanisms underlying HPV (Waypa *et al.*, 2001). Even more convincing are studies using mutant cells lacking mitochondrial DNA derived from PASMCs (p^0 cells). These cells retain contractility (tested with thromboxame A_2 analogue, U46619) but fail to respond to hypoxia (Waypa *et al.*, 2001). More specifically, Leach *et al.* (2001) described data supporting a fundamental role for the mETC in both the phase 1 and 2 parts of the response to hypoxia in PA rings. Any disparity with the mETC as the predominant O_2 sensor may

be explained by mitochondrial diversity between vascular beds, which has been proposed as an explanation for the difference in response to hypoxia in PA and systemic vasculature (Michelakis *et al.*, 2002).

1.6.2.1 *Mitochondrial oxidative phosphorylation*

Mitochondria occupy a considerable proportion of the cells cytoplasm and are crucial to cellular respiration, enabling up to 15 times more ATP to be produced than glycolysis alone (Fig. 1.4). This chemiosmotic process, by which large amounts of energy harnessed in the inner mitochondrial membrane are used to drive the production of ATP, was first proposed by Mitchell (1961). Mitchell continued to propose that uncouplers of oxidative phosphorylation or OXPHOS acted as proton conductors through the mitochondrial membrane from the matrix (Reid *et al.*, 1966). Wilkstrom furthered the hypothesis and his principles that oxidation of cytochrome c oxidase complex, catalysed by cytochrome c oxidase, is coupled to translocation of H^+ ions across the mitochondrial membrane also apply to the subsequent respiratory chain complexes (Wikstrom & Saari, 1977).

This mechanism by which protons are transferred across the membrane has been the focus of many years of investigation and still remains controversial. Recently it was even proposed that proton pumping by cytochrome *c* oxidase is not mechanistically coupled to internal electron transfer, but instead to O_2 at the catalytic site (Faxen *et al.*, 2005). However, the latest evidence has now demonstrated that electron transfer from haem *a* to the O_2 reduction site initiates the proton pump mechanism by being kinetically linked to an internal vectoral proton transfer (Belevich *et al.*, 2006).

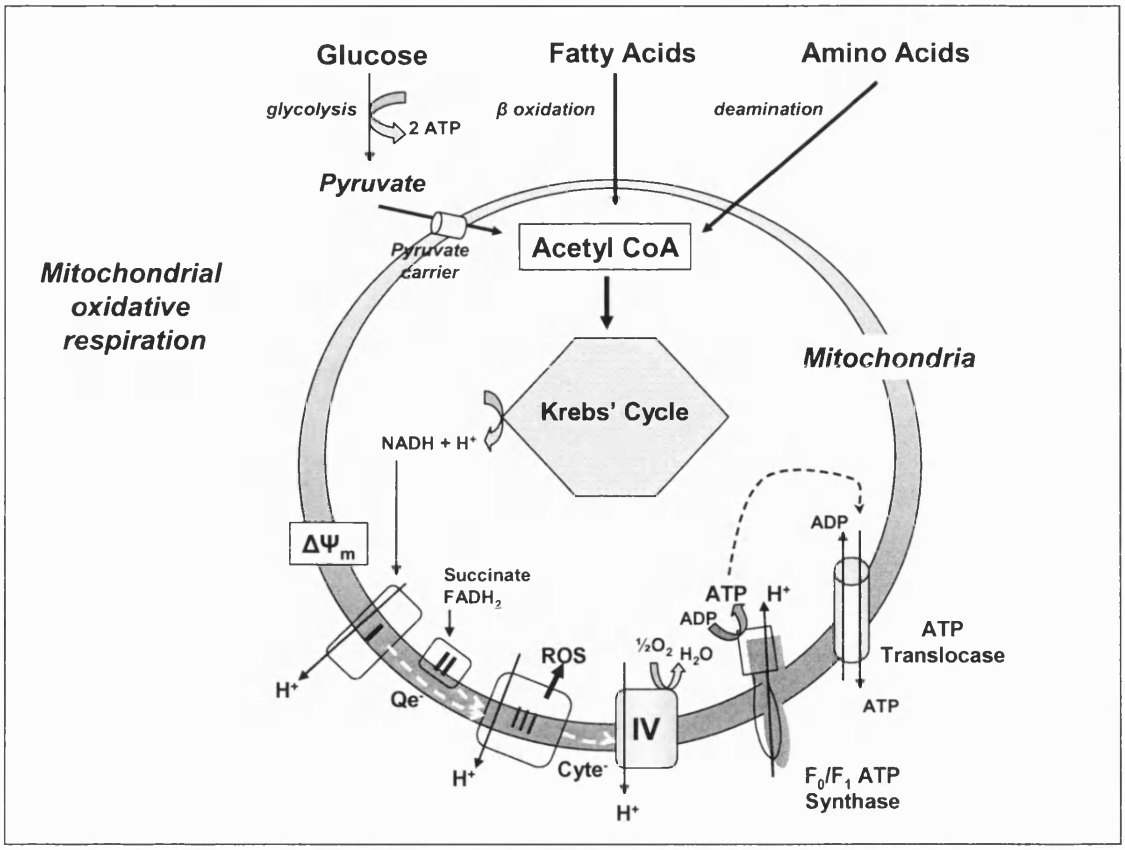

Figure 1.4 Simplified diagrammatical representation of cellular respiration. Glucose undergoes glycolysis to produce pyruvate and a net of 2 ATP molecules. Pyruvate is converted to Acetyl CoA and during this process is transported by a pyruvate carrier into the mitochondrion. Acetyl CoA then enters the Krebs' cycle. Here the acetyl group is further oxidised to generate NADH and ubiquinol. NADH acts as the reducing equivalent driving the mETC. Electrons are transported from complex I to III via coenzyme Q (Qe^-) and from complex III to IV via cytochrome c ($cyte^-$). The electrochemical gradient (Δp) created by movement of protons into the inter mitochondrial space drives H^+ back across the membrane via the F_0/F_1 ATP synthase, producing ATP which itself is transported out of the mitochondrion by the ATP translocase in exchange for ADP. Adapted from Leach *et al.*, (2002).

1.6.2.2 mETC

OXPHOS is the process by which a series of multi-subunit enzyme complexes interact passing electrons down a series of redox reactions and simultaneously storing energy as

an electrochemical proton gradient, which will ultimately drive the generation of mitochondrial ATP.

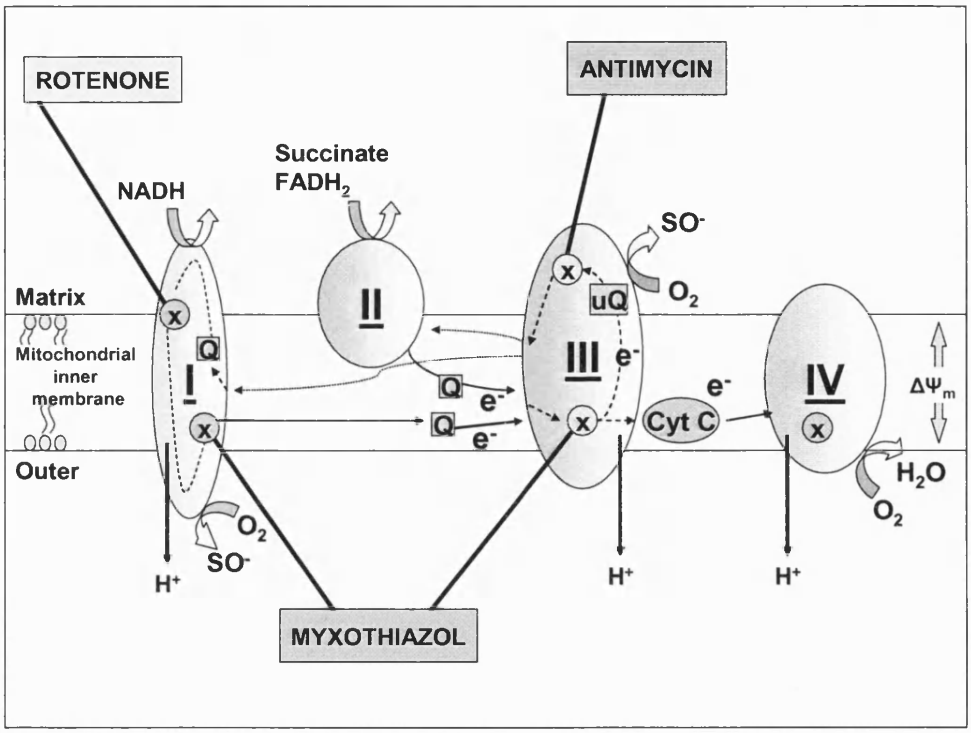

Figure 1.5. Simplified diagram of the mETC and its inhibition. NADH and $FADH_2$ are the reducing equivalents supplying complex I and II, respectively, the final electron acceptor in complex IV is molecular O_2, generating water. Superoxide (SO^-) is known to be produced at both complexes I and III. The correct functioning of the mETC complexes maintains $\Delta\Psi_m$. mETC inhibitors indicated are rotenone (inhibiting complex I), myxothiazol (inhibiting complexes I and proximally in III) and antimycin (inhibiting distally in complex III). Additionally, cyanide inhibits at Complex IV. Adapted from Ward, (2003).

Complex I

NADH and $FADH_2$ are high energy electron carriers generated by the Krebs' cycle and transferred to the inner mitochondrial membrane. Here NADH acts as a reducing equivalent feeding complex I of the mETC. Complex I or the NADH dehydrogenase complex is the largest complex consisting of over 40 polypeptide chains and is reduced by accepting e^- from NADH which looses a hydride ion to form NAD^+. Electrons are

passed via flavin and several iron-sulphur centres to ubiquinone which transports the electron to complex III, itself becoming reduced to ubiquinol.

Complex II

Complex II, the cytochrome b-c complex or co-enzyme Q reductase, consists of 11 polypeptide chains and is the only membrane bound complex in the chain. It passes the electron to cytochrome-c which transfers the electron down the mETC to complex III (cytochrome c reductase complex). Complex II functions to add additional electrons into the quinone pool by removing electrons from succinate and transferring them (via FAD^+) to coenzyme Q, thus bypassing complex I.

Complex III

Complex III comprises 13 polypeptide chains and includes two cytochromes and two copper ions. In complex III a phenomenon known as the Q cycle occurs; two electrons from ubiquinol (QH_2) are removed in a stepwise manner and accepted as single electrons sequentially by cytochrome c_1 from the Rieske protein. Concurrently, four protons move across the membrane, adding to the proton gradient initiated in complex I (Hunte *et al.*, 2003; Yu *et al.*, 1998). If the $\Delta\Psi_m$ changes or inhibitors such as antimycin are present, then the electron transport is disrupted. This may conversely alter the production of superoxide in this complex (Fig. 3.3).

Complex IV

Four electrons are subsequently passed, in a series of one-electron steps, to the final electron acceptor, molecular oxygen, which is reduced to form a water molecule. This occurs in complex IV, the cytochrome oxidase. Generated Δp drives the formation of ATP from ADP + P_i in complex V, the ATP synthase.

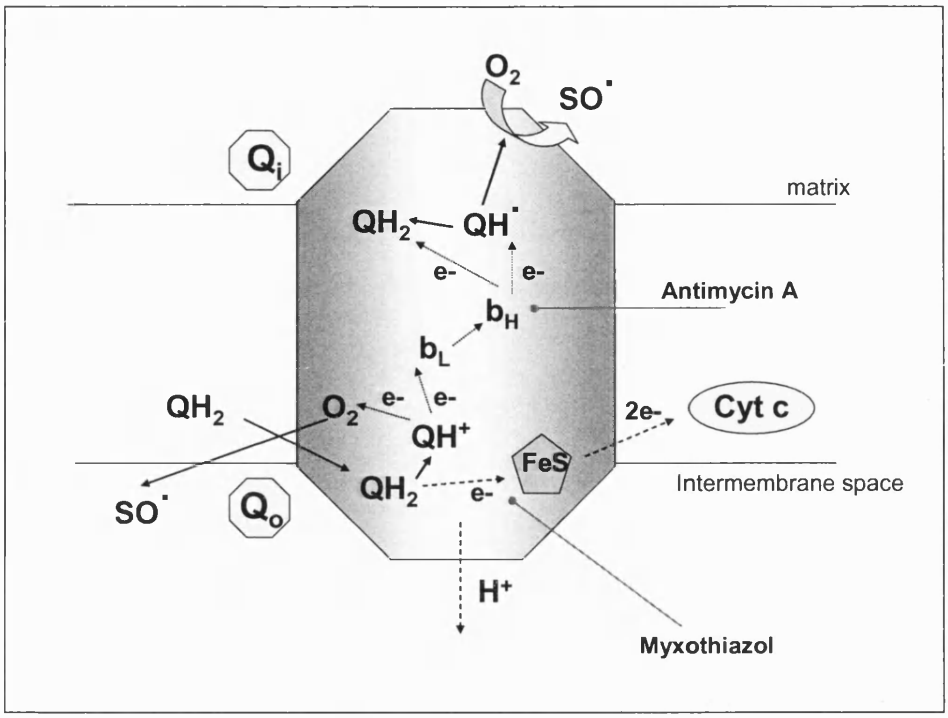

Figure 1.6. Detailed mechanisms of electron transport in complex III. Ubiquinol (QH_2) binds at the Q_o site, located near the outer surface of the inner membrane Rieske iron–sulphur protein (the inhibitory site of proximal inhibitor myxothiazol) accepts a single electron and generating semiquinone, which reduces the first cytochrome b heme (b_L) (Demin *et al.* 1998). The iron–sulphur group of the Rieske protein subsequently transfers the electron to cytochrome c_1. Concurrently, the second cytochrome b heme (b_H) accepts the electron from b_L and reduced uniquinone to form ubisemiquinone. This additional quinone reduction site is situated on the matrix side membrane (denoted Q_i, for inner membrane). Electrons from cytochrome b are then transferred to regenerate ubiquinol. The bc_1 complex is the inhibitory site of distal inhibitor antimycin (Bolgunas *et al.*, 2006).

Complex V

F_0F_1 ATP synthase present in the mitochondrial inner membrane catalyses the synthesis of ATP from ADP and phosphate. The F_0 part resides in the membrane whilst the F_1 part protrudes above the membrane into the matrix. It serves an important function in catalysing the synthesis of ATP and is driven by a flow of protons across the membrane (Stock *et al.*, 2000) (Fig. 1.6). An electrochemical gradient is created for protons during electron transfer in the mitochondrial inner membrane. This reaction is fully reversible

with ATP hydrolysis, generating a change in the proton motive gradient. The F_1-ATPase part is primarily responsible for the synthesis, as well as hydrolysis, by application of external torque rotating the γ subunit in reverse, of ATP (Itoh *et al.*, 2004). It is also proposed that there are different binding sites for the substrates of ATP synthesis (ADP and P_i) and hydrolysis (ATP) and for the products of these two processes (Gao *et al.*, 2005). Two commonly used inhibitors of the ATP synthase are oligomycin, binding between the F_o and F_1 subunits and dicyclohexylcarbodiimide (DCCD) binding in the F_o subunit (Matsuno-Yagi & Hatefi, 1993). The reaction for both ATP synthesis and hydrolysis by the F_0F_1 ATPase is represented by [EQN1.1].

[EQN 1.1] $\quad ADP + P_i + \uparrow H^+ <=> ATP + \downarrow H^+$

where $\uparrow H^+$ indicates high proton concentration and $\downarrow H^+$ indicates low proton concentration.

Situated in the inner mitochondrial membrane, the ATP translocase (ANT) facilitates the transport of ADP and ATP between the mitochondrion and the cytosol. ADP can only enter the mitochondrial matrix when it is directly coupled the exit of ATP. The reaction which is catalyzed by the translocase is represented in [EQN 1.2].

[EQN 1.2] $\quad ADP^{3-}_{cyt} + ATP^{4-}_{matrix} \longrightarrow ADP^{3-}_{matrix} + ATP^{4-}_{cyt}$

ATP and ADP (both devoid of Mg^{2+}) are bound with nearly the same affinity. Currently two different isoforms (ANT1 and ANT2) have been identified in the rat, each comprising of two subunits (Brandolin *et al.*, 1993). Interestingly, the levels of ANT transcription have been directly linked to the degree of OXPHOS with evidence for high levels of both isoforms present in energy demanding tissues such as the heart and muscle (Ning *et al.*, 1998). It has, however, also been proposed that the expression of these subunits is coupled more to the tissues ability to proliferate (Dorner *et al.*, 1999). If the mETC function is impaired, e.g. in the presence of inhibitors or uncouplers, the proton gradient will be reduced, but respiration will proceed. However, the ATP synthase will be active in the reverse mode culminating in ATP hydrolysis, not synthesis. In addition, ATP has a 10 fold higher affinity for Mg^{2+} than ADP and also acts as one of the main buffers of intracellular Mg^{2+}. Therefore, changes in the

ADP/ATP ratio will cause changes in the Mg^{2+} concentration (Kun, 1976). The translocation of ATP or ADP can be blocked by Mg^{2+}, because MgATP/MgADP complexes cannot be transported by the ANT (Gropp *et al.*, 1999). Mg^{2+}, however, is suggested to be very important in ATP synthesis, where it helps to bring the β-phosphate of ADP and P_i closer together (Chen *et al.*, 2006).

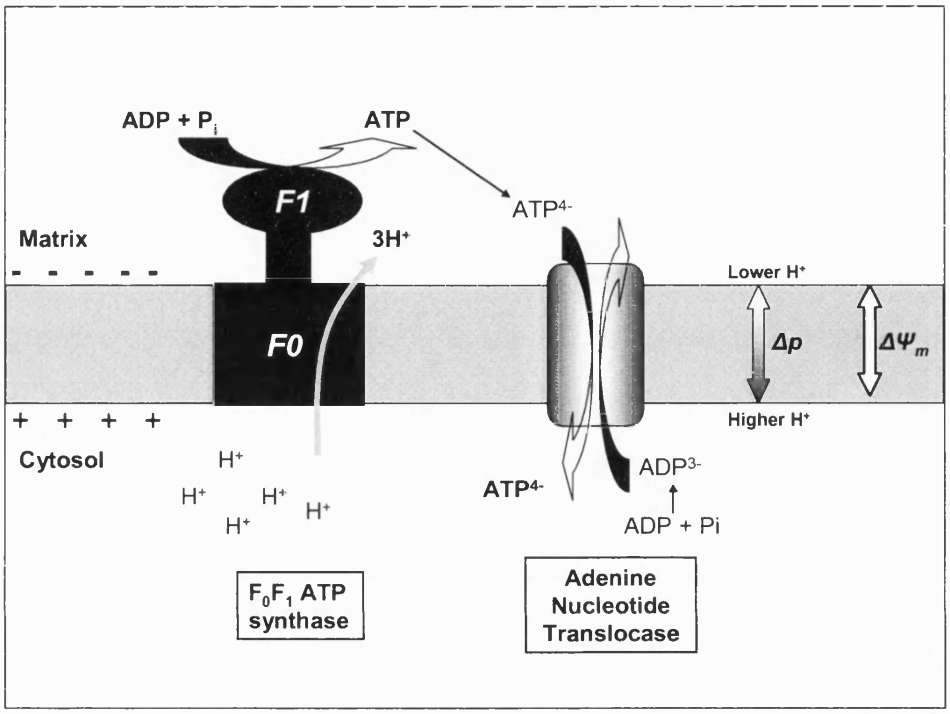

Figure 1.6. A diagrammatical representation of ATP synthesis and transport. Electron transport through the mETC, H^+ leaves the matrix creating a proton gradient (Δp) and generating a $\Delta\Psi_m$ that is negative to the matrix. This provides the driving force for the F_1F_o ATP synthase to synthesise ATP. The ANT is an antiporter that catalyses the exchange of ADP for ATP across the inner mitochondrial membrane.

1.6.2.3 Mitochondrial ROS production

ROS production occurs with a single electron reduction of O_2. Leaks in electron transport tend to arise at complexes I and III giving rise to superoxide production (Turrens, 1997). The mechanism of superoxide production at complex III is most extensively understood (Turrens *et al.*, 1985). Changes in ROS during hypoxia are well established and there is currently support for the involvement of the mETC in oxygen

sensing in PASMCs (Moudgil *et al.*, 2005; Waypa & Schumacker, 2005). H_2O_2 is the main and most stable intracellular oxidant formed by dismutation (by superoxide dismutase 2, SOD2) of SO^- in the mitochondria. There are three human forms of SOD (SOD1-3); in the mitochondria the SOD2 isoform with a manganese centre is present. Production of ROS has been shown to be sensitive to cyanide and particularly antimycin and is thus likely to involve a component of complex III. In addition, factors such as myxothiazol (by preventing the formation of ubisemiquinone) also reduced the production of H_2O_2. Cytochrome b was not involved in this mechanism as it remained reduced throughout (Turrens *et al.*, 1985), therefore leaving ubiquinone as the only reduced electron carrier capable of converting O_2 to O_2^-. The mechanism at complex I is currently thought to involve a single electron reduction of O_2 the source of which is now proposed to be an iron sulphur cluster (either the N1a, Kushnareva *et al.* (2002) or the N2, Genova *et al.* (2001) and not ubisemiquinone as has subsequently been shown (Lambert & Brand, 2004). Despite these advances the physiological relevance of ROS generation by Complex I still remains unclear (Lenaz *et al.*, 2006).

1.7 Transduction mechanisms

Currently and controversially cellular redox state and ROS are thought to represent the predominant transduction pathway in response to hypoxic conditions. In addition, pathways involving ATP and the cellular phosphorylation state are speculated to be involved. Both are discussed below.

1.7.1 Intracellular redox state

The role of intracellular redox state in the cellular response to hypoxia is widely recognised, however there is a difference in opinion, either siding for a paradoxical increase in ROS and activation of oxidant dependent signalling mechanisms to inhibit K^+ channels (Waypa *et al.*, 2001; Waypa & Schumacker, 2002; Ward *et al.*, 2006) or that decreased ROS production occurs with an associated change in redox couples inhibiting redox-sensitive K^+ channels (Archer *et al.*, 1993; Archer & Michelakis, 2002). An interesting, and entertaining, point:counterpoint article was recently published in the Journal of Applied Physiology between two groups of researchers, JP

Ward and SL Archer, at the forefront of this debate arguing the evidence for both hypothesis (Ward *et al.*, 2006;Weir & Archer, 2006a; Weir & Archer, 2006b).

1.7.1.1 Hypoxia and ROS

An increase in ROS in response to hypoxia in PASMC is thought to activate the release of Ca^{2+} from intracellular stores. RyR activation by ROS has been shown to have an important role in the sustained contraction in response to hypoxia (Du *et al.*, 2005). In turn Ca^{2+} channels in the plasma membrane will be recruited and contraction initiated. Using proximal (rotenone and myxothiazol) and distal (antimycin and cyanide) inhibitors Schumacker and colleagues concluded that proximal ROS act as second messengers to increase Ca^{2+} release in PASMCs during hypoxia (Waypa *et al.*, 2002). Further supporting this, proximal inhibitors abolished HPV but PAs still responded to vasoconstrictors, whereas HPV was maintained in the presence of distal inhibitors (Waypa *et al.*, 2001). Evidence obtained by other groups also supports the increase in ROS under hypoxic conditions; in isolated perfused rabbit lungs (Weissmann *et al.*, 2006a), in porcine distal PAs (Liu *et al.*, 2003), in rat PAs (Wang *et al.*, 2006) and in vascular walls of murine lung sections (Paddenberg *et al.*, 2003). In direct contrast, Archer and colleagues postulate that a decrease in ROS is responsible for vasoconstriction via inhibition of K^+ channels, which are demonstrated to be responsive to changes in cellular redox state (Weir & Archer, 1995). Such involvement of ROS in K^+ channel regulation during hypoxia is discussed in detail later in this chapter.

It is noteworthy that a number of other mechanisms have also been proposed to play a role in the regulation of ROS in response to hypoxia, in particular when hypoxia becomes more sustained (Wolin *et al.*, 2005; Waypa & Schumacker, 2005; Ward *et al.*, 2006). Complexes I and III of the mitochondrial ETC (discussed above) are believed to be the major sources of ROS production (Guzy *et al.*, 2005). ROS from complex III apparently essential for the stabilisation of hypoxia inducible factor 1α (HIF-1α) under sustained hypoxia (BelAiba *et al.*, 2004; Mansfield *et al.*, 2005; Chandel *et al.*, 2000). Controversially, Paddenbergs' group have suggested that complexes I and III regulate ROS only under normoxic conditions and that it is actually complex II that is responsible for the increase in ROS under hypoxic conditions and necessary for the development of HPV (Paddenberg *et al.*, 2003). They proposed that a change in the

catalytic activity of complex II from succinate dehydrogenase to fumarate reductase is principally responsible for this. Another group suggest that hypoxia induced increases in SO^- anions can increase endothelin 1 (ET-1) release and down regulate endothelin B (ET-B) receptors in SMCs (Wang *et al.*, 2006). In PASMCs, an increase in ROS can also increase vascular endothelial growth factor mRNA, thus a more reduced redox state may be a possible treatment for the remodelling that occurs in pulmonary hypertension (BelAiba *et al.*, 2004).

1.8 HPV effector components

As previously mentioned there are several effector components in HPV proposed. Most recently proposed is a role for AMP-activated protein kinase (AMPK) dependent, cADP ribose activated, Ca^{2+} release from the SR via RyR. Additionally, an increase in RhoA/ROK has been shown to increase myosin light chain phosphorylation and possibly be involved in Ca^{2+} sensitisation of the contractile apparatus.

1.8.1 AMP-activated protein kinase (AMPK)

Evans *et al* (2005, 2006a&b) have proposed a novel effector mechanism in PASMCs which may be particularly sensitive to the metabolic stresses induced by hypoxia. They report that hypoxia induced an increase in the AMP/ATP ratio with an ensuing AMPK dependent cADP-ribose activated Ca^{2+} release from the SR via RyRs Four AMPK isoforms are currently identified in PASMC with the $\alpha 1\beta 1\gamma 1$ isoform most prevalent and at higher expression levels than in systemic vasculature (Evans *et al.*, 2005). It is also worth noting that hypoxia has recently been shown to activate AMPK via increased ROS production, independent of the above-mentioned change in nucleotide ratio (Quintero *et al.*, 2006).

1.8.2 RhoA kinase and Ca^{2+} sensitisation

The ROK inhibitor Y27632 has recently been used to study the involvement of RhoA and its downstream effector ROK in the signalling pathways activated by hypoxia. Studies have demonstrated that cGMP effects RhoA/ROK directed Ca^{2+} sensitisation of the contractile apparatus in arteries (Sauzeau *et al.*, 2000). Ca^{2+} sensitisation was first

described by Leach *et al* (1994) in the PA who, while seeking an explanation for the lack of further increases in Ca^{2+}_i during the 2nd, endothelium dependent, phase of HPV proposed a possible Ca^{2+}-sensitisation of the contractile apparatus in PA (Robertson *et al.*, 1995; Leach *et al.*, 1994). RhoA/ROK have previously been shown to be central components of Ca^{2+} sensitisation in guinea-pig ileum smooth muscle (Swärd *et al.*, 2000). This has since been proven to have a role in both acute and chronic hypoxia (McMurtry *et al.*, 2003). Hypoxia has been shown to increase RhoA/ROK leading to an increase in myosin light chain phosphorylation (Wang *et al.*, 2001; Wang *et al.*, 2003). In addition, inhibition of ROK blocks both the sustained phase of HPV in PA and inhibits HPV development in perfused rat (Robertson *et al.*,2000a) and mouse (Fagan *et al.*, 2004) lungs. How RhoA/ROK is activated by hypoxia is currently unclear. It is speculated that either hypoxia induced elevation of Ca^{2+} itself (Sakurada *et al.*, 2003) or the hypoxia driven increase in ROS (Waypa *et al.*, 2001) activate the RhoA dependent Ca^{2+} sensitisation. After further experiments it is now concluded that a PKC and ET-1 independent Ca^{2+} sensitisation is responsible for the sustained response to acute hypoxia and that this is intrinsically reliant upon an intact endothelium (Aaronson *et al.*, 2002; Robertson *et al.*, 2003). This lead to the current hypothesis over the involvement of RhoA/ROK activation by an endothelium derived constrictor factor. It is noteworthy that inhaled Rho kinase inhibitors may possibly be useful as vasodilators in patients with PH (Nagaoka *et al.*, 2005).

1.8.3 K^+ channels

In PASMCs, as in other types of VSMCs, potassium channels play a crucial role in the maintenance of negative resting membrane potential (-60 to -50mV). Functional K^+ channels expressed in PASMCs include the K_v channels (Yuan, 1995), KCNQ (Kv7) (Joshi *et al.*, 2006 ;Yeung & Greenwood, 2005; Peng *et al.*, 1996), BK_{Ca} (Peng *et al.*, 1996; Barman *et al.*, 2003), K_{ATP} (Clapp & Gurney, 1992) and 2PK (Gurney & Joshi, 2006; Gurney *et al.*, 2003; Olschewski *et al.*, 2006).

BK_{Ca} channels are ubiquitously expressed in VSMC and are activated by both membrane potential and intracellular Ca^{2+} contributing to the control of membrane potential and consequently vascular tone (Korovkina & England, 2002). These

channels may act as a negative feedback mechanism in response to depolarisation and increased $[Ca^{2+}]_i$ during vasoconstriction, and could be a target for the action of vasoactive substances (Brayden, 1996). Cox & Rusch, (2002) showed that inhibition of Ca^{2+} efflux decreased the BK_{Ca} current and increased the K_v current, indicating that cytosolic Ca^{2+} levels are critical regulators of these channels. BK_{Ca} channels are expressed in PASMCs, though the relative contribution to the whole cell current has species diversity and varies in different PA tree regions (Mandegar *et al.*, 2002). Recent reports indicate an attenuation of BK_{Ca} currents during acute hypoxia via an inhibition of cAMP/PKA dependent pathway (Barman *et al.*, 2005). A role for BK_{Ca} channels in HPV is currently controversial.

Recently, 2PK have been identified in PASMCs having a non-inactivating current, denoted I_{KN}, which is characterised by having no time or voltage dependency (Evans *et al.*, 1996). In rat and rabbit PASMC (Gurney *et al.*, 2003) and, most recently in human PASMC (Olschewski *et al.*, 2006), it has been shown that the pharmacological profile of I_{KN} matches the TASK-1 (TWIK related Acid Sensitive K^+ channel, (Patel & Honore, 2001) subtype of 2PK, being insensitive to glybenclamide, TEA and Ca^{2+} channel blockers and having a high sensitivity to external pH but not $Ca^{2+}{}_i$. Reverse transcription polymerase chain reactin (RT-PCR) analysis has shown both TASK-1 and TASK-2 channels to be present in rat MA- and PA-SMCs (Gardener *et al.*, 2004). TASK-1, in particular, is able to regulate membrane potential by 10 mV in both a hyperpolarising and depolarising direction and as such is strongly implicated as being a predominant factor in regulating resting membrane potential, and thus vascular tone, in PASMCs (Olschewski *et al.*, 2006). It is also worth noting that TASK-1 exhibits sensitivity to hypoxia (Olschewski *et al.*, 2006) and, as such, these channels may be functionally important in mechanisms underlying HPV. There is no evidence yet to suggest a direct role of TASK in HPV. Additionally, there is no link shown between either BK_{Ca} or TASK channels, and the proposed ROS-dependent transduction mechanism, discussed previously.

K_{ATP} is another ubiquitous class of K^+ channels, which show little or no voltage dependence. It is believed that under basal conditions the open probability of K_{ATP} is low (Jackson, 2000a). Co-expression of SUR subunit 2B with K_{ir} 6.1or 6.2 produces

channels with characteristics of two distinct K_{ATP} families, K_{NDP} (named reflecting a primary role for various nucleotide diphosphates in their activation) and K_{ATP} (predominantly sensitive to ATP), respectively (Beech *et al.*, 1993). K_{ATP} channels are shown to be present in PASMC and activated under metabolic deprivation (Clapp & Gurney, 1993). The expression of K_{ir} 6.1 with SUR2B has been detected in human PASMCs (Cui *et al.*, 2001). Some evidence suggests they may contribute to resting membrane potential in PASMCs, although the regulatory mechanisms are still to be elucidated (Cui *et al.*, 2002). Additionally, there is no proposed role in HPV, Robertson *et al.* (1992) suggested that K_{ATP} channels are normally closed in the pulmonary arteries and are not activated by the levels of hypoxia that cause a constriction.

KCNQ (previously KVLQT1, Kv7 family) channels were first identified in cardiac cells where mutations in a chromosomal loci on the KVLQT1 gene encode for an inherited form of long QT syndrome (LQT) (Wang *et al.*, 1996). Since their discovery isoforms KCNQ 1-5 have been identified. They have been widely studied in neurones, where KCNQ2 associates with KCNQ3 or KCNQ4, and KCNQ3 associates with KCNQ5 (Robbins, 2001). KCNQ2 are the proposed molecular correlates for a slowly activating and slowly deactivating K^+ M-current ($I_{K(M)}$) that shows no inactivation (Tinel *et al.*, 2000 (heart); Robbins, 2001). KCNQ channels encode a "shaker like" 6 TM spanning channel with a single pore domain (Fig. 1.2A). In the vasculature, KCNQ1 channels have recently been identified and are thought to play an important role in the contractility of both rat portal veins (Ohya *et al.*, 2003; Yeung & Greenwood, 2005) and in mouse and rat PAs (Joshi *et al.*, 2006). Linopiridine and XE991, KCNQ blockers, were demonstrated to be potent and selective PA constrictors and data suggests that KCNQ channels could contribute to the regulation of resting membrane potential in the PAs (Joshi *et al.*, 2006). Again, a role in HPV is currently not established.

1.9 K_v channels

The Kv channels are the most diverse group of K^+ channels ubiquitously expressed in VSMCs. The variety of Kv channel subtypes and their regulatory components found in the vasculature are summarised in Table 1.2. Kv channels, similar to BK_{Ca}, are composed of a tetramer of Kv α subunits (pictured in Fig 1.2A) which come together to

form a pore selective to the conduction of K^+ ions. Accessory β subunits have been shown to alter the kinetic properties of associated Kv1 α subunits (Accili *et al.*, 1997). Kv channels are activated by depolarisation (Beech & Bolton, 1989) and are central to the regulation of resting membrane potential throughout the vasculature; aortic (Tammaro *et al.*, 2004), mesenteric (Kharkhun *et al.*, 2000), cerebral (Knot & Nelson, 1995) and pulmonary (Yuan, 1995) SMCs.

A prominent voltage-gated K^+ current (I_{Kv}) which plays an important role in the regulation of the resting membrane potential is present in freshly isolated rat PASMCs (Yuan, 1995; Smirnov *et al.*, 2003; Smirnov & Aaronson, 1994). A heterogeneity of K_v channel currents in conduit PASMCs has been described (Archer *et al.*, 1996, Smirnov *et al.*, 2002). Firstly, Archer *et al.* (1996) identified a differential expression of a K_{Ca} current; in larger elongated cells a low current density and sensitivity to TEA and ChTX was predominantly found, whereas in smaller cells a high current density and sensitivity to 4-aminopyridine (4-AP, a delayed rectifier K^+ current inhibitor) existed. The K_{Ca} was the representative current in the conduit arteries whereas the K_{DR} was more prominent in the resistance. Smirnov *et al.* (2002) furthered this work by focusing on Kv channels and Kv channel currents in conduit arteries, termed I_{Kv1} and I_{Kv2}. I_{Kv1} constituted 67% of the population and demonstrated large, rapidly activating I_{Kv} inhibited by 4-AP but insensitive to TEA. The remaining 33% of cells expressed I_{Kv2}, a smaller and slower activating current, which, in contrast, was more sensitive to TEA than to 4-AP. Resistance arteries were found to demonstrate a third uniform I_{KvR} subtype with a large current resembling that of I_{Kv1} but distinguished by a higher current density, a significantly larger time constant for activation and I_{Kv} activation and inactivation were 7 mV more negative than I_{Kv1}. Notably, I_{KvR} was also more sensitive to 4-AP that I_{Kv1} (Smirnov *et al.*, 2002).

Post *et al.* (1992) first demonstrated that I_{Kv} in PASMCs is diminished by hypoxia and it has since been proposed that it may contribute to HPV. Yuan *et al.* (1993a) showed that the inhibition of I_{Kv} amplitude is specific for PA since it was not observed in MA. The importance of Kv channels in the regulation of pulmonary vascular tone has been further supported by Smirnov *et al.* (1994) who showed that chronic hypoxia (P_{O2} 30-35 mmHg) was associated with a marked (40-50%) reduction in the I_{Kv} amplitude. Similar to acute hypoxic episodes, chronically hypoxic animals had a PASMC resting

membrane potential that was significantly more positive (-43.5±2 mV) than that observed in PASMCs from normoxic animals (-54.3±2 mV) (Smirnov *et al.*, 1994). Application of 1 mM 4-AP mimicked this depolarisation. Platoshyn *et al.* (2001) provided evidence for decreased mRNA expression and attenuated protein expression of the K_v channel α -subunits (Kv1.1, Kv1.5, Kv2.1, Kv4.3, and Kv9.3) in primary cultured PA- but not in MA- SMCs. This work has been supported by work from other groups; Wang *et al.* (2005) in rat distal PASMCs and Hong *et al.* (2004) under sub-acute hypoxic conditions. Furthermore, in chronic hypoxia, it has been proposed that hypoxia-induced down regulation of I_{KN} would subsequently promote Kv channel opening and it was thus suggested that there is a switch during chronic hypoxia in the K^+ current determining resting potential from I_{KN} to I_{Kv} (Osipenko *et al.*, 1998).

Several attempts to identify the molecular components of native PASMC O_2 sensitive K_v channel currents have been carried out (Patel *et al.*, 1997; Archer *et al.*, 1996). All studies verify a potential role for the K_v α subunits $K_v1.2$, $K_v1.5$, $K_v2.1$, $K_v3.1b$ and $K_v9.3$ which display similar hypoxic inhibition and are all slowly inactivating voltage-gated channels sensitive to 4-AP but not ChTX. Several β subunits are expressed in PASMCs and may possibly interact with the K_v1 family as oxidoreductase enzymes and can function as redox sensors (MacKinnon, 1991b; Yuan, 2001). β subunits may have a significant role in O_2 response as the $K_v1.2\beta$ subunit demonstrates O_2 sensitivity on the Kv4.2α subunit (Archer *et al.*, 1999). Co-expression of any of the β subunits with one of the O_2 sensitive α subunits affects the time and voltage dependant properties of the resulting current, suggesting that the α subunits may not be the only O_2 sensors and further implicating a role for the β subunit in O_2 sensing in PAs (Coppock & Tamkun, 2001).

Archer and colleagues (1993) were the first group to propose a redox based O_2 sensor as a regulatory point in the response of pulmonary vasculature to hypoxia and also suggested that a decrease in ROS is responsible for vasoconstriction via inhibition of K^+ channels, which were demonstrated to be responsive to changes in cell redox state (Weir & Archer, 1995). Since this initial observation this group has continued extensive research in support of this hypothesis. They progressed to show opposing effects of oxidants (increasing) and antioxidants (decreasing) whole cell potassium channel

currents (Reeve *et al.*, 1995). Archers' group now postulates that, the high basal levels of H_2O_2 in PA may actually activate K^+ channels and therefore in hypoxia a decrease in mitochondrial H_2O_2 production would block them (Michelakis *et al.*, 2004). Inhibition of I_{Kv} by mETC inhibitors, particularly those acting at complexes I and III (being most responsible for ROS generation, Archer *et al.* (1993), supports this concept. Conversely, mitochondrial uncouplers, which decrease mitochondrial membrane potential ($\Delta\Psi_m$) (Yuan *et al.*, 1996), and metabolic inhibition of PASMCs with 2-deoxyglucose (Yuan *et al.*, 1994) also inhibited I_{Kv}, suggesting the presence of multiple, presently undetermined, mitochondria-dependent mechanisms which affect I_{Kv} in PASMCs. Notably, these studies were only focused on the inhibition of I_{Kv} amplitude, which does not allow for discrimination between mitochondria-specific and non-specific actions of inhibitors (Searle *et al.*, 2002). Enhancement of I_{Kv} at negative voltages and inhibition at positive voltages was observed, but mostly ignored, by number of researchers in both canine (Post *et al.*, 1992) and rat (Archer *et al.*, 1993; Turner & Kozlowski, 1997) PASMCs. Furthermore, it is unknown whether and how changes in mitochondrial function affect Kv channel activation and inactivation, two other important voltage-dependent characteristics. These characteristics determine the proportion of available Kv channels in the physiological range of membrane potentials (Nelson & Quayle, 1995) and understanding of the mechanism of their regulation should provide an invaluable insight into the Kv channel function in the pulmonary circulation.

1.10 Aims and objectives

The mechanism by which the pulmonary arteries sense O_2 and constrict in response to hypoxic levels remains highly controversial and currently unknown. The interaction between the mitochondria, as a sensor for O_2, and Kv channels, as an effector, has been proposed; however the two phenomena have not been studied in detail. Furthermore, agreement over evidence for an involvement of ROS in Kv channel regulation is yet to be sought.

Therefore, the main aim of this thesis was to comprehensively investigate the mechanisms of interaction between Kv channel function and the mitochondria in rat PASMCs and to determine a potential physiological significance of such an interaction. To determine specificity to the pulmonary circulation, the key observations will also be compared in mesenteric arterial SMCs, as a representative of the systemic circulation.

Thus, the initial objectives were set as follows:

1) To identify and characterise the role of mitochondria and individual mETC complexes in the regulation of Kv channels in PASMCs using the whole cell and perforated patch clamp techniques.

2) To assess a role of intracellular redox state in the mitochondria dependent regulation of Kv channels in PASMCs.

3) To determine tissue specificity of the mitochondria-dependent modulation of Kv channels by comparing the results obtained in PASMCs to those in MASMCs, as a model of systemic circulation.

4) To determine the potential relevance of the interactions between mitochondria and Kv channels to HPV.

5) As a result of my investigation, the involvement of Na^+ dependent extrusion mechanisms and in particular the NME became apparent. These were therefore characterised in the last chapter of this thesis.

The experiments were performed using the whole cell and perforated patch clamp techniques, confocal imaging microscopy and small vessel wire myography in PA- and MA-SMCs and whole vessels isolated from the rat.

Chapter 2

MATERIALS AND METHODS

2.1 Solutions

Table 2.1 Composition of solutions for cell isolation

Table 2.2 Composition of extracellular solutions for electrophysiological recordings

Table 2.3 Composition of intracellular solutions for electrophysiological recordings

Table 2.4 Composition of solutions for wire myography and solutions for confocal imaging

Table 2.1. Solutions for cell isolation (in mM)

Composition	PSS	Ca^{2+} free PSS
NaCl	110	110
KCl	5	5
$MgCl_2$	1.2	1.2
$CaCl_2$	1.5	0
HEPES	10	10
Glucose	10	10
pH 7.2 adjusted with	NaOH	NaOH

PSS – Physiological saline solution

Table 2.2. Extracellular solutions for electrophysiology (mM)

Composition	PSS	Na^+-free			
		NMDG	KCl	Tris-Cl	LiCl
NaCl	110	0	0	0	0
KCl	5	5	140	5	5
$MgCl_2$	1.2	1.2	1.2	1.2	1.2
$CaCl_2$	1.5	1.5	1.5	1.5	1.5
HEPES	10	10	10	10	10
Glucose	10	10	10	10	10
NMDG		110			
LiCl					110
Tris-Cl				110	
pH 7.2 adjusted with	NaOH	HCl	KOH	KOH	KOH

PSS – Physiological saline solution

All extracellular solutions contained 1 μM paxilline and 10 μM glybenclamide to inhibit BK_{Ca} and K_{ATP} channels respectively.

Table 2.3. Intracellular electrophysiology solutions (in mM)

Composition	Standard pipette soluion	5 $MgCl_2$	5 Na_2ATP	5 MgATP	5 EDTA	1 GSH	Perforated Patch
KCl	140	140	140	140	140	140	140
$MgCl_2$	0.5	5	0.5			0.5	
$CaCl_2$	0.5	0.5	0.5	0.5	0.5	0.5	
HEPES	10	10	10	10	10	10	10
EGTA	10	10	10	10	5	10	1
MgATP				5			
Na_2ATP			5				
EDTA					5		
GSH						1	
Amphotericin B							100 µg/ml
pH 7.2 adjusted with	KOH	KOH	KOH	KOH	KOH	KOH	KOH

Table 2.4. Intracellular solutions for electrophysiology (in mM)

Composition	Standard pipette solution	10 $MgCl_2$	High $CaCl_2$ (220nM)	10 EDTA	BAPTA	HEPES
KCl	140	140	140	140	140	30
$MgCl_2$	0.5	10	0.5		0.5	0.5
$CaCl_2$	0.5	0.5	5.67	0.5		0.5
HEPES	10	10	10	10	10	
EGTA	10	10	10			10
K-HEPES						110
BAPTA					10	
EDTA				10		
pH 7.2 adjusted with	KOH	KOH	KOH	KOH	KOH	KOH

Table 2.5. Solutions for wire myography (mM).

Composition	Standard Krebs	80 K^+ Krebs
NaCl	118	42
$NaCHCO_3$	24	24
$MgSO_4$	1	1
NaH_2PO_4	0.5	0.5
KCl	4	80
Glucose	11	11
$CaCl_2$	1.8	1.8

For the Krebs solutions (Table 2.5) pH was stabilised by continuous gassing with either air, 95 % O_2/5 % CO_2. For dose dependent response curves to KCl concentrations of 10, 15, 20, 40, 80 and 100 mM K^+ were studied. Changes in osmolarity were compensated by respective reductions in the NaCl concentration.

Solutions for confocal imaging

For cell and tissue imaging PSS (Table 2.1) and Krebs (Table 2.5) were used, respectively, whereas Ca^{2+} free PSS (Table 2.1) also contained 1mM EGTA.

The free [Ca^{2+}] (10 nM and 220 nM) and [Mg^{2+}] in the pipette solution was calculated using Maxchelator software (Stanford University, USA). Different Mg^{2+}_i concentrations were achieved by adding corresponding amounts of $MgCl_2$ to the pipette solution giving free [Mg^{2+}] of 350 μM, 3.55 mM and 7.4 mM for 0.5 mM, 5 mM and 10 mM $MgCl_2$, respectively.

The pH of the pipette solution was adjusted to 7.2 using KOH, the total K^+ was adjusted as necessary to be 140 mM with KCl.

2.2 Materials and Reagents

Basic chemicals were purchased from BDH Merck (UK) or Fisher (UK). Enzymes for cell isolation, channel and exchanger inhibitors, ETC inhibitors and fluorescent imaging probes were purchased from Sigma (UK) or Roche (UK). The stainless steel wire was provided by DMT A/S (DEN).

2.3 Tissue preparation

2.3.1 Rat vasculature

Preparation for cell isolation

Male Wistar rats (weight 225–300 g) were killed by cervical dislocation in accordance with UK Home Office guidelines. The heart and lungs were removed *en bloc* after opening of the chest cavity from the diaphragm and cutting the rib cage. Subsequently, the abdominal area was opened midline and the whole mesenteric bed was removed. All tissues were placed in 30ml of PSS solution and maintained on ice for micro dissection. Small intra pulmonary arteries (<500 μm external diameter, 3rd to 5th order) and 3rd to 4th order mesenteric arteries were micro-dissected, cleaned of connective tissue, cut into sections ~3mm wide and used for enzymatic cell isolation.

Preparation for wire myography

Tissues were removed as above; micro dissected and cleaned of connective tissue whilst remaining intact in the organ. 40μm diameter stainless steel wire (DMT/AS) was carefully inserted through a 2mm length of artery, which was subsequently freed before mounting into the wire myograph.

All of the above procedures were carried out using a stereo-microscope (Leica, zoom 2000 or Meiji, Optech scientific instruments) and KL 1500 LCD light source (Olympus).

2.3.2 Isolation of single VSMCs

PA sections bathed in normal physiological salt solution (PSS, Table 2.2) were left on ice for 30 min followed by incubation in Ca^{2+}-free PSS for 10 min at 37°C. Tissue was then transferred into pre-warmed nominally Ca^{2+}-free PSS (2 ml, Table 2.1) containing 1 mg/ml collagenase (Type XI or, in the most recent experiments Collagenase P (Roche) was used yielding a better quantity of PASMCs), 0.5 mg/ml papain and 1 mM dithiothreitol (a reducing agent used to activate the papain) and incubated for 20 min at 37°C. Also, 10 µl/ml PSS was added to Ca^{2+} free PSS to elevate Ca^{2+} concentration and thus increase collagenase activity. Digested tissue was transferred into pre-warmed Ca^{2+}-free PSS and cooled on ice for 5 minutes. The tissue pieces were then triturated to remove the surface layers of the tissue (*tunica intima* and *tunica adventizia*), mainly containing non-smooth muscle cell types with a wide bore Pasteur pipette (to avoid bubbles in the solution) in 2 ml Ca^{2+}-free PSS. This was repeated and the resulting two volumes of Ca^{2+}-free PSS containing dispersed cells were combined and filtered through 95µm nylon mesh. Cells were stored at +4°C in the presence of Ca^{2+}. It is worth mentioning that under these conditions cells tend to contract partially with time, similar to those shown in Fig. 3.17. Only elongated cells were used in experiments

Cells from MAs were isolated using the same procedure except using 2 and 1 mg/ml collagenase and papain, respectively. Also, the tissue incubation time in enzyme was increased to 30 min.

2.4 Wire myography

Small PA and MA obtained from the same rat and threaded onto 40µm stainless steel wire were carefully mounted into a two vessel Mulvany–Halpern myograph (model 400A; Danish Myotechnology) at room temperature. The temperature was increased to 37°C and gassed with 5% CO_2 balanced with O_2. At 37°C the tissue was equilibrated to a resting tension of 30 mmHg (pulmonary) or 100 mmHg (mesenteric) and internal vessel diameter was estimated using a normalisation program. Following a 20 minute stabilisation period the vessels were contracted using 80mM Krebs (Table 2.5) for 2

minutes, only vessels developing a tension of >3mN were used for recording. The endothelium was removed using a hair to gently rub the intimal surface of the vessel, 10μM ACh was used to verify successful removal. Four to six 80mM KPSS applications were performed to establish a steady maximal contraction.

2.5 Confocal Microscopy

2.5.1 Confocal Imaging of $Mg^{2+}{}_i$ and $Ca^{2+}{}_i$

2.5.1.1 Individual smooth muscle cells

Changes in free $Mg^{2+}{}_i$ were measured using a membrane-permeable fluorescent indicator MagFluo-4-AM (Molecular Probes) and an Olympus FV300-SU laser scanning confocal microscope. A drop of cell suspension was placed on a microscope coverslip and loaded with 5 μM MagFluo-4-AM for 45-60 min in the dark at room temperature. The loading solution also contained 50 μM BAPTA-AM (Molecular Probes) to suppress possible changes in MagFluo-4 fluorescence due to increases in $Ca^{2+}{}_i$ and 20% (w/v) Pluronic F-127, (vortexed thoroughly). After loading, PASMCs were continually superfused with PSS (2 ml/min) for 10-30 min to allow de-esterification of both agents. Integral MagFluo-4 fluorescence was measured by using excitation and emission wave lengths of 488 and 505 nm respectively. Images were acquired at 0.33Hz using Fluoview software (Olympus, USA). Measurements were performed in Ca^{2+}-free PSS containing 1 mM EGTA to inhibit Ca^{2+} influx. Data were analysed off-line with MetaMorph v.6.1 (Universal Instruments), corrected for photobleaching, occurring at this acquisition rate under control conditions, using a monoexponential decay function [EQN 2.1], and expressed as a relative intensity normalised to the maximal fluorescence observed in the presence of 1 μM A23187, added at the end of experiment.

[EQN 2.1] $y = y_0 + Ae^{-x/t}$

where y_0 = y offset, A = amplitude and t = the decay constant.

$Ca^{2+}{}_i$ fluorescence imaging in PASMCs was performed in a similar manner to $Mg^{2+}{}_i$. Fluo-4 loading solution was prepared by a dispersion of the AM ester Fluo-4 AM ester in 4ml PSS containing 20% (w/v) Pluronic F-127, which was vortexed thoroughly.

Cells were plated on a glass coverslip and incubated with the loading solution for 45-60 min at room temperature in which the final concentration of Fluo-4 was 12.5 μg/ml. As for Mg^{2+}, cells were then superfused with PSS for 10-30 min before commencing fluorescence measurements. Fluorescent intensity was corrected as described above for Mg^{2+} measurements, and expressed as the relative intensity normalised to the maximal fluorescence observed in the presence of ionomycin (1 μM) added at the end of experiment.

2.5.1.2 Isolated vessels

Whole vessels were mounted on a single channel wire myograph (described in 2.4) and loaded with MagFluo-4AM (as previously described in 2.5.1.1) except the bath volume was 5 ml. To maximise loading of the smooth muscle cells the connective tissue was partly digested with 0.5-1 mg/ml of papain and collagenase and DTT (for 3-10 mins). The enzymes were removed by washing every 5 minutes for 30 minutes before loading. The vessel was then loaded with MagFluo-4AM for 90 minutes, replacing the dye after 45 minutes. After successful loading, monitored by observation of changes in the fluorescence every 5 minutes, the dye was washed for a further 30 minutes before any recording and 10μM wortmannin was added to prevent tissue contraction and thus movement which subsequent data analysis (Hong & Chang, 1998). Wortmannin, preventing contraction by inhibiting myosin light chain kinase, was present throughout all subsequent measurements.

2.6 Electrophysiological recordings

2.6.1 Patch clamp set up and electrical recordings

Neher & Sakmann (1976) were the first to describe the patch clamp technique and its use in the study of ion channel distribution and characteristics. The technique was later refined by Hamill and coworkers in 1981. A successful patch clamp set up requires mechanical stability and shielding from electrical noise (Neher & Sakmann, 1976). The latter is achieved by shielding with a Faraday cage and connecting items capable of electrical conductivity to a ground point thus preventing current passage between parts of the set up. An anti-vibration table was used to mount the inverted microscope (Nikon, Japan), the recording chamber and the micromanipulator (Sutter Instruments,

UK). The micromaniopulator is used to control the movement of the patch pipette. The chamber for the cell suspension is sealed with a cover slip over the bottom, to facilitate a visual control over the approach of the pipette to the cell. Membrane currents were measured using an Axopatch 200B amplifier (Axon Instruments) and data acquisition was controlled by a personal computer using pClamp 6 software (Axon Instruments, Foster city, CA).

2.6.2 Pipette fabrication

Pipettes were fabricated from hard borosilicate glass capillaries (Sutter Instruments); internal diameter 0.86mm, external diameter 1.5mm. Thick glass wall capillaries were used to reduce electrical noise between the pipette and bath solutions via the glass. Pipettes were cut to size and the ends gently smoothed in a Bunsen flame to prevent damage to the electrode and the rubber seal in the pipette holder. A Narishige (Japan) PC-10 two stage pipette puller was used to pull the pipettes. To facilitate the formation of the gigaohm seal to the cell the pipette tips were fire polished by a hot platinum wire mounted on a Micro forge MF-830, Narishige (Japan) under observation, at a magnification of 45x. Patch pipettes were produced on the day of use and stored in a sealed container. Both the pipette and reference electrode were formed from silver wire (Ag) 0.25mm diameter coated with silver chloride, according to the reaction $Cl^- + Ag \leftrightarrow AgCl + e^-$ under a constant electrical current for ~10 minutes. Pipettes had a resistance of 4-6 MΩ when filled with the pipette solutions (for whole cell and perforated patch recordings). Pipette resistance was calculated from the following equation (Ohms Law) using a 10 mV step protocol: V=IR, where V = voltage in volts, I = current in amps, and R = pipette resistance in Ohms.). At the start of each experiment the liquid-junction potential between the two electrodes, caused by differences in the composition of the bath and pipette solutions, was compensated (Neher, 1992).

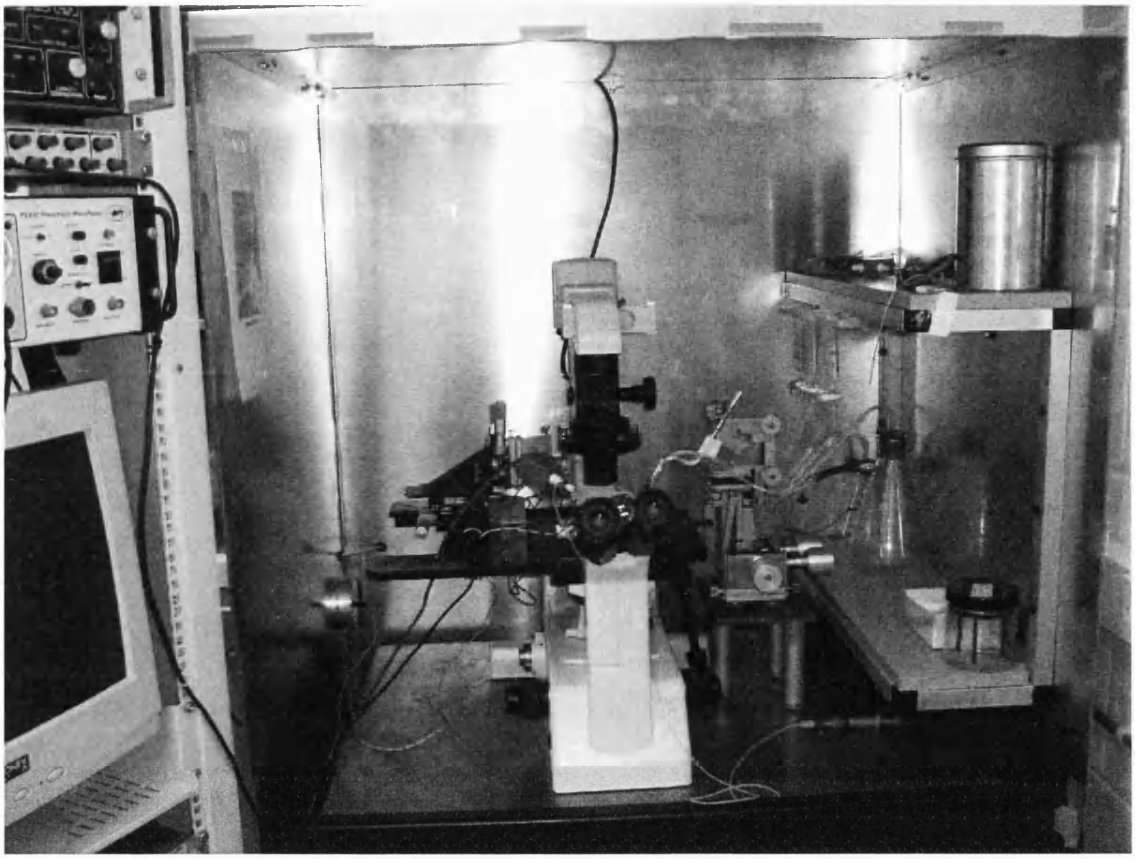

Figure 2.1. Photograph of the Patch clamp rig. On the right is a home made 6 barrel pipette perfusion system. Centre inverted microscope with head stage. On the left are the amplifier, digitizer and computer. All is surrounded by a faraday cage.

2.6.3 Whole cell recordings from VSMCs

Cells were placed in a chamber (100-200 µl) and left for 5 minutes to adhere to the glass cover. Throughout the experiment the cells were superfused (~1 ml/min) with either PSS or the test solutions via a 6 barrel pipette perfusion system. After breakthrough into the whole-cell mode cells were left to equilibrate with the pipette solution for 5 min preceding any recordings (Hille, 2001). Capacitance transients were routinely measured during this period in response to a 10mV hyperpolarising step (filtered at 10 kHz and sampled at 200 kHz). The area under the transient capacitance divided by 10mV (size of the depolarising step) was used to calculate the cell capacitance (C_m). The mean C_m recorded in different pipette solutions was similar and equal to: 12.3±0.36 pF (n=94, standard pipette solution); 11.6±0.5 pF (n=43, 1mM GSH); 11±0.45 pF (n=61, PP) and 13.4±1.3 pF (n=8, 5mM Mg^{2+}). The holding potential was -80mV unless otherwise stated. All electrophysiological experiments were performed at room temperature.

Whole cell voltage-gated K^+ channel currents (I_{Kv}) (sampled at 10 kHz and filtered at 2 kHz) were recorded using the standard patch-clamp technique using the protocols described in 2.6.4. Series resistance was measured to be: 11.8±0.42 mΩ (n=94, standard pipette solution); 13.3±0.65 mΩ (n=43, 1 mM GSH); 14.3±0.6 mΩ (n=61, PP) and 10.9±1.46 mΩ (n=8, 5 mM Mg^{2+}).

2.6.4 Electrophysiological stimulation protocols

To study and compare the voltage dependent characteristics of I_{Kv} under a variety of conditions and in different cell types, a set of standard voltage protocols were designed using PCLAMP 6 software, which are detailed below and will subsequently be referred back to in the text, avoiding unnecessary repetition.

2.6.4.1 Measurement of the I_{Kv} activation – I-V step protocol

The peak I_{Kv} amplitude and tail currents were recorded using a 200 ms step depolarisation applied from -100 mV to +50 mV in 10 mV increments every 10 s, followed by a 160 ms step to -20 mV (Fig 2.2 A). Due to inactivation of the current with time and in particularl at more positive potentials the peak I_{Kv} was measured from the onset of membrane depolarisation by fitting to a monoexponential function (indicated by the red line in Fig. 2.2 A).

[EQN 2.2] $f(t) = A \exp(-t/\tau) + C$

where f(t) is the current as a function of time (t), τ is the time constant of activation, A is a scaling factor and C is an asymptotic value used as evaluation of I_{Kv} peak. The ratio of the I_{Kv} peak measured at +50 mV in the presence and absence of inhibitors (I_{Kv} Block) was used to evaluate I_{Kv} inhibition (Smirnov *et al.*, 2002).

The current was leak-corrected, where $I_{(leak)}$ was calculated from the fit of the current measured in the negative range of -90mV to -50mV (where there was negligible activation of I_{Kv}), with a linear regression function to obtain the slope resistance (a) and intercept on the V_m axis (b) ([EQN 2.3]);

[EQN 2.3] $I_{(Leak)}(V_m) = aV_m+b$

The leak-subtracted current at each membrane potential was subsequently calculated ([EQN 2.4]);

[EQN 2.4] $I_{Kv}(V_m) = I'_{Kv}(V_m) - I_{(Leak)}(V_m)$,

and divided by C_m to derive current density. I'_{Kv} is the non-leak subtracted I_{Kv}

2.6.4.2 Measurement of the steady state activation: I_{Kv}–tail current protocol

Tail currents were measured at -20 mV following 200 ms depolarising steps between -100 and +50 mV. They were measured 2-3ms after the step to minimise contamination from capacitance transients. The amplitude of the tail current, corrected for the minimum tail current amplitude ($I_{(min)}$) measured between -60 and -100 mV ([EQN 2.5]), was normalised to its maximal value and plotted against V_m.

[EQN 2.5] $\text{Normalised } I_{Kv(tail)} = (I_{(tail)}-I_{(min)})/(I_{(max)}-I_{(min)})$

The instantaneous I-V relationship value that is thus derived is proportional to the number of channels open at each V_m. The resulting dependence was then fitted to the Boltzmann function.

[EQN 2.6] $$I_{norm} = \frac{1}{1+\exp((V_a - V_m)/k_a)}$$

where V_a is the half activation potential and k_a is the slope factor of activation.

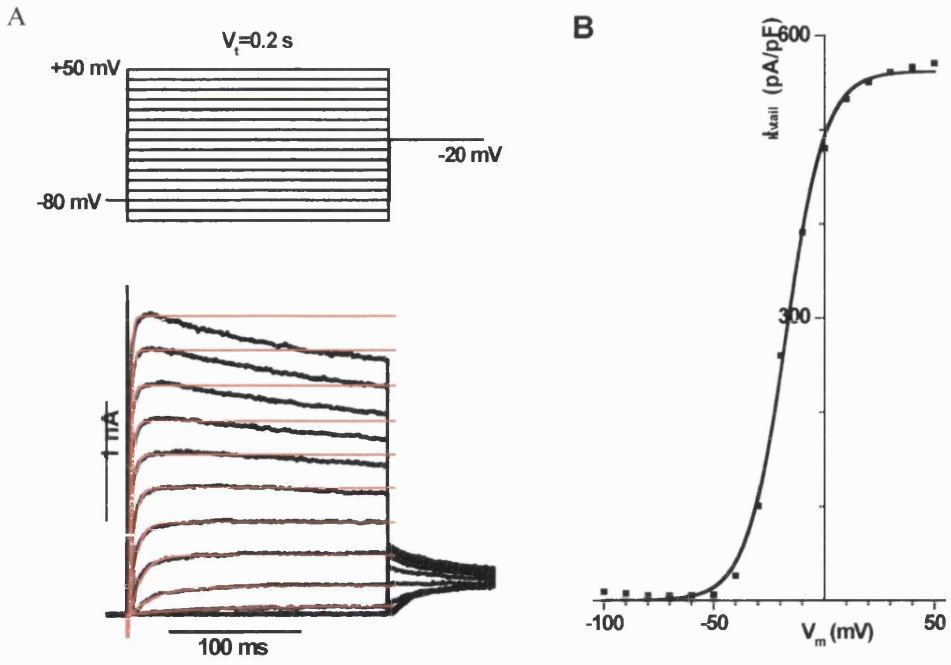

Figure 2.2. Measurements of I_{Kv} peak and I_{Kv} steady-state tail activation with tail current protocols. A; representative current traces recorded with the I-V protocol shown above in control conditions (C_m =14.6 pF). The red lines represent the monoexponential fit of the peak current ([EQN 2.2]). B; the dependence of the normalised I_{Kv} tail on V_m, recorded from the cell shown in A, fitted with the Boltzmann function ([EQN 2.6], solid line).

2.6.4.3 Measurement of I_{Kv} activation – Ramp protocol

In experiments described in chapter 7, I_{Kv} was recorded using 2s voltage ramp protocol between -100mV and +100mV from a holding potential of -80mV and applied every 20s. This protocol allows to rapidly record I-V relationships under various experimental conditions. To quantitatively analyse the changes in I_{Kv} activation the last 3 ramp episodes in any particular condition were averaged. A minimum of 5 traces were always recorded to establish a stable control for comparison.

The I_{Kv} was leak-corrected in the same manner as described for the I-V protocol in section 2.6.4.2. The I-V relationship was then fitted to the following equation ([EQN 2.7];

[EQN 2.7] $$g_{Kv}/G_{max} = \frac{1}{1+[\exp(V_m - V_a)/(-k_a)]},$$

Where G_{max}, V_a and k_a are the maximal whole-cell I_{Kv} conductance, the half-activation potential (where 50% of the channels are open) and the slope factor, respectively; and g_{Kv} is I_{Kv} conductance at each membrane potential (V_m) derived as a ratio of the peak I_{Kv} over the difference between the test V_m and the K^+ equilibrium potential ([EQN 2.8]).

[EQN 2.8] $$g = I_{Kv} / (V_m - E_k)$$

The E_k was calculated to be equal to -83 mV according to the Nernst equation ([EQN 2.9]);

[EQN 2.9] $$E_k = \frac{RT}{zF} \ln\left(\frac{[K^+_o]}{[K^+_i]}\right)$$

Where R = gas constant (1.987 cal mol^{-1} K^{-1}, T = room temperature in Kelvin, z = valance of ion, F = Faraday constant ($9.6485*10^4$ C mol^{-1}) and $[K^+]_o$ = extracellular K^+ concentration equal to 5 mM and $[K^+]_i$ = intracellular K^+ concentration equal to 140mM.

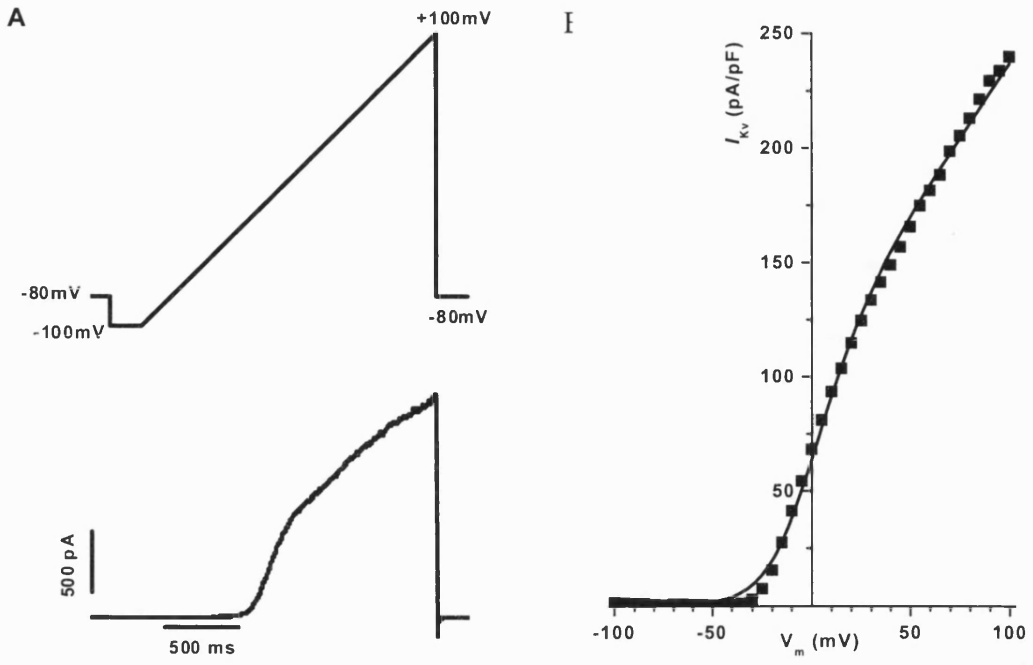

Fig. 2.3. The voltage ramp protocol. A; the voltage protocol with a representative trace below from a PASMC with C_m = 9.68 pF. B; the leak subtracted I-V relationship from -100mV to + 100mV for the representative cell shown in A fitted with the Boltzmann function (EQN 2.7], solid line). Note that the quality of fit was better at positive potentials than at negative V_m. A justification of this protocol and possible explanation of the differences between real data and the theoretical fit are given in chapter 7.

2.6.4.4 Measurement of steady state inactivation - Availability protocol

I_{Kv} inactivation was recorded using a two pulse protocol. A 200ms test pulse to +60mV was applied subsequent to a 10 s conditioning pre-pulse in 10 mV increments from -100mV to + 40mV, every 30s. The second pulse, to + 60mV, measures the degree of I_{Kv} inactivation. I_{Kv} measured at the end of the second pulse was normalised to its maximal value and fitted to the following equation [EQN 2.10].

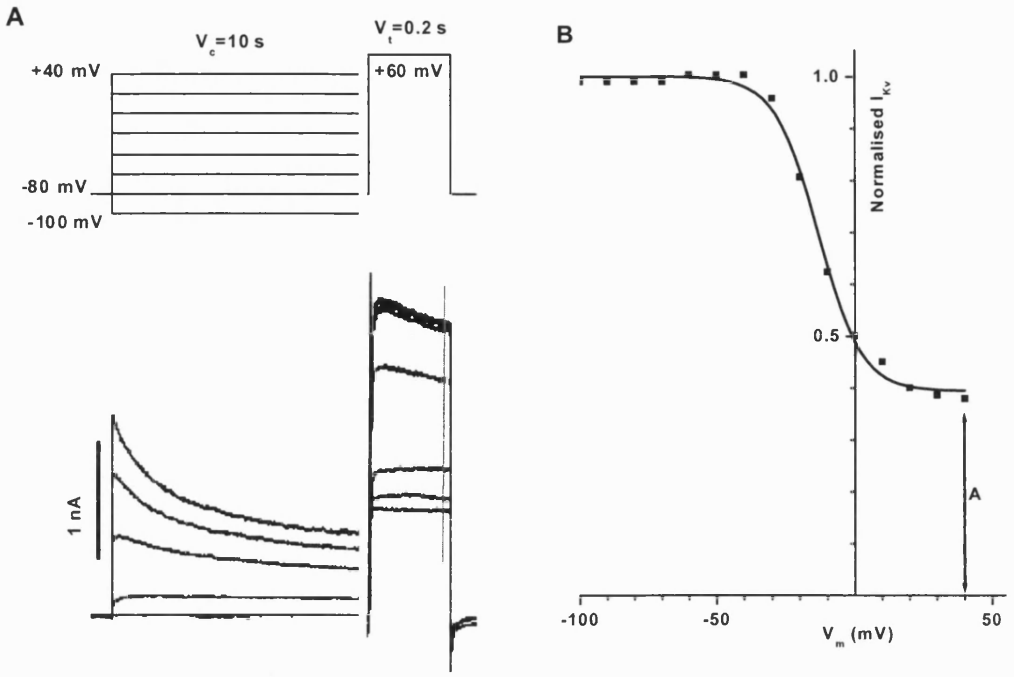

Fig. 2.4. Steady state I_{Kv} inactivation – availability protocol. (A); I_{Kv} traces recorded with the availability protocol in a representative PASMC, C_m = 8.67 pF. The solid line at the end of the pulse indicates where the inactivation was measured. (B); normalised steady state I_{Kv} inactivation dependence for the cell shown in A. The data at each potential was normalised to the average of the data between -80 and -100mV where there was minimal channel inactivation. A represents the non-inactivating component.

[EQN 2.10]
$$I_{norm} = \frac{1-A}{1+\exp((V_C - V_h)/k_h)} + A,$$

where V_h is the half-inactivation potential, k_h is the slope factor of inactivation and A is the non-inactivating component of the current.

2.6.4.5 Measurement of membrane potential – current clamp protocol

V_m was measured in the current-clamp mode acquired at 100 Hz for 300 s by applying a 4.5 ms pulse every 1s. The drug was applied for 300 s after a stable resting membrane potential was achieved (~ 60 s).

2.7 Comparison of the changes in I_{Kv} activation and inactivation

Only relative changes in the half-activation (V_a) and half-inactivation (V_h) potentials (calculated at the absolute V_a/V_h in test conditions minus absolute V_a/V_h in control conditions and defined as ΔV_a and ΔV_h respectively) were compared, to take into consideration individual variation in the I_{Kv} voltage-dependent parameters. Absolute values of V_a and V_h, as well as k_a, k_h and A, are given in the corresponding tables.

2.8 Variability in I_{Kv} Parameters

The relative changes in the voltage dependent characteristics of V_a, V_h, k_a, k_h and I_{Kv} block were compared in paired cells due to variability in the parameters. Variations in I_{Kv} parameters were observed in PASMCs either dialysed with the control pipette solution (whole-cell recording) or non-dialysed (perforated-patch recording). For example, the V_a ranged between -35 and +24 mV with a mean of -13.2±0.6 mV, n=184, in the whole-cell mode, and between -32 and +7 mV with a mean of -9.6±1 mV, n=63, in the perforated-patch configuration (Fig 2.5 A&B, respectively). Similar variations in V_h (whole-cell recording) were also seen (ranged between -47 and +2 mV with a mean of -23.7±1.1 mV, n=69). All the conditions are represented by a normalised distribution as indicated by the histogram analysis of V_a parameters (Fig 2.5 A&B). Analysis of the correlation between C_m, which is proportional to cell surface area, and the I_{Kv} amplitude at +50 mV and also between cell surface area and V_a (Fig. 2.5 C&D) showed no relationship between either C_m and $I_{Kv(50)}$ or V_a (the regression co-efficient, R, were equal to 0.095 and 0.155, respectively).

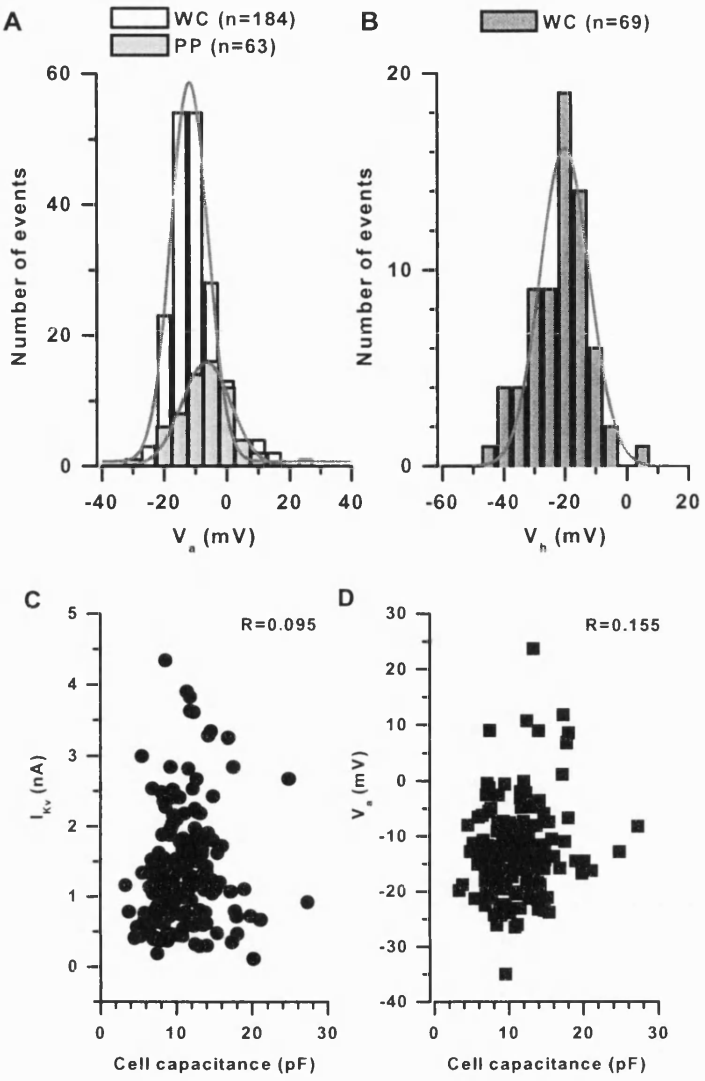

Figure 2.5. Normal distribution of I_{Kv} voltage-dependent parameters, V_a and V_h. (A) I_{Kv} was recorded in PASMCs either dialysed with the control pipette solution (WC) or in perforated-patch mode (PP) and bathed in PSS. Solid lines represent the Gaussian model fit with the mean V_a values of -12 (WC) and -7 mV (PP) (A) and V_h value of -20 mV (B). (C and D) Correlation between the cell membrane capacitance and I_{Kv} amplitude at +50 mV in pA (A) and V_a values (B) measured in the same cell (n=184) in the WC mode. R is the regression coefficient.

2.9 Data analysis, presentation and statistics

All data analysis, curve fitting and graphical representation of the results were performed using Clampfit 8.02 (Axon Instruments, Foster City, CA, USA) and Origin 6.0 (Microcal Software, Northampton, MA, USA) software. The data are presented as mean ± s.e.m (standard error of the mean). Statistical comparisons were performed using a paired(*) or non-paired(#) two-tail *t*-test with $^{*,\#}p<0.05$, $^{**,\#\#}p<0.01$, $^{***,\#\#\#}p<0.001$ and $^{****,\#\#\#\#}p<0.0001$ deemed significant unless stated otherwise. A paired *t*-test was used to compare the difference in parameters obtained in control (which could be either PSS or pre-treatment with another inhibitor) and test conditions in the same cell, whereas a non-paired t-test was used to compare differences between two groups of cells. Additionally when V_a or V_h were compared in control in the different intracellular solutions an ANOVA was used to assess the statistical difference between all the groups.

Chapter 3

INVOLVEMENT OF MITOCHONDRIAL DEPENDENT MECHANISMS IN THE REGULATION OF I_{KV}

To assess how I_{Kv} is regulated by mitochondrial dependent mechanisms this chapter investigates the interaction between Kv channels and mitochondria using changes in I_{Kv} activation, inactivation and I_{Kv} block as the indicators of Kv channel activity, and specific mitochondrial inhibitors to alter mitochondrial function under a variety of extracellular and intracellular conditions.

3.1 *Results*

3.1.1 Effect of mitochondrial uncoupling on I_{Kv}

The effect of mitochondrial uncoupling on I_{Kv} was investigated using 2 μM CCCP, a widely used mitochondrial uncoupler (Kadenbach, 2003; Kang *et al.*, 2002). Incubation of PASMCs with CCCP for 5 minutes caused a parallel leftward shift in both I_{Kv} activation (ΔV_a=-8.1±1.4 mV, n=20, p<0.00001) and inactivation (ΔV_h=-6.8±2.4 mV, n=12, p<0.018) dependencies (Fig. 3.1). A small, but consistent, I_{Kv} peak inhibition was also observed at positive voltages ($I_{Kv(50)}$ block = 22±4.8 %, n=20, p<0.006, Fig. 3.1 C). There was, however, no significant effect of CCCP upon the slope of the steady state activation or inactivation dependencies (Table 3.1). These results suggest that uncoupling of the mitochondria with CCCP, which should lead to a significant decrease in mitochondrial membrane potential ($\Delta\Psi_m$), caused significant effects on the properties of I_{Kv} in PASMCs.

Additionally, acceleration of the current decay was evident (observed in traces in Fig. 3.1 A&D), resulting in a significant reduction of the non-inactivating component of I_{Kv} from 0.32±0.05 (control) to 0.18±0.02 (CCCP) (n=12, p<0.001). Two processes could be possible for such acceleration 1) more channels become inactivated, 2) direct blocking effect of the drug on open channel. The data providing evidence for both possibilities, at least for some of the mitochondrial inhibitors, will be addressed later in this chapter.

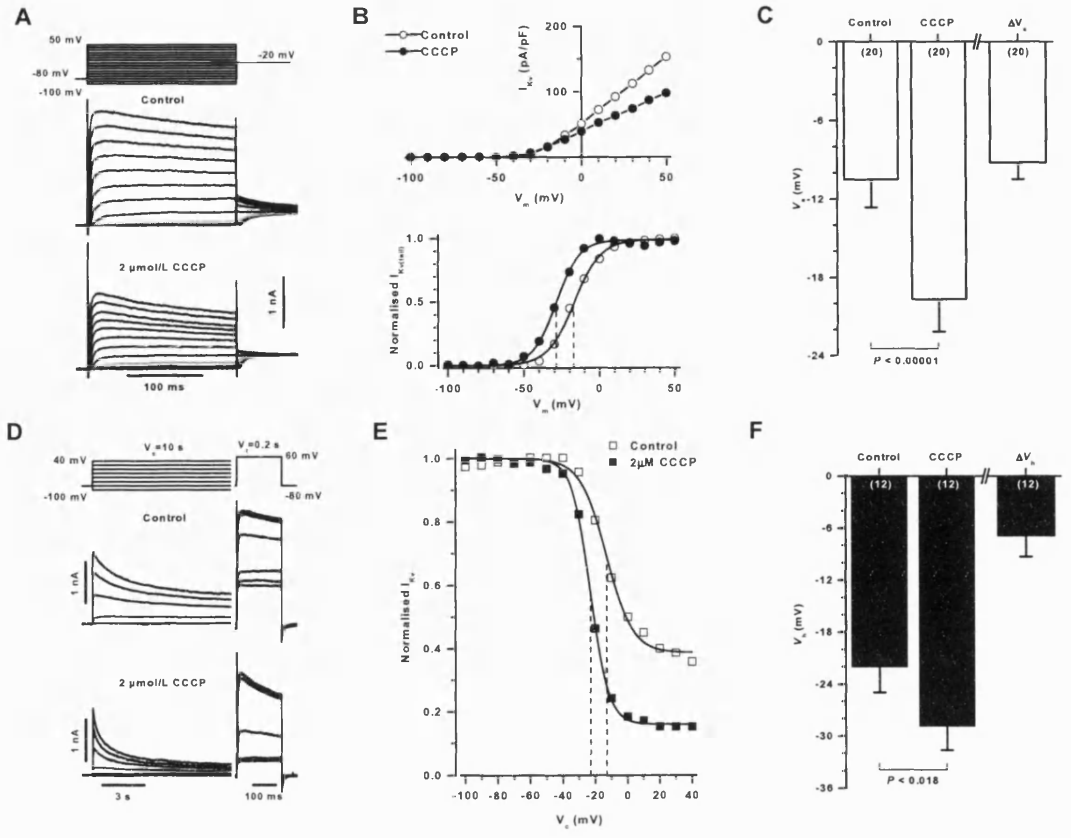

Figure 3.1. Effect of mitochondrial uncoupling with CCCP on I_{Kv} activation, inactivation and block. A-C, Modulation of I_{Kv} activation. (A) Voltage protocol and original current traces recorded from a representative PASMC 5 min after pre-incubation with the mitochondrial uncoupler CCCP (2 µM). Traces in grey in A correspond to a V_m = -30mV. (B) Comparison of CCCP-induced changes in the peak I_{Kv} measured from a single exponential fit of the current activation at each V_m, and normalised tail currents (upper and lower panel respectively). (C) The mean absolute (V_a) and relative (ΔV_a) changes in I_{Kv} activation. D-F, Effect on I_{Kv} inactivation. (D) Current traces recorded with the availability protocol (shown at the top of the panel) in the absence and presence of CCCP from a representative PASMC. (E) CCCP-induced changes in the normalised I_{Kv} measured with the availability protocol. (F) Compares the mean absolute (V_h) and relative (ΔV_h) changes in I_{Kv} inactivation. A and D were obtained from different cells with C_m=14.6 and 8.7 pF, respectively. Lines in B were drawn with V_a=-17 and -28.9 mV (dashed lines) and k_a=8.9 and 7.7 mV, for control and CCCP respectively. Lines in E were drawn with V_h=-12.9 and -22.9 mV (dashed lines) and k_h=8.1 and 5.7 mV and the non-inactivating component equal to 0.39 and 0.16 in control and CCCP-containing solutions respectively.

3.1.2 Role of the mETC in I_{Kv} modulation

Since the mitochondrial membrane potential ($\Delta\Psi_m$) is maintained by the mETC, a putative involvement of individual mETC complexes in the mitochondrial dependent modulation of I_{Kv} was further investigated with widely used mETC inhibitors: rotenone (inhibiting at complex I), myxothiazol and antimycin (inhibiting at complex III) (all at 1 μM) and NaCN (inhibiting at complex IV, 1 mM).

Figure 3.2 summarises the effects of mETC inhibitors on ΔV_a, ΔV_h and I_{Kv} block. A significant negative shift in the I_{Kv} activation and increased I_{Kv} block was observed with all mETC inhibitors (Table 3.1), mimicking those caused by CCCP. Interestingly, a noticeable larger shift in I_{Kv} activation and block was observed with distal mETC inhibitors (antimycin and cyanide) in comparison to the proximal inhibitors (rotenone, and myxothiazol) with the effects caused by antimycin were most pronounced ($I_{Kv(50)}$ block = 39.6±8.8, ΔV_a = -13.6±2 mV, n=9, p<0.011) (Fig. 3.2 A-C). A significant decrease in I_{Kv} block for antimycin was observed at all potentials from 10 to 50 mV (Fig. 3.2 D). It is also worth noting that the slope of the steady-state activation dependencies was significantly increased in the presence of myxothiazol and antimycin (acting at complex III, Table 3.1). Similar to I_{Kv} activation, all mETC inhibitors, except myxothiazol, induced significant changes in $\Delta V_{h,}$, again antimycin had the most pronounced effects (ΔV_h = -15.6±2.1 mV, n=8, p<0.0002). Furthermore, antimycin, 12.6±0.8 to 8±0.8 p<0.006, and rotenone, 11.8±1.2 to 8.6±1.1 p<0.0024, increased the slope of the steady state I_{Kv} inactivation dependencies (Table 3.1). It is also worth noting that there was a substantial decrease in the non-inactivating component for all inhibitors, with all but rotenone being significant; for antimycin this was decreased from 0.31±0.03 to 0.08±0.02, p<0.0005, n=8. Therefore, for characterisation of the mechanisms involved in the interaction between mitochondria and I_{Kv}, antimycin was chosen as the main modulatory agent of mitochondrial function.

It is noteworthy that changes in the $I_{Kv(50)}$ block under different conditions were similar to those calculated for the maximal whole-cell conductance determined from the conductance-voltage relationships (for example; antimycin 47.6±5.9 %, n=9, rotenone 44.7±9.9 %, n=6 and myxothiazol 56.7±4.9 %, n=7, in comparison to $I_{Kv(50)}$ in Table 3.1).

TABLE 3. 1. Effect of CCCP and mitochondrial ETC inhibitors on voltage-dependent parameters of I_{Kv}.

	Steady-state I_{Kv} activation and $I_{Kv(50)}$ block					**I_{Kv} inactivation**				
	V_a (mV)	k_a (mV)	ΔV_a (mV)	$I_{Kv(50)}$ *block* (%)	*n*	V_h (mV)	k_h (mV)	*A*	ΔV_h (mV)	*n*
PSS	-12.9±1.5	9.9±0.7				-21.9±3	11.6±0.8	0.32±0.05		
CCCP (2 μM)	-21±2 (p<0.00005)	10±1	-8.1±1.4	22±4.8 (p<0.006)	20	-28.8±2.8 (p<0.018)	9.8±0.8	0.18±0.02 (p<0.0008)	-6.8±2.4	12
PSS	-15.4±1.5	8.3±0.4				-29.6±1.7	11.8±1.2	0.32±0.03		
Rotenone (1 μM)	-20.4±1.9 (p<0.00003)	8.7±0.7	-5±0.8	10.3±10.3 (p<0.039)	21	-34.8±2.3 (p<0.04)	8.6±1.1 (p<0.024)	0.23±0.03	-5.1±1.9	7
PSS	-16.5±0.9	9.2±1.3				-24.4±1.9	10.5±1.3	0.28±0.03		
Myxothiazol (1 μM)	-22.7±1.2 (p<0.00001)	7.9±0.4 (p<0.031)	-6.1±0.7	10.6±3.9 (p<0.034)	10	-26.7±1.7	9.1±0.9	0.15±0.02 (p<0.014)	-2.2±2.4	6
PSS	-10.6±1.1	11.3±1				-16.1±1.7	12.6±0.8	0.31±0.03		
Antimycin (1 μM)	-24.2±1.9 (p<0.0002)	8.2±0.7 (p<0.026)	-13.6±2	39.6±8.8 (p<0.011)	9	-32±2.6 (p<0.0002)	8±0.8 (p<0.006)	0.08±0.02 (p<0.0005)	-15.6±2.1	8
PSS	-17.4±1.9	8.4±0.5				-30.5±1.4	10.2±1	0.25±0.01		
NaCN (1 mM)	-28.5±1.2 (p<0.00008)	8.7±0.6	-11.1±1.9	23.8±9.5 (p<0.01)	14	-37.7±2.2 (p<0.023)	9.9±1	0.14±0.02 (p<0.0002)	-7.2±2.6	10

Here and in subsequent Tables p values show significant differences between the values measured in control conditions and in the presence of the tested inhibitor obtained in the same PASMCs (paired two-tail t-test) unless indicated otherwise.

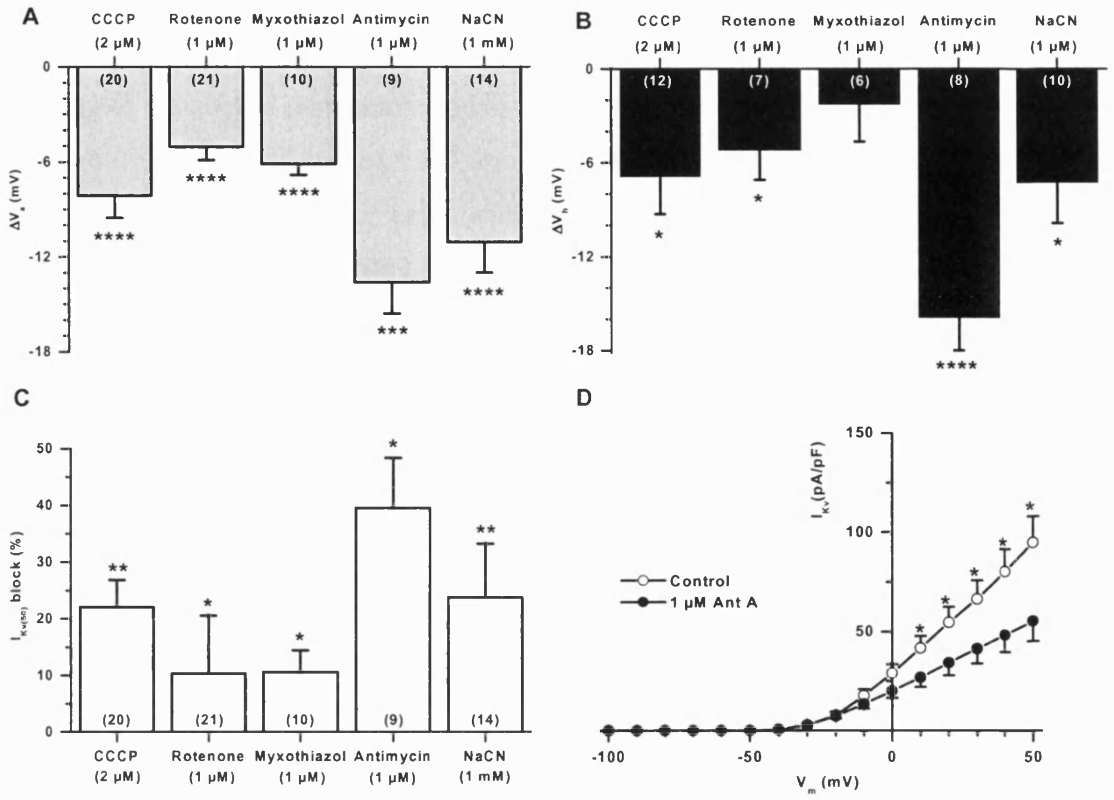

Figure 3.2. Effect of the mETC inhibition on the I_{Kv} characteristics: activation (A), inactivation (B) and $I_{Kv(50)}$ block (C). (D) Comparison of antimycin-induced changes in the peak I_{Kv} measured from a single exponential fit of the current activation at each potential.

3.1.3 Specificity of the I_{Kv} modulation to the mETC

One common feature for antimycin and the other mitochondrial inhibitors is their modulation of $\Delta\Psi_m$ by reducing the proton gradient across the inner mitochondrial membrane. If the inhibitors are specifically targeting the mETC, and therefore $\Delta\Psi_m$ then, using antimycin as the test inhibitor, it would be expected that the antimycin-induced effects should be attenuated either: 1) in the presence of CCCP (by collapsing $\Delta\Psi_m$), and 2) after pre-treatment with the proximal mETC inhibitors, such as rotenone or myxothiazol (by reducing electron flow proximally to the mETC complex III). It could also be expected that enhancing the drive of the mETC, by increasing electron flow to distal regions with Complex II substrate succinate would augment the effects of

antimycin. All of these conditions were investigated. Cells were pre-incubated for 5 minutes in CCCP or a proximal inhibitor (rotenone or myxothiazol) prior to any recording of the control parameters and antimycin was then added in addition to the pre-incubated drug and equilibrated for 5 minutes before recording the test I_{Kv} parameters. Succinate was dialysed into cells and again equilibrated for 5 minutes before commencing recording using the I_{Kv} protocols.

Although pre-incubation of PASMCs with CCCP did not alter the antimycin-mediated I_{Kv} inhibition (44.4±7.1 %, n=8, $p<0.007$) (Fig 3.3 B), the antimycin-induced shift in both I_{Kv} activation (from -13.6±2 mV, n=9 to -3.1±1 mV, n=8 ($p<0.0004$)) and inactivation dependencies (from -15.6±2.1 mV, n=9 to -2.7±1.9 mV, n=10 ($p<0.005$)) were significantly reduced (Fig. 3.3 A). Additionally, antimycin caused an increase, instead of decrease, in the slope of I_{Kv} activation following pre-treatment with CCCP (Table 3.2). Conversely, despite the complete inhibition of ΔV_h (from -15.6±2.1 mV to -2.7±1.0 mV, $p<0.005$) (Fig. 3.3 A), the non-inactivating component of I_{Kv} was still significantly reduced by antimycin, indicating a possible direct open channel block during the prolonged membrane depolarisation. The antimycin-mediated increase in the slope of I_{Kv} inactivation from 11.8±1.2 mV to 8.8±1.1 mV ($p<0.0007$) is also consistent with this concept (Table 3.2). Similarly to antimycin, CCCP also attenuated, but not significantly, the effect of inhibition of complex I by rotenone on I_{Kv} activation. In contrast to antimycin the effect of rotenone on I_{Kv} inactivation was not affected by CCCP (Fig. 3.3 D).

Similar to CCCP, cell pre-treatment with myxothiazol and rotenone, significantly attenuated the antimycin-induced changes in I_{Kv} activation and inactivation (Fig. 3.3 C). Consequently, no significant changes in k_a were found in the presence of both proximal inhibitors (Table 3.3). It is noteworthy that, although it was not possible to record I_{Kv} availability in the presence of antimycin with myxothiazol or rotenone since prolonged exposure to both inhibitors often caused cell blebbing and deterioration, the absolute value of V_h obtained in myxothiazol and antimycin (-32.1±3.6 mV, n=6) was comparable to that measured in antimycin alone (-32±2.6 mV, n=8), suggesting that the effects of these agents on ΔV_h were also not additive. Significant potentiation of the antimycin-induced $I_{Kv(50)}$ block was observed with myxothiazol, but not with rotenone (Fig. 3.3 C).

TABLE 3.2. Effect of the cell pre-treatment with the mitochondrial uncoupler CCCP (2 μM) on antimycin (1 μM) induced changes of I_{Kv} characteristics.

	Steady-state $I_{Kv\ activation}$ and $I_{Kv(50)}$ block					**I_{Kv} inactivation**				
	V_a (mV)	k_a (mV)	ΔV_a (mV)	$I_{Kv(50)}$ *block* (%)	*n*	V_h (mV)	k_h (mV)	*A*	ΔV_h (mV)	*n*
CCCP	-19.4±1.4	10.5±1.1				-27.8±3.6	11.8±1.2	0.21±0.03		
Antimycin	-22.5±1.5	12.1±1.4	-3.1±1	44.4±7.1	8	-30.5±4.2	8.8±1.1	0.1±0.02	-2.7±1.9	10
+ CCCP	(p<0.015)	(p<0.03)[b]	(p<0.0004)[a]	(p<0.007)			(p<0.0007)		(p<0.005)[a]	
CCCP	-22.3±3.1	10.3±1.5				-28.4±3	9.5±0.6	0.19±0.03		
Rotenone	-24.5±2.9	12.2±1.4	-2.2±1.9	25..9±3.7	11	-33.7±2.5	7.6±0.6	0.16±0.01	-5.3±1.2	11
+ CCCP		(p<0.04)		(p<0.008)		(p<0.002)	(p<0.02)			

[a] Compares the mean values obtained in this condition and those measured in the presence of antimycin A alone (Table 3.1) (non-paired two-tail *t*-test). Cells were incubated with CCCP for 5 min prior to commencing recordings.
[b] Denotes significant differences only with the one-tail *t*-test.

TABLE 3.3. Effect of the proximal mETC inhibitors rotenone and myxothiazol on the effects of the distal ETC inhibitor antimycin (all at 1 μM).

Steady-state I_{Kv} activation and $I_{Kv(50)}$ block					
	V_a (mV)	k_a (mV)	ΔV_a (mV)	$I_{Kv(50)}$ *block* (%)	*n*
Rotenone	-16.9±3.5	7.9±0.6			
Antimycin + Rotenone	-21.3±4.6 ($p<0.05$)	7.8±1.2	-4.5±1.9 ($p<0.005$)[a]	39.8±8.2 ($p<0.005$)	8
Myxothiazol	-20.6±1.3	7.9±0.4			
Antimycin + Myxothiazol	-24.9±1.1 ($p<0.002$)	8.2±0.6	-4.3±0.8 ($p<0.002$)[a]	60.3±4.5 ($p<0.005$) ($p<0.039$)[a,b]	7

[a] Compares the mean values obtained in these conditions and those measured in the presence of antimycin alone (Table 3.1) (non-paired two-tail *t*-test). Cells were incubated with rotenone or myxothiazol for 5 min before I_{Kv} characteristics were recorded.
[b] Denotes a significant difference only with the one-tail *t*-test.

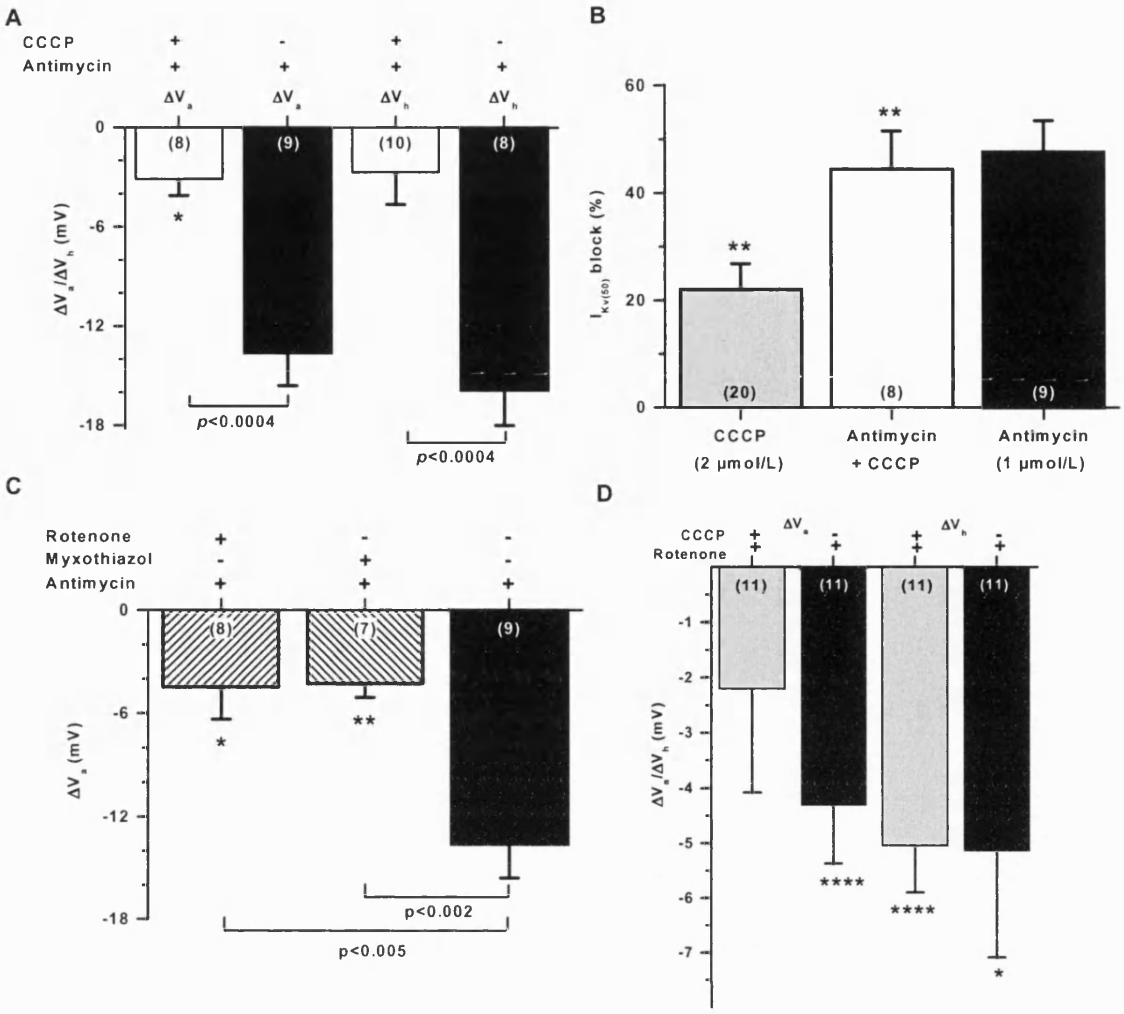

Figure 3.3. Specificity of the antimycin-induced effects on the mETC. A, Effect of the mitochondria uncoupler CCCP (2 μM) on antimycin-induced changes in I_{Kv} activation and inactivation. B-C, Effect of the proximal mETC inhibitors rotenone and myxothiazol (all at 1 μM) on the antimycin-induced changes in I_{Kv} activation (B) and block (C). (D) Effect of CCCP on rotenone-inducted changes in I_{Kv} activation and inactivation. Black bars on the right of each panel show the effect of antimycin or rotenone, respectively, alone for comparison. Cells were pre-incubated with each drug for at least 5 min before recording I_{Kv}.

If the effects of rotenone are specific to the mETC, increased supply of substrate to mETC via complex II would be expected to block rotenone dependent changes in I_{Kv}. It has previously been shown that rotenone and antimycin have direct actions on ion

channels including Kv channels (Lopez-Barneo *et al.,* 2001; Mason *et al.,* 2004). Dialysing cells with a Na succinate containing pipette solution (Table 2.3) an exogenous substrate for the mETC complex II, could enhance transfer of electrons from $FADH_2$ (reduced ubiquinone) to FAD^+ (oxidised ubiquinol) to the Reiske Fe-S protein in complex III. The changes in ΔV_a and ΔV_h induced by rotenone remained unaltered (Fig 3.4).

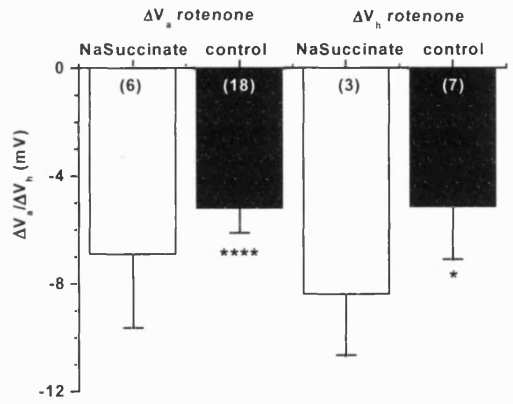

Figure 3.4. Effects of cell dialysis with 5 mM Na succinate (Table 2.3) on rotenone-induced changes in I_{Kv} activation and inactivation. Black bars on the right of each panel show the effect of rotenone alone for comparison. Cells were pre-incubated with each drug for at least 5 min before recording I_{Kv}.

3.1.4 Effect of mETC inhibition on membrane potential.

Antimycin caused a reversible membrane depolarisation in PASMCs (ΔV_m = 31.2±10.3 mV, n=2). CCCP also caused a small, but significant and reversible, depolarisation (ΔV_m = 4.7±1.5, n=5, $p<0.05$) in dialysed cells. It was interesting to note that when the cell was more depolarised the effect of CCCP was much more substantial, this is particularly evident in the representative trace in Fig. 3.5 D, after the second application of CCCP. In this cell, when RMP was on average -39 mV, CCCP caused a 4.6 mV depolarisation and, subsequent to the first application when RMP had changed to -33 mV, the effect of CCCP was much more substantial with a 29 mV depolarisation. This was similar to the depolarisations in response to antimycin (Fig. 3.5 A).

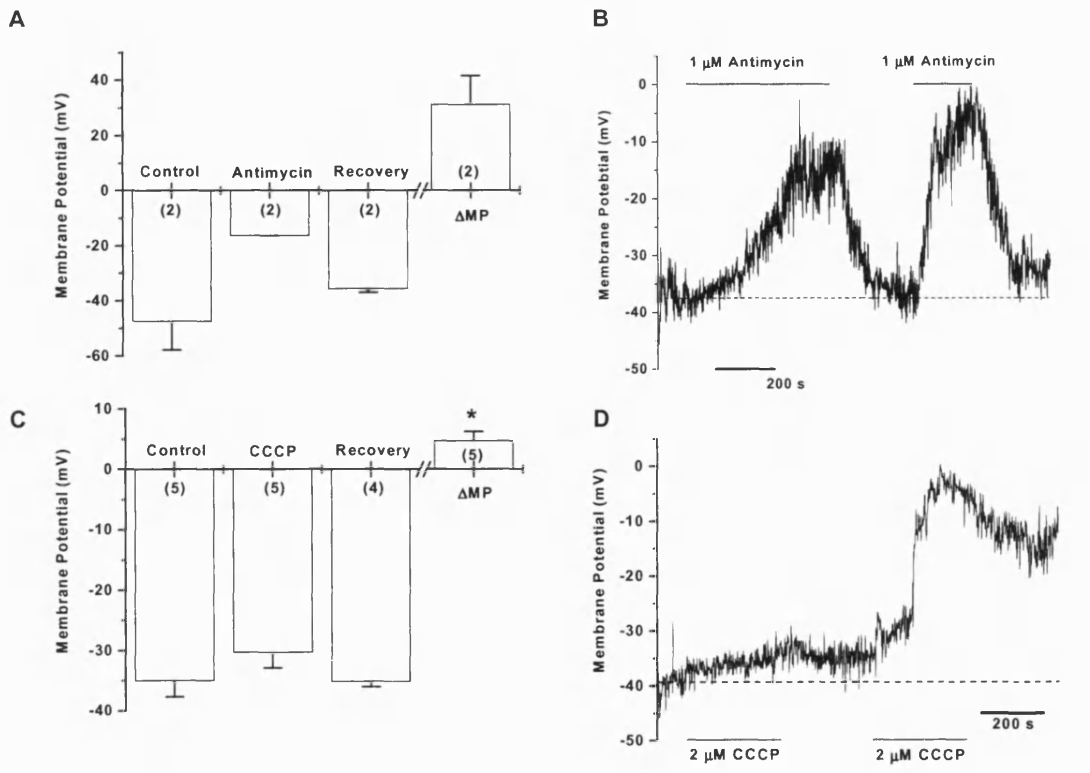

Figure 3.5. Effect of antimycin and CCCP on PASMC membrane potential. (A-B) Depolarisation and recovery after perfusion with antimycin in WC configuration (change in membrane potential, ΔV_m). (C-D) Depolarisation induced by CCCP in WC. (B and D) Representative traces from separate cells showing the effects of antimycin (C_m = 12.3 pF) and CCCP (C_m = 10 pF), respectively. The dashed lines in B and D indicate average resting membrane potential in that cell.

3.1.5 Effect of mETC on I_{Kv} activation in intact PASMCs

To address a potential influence of cell dialysis on I_{Kv} activation the WC mode patch clamp was compared to non-dialysed cells using the perforated patch clamp (Table 2.3) in PASMCs. The effects of the mETC inhibitors in whole cell mode were mimicked by antimycin, but not rotenone, in intact cells causing a significant leftward shift in I_{Kv} activation (Fig. 3.4). Notably, the antimycin-induced shift in V_a measured in the perforated-patch mode was significantly smaller than that recorded in the whole-cell configuration (ΔV_a = -4.6±1.6 mV, n=8 in perforated patch compared to -13.6±2 mV, n=9 in whole cell configuration, p<0.004), suggesting a possible presence of an additional factor(s) or influence of other process's that are altered by or lost during cell

dialysis. No significant effect on I_{Kv} amplitude was observed for rotenone, though with antimycin a significant, 30.2±11.2 % I_{Kv} block was evident (Table 3.5). No notable changes in the slope of I_{Kv} activation were recorded (Table 3.5). The significant leftward shift in ΔV_h still occurred shifting the dependence by -8±1.6 mV (n=7, p<0.003). It is also worth noting that the non-inactivating component is still significantly decreased from 0.28±0.05 mV to 0.11±0.03 mV (n=7, p<0.036). However, the antimycin induced increase in the steady state inactivation dependencies in whole cell mode did not occur in the intact cells.

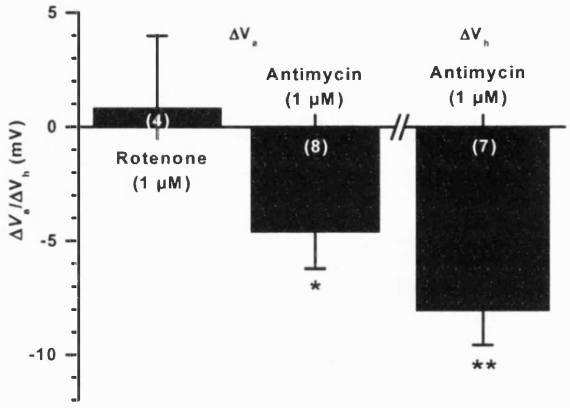

Figure 3.6. Effect of mETC inhibition in intact PASMCs. Comparison of the effect of rotenone (complex I) on I_{Kv} activation and antimycin (distally in complex III) on I_{Kv} activation and inactivation in non-dialysed PASMCs. All experiments were performed in the perforated-patch mode using 100 μg/ml amphotericin B (Table 2.3).

TABLE 3.4. Effect of mETC inhibitors and ROS on I_{Kv} activation recorded in perforated-patch mode.

	Steady-state I_{Kv} activation and $I_{Kv(50)}$ block				
	V_a (mV)	k_a (mV)	ΔV_a (mV)	$I_{Kv(50)}$ *block* (%)	*n*
PSS (all controls)	-9.6±1 (p<0.002)[a]	8.3±0.4	-	-	63
PSS	-13.3±4.6	7.5±0.8			
Rotenone	-12.5±2.3	9.2±1.3	0.8±3.2	16.3±19.3	4
PSS	-15.2±2.2	7.9±0.9	-4.6±1.6	30.2±11.2	
Antimycin	-19.7±2.1 (p<0.027)	7±0.5	(p<0.004)[b]	(p<0.035)[c]	8
PSS	-7.1±2.7	11.5±1.2			
Oligomycin	-9.1±2.3	11.6±1.1	-2±1.6	6.3±9.9	8
PSS	-17.5±3.1	8.4±0.5			
H_2O_2	-17.7±3.2	9.1±0.7	-0.2±0.7	2.2±16.5	6
PSS	-8.7±1.6	8.5±1			
Menadione (10 μM)	-8.1±1.6	8.2±1.6	0.6±0.9	8±9.3	6
PSS	-7.1±2.6	9.8±1.5			
Menadione (100 μM)	-1.6±1.2	10.2±0.6	5.5±2.6	23.1±17.7	4

Concentration of rotenone, antimycin and oligomycin was 1 μM, concentration of H_2O_2 was 300 μM.
[a] Compares the mean values between perforated-patch and control (In: 0.5 mM $MgCl_2$) whole-cell modes (Table 3.5) (non-paired *t*-test).
[b] Compares the mean values obtained in these conditions and those measured in the presence of antimycin and oligomycin alone (Tables 1 and 5 respectively) (non-paired *t*-test). [c] Denotes a significant difference only with paired one-tail *t*-test.

3.1.6 Dependence of I_{Kv} on intracellular redox state

The results presented so far strongly support a specific mitochondria-mediated action of antimycin on I_{Kv} in PASMCs. One of the possible contributing mechanisms could be associated changes in cellular redox state (Archer *et al.*, 1993; Waypa *et al.*, 2001). Indeed, inhibition of the mETC could alter Δp and thus change $\Delta\Psi_m$ and, as the rate of ROS production is highly influence by both Δp and $\Delta\Psi_m$ (Demin *et al.*, 1998), it is necessary to assess the involvement of ROS in the mitochondria-dependent regulation of I_{Kv}. Therefore, the consequences of changing cellular redox state on I_{Kv} were studied in cells pre-incubated for 5 mins in 300 μM H_2O_2, applied in the extracellular solution, or cells dialysed for 5 mins with reduced glutathione (GSH, 1 mM in the pipette) to either decrease or increase cellular redox state, respectively. The effects of redox modulation by 300 μM H_2O_2 and 1 mM GSH on the shifts in V_a and V_h induced by antimycin were investigated in PASMCs. In addition, the effects of H_2O_2 and the cell permeable activator of SO^-, menadione, were assessed in intact PASMCs.

In dialysed PASMCs, 300 μM H_2O_2 alone caused a small, but consistent, decrease in the $I_{Kv(50)}$ peak (9.5±4.2 %, n=28, $p<0.0008$; Fig. 3.7 A) and a significant leftward shift in I_{Kv} activation (-5.1±1.3 mV, $p<0.0007$; Fig. 3.7 B), thus mimicking the effect of the mETC inhibitors (Fig. 3.5). Although a small difference was also observed in ΔV_h, the effect was not significant (Fig. 3.7 B). As expected, in cells dialysed with 1 mM GSH (5 min dialysis in GSH to enable equilibration prior to any recording), the H_2O_2-induced changes in ΔV_a were virtually eliminated (Fig. 3.7 C) and, although not significantly different from the effects of H_2O_2 alone, caused a small reversal of the shift in V_h to +4.5± 3.6 mV, n=7 ($p<0.041$, one tailed *t*-test).

It is worth noting that cell dialysis with 1 mM GSH alone had a significant effect upon I_{Kv} activation (V_a = -15.2±0.7 mV (GSH) and -13.1±0.6 mV (control), $p<0.03$), resembling the shifts observed with the oxidant H_2O_2. There were, however, no effects in cells dialysed with GSH alone upon inactivation (Table 3.5). Notably, both parameters (V_a and V_h) measured in PASMCs were normally distributed (Fig. 3.8 A&B), similarly to those measured under control conditions, supporting the previously made statement of a relatively homogenous population of I_{Kv} in resistance PASMCs.

In agreement with the effects of H_2O_2 on I_{Kv} activation, 300 μM H_2O_2 had no effect upon membrane potential in both dialysed (ΔV_m = -1.6±1.5 mV, n=7) (Fig. 3.9) and non-dialysed cells (ΔV_m = -2.4, n=1 (data not shown)).

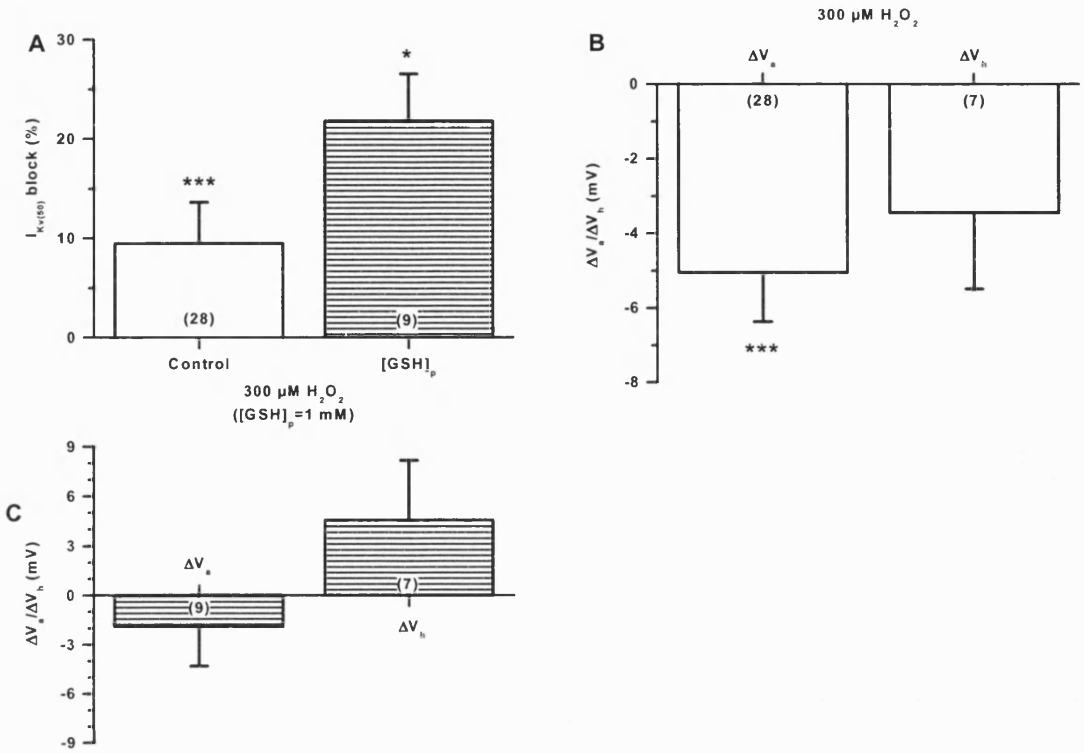

Figure 3.7. Effect of cellular redox state on I_{Kv} activation and inactivation. Effect of 300 μM H_2O_2 on I_{Kv} characteristics in PASMCs dialysed with the control solution (A & B) or with 1 mM GSH added to the pipette solution ($[GSH]_p$) (A & C).

TABLE 3.5 Effect of various intracellular (pipette) solutions on voltage-dependence of I_{Kv} activation and inactivation in PSS in the absence of any inhibitors

Pipette solutions	Steady-state I_{Kv} activation			I_{Kv} inactivation			
	V_a (mV)	k_a (mV)	n	V_h (mV)	k_h (mV)	A	n
$[MgCl_2]_p$=0.5 mM (Control)	-13.2±0.6	10.6±0.3	184	-23.7±1.1	11.5±0.4	0.28±0.01	69
$[GSH]_p$=1 mM	-15.4±0.7 (p<0.018)	9.5±0.3 (p<0.011)	90	-23.7±1	8.5±1 (p<0.006)	0.24±0.01 (p<0.019)	67
$[Na_2ATP]_p$=5 mM	-8.1±1 (p<0.004)	8.9±0.5 (p<0.032)	22	-10.6±1.9 (p<0.00001)	11.5±0.9	0.4±0.02 (p<0.00003)	20
$[MgATP]_p$=5 mM	-14.8±1.4	9.5±1	9	-19.7±1.5	10.4±0.6	0.34±0.02	9
$[EDTA]_p$=5 mM	-9.6±1.2 (p<0.005)	9±0.5	21	-15.3±2 (p<0.009)	13.9±1.2 (p<0.047)	0.29±0.02	10
$[MgCl_2]_p$=5 mM	-14.1±1.8	10.6±0.7	24	-30.7±2.8 (p<0.02)	10.5±0.5	0.21±0.02 (p<0.035)	12

Statistical comparison was performed using all pooled data for the I_{Kv} recorded in PASMCs bathed in PSS and dialysed with a specified pipette solution (one way ANOVA).

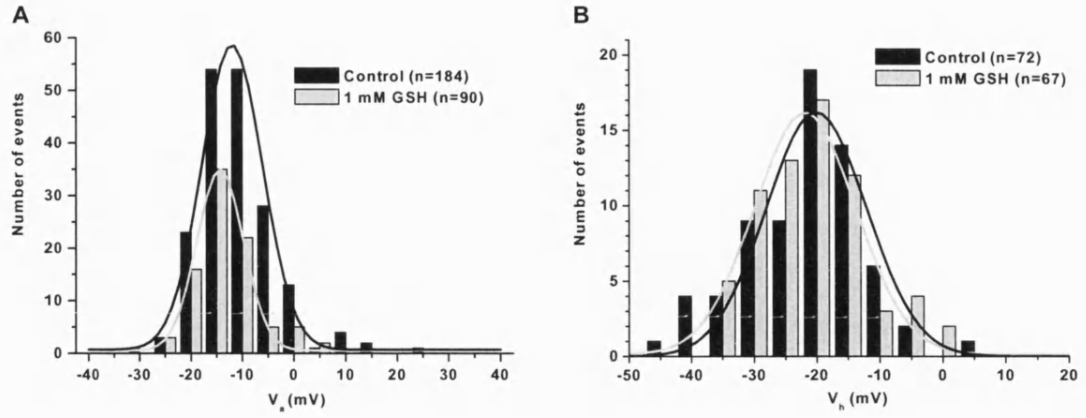

Figure 3.8. Comparison of the distribution of I_{Kv} voltage-dependent parameters, V_a (A) and V_h (B) in cells dialysed with control and 1 mM GSH containing pipette solutions. I_{Kv} was recorded in PASMCs either dialysed with either the control pipette solution or pipette solution containing 1 mM GSH and bathed in PSS containing paxilline and glybenclamide. Solid lines represent the Gaussian model fit with mean V_a values of -12 mV (control) and -14 mV (GSH) (A) and mean V_h values of -20 mV (control) and -22 mV (GSH) (B).

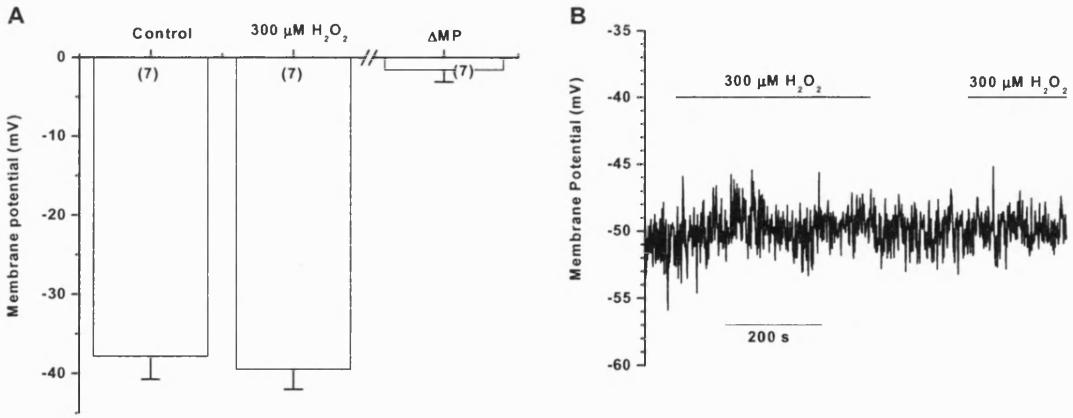

Figure 3.9. Effect of 300 µM H_2O_2 on membrane potential. (A) Change in membrane potential (ΔV_m) induced by H_2O_2 in whole cell patch clamp mode. (B) A representative recording from a cell with C_m = 12.6 pF.

3.1.7 Effects of cellular redox state on antimycin induced changes in I_{Kv}

Antimycin-mediated changes in I_{Kv} activation and inactivation were not significantly affected by pre incubation of cells in 300 μM H_2O_2 (Fig. 3.10 A&B). Interestingly, similar to data where cells were preincubated in myxothiazol (Fig. 3.3), the antimycin-induced I_{Kv} block was also enhanced by H_2O_2 from 39.6±8.8 % (n=9) to 64.6±6.8 %, n=8, $p<0.05$ (Fig. 3.10 C). Conversely, cell dialysis with GSH caused a significant decrease in the antimycin-dependent changes in V_a from -13.6±2 mV, n=9 (antimycin alone), to -4±1.8 mV, n=15, $p<0.003$ (antimycin in the presence of GSH), and V_h from -15.6±2.1 mV, n=9 (antimycin alone) to -8.7±2.5 mV, n=14, $p<0.033$ (antimycin in the presence of GSH) (Fig. 3.10 B&C) without affecting the $I_{Kv(50)}$ block (Fig. 3.10 A). This data suggests a potential link between the antimycin-dependent modulation of the voltage-dependent characteristics of I_{Kv} (activation in particular) and intracellular redox state. The lack of an inhibitory effect of H_2O_2 on the antimycin-induced $I_{Kv(50)}$ block might suggest that Kv channels are already oxidized (as proposed by Archer *et al.*, 1993; Michelakis *et al.*, 2004). This, however, seems unlikely since cell dialysis with GSH caused a significant leftward shift in I_{Kv} activation in the absence of any inhibitors (Fig. 3.8 and Table 3.5), mimicking the effect of H_2O_2. Additionally, H_2O_2 had no effect upon membrane potential as shown in Fig. 3.9, which suggests against an additional effect of an oxidised cellular redox state in the regulation of Kv channels in PASMCs.

Interestingly, cell dialysis with 1 mM GSH did, although not significantly compared to the control, reduce the rotenone induced shifts in I_{Kv}. In this, more reduced, cellular redox state rotenone caused very small and non-significant shifts in both V_a, -2.7±2.1 mV (n=13) and ΔV_h, -2.7±2 mV (n=11). In addition, no significant effects on the slope of the steady state activation dependencies or the I_{Kv} block were now evident (Table 3.6). Despite this, the slope of the inactivation dependency was still increased from 10.8±0.4 mV (n= 11 in control) to 8.2±0.5 mV (n= 11 in rotenone 1μM), $p<0.0013$.

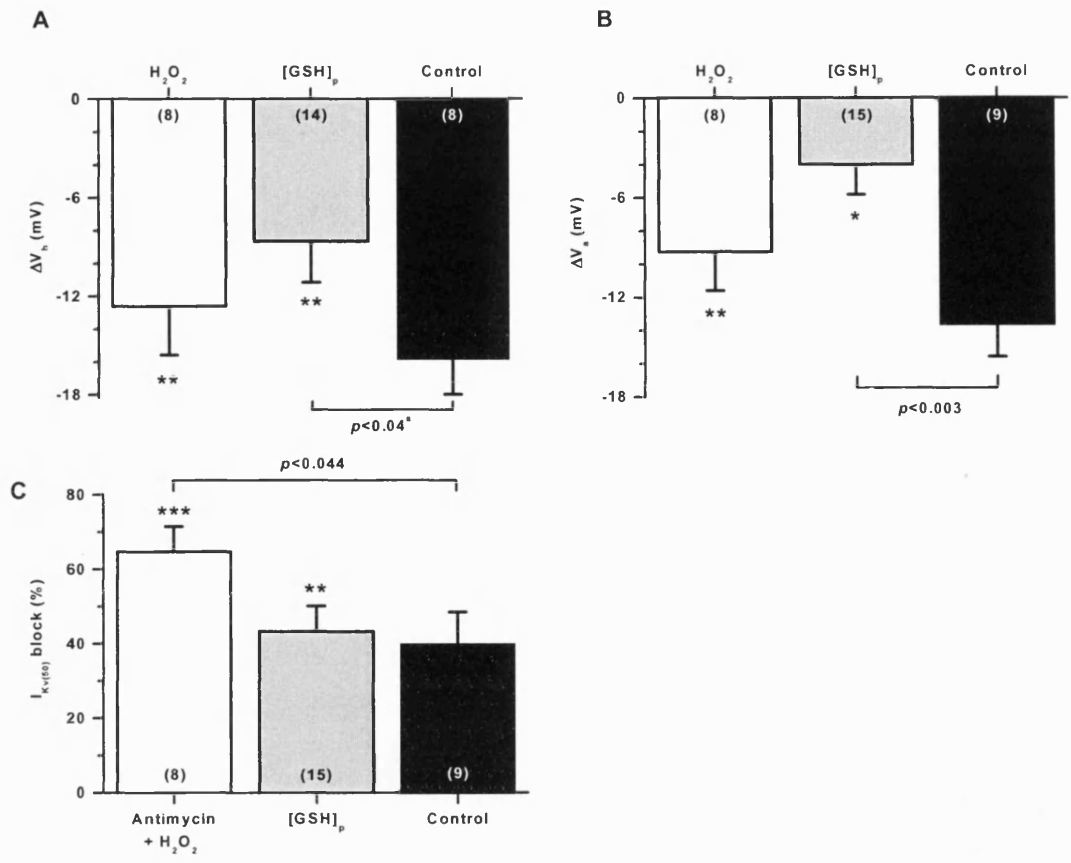

Figure 3.10. Effect of cellular redox state on the modulation of I_{Kv} by antimycin. Effect of H_2O_2 and $[GSH]_p$ on antimycin-mediated changes in I_{Kv} ΔV_a (A), ΔV_h(B) and I_{Kv} block (C). Black bars show the effect of antimycin alone for comparison. [a] denotes one-tail *t*-test.

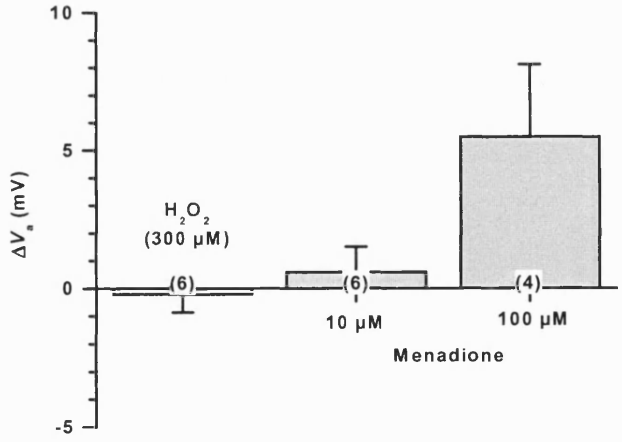

Figure 3.11. Effect H_2O_2 and menadione on I_{Kv} activation in non-dialysed PASMCs. All experiments were performed in the perforated-patch mode (with 100 µg/ml amphotericin B in the pipette).

TABLE 3.6. Modulation of the I_{Kv} characteristics by extracellular hydrogen peroxide (H_2O_2, 300 μM) and its effect in the presence of intracellular reduced glutathione (GSH, 1 mM) and antimycin and rotenone (both at 1 μM) induced changes in the presence of H_2O_2 and GSH.

	Steady-state I_{Kv} activation and $I_{Kv(50)}$ block					I_{Kv} inactivation				
	V_a (mV)	k_a (mV)	ΔV_a (mV)	$I_{Kv(50)}$ *block* (%)	*n*	V_h (mV)	k_h (mV)	*A*	ΔV_h (mV)	*n*
PSS	-16±1	10.3±0.4				-20.7±2.3	10.5±0.5	0.3±0.03		
H_2O_2	-21.1±1.3 (p<0.0007)	11.1±0.6	-5.1±1.3	9.5±4.2 (p<0.0008)	28	-24.1±2.4	9±1.2	0.24±0.04 (p<0.01)	-3.4±2.1	7
PSS (In: GSH)	-16.2±1.7	9.2±0.7				-31.7±5.5	12±1.6	0.29±0.04		
H_2O_2 (In: GSH)	-18.1±2.7	8.5±0.5	-3±2.5	21.8±4.8 (p<0.023)	9	-27.2±6.1	11.5±1.3	0.21±0.04 (p<0.043)	4.5±3.6	7
H_2O_2	-18.8±2.1	13±2.1				-24.6±3.1	10.4±1.1	0.24±0.03		
Antimycin (H_2O_2)	-28.1±3.2 (p<0.006)	9.4±1.4 (p<0.022)	-9.3±2.3	64.6±6.8 (p<0.0002)	8	-37.2±3.5 (p<0.004)	6.7±0.5 (p<0.023)	0.09±0.02 (p<0.006)	-12.6±3	8
PSS (In: GSH)	-19.1±1.4	8.2±0.5				-21.7±2.3	11.5±1.1	0.22±0.02		
Antimycin (In:GSH)	-23.1±1.7 (p<0.044)	7.8±1.7	-4±1.8	43.2±6.9.2 (p<0.007)	15	-30.4±2.8 (p<0.005)	8.4±0.5 (p<0.031)	0.07±0.03 (p<0.00001)	-8.7±2.5 (p<0.033)[a]	14
PSS (In: GSH)	-17.4±1.1	8.7±0.3	-2.7±2.1	10.8±17.6	13	-23.7±2.1	10.8±0.4	0.28±0.03	-2.7±2	11
Rotenone (In: GSH)	-20.6±2.7	5.8±2		(p<0.01)		-26.4±3.2	8.2±0.5 (p<0.002)	0.18±0.02 (p<0.003)		

[a] Compares the mean values obtained in the specified condition and those measured in the presence of antimycin alone (Table 3.1) (non-paired two-tail *t*-test).
[b] Compares the mean V_a, k_a, V_h and k_h values obtained in PASMCs dialysed either with the control pipette solution or with solution containing 1 mM GSH in the absence of any inhibitors (non-paired two-tail *t*-test).

3.1.8 Effect of H_2O_2 and menadione on I_{Kv} activation in non-dialysed cells.

Again it was important to assess a potential influence of cell dialysis on I_{Kv} activation the WC mode patch clamp and this was done by compared to non-dialysed cells using the perforated patch clamp technique. 100 μg/ml amphotericin B was included in the pipette solution to gain electrical access to the cell (Table 2.3). In contrast to dialysed cells, modulation of cellular redox state by H_2O_2 had no significant effects upon I_{Kv} activation nor the slope of the steady state activation dependencies and there was no I_{Kv} block (2.2±16.5 %, n=6) in non-dialysed cells. In addition to 300 μM H_2O_2, cells were perfused with the membrane permeable activator of superoxide, menadione, at 10 and 100 μM. Both concentrations caused a small, but not significant, rightward shift in I_{Kv} activation, opposite to the shifts in dialysed cells (Fig. 3.11). Additionally no changes in the slope of the steady state activation of the I_{Kv} block were observed with either menadione concentration. This could suggest that an anti-oxidative cellular mechanism for the maintenance of cellular redox levels is sufficient to counteract of externally applied oxidants like H_2O_2 and intracellular increases in superoxide production which might be induced by menadione. This data therefore advocates against a major role for cellular redox levels in the mitochondria-dependent regulation of I_{Kv}.

3.1.9 Involvement of the F_0/F_1 ATP synthase

Inhibition of the mETC could reduce F_0/F_1 ATP synthase activity, thus decreasing local ATP levels. If ATP synthase is involved, then its inhibition with the selective inhibitor oligomycin should mimic the effects of the mETC inhibitors on I_{Kv}.

3.1.10 Inhibition of the F_0/F_1 ATP synthase

Oligomycin (1μM), a potent inhibitor of mitochondrial ATPase, was applied to PASMCs for 5 minutes after recording I_{Kv} control parameters. Figure 3.12 shows that changes in I_{Kv} block (A) V_a (C) and V_h (E) caused by oligomycin were indeed comparable to those induced by antimycin. There was a substantial leftward shift in both V_a (ΔV_a = -11.4±1.9 mV, n=12, p<0.00007) and V_h (ΔV_h = -14.8±2.5 mV, n=11, p<0.0002). In addition the I_{Kv} block was reduced by 29.6±1.8 % and there was significant increases in the dependencies of both the steady state I_{Kv} activation (9.9±0.5

mV to 8.8±0.6 mV, n=12, $p<0.039$) and inactivation (12.2±1.3mV to 9±0.7 mV, n=11, $p<0.00001$). Additionally, a significant decrease in the non-inactivating component was evident; reduced from 0.25±0.01 mV to 0.11±0.01, n=11, $p<0.00001$) (Table 3.7).

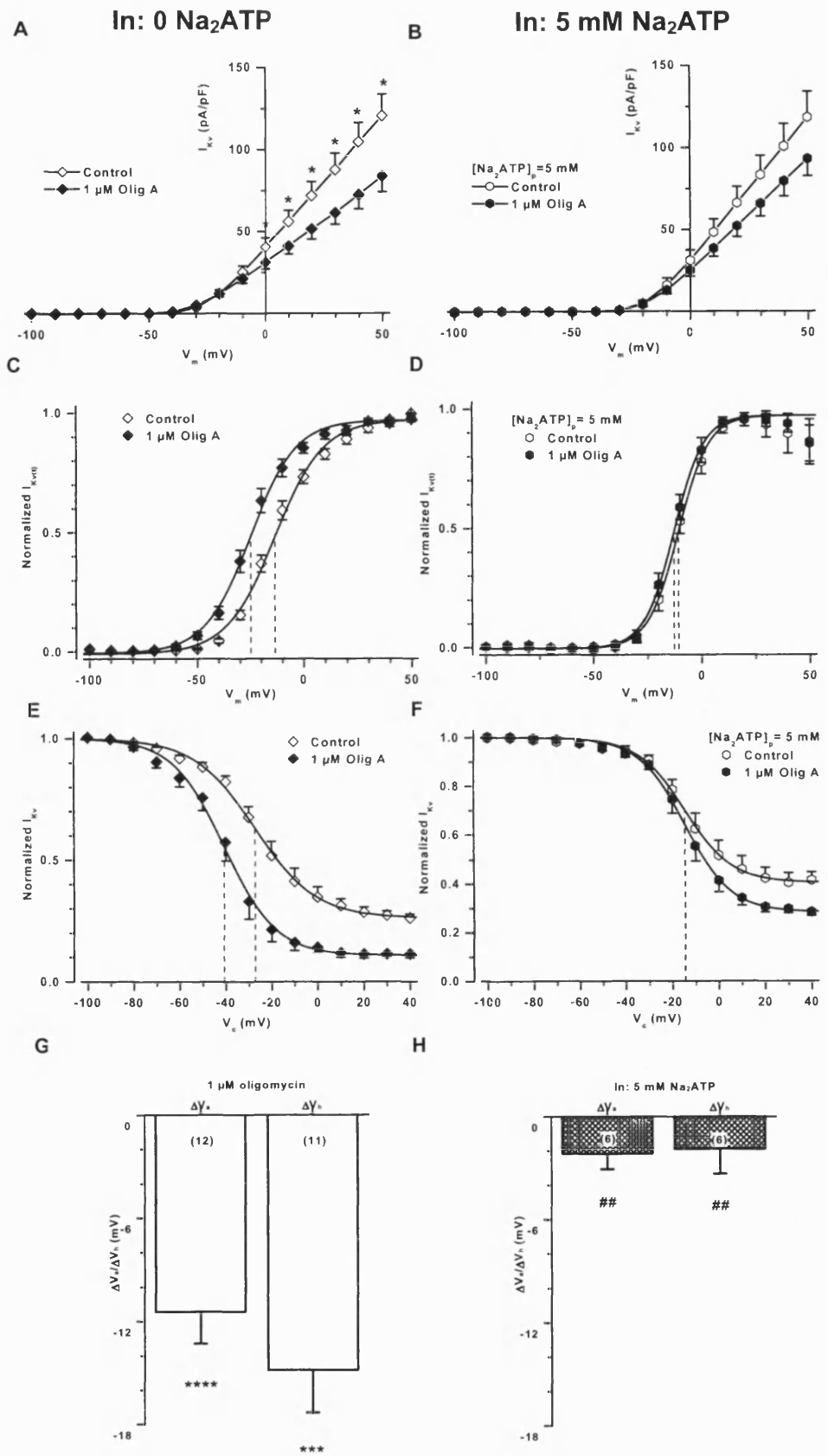
A
In: 0 Na2ATP
B
In: 5 mM Na2ATP
Control
1 μM Olig A
[Na2ATP]p=5 mM
Iκv (pA/pF)
Vm (mV)
C
D
Normalized Iκv(t0)
E
F
Normalized Iκv
Ve (mV)
G
1 μM oligomycin
H
In: 5 mM Na2ATP
ΔVa/ΔVh (mV)
(12)
(11)
(6)
****
***
##

Figure 3.12. Effect of F_0/F_1ATP synthase inhibitor oligomycin (1 μM) on I_{Kv}. A-B, Effect of olgomycin on current density to highlight I_{Kv} block at potentials up to +50 mV. Effect of oligomycin on I_{Kv} activation (C&D) and inactivation (E&F) measured and normalised to the maximal current using tail currents and I_{Kv} availability protocols (as described in chapter 2.6) in the absence (C&E) and presence (D&F) of 5 mM Na_2ATP. G&H compares the ΔV_a and ΔV_h also in the absence (G) and presence (H) of 5 mM Na_2ATP. $^{\#\#}$Compares the mean values in (G) and (H). The controls had 0 mM Na_2ATP (as shown in Fig. 3.1).

Similarity between the effects of antimycin and oligomycin could suggest that local changes in ATP concentration are important in I_{Kv} modulation by the inhibitors. Cell dialysis with 5 mM Na_2ATP, increasing intracellular ATP levels, practically abolished the effect of oligomycin on ΔV_a and ΔV_h (Fig. 3.12). An attenuation of the effects of oligomycin by dialysis with an elevated ATP concentration is clearly shown in the figures comparing; 1) I_{Kv} current densities where the current block at and above 0 mV is now not significant (Fig. 3.12 A, control vs. B 5 mM Na_2ATP); 2) normalised tail current densities where the leftward shift in V_a is practically abolished (ΔV_a = -2.2±0.9 mV, n=6, p<0.004 unpaired t-test shown in Fig 3.12 (C), control vs. (D) 5 mM Na_2ATP) and 3) the shift in I_{Kv} inactivation is significantly blocked (p<0.003, non-paired *t*-test to oligomycin in control conditions, Fig. 3.12 E, control and F, 5 mM Na_2ATP). It is interesting to note that in the presence of Na_2ATP there is rectification of the current positive to +30 mV, shown in Fig. 3.12 D. It is also worth noting that the changes in the slopes of the steady state I_{Kv} activation dependencies caused by oligomycin alone were completely blocked by Na_2ATP (Table 3.7) and, despite having an insignificant smaller 18.9±7.2 % (n=6) reduction in I_{Kv} block, there was no significant difference to the oligomycin in control condition. Additionally, there was no effect upon the slope of the steady state dependencies of I_{Kv} inactivation, however, despite being significantly reduced from 0.38±0.04 mV to 0.28±0.01 (n=6, p<0.035) a significant block of the effects of oligomycin on the non-inactivating component was nevertheless evident (p<0.00001, non-paired *t*-test) (Table 3.7).

TABLE 3.7. Effect of F_1/F_0 ATP Synthase inhibitor oigomycin (1 μM) on I_{Kv}.

	Steady-state I_{Kv} activation and $I_{Kv(50)}$ block					**I_{Kv} inactivation**				
	V_a (mV)	k_a (mV)	ΔV_a (mV)	$I_{Kv(50)}$ *block* (%)	*n*	V_h (mV)	k_h (mV)	*A*	ΔV_h (mV)	*n*
$[MgCl_2]_p$=0.5 mM										
PSS	-14.7±1.5	9.9±0.5				-25.2±3.5	12.2±1.3	0.25±0.01		
Oligomycin	-26.1±1.9 (p<0.00007)	8.8±0.6 (p<0.039)	-11.4±1.9	29.6±1.8 (p<0.0001)	12	-40.1±3.4 (p<0.0002)	9±0.7 (p<0.014)	0.11±0.01 (p<0.00001)	-14.8±2.5	11
$[Na_2ATP]_p$=5 mM										
PSS	-10.2±1.6	7±0.7				-12±2.9	11.3±2.3	0.38±0.04		
Oligomycin	-12.4±1.7 (p<0.031)[b]	7±0.7	-2.2±0.9 (p<0.004)[a]	18.9±7.2	6	-13.8±2.6	9.4±1.3	0.28±0.01 (p<0.035) (p<0.00001)[a]	-1.9±1.5 (p<0.003)[a]	6
$[MgCl_2]_p$=0.5 mM										
Antimycin	-21.8±2	6.3±0.5				-33.6±2.1	8.9±1.1	0.04±0.01		
Antimycin + Oligomycin	-30.5±3.9 (p<0.008)	7.2±0.7 (p<0.045)[b]	-8.7±2.2	44±6.3 (p<0.017) (p<0.033)[a, b]	7	-41.9±2.6 (p<0.007)	7.7±1.2	0.1±0.01 (p<0.011)	-8.3±2 (p<0.041)[a,b]	7

Concentration of antimycin was 1 μM; cells were pre-treated for 5 min before commencing I_{Kv} recording.
[a] Compares the mean values obtained in the specified condition and those measured in the presence of oligomycin alone (non-paired two-tail *t*-test).
[b] Denotes a significant difference only with the one-tail *t*-test.

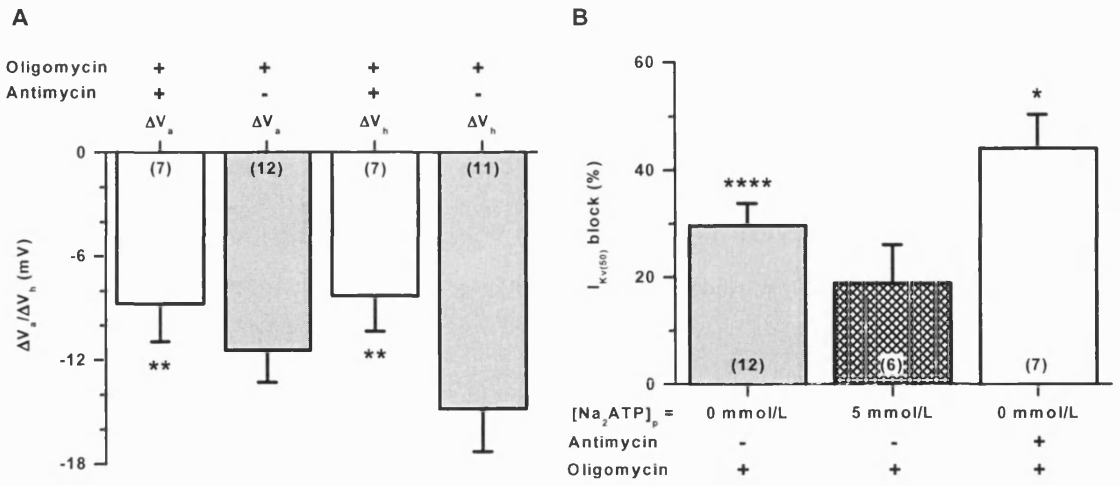

Figure 3.13. Effect of antimycin on the oligomycin induced shift in I_{Kv} parameters. (A) Cell pre-treatment with antimycin (1 μM) does not block the effect of oligomycin on I_{Kv} activation or inactivation. (B), $I_{Kv(50)}$ block in oligomycin (control and 5 mM Na_2ATP pipette solutions) and in the additional presence of antimycin when dialysed with control pipette solution. Grey bars indicate effect of oligomycin alone for comparison.

3.1.11 Effects of intracellular ATP on the antimycin dependent changes in I_{Kv}

The effects of oligomycin on I_{Kv} essentially mimic those of antimycin raising the possibility of a similar mechanism of action. Pre-treatment of PASMCs with antimycin however, despite reducing, did not prevent the subsequent effects of oligomycin on ΔV_a and ΔV_h (Fig. 3.13 A&B), suggesting an additive action of these inhibitors. Conversely, the oligomycin-induced reduction in k_a was reversed (from 6.3±0.5 mV in antimycin to 7.2±0.7 mV in both inhibitors, $p<0.045$, n=7) and changes in k_h were blocked in the presence of antimycin (Table 3.7), thus indicating a possible cross-talk between the mETC and the ATP synthase. It is also interesting to note an increase of the non-inactivating component in the additional presence of oligomycin (from 0.04±0.01 to 0.1±0.01, $p<0.011$, n=7, Table 3.7). In contrast, oligomycin and antimycin had an additive effect on I_{Kv} amplitude, I_{Kv} block was enhanced in the presence of both drugs to 44±6.3 %, $p<0.017$ (paired to antimycin alone) and $p<0.033$ (unpaired to oligomycin alone) (Fig. 3.13 B)

TABLE 3.8. Effect of intracellular ATP, EDTA and Mg^{2+} on antimycin-induced changes in the I_{Kv} characteristics.

	Steady-state I_{Kv} activation and $I_{Kv(50)}$ block					**I_{Kv} inactivation**				
	V_a (mV)	k_a (mV)	ΔV_a (mV)	$I_{Kv(50)}$ *block* (%)	*n*	V_h (mV)	k_h (mV)	*A*	ΔV_h (mV)	*n*
$[Na_2ATP]_p$=5 mM										
PSS	-10.1±1.8	10.1±0.9				-12±4.6	13.8±1.6	0.4±0.04		
Antimycin (1 µM)	-13.1±1.6 (p<0.034)	9.5±1.2	-3±1.1	2.7±7.7	8	-21.1±3.2 (p<0.016)	7.8±0.8 (p<0.0004)	0.12±0.02 (p<0.0002)	-9.1±2.8 (p<0.037)[a,b]	7
$[MgATP]_p$=5 mM										
PSS	-14.8±1.4	9.5±1				-19.7±1.5	10.4±0.6	0.34±0.02		
Antimycin (1 µM)	-21.7±1.8 (p<0.0002)	7.8±0.8 (p<0.031)[b]	-6.9±1.1 (p<0.009)[a]	26.2±4.5 (p<0.0005)	9	-28.7±2.1 (p<0.0002)	7.2±0.4 (p<0.0004)	0.05±0.01 (p<0.00001) (p<0.035)[a,b]	-8.9±1.4 (p<0.014)[a]	6
$[EDTA]_p$=5 mM										
PSS	-11.6±1.4	9.2±0.6				-19.6±2.1	12.2±1.3	0.31±0.03		
Antimycin (1 µM)	-14.8±1.8 (p<0.013)	9.5±0.7	-3.3±1 (p<0.0005)[a]	22.9±5.7 (p<0.014)	8	-24±1.9	7.3±1.1 (p<0.019)	0.08±0.02 (p<0.0004)	-4.4±2.6 (p<0.005)[a]	8
$[MgCl_2]_p$=5 mM										
PSS	-10.4±4.1	11.2±1.7				-31.5±4.5	10.7±0.8	0.22±0.04		
Antimycin (1 µM)	-17.1±4.5 (p<0.00007)	10.2±2.1	-6.7±1 (p<0.005)[a]	58.5±6.9 (p<0.002)	10	-39.7±3.6 (p<0.027)	7.4±0.7 (p<0.032)	0.06±0.02 (p<0.002)	-8.2±2.7 (p<0.043)[a]	6

[a] Compares the mean values obtained in these conditions and those measured in the presence of antimycin alone (Table 3.1) (non-paired two-tail *t*-test).
[b] Denotes a significant difference only with the one-tail *t*-test.

The similarity between the changes in the I_{Kv} characteristics caused by the complex V (ATP synthase) and complex III inhibitors could, nevertheless, advocate that an ATP-dependent process could be involved in the action of antimycin. To verify this notion, the effects of antimycin were also studied in cells dialysed with 5 mM Na_2ATP. Fig. 3.14 C&D demonstrates that, like oligomycin, the effect of antimycin on both I_{Kv} activation (ΔV_a = -3±1.1 mV, p<0.0005, n=8) and inactivation (ΔV_h = -9.1±2.8 mV, p<0.037 one-tailed t-test, n=7) was indeed significantly reduced, although changes in I_{Kv} inactivation appeared to be less sensitive. The example traces in Fig. 3.14 B also indicate an increase in the slope dependency of the steady state inactivation (13.8±1.6 mV to 7.8±0.8 mV, p<0.0004, n=7), changes for activation were blocked (see Table 3.8). Also, the antimycin-induced $I_{Kv(50)}$ block was virtually abolished by Na_2ATP (Table 3.8), with only a small decrease (11.6 %) evident in the traces from a representative cell in the absence and presence of Na_2ATP (Fig. 3.14 B). It is worth mentioning that a similar decrease in the non-inactivating component from 0.4±0.04 to 0.12±0.02, p<0.0002, n=7 was still observed as seen with antimycin in control conditions, suggesting that the effects of antimycin on the non-inactivating component are independent of changes in V_a and V_h and probably reflect a direct effect of the inhibitor on I_{Kv}.

Interestingly, cell dialysis with 5 mM MgATP, a condition that would be expected to favour protein phosphorylation, partly recovered antimycin-mediated effects on at least I_{Kv} (Fig. 3.14 C & D). More notable were changes on I_{Kv} activation parameters with a partial recovery of ΔV_a increasing to -6.9±1.1 mV, n=9, p<0.09 when compared to Na_2ATP. I_{Kv} block was also increased to 26.2±4.5 %, p<0.0005 and the slope of the steady state activation dependency increased from 9.5±1 to 7.8±0.8, p<0.031 (one tailed t-test) in comparison to the Na_2ATP and thus reflecting the antimycin induced shifts. However, inactivation parameters were not dissimilar from those dialysed with Na_2ATP

One possible explanation of the differences between the two ATP salts could be the Mg^{2+}-chelating property of ATP. To account for this possibility the effect of equimolar replacement of 5 mM EGTA with EDTA (a much more potent chelator of Mg^{2+}) in the pipette was examined (Table 2.3 in methods). Cell dialysis with the increased buffering capacity for Mg^{2+} significantly attenuated antimycin-induced changes in both ΔV_a (-3.3±1 mV, n=8, p<0.0005) and ΔV_h (-4.4±2.6 mV, n=8, p<0.003) and reduced its

$I_{Kv(50)}$ block by an average of 17.7 % (Table 3.8), thus mimicking the effect of Na_2ATP (Fig. 3.14 C-E). Furthermore, the increase in the dependency of I_{Kv} activation as seen with antimycin under control intracellular conditions was completely blocked when cells were dialysed with increased EDTA, akin to Na_2ATP (Table 3.8). It is also noteworthy that the mean V_a and V_h values obtained in cells dialysed with Na_2ATP and EDTA, but not with MgATP, in the absence of any inhibitors were significantly more positive when compared to those in cells dialysed with the control pipette solution (Table 3.8).

3.1.12 *Direct effect of antimycin on I_{Kv}*

Notably, although significantly reducing ΔV_h, these conditions did not change the effect of antimycin on the non-inactivating component strongly suggesting a possible direct effect of antimycin. To investigate this possibility the following analysis was performed. This non-specific effect is most clearly demonstrated by comparison of the effects of antimycin and oligomycin on I_{Kv} kinetics under conditions (5 mM EDTA for antimycin and 5 mM Na_2ATP for oligomycin) when changes in I_{Kv} inactivation (ΔV_h) were eliminated (Fig. 3.12). The effect of antimycin on the I_{Kv} decay measured during the 10 sec conditioning pre-pulse was practically unchanged by cell dialysis with 5 mM EDTA (Fig. 3.15 A&B), which virtually eliminated the antimycin-induced leftward shift in the I_{Kv} inactivation dependency (Fig. 3.15 C). In contrast, cell dialysis with Na_2ATP significantly reversed both the oligomycin-mediated shift and the inhibition of the non-inactivating component of I_{Kv} (Fig. 3.15 D-F).

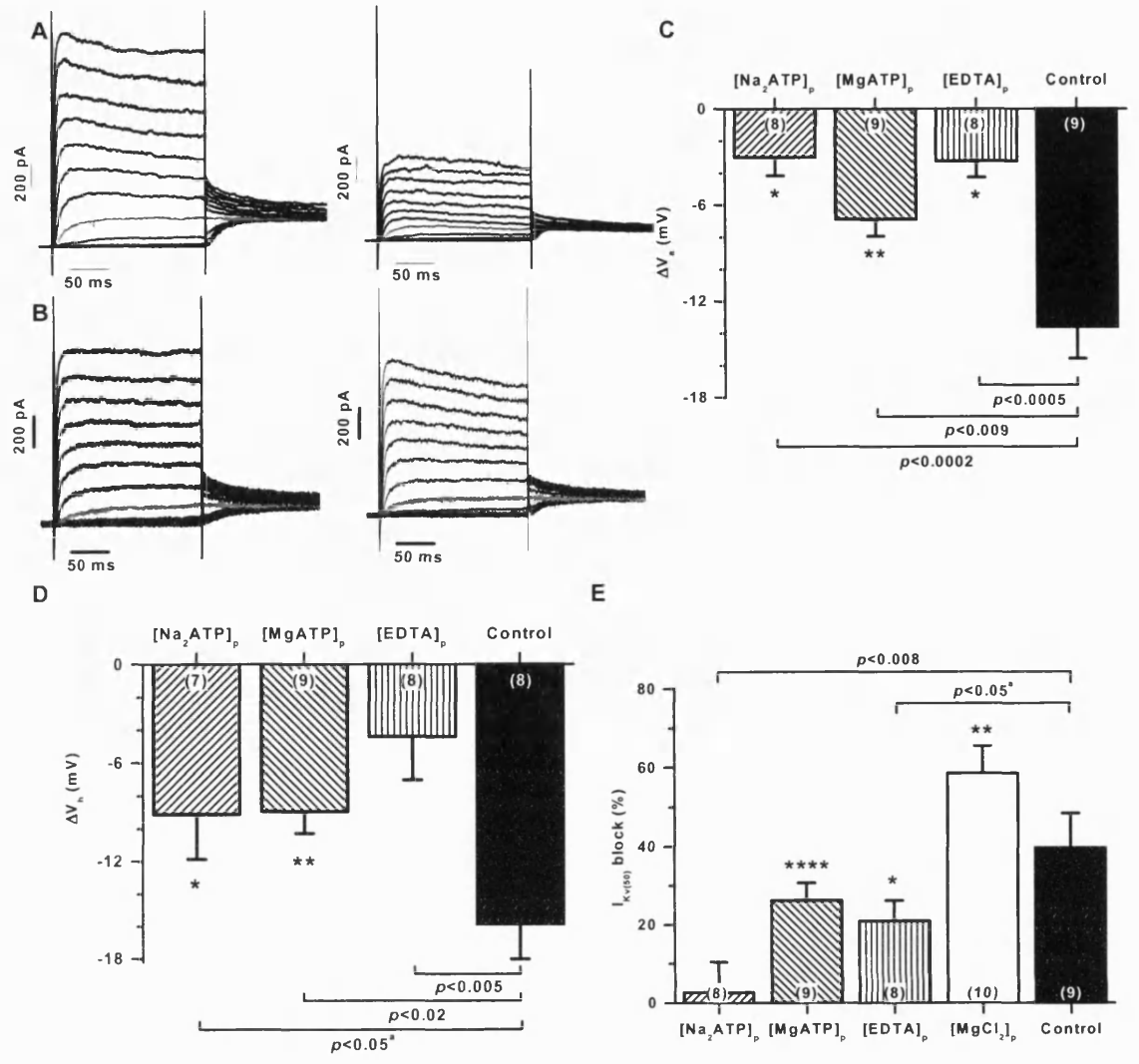

Figure 3.14. Dependence of I_{Kv} modulation on Mg^{2+}_i. A & B are representative I_{Kv} traces from two PASMCs in control (left) and in 1μM antimycin (right); (A) dialysed with control pipette solution (C_m = 12.3 pF, ΔV_a = -20.8 mV and $I_{Kv(50)}$ = 63.6 %.) and (B) dialysed with 5 mM Na_2ATP (C_m = 17.8 pF, ΔV_a = -1.3 mV and $I_{Kv(50)}$ = 11.6%). Comparison of the effect of intracellular (pipette) Na_2ATP, MgATP and EDTA (no $MgCl_2$ was added to the pipette solutions) on antimycin-induced changes in I_{Kv} activation (C), inactivation (D) and $I_{Kv(50)}$ block (E). Black bars show the effect of antimycin alone for comparison. [a] in C and D denotes significant difference with one-tail non-paired *t*-test.

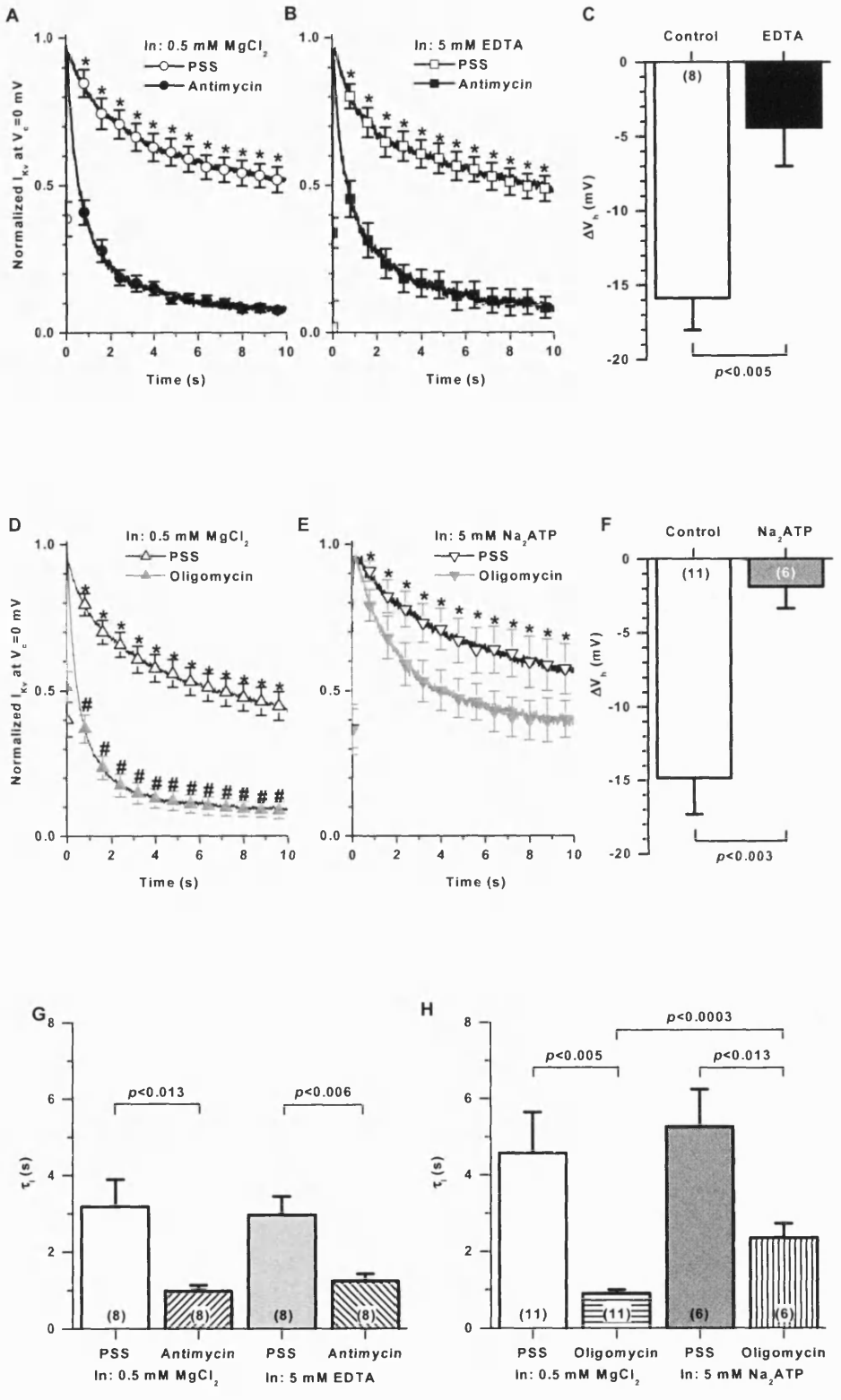

Figure 3.15. Demonstration of the direct block of I_{Kv} by antimycin. Comparison of the kinetics of I_{Kv} inactivation induced by antimycin (A-C) and oligomycin (D-F) (both at 1 μM) in PASMCs dialysed with control (A, D), EDTA (B) or Na_2ATP (E) containing

pipette solutions. G and H, changes in the time constant of inactivation calculated from a mono-exponential fit of the I_{Kv} elicited by a 10 s conditioning pre-pulse at 0 mV (availability protocol) for antimycin in control and EDTA (G) and oligomycin in control and Na_2ATP (B). I_{Kv} was normalised to its peak amplitude and averaged (solid lines). Symbols and error bars represent mean and s.e.m. for 8 (A and B), 11 (D) and 6 (E) PASMCs. *indicates the level of significance between data obtained in the presence and absence of an inhibitor using the paired *t*-test, while #indicates a significant difference between oligomycin-induced changes in cells dialysed with Na_2ATP and those recorded with the control pipette solution. Note that no significant difference in the antimycin-induced I_{Kv} decrease was observed, although EDTA significantly inhibited the shift in the I_{Kv} inactivation dependency (C). Conversely, the reduction in the oligomycin-mediated effect was well correlated with ΔV_a changes (F).

3.1.13 Dependence of antimycin- mediated effects on $Mg^{2+}{}_i$

If $Mg^{2+}{}_i$ is involved in the effect of the mitochondrial inhibitors on I_{Kv} activation and inactivation, then it would be expected that cell dialysis with elevated $Mg^{2+}{}_i$ should 1) mimic their effect and 2) attenuate the effect of antimycin. This was assessed by increasing [$MgCl_2$] in the pipette solution from 0.5 to 5 mM. Although the change in $[Mg^{2+}]_i$ alone did not affect I_{Kv} activation (Table 3.5), the inactivation dependency was significantly shifted to the left, V_h = -23.7±1.1 mV, n=69 (control) compared to -30.7±12.8, n=12 (5 mM $MgCl_2$), $p<0.02$, in the absence of any inhibitors (Fig. 3.16 A). Elevated Mg^{2+} also significantly decreased the non-inactivating component from 0.28±0.01 to 0.12±0.02, $p<0.035$, possibly via a direct effect on the Kv channel that might occur at positive potentials. Nevertheless, antimycin-induced changes in both ΔV_a from -13.6±2 mV, n=14, (control) to -6.7±1 mV (5 mM $MgCl_2$), and ΔV_h from -15.6±2. mV, n=9, (control) to -8.2±2.7 mV, n=6, (5 mM $MgCl_2$), were significantly reduced when compared to those in low $[Mg^{2+}]$ ($p<0.005$ and $p<0.043$, respectively, Fig. 3.16 B). Only the steady state dependencies of inactivation were increased significantly from 10.7± 0.8 mV to 7.4±0.7 mV (n=6, $p<0.032$). Consequently supporting a role for a mitochondria-mediated increase in $[Mg^{2+}]_i$ in the regulation of Kv channels. Interestingly, the antimycin-dependent $I_{Kv(50)}$ block was markedly enhanced in the elevated $[Mg^{2+}]_i$ (Fig. 3.14 E), a similar potentiation of the antimycin

induced block to that occurring with H_2O_2 (Fig. 3.10 C). Similarly to other conditions antimycin induced a significant decrease in the non-inactivating component from 0.22±0.04 to 0.06±0.02, $p<0.002$, n=6.

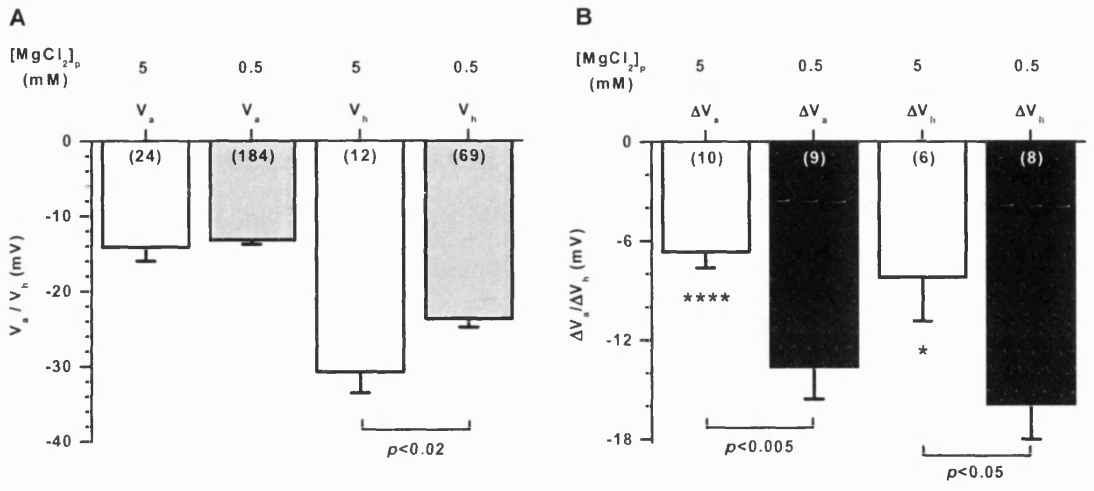

Figure 3.16. Comparison of the effect of increased pipette $MgCl_2$ ($[MgCl_2]_p$) on I_{Kv} characteristics. (A) Effects of 0.5 and 5 mM $[MgCl_2]_p$ on V_a and V_h in the absence of inhibitors (non-paired t-test). (B) Increased $[MgCl_2]_p$ significantly attenuates the antimycin-induced shifts in I_{Kv} activation and inactivation.

3.1.14 Confocal imaging of Mg^{2+}_i and Ca^{2+}_i in single PASMCs

An increase in Ca^{2+}_i and Mg^{2+}_i in response to mitochondrial inhibition has previously been demonstrated in cardiac myocytes (Leyssens *et al.*, 1996), but not in pulmonary arteries. Therefore, confocal imaging of PASMCs loaded with Mg^{2+}-sensitive dye, MagFluo-4-AM, was carried out in order to study the effect of CCCP and antimycin on Mg^{2+}_i concentration and to verify a possible role for Mg^{2+} in the mitochondrial dependent regulation of I_{Kv}. The Mg^{2+} imaging was investigated in the presence of BAPTA-AM and Ca^{2+} free Krebs (Table 2.4) to minimise Ca^{2+}_i-dependent contamination of the fluorescent signal which also occurs in response to these inhibitors, as demonstrated in (Fig. 3.18). CCCP caused a significant increase in Mg^{2+}_i in PASMCs. The images in Fig. 3.17 A show two individual PASMCs (a and b) under optical light and showing MagFluo-4-AM fluorescence taken at 0, 5 and 10 minutes after application of 2 μM CCCP. The final panel shows maximal fluorescence after

stimulation with A23187. In Fig. 3.17 B these images are converted to a normalised MagFluo-4-AM expressed as a percentage of the maximal response to A23187 and shows the CCCP induced increase in MagFluo-4-AM fluorescence over a 10 minute period. Similar significant increases in MagFluo-4-AM intensity were also observed for antimycin (Fig. 3.17 C&D).

To confirm that the increased intensity of MagFluo-4-AM was attributed to a change in Mg^{2+} concentration and not Ca^{2+} concentration, changes in Ca^{2+} intensity were also measured in a separate set of experiments using Fluo-4, a dye more selective for Ca^{2+}. Note that there is a relatively small level of control fluorescence after the correction procedure (less then 0.5 %, Fig. 3.18 B). As shown in Fig. 3.18 a significant increase in Ca^{2+}_i did also occur in response to both CCCP and antimycin. These changes in Ca^{2+}_i were abolished in cells pre-incubated with 50 μM BAPTA, conditions that the Mg^{2+} measurements were recorded in, completely blocking Fluo-4 fluorescent signals (n=7, data not shown). Additionally, cell dialysis with 220 nM Ca^{2+} alone caused a significant rightward shift in I_{Kv} activation (from V_a = -13.1±0.6 mV (control, n=184) to -7.6±1.9 mV (220 nM Ca^{2+}_i, n=11), $p<0.02$), an effect opposite to that caused by the mitochondrial inhibitors.

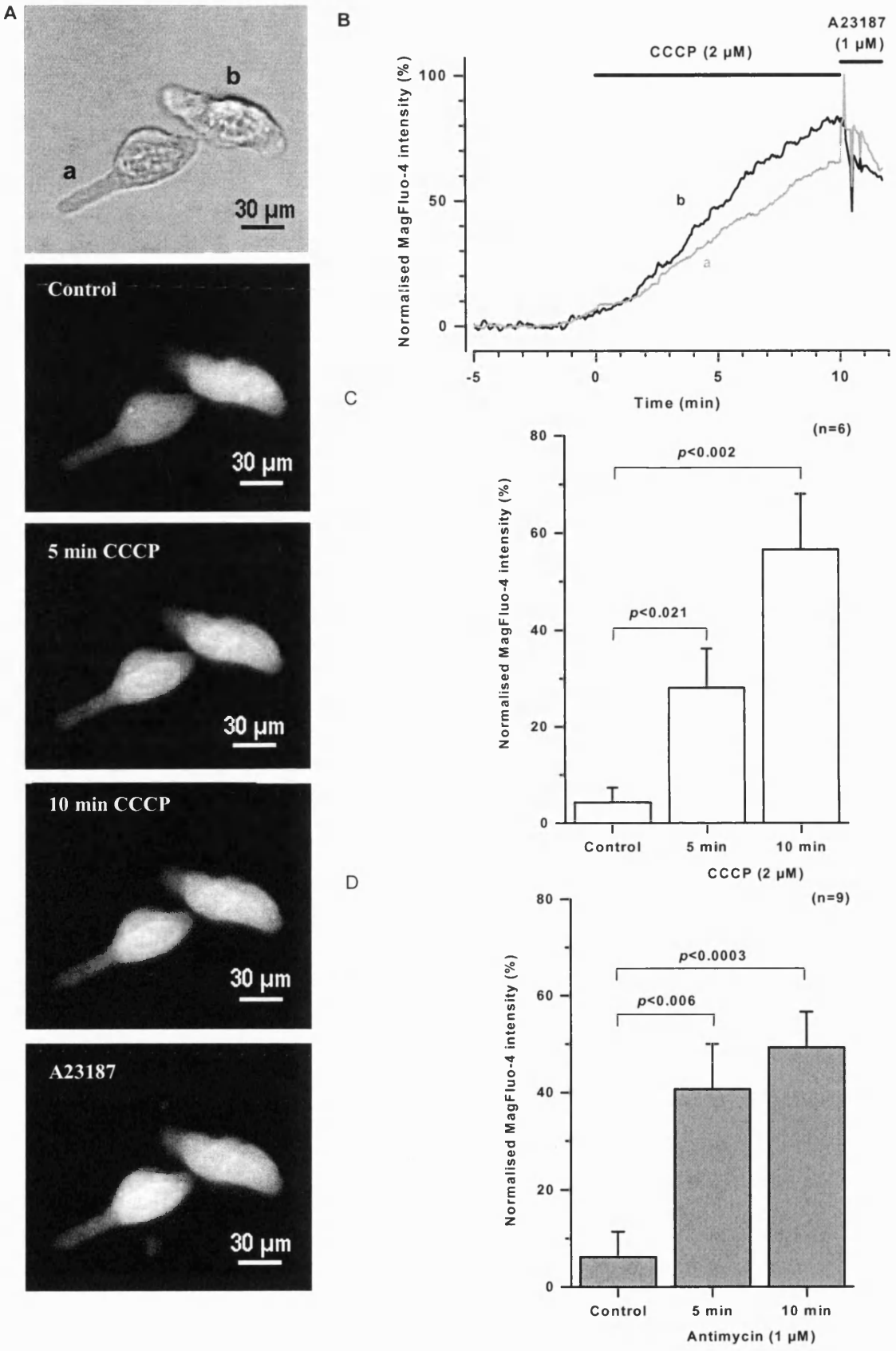
A
b
a
30 µm
Control
30 µm
5 min CCCP
30 µm
10 min CCCP
30 µm
A23187
30 µm
B
A23187
(1 µM)
CCCP (2 µM)
Normalised MagFluo-4 intensity (%)
100
50
0
b
a
-5
0
5
10
Time (min)
C
(n=6)
p<0.002
p<0.021
Normalised MagFluo-4 intensity (%)
80
60
40
20
0
Control
5 min
10 min
CCCP (2 µM)
D
(n=9)
p<0.0003
p<0.006
Normalised MagFluo-4 intensity (%)
80
60
40
20
0
Control
5 min
10 min
Antimycin (1 µM)

Figure 3.17 mETC inhibition induces increases in Mg^{2+}_i. CCCP- (A-C) and antimycin- (D) induced increases in Mg^{2+}_i in single PASMCs. (A) Images from two representative individual freshly isolated PASMCs (a and b). (B) Normalised MagFluo-4 intensity for the representative cells in (A). (C) & (D) Mean normalised intensities in 8 cells with CCCP and 8 cells with antimycin. Intensities were normalised to the peak MagFluo-4 fluorescence measured in A23187 and compared using paired *t*-test. Dr. Kathryn Yuill contributed to this figure.

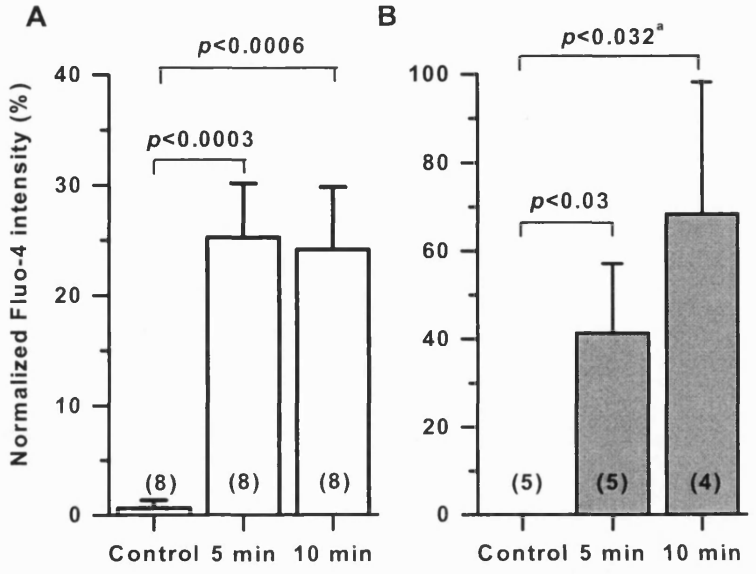

Figure 3.18. Effects of CCCP (2 μM, A) and antimycin (1 μM, B) on Ca^{2+}_i in PASMCs. Experiments were performed at room temperature with the cells were bathed in PSS. [a]Denotes one-tail paired *t*-test. Dr. Kathryn Yuill contributed to this figure.

3.2 Discussion

Mitochondria in the regulation of Kv channels

The major findings in this chapter reveal the existence of a potent mitochondria-mediated regulatory pathway in the Kv channel activity in PASMCs. The mitochondrial uncoupler CCCP, and mETC inhibitors, rotenone, antimycin and cyanide induced similar changes in all three I_{Kv} parameters. Antimycin-induced effects (the most pronounced) were studied in detail. It was found that these effects 1) cannot be entirely explained by changes in cellular redox state, 2) are mimicked by the ATP synthase inhibitor oligomycin, 3) were significantly inhibited by cell dialysis with 5 mM Na_2ATP, EDTA or with increased, 5 (instead of 0.5) mM, $MgCl_2$, whereas intracellular MgATP partially reversed this effect and 4) both CCCP and antimycin caused a significant increase in Mg^{2+}_i. Collectively, these findings suggest the presence of a novel mitochondrial-mediated Mg^{2+}_i-dependent mechanism in the regulation of Kv channels in PASMCs.

3.2.1 Variability in I_{Kv} parameters

A wide variation in the absolute V_a and V_h values under control conditions existed in PASMCs which was consistent with a normalised distribution. Variability may be representative of different populations of cells present. Differences in the intracellular micro-environment close to the Kv channel mouth (e.g. variations in local divalent cation concentration (Gelband *et al.*, 1993), different heteromultimeric composition, and/or the presence of multiple Kv channel isoforms (Davies & Kozlowski, 2001; Archer *et al.*, 1998)) in PASMCs could potentially contribute to such variability. It is noteworthy, however, that histogram analysis of V_a and V_h showed a normal Gaussian distribution of the parameters (Fig. 3.4 A&B), arguing against the presence of separate sub-types of PASMCs expressing different types of I_{Kv} with distinctive voltage-dependent characteristics as has previously been demonstrated in conduit PAs (Smirnov *et al.*, 2002). Also, in contrast to conduit PASMCs (Smirnov *et al.*, 2002), no correlation between the maximal I_{Kv} amplitude and the cell membrane capacitance was observed (Fig. 3.3 C). Similarly, no correlation was found between the cell size and V_a (Fig. 3.4

D). Thus, this analysis strongly supports the presence of a relatively homogenous population of the *whole-cell* I_{Kv} in small PASMCs.

3.2.2 Specificity of the effects of mitochondrial inhibitors

It has been demonstrated that other specific protein kinase inhibitors can directly affect Kv channels in PASMCs (Smirnov & Aaronson, 1996). It was therefore important to show that the mETC inhibitors act via modulation of the mitochondrial function and not directly on I_{Kv}. Although a reversal of the effects of inhibitors was not possible to assess under my experimental conditions (designed to study their action at equilibrium) full reversibility of the inhibitor-mediated inhibition of I_{Kv} has been previously demonstrated during acute application of higher concentrations of inhibitors in this cell type (Yuan *et al.*, 1996; Yuan *et al.*, 1995). Furthermore, the usage of relatively low concentrations of mitochondrial inhibitors (1-2 μM) in this study ensured minimisation of possible non-specific actions. Importantly, the inhibition of antimycin-mediated changes in I_{Kv} by CCCP and by the proximal mETC inhibitors, rotenone and myxothiazol strongly suggest that the inhibitor-mediated effects on I_{Kv} are due to modulation of mitochondrial function. It is interesting to note that CCCP had no significant effect on the rotenone induced shift in both I_{Kv} activation and inactivation. In addition, the lack of attenuation of the rotenone induced shifts in I_{Kv} by cellular dialysis with Na succinate, acting as a substrate for mETC complex II, suggests either towards a non mETC specific effect of rotenone on I_{Kv} in PASMCs, or to other yet unknown factors which may influence its specific action on complex I. Nevertheless, the direct effect of inhibitors particularly at the prolonged depolarisations, cannot be excluded.

Conversely, the absence of such correlation for antimycin-induced effects strongly suggests that the inactivation-dependent effect is masked by another process which is likely to represent an open channel block. In favour of this, the peak I_{Kv} amplitude during V_c did not reduce much suggesting that the channel has to be opened first. Correlation between the inhibition of the oligomycin-mediated acceleration in the current decay and the shift in V_a by cell dialysis with Na_2ATP suggests that the effect of oligomycin on I_{Kv} kinetics is predominantly due to changes in channel inactivation.

This effect of antimycin resembles the direct block of Kv channels by specific protein kinase inhibitors staurosporine (Park *et al.*, 2005) and bisindolylmaleimide (Choi *et al.*, 2000). It is also worth noting that antimycin did induce a similar block independent of the conditions. An inhibitor-mediated open channel block however is unlikely to significantly interfere with measurements of I_{Kv} activation, since it develops over much longer membrane depolarisations than those used for the activation protocol. Due to difficulties in separation of mitochondria-mediated changes in I_{Kv} inactivation from a non-specific I_{Kv} block by inhibitors, changes in the non-inactivating I_{Kv} component are difficult to interpret.

3.2.3 Role of $\Delta\Psi_m$

Incubation of PASMCs with the mitochondrial uncoupler CCCP, which should significantly reduce $\Delta\Psi_m$, caused a significant effect on all three measured characteristics of I_{Kv}; V_a, V_h and $I_{Kv(50)}$ block (Fig 3.5). These effects of CCCP were mimicked by rotenone, myxothiazol (on activation only), antimycin and cyanide, inhibitors of the mETC complexes I, III and IV, respectively (Fig.3.6). Since $\Delta\Psi_m$ is predominantly maintained by the activity of the mETC complexes I, III and IV which create an electrochemical proton gradient (Δp) across the inner mitochondrial membrane, it is likely that inhibitor-induced decreases in Δp and thus in $\Delta\Psi_m$ are primarily responsible for their effects on I_{Kv}. The ability of CCCP and the proximal mETC inhibitors rotenone and myxothiazol to block the antimycin-dependent relative shifts in activation and inactivation (Fig. 3.7) strongly supports this conclusion. Furthermore, depolarisation induced by antimycin and CCCP reflects that observed in response to 4-AP (Yuan, 1995), a known blocker of Kv channels in PASMCs.

$\Delta\Psi_m$ and Δp provide the electrochemical driving force for three fundamental cellular processes, ROS generation by mETC complexes I and III, ATP synthesis by complex V (ATP synthase) and ion transport across the inner mitochondrial membrane (the latter is crucial for maintenance of mitochondrial integrity and regulation of mitochondrial function). Therefore, mETC inhibitor-induced changes in $\Delta\Psi_m$ are likely to affect any of these processes alone or in combination. It is highly possible that inhibition of the mETC by antimycin would increase ROS production by this complex due to its increase in the lifetime of the electron donor, ubisemiquinone (Turrens *et al.*, 1985).

3.2.4 Role of ROS

Antimycin acts at complex III, which is the main proposed site of electron leak and ROS production in the mETC (Chen *et al.*, 2003). A putative involvement of ROS was therefore assessed using variety of experimental approaches. It was found that 1) extracellular H_2O_2 mimicked the effect of the mETC inhibitors only on activation, and failed to attenuate the antimycin-induced effects on ΔV_a and ΔV_h in dialysed PASMCs, 2) cell dialysis with GSH alone had an effect on the I_{Kv} activation, but not inactivation, and significantly reduced the antimycin-induced changes in ΔV_a and ΔV_h, 3) in dialysed cells H_2O_2 had no effect upon cell resting membrane potential, 4) in non-dialysed PASMCs neither H_2O_2 nor menadione had significant effect on I_{Kv} activation and preliminary data also indicates no effect upon resting membrane potential.

Overall, these results demonstrate that I_{Kv} activation is more susceptible to the changes in cellular redox state than I_{Kv} inactivation is. The H_2O_2-mediated leftward shift in I_{Kv} activation should lead to an increase in the Kv channel activity in the physiological range of membrane voltages, as previously proposed (Archer *et al.*, 1993; Michelakis *et al.*, 2004). However, a similar shift in cells dialysed with GSH (which should increase the reduced state of Kv channels) and failure of H_2O_2 to alter the antimycin-dependent effects argue against the direct involvement of H_2O_2 in I_{Kv} modulation by the mitochondrial inhibitors. Furthermore, the lack of the effect of H_2O_2 and the pro-oxidant menadione (10-100 μM) on I_{Kv} activation in non-dialysed PASMCs (Fig. 4.5) suggests the presence of effective anti-oxidant mechanisms in intact PASMCs (Smith *et al.*, 2005).

Additionally, this data only adds to the current controversies regarding the regulation of ROS in hypoxia and does not divulge a putative role for ROS in the regulation of I_{Kv} in PASMCs. Contribution of neither a decrease nor an increase (debated extensively in Ward *et al.*, 2006) in mitochondrial derived ROS in the regulation of I_{Kv} is fully supported by the data in this chapter. An increase in ROS acting on Kv channels is implicated in the whole cell recordings; however in intact cells this is not evident. Nevertheless, increasing cellular redox state through dialysis with 1mM GSH does modulate I_{Kv} directly and attenuate the effects of antimycin, mainly on activation. A predominant role for mitochondrial derived ROS in the regulation of I_{Kv} may not be

supported, however changes in the I_{Kv} activation do occur in the presence of increased ROS and, therefore, there is an involvement of ROS in Kv channel regulation in PASMCs (Fig. 3.7 & 3.9-10). Changes in intracellular ROS are not easy to confirm because dyes such as dichlorofluorescein (DCF), luminol and lucigenin are generally deemed as unreliable fluorescent indicators of ROS, for example they may detect extracellular NADPH oxidise induced ROS instead of intracellular changes (Wolin *et al.*, 2005). However a, perhaps more reliable, FRET-based intracellular sensor has recently shown a hypoxia induced increase in ROS (Guzy *et al.*, 2005). This increase in ROS is unlikely to act directly on Kv channels, but may influence their activity or expression indirectly via increasing ET-1 (Wang *et al.*, 2006) or stabilising HIF-1α (BelAiba *et al.*, 2004; Mansfield *et al.*, 2005; Chandel *et al.*, 2000).

3.2.5 Role of F_0F_1 ATP Synthase

As changes in ROS cannot solely account for the changes in the mitochondrial dependent regulation of I_{Kv} in PASMCs then it is possible that, by changing the proton gradient and $\Delta\Psi_m$, the F_0F_1 ATP synthase activity may be altered. Selective inhibition of ATP synthase with oligomycin affected I_{Kv} similarly to other mitochondrial inhibitors in spite of the fact that their effect on mETC electron flow is different. CCCP increases electron transport by increasing the permeability to H^+, uncoupling OXPHOS at $\Delta\Psi_m$ >140mV and driving electron flow (Kadenbach, 2003) and mETC inhibitors block the transport of electrons to more distal ETC complexes. A block of the ATP synthase, however, has no direct effect on the electron flow but may indirectly alter it due to an increased H^+ gradient (Andersson *et al.*, 1987). In addition, a reversal of the ATP synthase block by intracellular dialysis with Na_2ATP (Fig. 3.12 G&H) implies that changes in ATP levels are important in mitochondria-dependent regulation of I_{Kv}. Conversely, the lack of a complete reversal of the oligomycin-induced effects by the inhibition of the mETC with antimycin suggests that they might act synergistically. The experimental data presented here does not allow this question to be directly answered. It is, however, entirely possible that antimycin would be expected to reduce the synthesis of ATP and, through reversal of the ATP synthase, accelerate its consumption secondary to mitochondrial depolarization. On the other hand oligomycin, by binding to the ATP synthase blocking the proton channel, has no direct effect on the electron chemiosmotic gradient and thus has no effect on state 4 respiration. Although the exact

to the ATP synthase blocking the proton channel, has no direct effect on the electron chemiosmotic gradient and thus has no effect on state 4 respiration. Although the exact mechanism is still unclear, a switch from state 3 (active respiration utilising substrate ADP) to state 4 (controlled after an increase in conversion of ADP to ATP) respiration as a result of intracellular ATP being elevated (Nicholls, 2004) might be responsible for a combined effect of the inhibitors. Such effects on mitochondrial ATP levels/synthesis have additionally been proposed to possibly alter the production of an unknown signalling molecule in rat carotid body type 1 cells which is involved in the regulation of ion channel function (TASK channels in this particular investigation) (Wyatt & Buckler, 2004).

3.2.6 Mg^{2+}_i as a mitochondrial mediator

The ATP-dependence of the oligomycin-induced shifts in both I_{Kv} activation and inactivation might indicate the involvement of a phosphorylation-mediated process as the end point of the mitochondria-mediated regulation of the Kv channels. However, my findings in this and previous chapters, showing that: i) Na_2ATP has a greater ability to reverse the effect of antimycin on I_{Kv} activation and $I_{Kv(50)}$ block compared to MgATP, ii) EDTA, a more potent chelator of Mg^{2+} than EGTA, inhibits of antimycin-induced effects on I_{Kv} voltage dependent characteristics iii) elevation of Mg^{2+}_i (Fig. 3.16), significant attenuates the antimycin induced effects and iv) CCCP and antimycin significantly increase Mg^{2+}_i (Fig. 3.15), strongly suggest that mitochondria-mediated changes in Mg^{2+}_i play a pivotal role in the regulation of Kv channels in PASMCs, possibly in addition and/or subsequent to changes in the ATP/ADP ratio. Additionally, in PSS, both Na_2ATP and EDTA strongly buffering Mg^{2+}_i shifted V_a to more positive potentials (-9.6±1.6 mV, n=21, p<0.0006 and -8.1±1 mV, n=22, p<0.002, respectively) and shifted V_h to more positive potentials (only significant for Na_2ATP, Table 3.8); the significant negative shift in V_h when Mg^{2+} is elevated (Fig. 3.16) is also supportive.

A lack of effect of increased Mg^{2+} alone on V_a may either indicate that the control (0.5 mM $MgCl_2$) was sufficient Mg^{2+}_i to maximise effects on I_{Kv} or that 5 mM $MgCl_2$ was insufficient to change Mg^{2+}_i or that there may be an additional factor which contributes to modulation of I_{Kv} activation, but is suppressed in high Mg^{2+}. This factor could be of mitochondrial origin (e.g. ROS or ATP production) or represent an unknown cellular

intermediate. There is very little known in the pulmonary circulation regarding intracellular Mg^{2+} regulation, however, the conclusions above are supported by the observations of the effect of mitochondrial depolarisation or inhibition of oxidative phosphorylation on Mg^{2+}_i in cardiac myocytes (Leyssens *et al.*, 1996) and in PC12 cells (Kubota *et al.*, 2005). In particular, both studies surmised an increase in $[Mg^{2+}]_i$ in response to FCCP to be associated with the release of Mg^{2+}_i following ATP hydrolysis by the mitochondrial F_1F_0-ATPase. Importantly, with respect to Kv channels, Tammaro *et al* (2005) have also shown increases in $MgCl_2$ in the pipette solution significantly shifted the activation of Kv1.5 and Kv2.1 channels (known to be expressed in PASMCs and potentially involved in HPV, (Archer *et al.*, 1998; Hogg *et al.*, 2002; Pozeg *et al.*, 2003), expressed in *Xenopus* oocytes, to more negative potentials (Tammaro *et al.*, 2005).

Changes in Ca^{2+}_i, which would also occur under these conditions (Fig. 3.18) (Kubota *et al.*, 2005; Wyatt & Buckler, 2004), are unlikely to contribute to the observed effects because: 1) data were obtained from cells where free $[Ca^{2+}]_i$ was strongly buffered with EGTA (~10 nM); 2) cell dialysis with 220 nM Ca^{2+} alone caused a significant rightward shift in I_{Kv} activation, opposite to that caused by the mitochondrial inhibitors.

The results presented so far provide, for the first time, evidence for the existence of a novel mitochondria-dependent mechanism of Kv channel regulation, occurring via local changes in Mg^{2+}_i homeostasis. This hypothesis is summarised in Fig 3.19. As shown in this figure a primary factor influencing Mg^{2+}_i is the change in the $\Delta\Psi_m$ upon inhibition of the mETC leading to local changes in the ATP-to-ADP ratio. Furthermore, reduction in $\Delta\Psi_m$ itself would reduce the electrophoretic diffusion force which drives Mg^{2+}_i into mitochondria causing a further increase in $[Mg^{2+}]_i$. Resulting increases in the local concentration of Mg^{2+} ions are known to act on Kv channels changing their voltage-dependency (Tammaro *et al.*, 2004; Lopatin & Nichols, 1994). Additionally, Mg^{2+} can directly block Kv channels by interfering with K^+ efflux from the cytosol (Tammaro *et al.*, 2004; Tammaro *et al.*, 2005; Gelband *et al.*, 1993), thus explaining I_{Kv} inhibition at positive potentials.

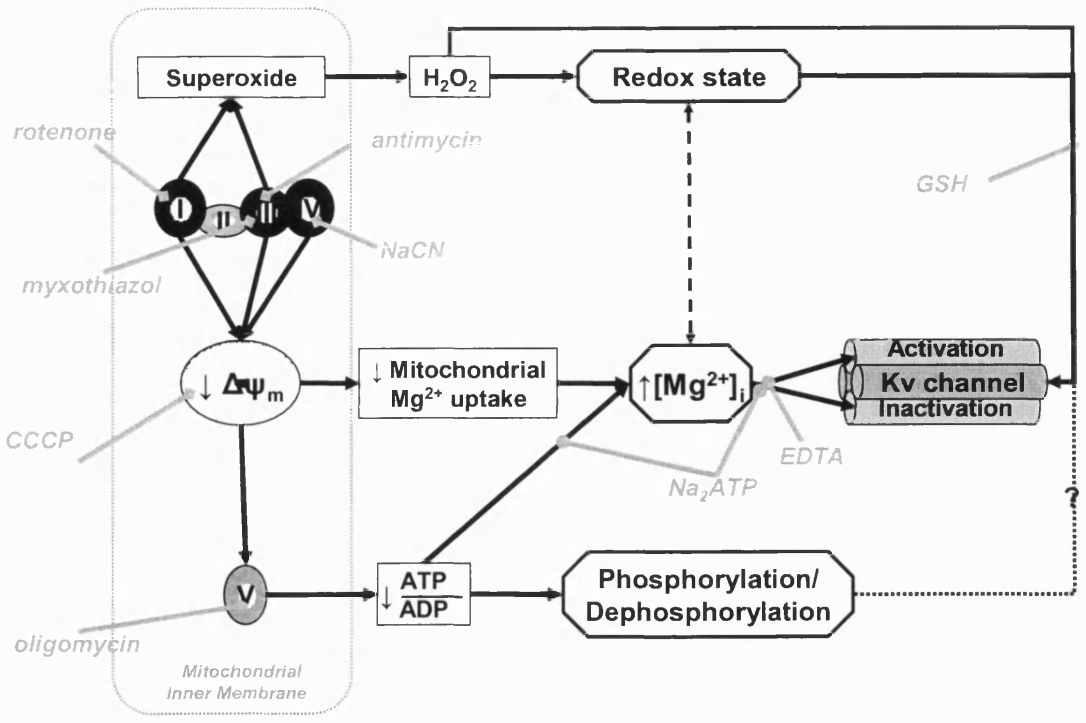

Figure 3.19 Hypothetical mechanism of mitochondrial-mediated regulation of Kv channels in PASMCs. Sites of action of inhibitors and reagents used in this study are shown in grey. Dashed lines indicate possible, yet to be confirmed, ways of interaction.

Influenced by both cellular redox state and by the ATP-to-ADP ratio this mechanism might serve as an important link between redox state (Archer *et al.*, 1993) Kv channels (Michelakis *et al.*, 2004) and ATP-dependent phosphorylation (Yuan *et al.*, 1995). Although, a direct affect of ROS on Kv channels unlikely under physiological conditions, the results with GSH could indicate an indirect modulatory role. The current findings do not allow for this to be completely answered, however, increased ROS production at complex III in the presence of antimycin, which leads to rapid $\Delta\Psi_m$ reduction, ATP depletion and rigor contraction of cardiac myocytes, could be one possible explanation (Hudman *et al.*, 2002). If this occurs in PASMCs, it could lead to a greater increase in $Mg^{2+}{}_i$ and might be responsible for a greater effect of antimycin than that of other mETC inhibitors (Fig. 3.2) and its attenuation in the presence of GSH (Fig. 3.7).

Additive effects of antimycin and oligomycin (Fig. 3.13) and significant differences between the control antimycin-mediated effects and those in cells dialysed with MgATP

(Fig. 3.14) do not rule out a potential involvement of phosphorylation or dephosphorylation mediated process in I_{Kv} modulation as previously suggested (Yuan *et al.*, 1995). A simple mechanism could involve a direct phosphorylation of the channel protein causing changes in the number of negative surface charges, thus leading to the alteration of static Mg^{2+} interactions and thus Kv channel gating (Perozo & Bezanilla, 1990). Conversely, more complex interactions involving the actin cytoskeleton organization also cannot be excluded and has been demonstrated for the Kv1.5 channels in Xenopus laevis oocytes (Mason *et al.*, 2002). An alternative possibility is that antimycin and oligomycin could influence Mg^{2+}_i via different pathways. Antimycin could impose a stronger influence over $\Delta\Psi_m$ and the, non-specified, uptake and release mechanisms of Mg^{2+} by the mitochondria, oligomycin could exert a stronger influence over ATP hydrolysis, decreasing ATP-to-ADP ratio and thus decreasing the binding affinity for Mg^{2+} (Leyssens *et al.*, 1996).

Despite the substantial evidence presented here favouring an involvement of Mg^{2+}_i it is not possible to determine the exact contribution of ATP and Mg^{2+}_i to the changes in I_{Kv} as modulation of the concentrations of these components in the vicinity of the channels is not easily achievable. It has been previously proposed a limited diffusion space exists close to Kv channels in PASMCs (Smirnov & Aaronson, 1994). Complete inhibition of the H_2O_2 mediated shifts in I_{Kv} by cell dialysis with GSH and a significant attenuation of the antimycin induced shifts by EDTA and GSH suggests that in the dialysed cells this compartment is relatively well controlled under conditions when the pipette solution is equilibrated with the cell interior. It is possible that there may be either an under or over estimation of the potential effects on I_{Kv}, as seen with the perforated patch technique with maintained cellular integrity, where a significant decrease in the effects of antimycin was evident, compared to those in WC recordings.

Chapter 4

EFFECT OF HYPOXIA ON I_{KV} ACTIVATION AND INTRACELLULAR Mg^{2+} IN PASMCS

4.1 Introduction

Kv channels have been proposed to have an important, yet controversial, physiological role in the cellular response to hypoxia. Despite being proposed to be molecular correlates for O_2 sensing in PASMCs (López-Barneo, 1994) it is more generally accepted that their function in altered by a factor stimulated by hypoxia causing inhibition of the channel, membrane depolarisation and subsequent Ca^{2+} entry through L-type VDCC. Kv channel inhibition was proposed reflecting data that showed a decreased I_{Kv} amplitude and membrane depolarisation in response to acute hypoxia in both rat and mouse PASMCs (Archer *et al.*, 1993; Archer *et al.*, 2001; Yuan *et al.*, 1993; Turner & Kozlowski, 1997; Archer *et al.*, 2004). Additionally, effects on amplitude were often only compared at more positive potentials, outside a physiological range, and therefore investigating the kinetics and parameters of channel activation and inactivation may provide a more accurate picture of Kv channel regulation in PASMC during hypoxia. For these reasons, the effects of acute (25-40 mmHg) hypoxia was investigated on the channel characteristics and comparisons were made to those observed for mitochondrial inhibition described in the previous chapter.

4.2 Results

4.2.1 Measurements of hypoxia levels in the electrophysiological recording chamber

Due to the small size of the experimental chamber (100-200 µl) it was not possible to simultaneously measure changes in O_2 level and current recordings. Therefore, the level of hypoxia was measured separately using an ISO_2 oxygen meter (WPI Incorporation, USA) under the same conditions as for electrophysiological recordings. A mean level of hypoxia of 30±3 mm Hg (n=6, with variation ranging from 22 and 40 mm Hg) was achieved 5 min after the perfusion (~1 ml/min) of the recording chamber with PSS saturated with 100% N_2 (Fig. 4.1). The control PSS was bubbled with air.

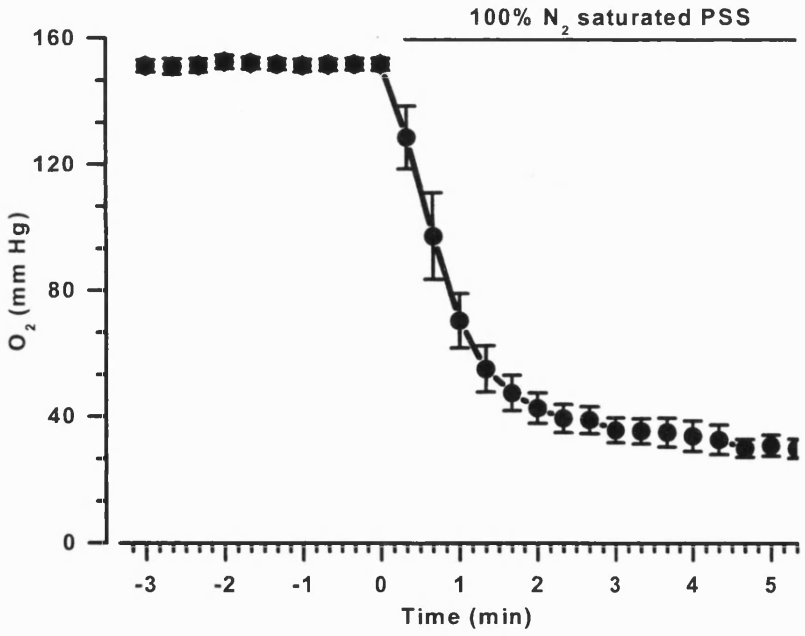

Figure 4.1. Oxygen level changes in the electrophysiological recording chamber during hypoxia. Each symbol represents the mean of 6 separate measurements. The position of the oxygen electrode, the perfusion tube and the suction outlet was altered during each measurement to account for possible variations in O_2 levels during electrophysiological recordings.

4.2.2 Effect of acute hypoxia on I_{Kv} activation in intact PASMCs

To address a potential relevance of the mitochondrial dependent changes in I_{Kv} to HPV and its specificity to PASMCs, I_{Kv} activation was compared during acute hypoxia in non-dialysed PASMCs and MASMCs. Hypoxia caused a significant enhancement in I_{Kv} in PASMCs at negative potentials (Fig. 4.2 A) associated with a significant leftward shift in the activation dependency in PASMCs, but not in MASMCs (Fig. 4.2 B). Additionally, a significant increase in the dependency of the steady state activation was observed only in PASMCs shifting it from 8.7±0.8 mV to 7.4±0.6 mV (n=6, $p<0.018$) reflecting changes observed for antimycin in intact cells (Fig. 3.6). The effect on the peak I_{Kv} amplitude was not significant in either tissue at this level of hypoxia at any membrane potential (Table 4.1).

It is noteworthy that, although the data does not show a significant hypoxia-mediated inhibition of the *peak* Kv current as other researchers have suggested (Post *et al.*, 1992; Hogg *et al.*, 2002; Archer *et al.*, 2004), if the block is calculated at the end of pulse to +50 mV a small 8.4±7.1 % (n=6) but significant ($p<0.05$, one-tail t-test) decrease was observed. Also, to monitor the cell state and the development of the effect, the ramp protocol was applied every 20 sec between recording the I-Vs with the step protocol. By ramping the voltage between -100 and +100 mV a wider voltage range was used to measure the tail currents. Analysis of the ramp data demonstrated both significant activation of the I_{Kv} in the negative voltage range and a small (5-8 %) but significant ($0.02<p<0.05$, paired two-tailed *t*-test) hypoxia inhibition of the whole cell Kv current between +45 and +100 mV in 12 cells studied. The difference in the cell number is because some cells died before the recording of the second I-V was completed. Importantly, inhibition of the current was only obvious at positive, non-physiological, membrane potentials and, although it may help to elucidate the mechanisms involved, it is unlikely to have a major impact on cell excitability under these conditions.

TABLE 4.1. Effect of hypoxia on I_{Kv} activation recorded in perforated-patch mode in PASMCs and MASMCs arterial smooth muscle cells.

	Steady-state I_{Kv} activation and $I_{Kv(50)}$ block				
	V_a (mV)	k_a (mV)	ΔV_a (mV)	$I_{Kv(50)}$ *block* (%)	*n*
PASMCs					
Control (air)	-5.1±1.5	8.7±0.8			
Hypoxia (30 mm Hg)	-13.3±0.7 (p<0.0009)	7.4±0.6 (p<0.018)	-8.2±1.1	3±6.7	6
MASMCs					
Control (air)	-9.5±2	9.8±1.9			
Hypoxia (30 mm Hg)	-7.6±2.8	10.8±1.4	1.8±1.7	-5.1±4.8	6

Note that the negative values for $I_{Kv(50)}$ block in MASMCs indicates an enhancement of I_{Kv}.

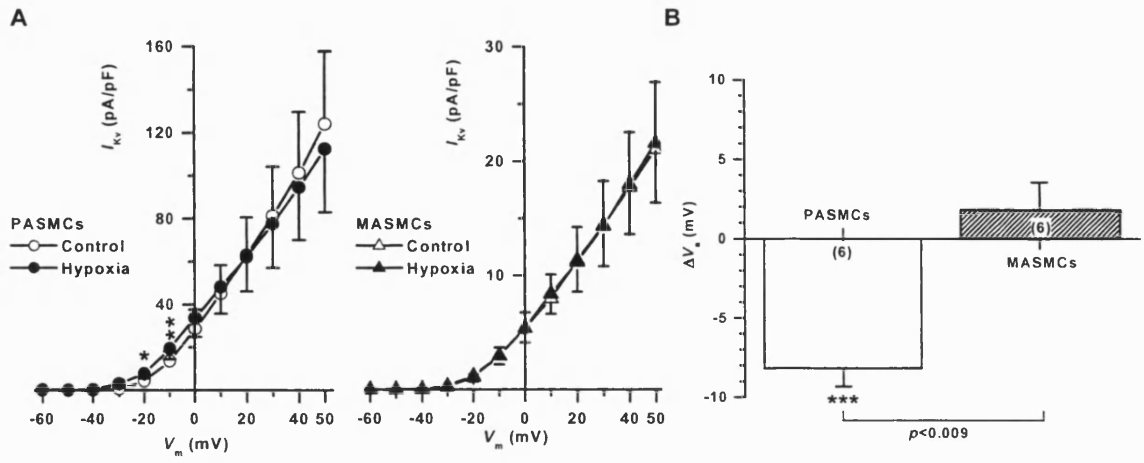

Fig 4.2 Comparison of the effect of acute hypoxia on I_{Kv} I-Vs (A) and ΔV_a (B) in PASMCs and MASMCs. All experiments were performed in the perforated-patch mode.

4.2.3 Hypoxia causes an increase in free $Mg^{2+}{}_i$

The results described in chapter 3 strongly suggest that $Mg^{2+}{}_i$ is involved in the regulation of I_{Kv}. Currently, $Ca^{2+}{}_i$ has been shown to be elevated in hypoxia, however, direct measurements of changes in $Mg^{2+}{}_i$ during hypoxia have not been performed in PASMCs. Mg^{2+} has been measured in hepatocytes where it increased from 0.63±0.05 to 1.42±0.11 mM during hypoxia (Brecht & De Groot, 1994). Furthermore, increase in $Ca^{2+}{}_i$ and $Mg^{2+}{}_i$ in response to mitochondrial inhibition has previously been demonstrated in cardiac myocytes (Leyssens *et al.*, 1996), but not in pulmonary arteries. Therefore, the effect of hypoxia was investigated in intact PAs and PASMCs loaded with Mg^{2+}-sensitive dye, MagFluo-4-AM.

A 20 min exposure of whole PAs to hypoxia (25-40 mmHg) caused a significant increase in free $Mg^{2+}{}_i$ which reaches its peak within 4-5 min and then slowly recovers following re-oxygenation (Fig. 4.3 A). The specificity of $Mg^{2+}{}_i$ measurement with MagFluo-4-AM was confirmed by the lack of response to 80 mM KCl (Fig. 4.3 B), that would be expected to cause a significant increase in $Ca^{2+}{}_i$ (Kobayashi *et al.*, 1986).

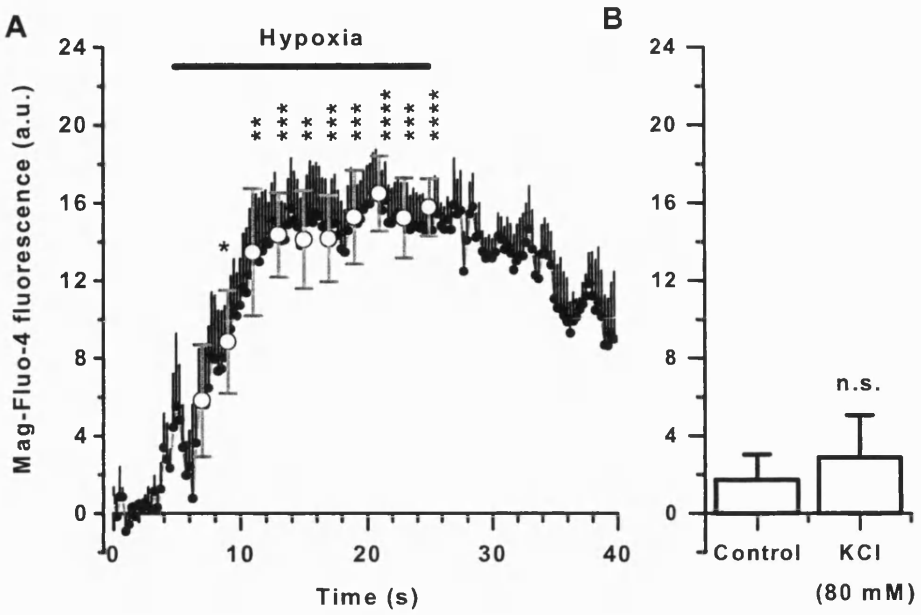

Figure 4.3. Hypoxia-induced increase in free Mg^{2+}_i (n=7) (A). (B) Lack of effect of KCl on Mg^{2+}_i (n=13). (A) and (B) were measured in endothelium-denuded whole PAs in the presence of 10 μM wortmannin. Intensities were normalised to the peak MagFluo-4 fluorescence measured in A23187 and compared using paired *t*-test. Dr. Kathryn Yuill contributed to this figure.

4.3 Discussion

4.3.1 Effect of hypoxia on I_{Kv} activation

The main observation in this chapter was that hypoxia causes activation of I_{Kv} at negative membrane potentials in intact PASMCs. This effect was not observed in MASMCs. Although this observation is apparently against the current opinion that hypoxia should inhibit Kv channels, activation of the whole cell K^+ currents by hypoxia was previously observed in canine (Post *et al.*, 1992) and rat (Archer *et al.*, 2004) PASMCs. This was, however, ignored and not discussed by the researchers.

The similarity between the effects of hypoxia on I_{Kv} activation to that of antimycin, as discussed in chapter 3, may reflect a mitochondrial dependent component serving a protective role in the response of PASMCs to the early stages of the detection of hypoxia. It is therefore entirely possible that the observations of cell depolarisation in response to hypoxia reported previously (Archer *et al.*, 1998) could initially be induced by another mechanism such as inhibition of TASK channels (observed in rat PAs (Gurney & Joshi, 2006), human PAs (Olschewski *et al.*, 2006) and rat carotid body type 1 cells (Wyatt & Buckler, 2004)) and/or Ca^{2+} entry via activation of SOCC and ROCC channels, for which the molecular correlates are proposed to be TRP channels (Kunichika *et al.*, 2004). Additionally, inhibition of I_{Kv} amplitude may occur once the cell becomes more depolarised enhancing, rather than initiating depolarisation and contraction, which may explain the initial lack of effect of hypoxia on Kv1.5 channels (Archer *et al.*, 1998) and why only poor attenuation of HPV in whole lung preparations after treatment with 5 mM 4-aminopyridine and 10 mM TEA was seen (Hasunuma *et al.*, 1991). Increased Ca^{2+} can cause activation of Ca^{2+} activated chloride channels also causing membrane depolarisation (Pacaud *et al.*, 1989). Additionally, at P_{O2} of 60-80 mmHg there is a lack of depolarisation and Kv channel inhibition (Olschewski *et al.*, 2002), though HPV is still triggered. The proposed role of $Mg^{2+}{}_i$ in the regulation of Kv channels by hypoxia is further supported by hypoxia-induced increases in $Mg^{2+}{}_i$ in intact arteries. This is the first observation of this kind in the PA, although it has previously been demonstrated in hepatocytes (Brecht & De Groot, 1994; Gasbarrini *et al.*, 1992) and cardiac myocytes (Silverman *et al.*, 1994) that anoxia also causes increased $Mg^{2+}{}_i$.

4.3.2. Effect of hypoxia on I_{Kv} block

Interestingly, 20-40 mmHg used in these experiments did not cause a decrease in I_{Kv} amplitude as previously observed by other groups (Archer *et al.*, 2004; Hogg *et al.*, 2002; Yuan *et al.*, 1993; Turner & Kozlowski, 1997; Archer *et al.*, 1996). In fact, a significant inhibition of the whole-cell K^+ currents in rat PASMCs over the negative range of membrane potentials was actually only reported by two groups, Hogg *et al.*, (2002) and Olschewski *et al.*, (2002). The majority of workers, who originally studied the effect of acute hypoxia on the whole-cell K^+ currents in both rat and mouse PASMCs (Archer *et al.*, 1993; Archer *et al.*, 2001; Archer *et al.*, 2004), have observed a significant inhibition only at membrane potentials positive +50 mV (the most positive membrane potential we have used in our study), whilst Patel *et al.*, (1997) reported the inhibitory effect of hypoxia only at +30 mV in cultured PASMCs, but failed to mention whether the effects were significant. Notably, Turner & Kozlowski, (1997), who did show a decrease of the current by hypoxia (20-30 mmHg) in PASMCs over the same range of membrane potentials, did not report any significance of the effect in either dialysed or non-dialysed cells. Therefore, the data presented in this chapter does not principally contradict the majority of the reports where the effect on the whole cell K^+ current was studied.

Differences may be due to the use of different experimental conditions; for example whole cell versus perforated patch. In general, experiments using the whole cell patch clamp technique observed greater inhibition of I_{Kv} (50-70 %), (Archer *et al.*, 2004; Hogg *et al.*, 2002). Additionally, a differential expression of Kv channel subtypes may affect the response to hypoxia; expression studies of Kv subunits, known to be expressed in PASMCs, in mouse L cells have shown that homomeric channels Kv1.2 and Kv2.1, but not Kv1.5 are reversibly inhibited by hypoxia; heteromeric channels composed of Kv1.2/Kv1.5 and Kv2.1/Kv9.3 are O_2 sensitive and reversibly inhibited by hypoxia in the physiological voltage range (Hulme *et al.*, 1999). It is worth noting that a recently reported finding that overexpression of the Kv1.5 α-subunit, one of the main components of the Kv channel in PASMCs, induced a hypoxia-sensitive Kv current only when the same channel was overexpressed in pulmonary, but not mesenteric arterial SMCs or HEK-293 or COS-7 cell lines (Platoshyn *et al.*, 2006), suggesting that hypoxia-sensitivity of Kv channels may be cell specific and not subunit-type specific.

Chapter 5

MITOCHONDRIAL DEPENDENT REGULATION OF I_{KV} IN MASMCS

5.1 Mesenteric circulation and hypoxia

In the early 1990s researchers, using mesenteric arteries directly compared the effects of hypoxia in systemic and pulmonary circulation in an attempt to try to elucidate the complex mechanisms involved in the phenomenon of HPV. In contrast to pulmonary circulation, no increase in artery tension (Yuan *et al.*, 1990) alongside a decrease in arterial pressure and increase in vascular conductance was observed in mesenteric arteries in response to hypoxic exposure (Langdown & Marshall, 1995). However, a transient and small initial contraction was observed in some experiments (Leach *et al.*, 1994). Additionally, hypoxia failed to attenuate I_{Kv} and caused little or no depolarisation in isolated MASMCs (Yuan *et al.*, 1993a). Figure 7.1, reproduced with kind permission of Prof. J.P. Ward, shows a typical example of the differences observed in the two phase response to hypoxia in PA and MAs (Leach *et al.*, 1994). A brief and much smaller contraction is initially observed followed by a sustained relaxation of MA pre-constricted with prostaglandin $F_{2\alpha}$ ($PGF_{2\alpha}$). It was therefore concluded that different mechanisms must exist in response to hypoxia that are inherent to particular smooth muscle types. With respect to Kv channels this conclusion was recently supported by the observation that the hypoxic sensitivity of the Kv1.5 channel is only seen in PAs and not in MAs (Platoshyn *et al.*, 2006).

As such tissue specificity exists to hypoxia it is therefore physiologically important to determine if the postulated mechanism of mitochondrial mediated increased $Mg^{2+}{}_i$ in the regulation of I_{Kv} is specific to the pulmonary circulation. Comparisons were therefore made for the effects of mETC inhibitors, ROS and ATP on I_{Kv} using cells isolated from mesenteric arteries.

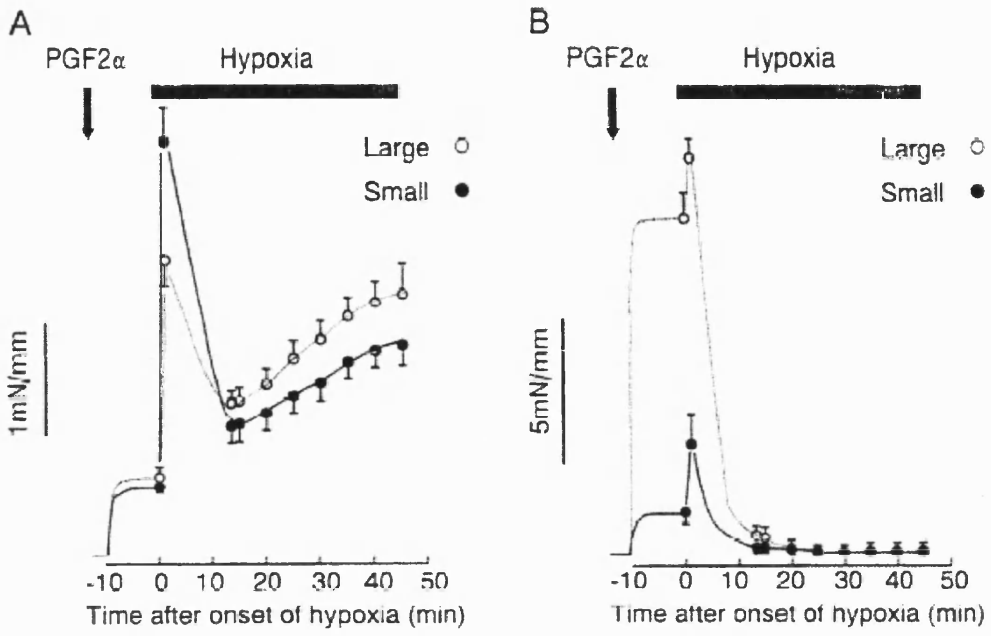

Fig 5.1 Different responses to hypoxia in pulmonary and mesenteric, large and small arteries. Pre-constriction with 10 μM $PGF_{2\alpha}$ followed by 50 minutes hypoxia in (A) pulmonary and (B) mesenteric arteries. Figure is reproduced from Leach *et al.*, 1994) with permission.

5.2 Results

The effects of H_2O_2, mitochondrial uncoupler CCCP and inhibitors antimycin and oligomycin, targeting the most pronounced effects in the PASMCs were compared in the MASMCs to assess the specificity of the mitochondrial dependent mechanism to the pulmonary circulation.

5.2.1 Effect of external H_2O_2

Similar to PAMSCs, 300 μM H_2O_2 was used to decrease intracellular redox state. In MASMCs, H_2O_2 caused a significant shift to more negative potentials in both the activation and inactivation dependencies. Notably the shift in activation was 5.2 mV larger than that in PASMCs with ΔV_a = -10.3±3.8 mV, $p<0.05$ and, more importantly V_h also shifted significantly with ΔV_h = -5.2±1.8 mV, $p<0.04$ (Fig. 5.2 A, B&D). Also, unlike in PASMCs no significant effect on the current amplitude was observed (Fig. 5.2 C).

5.2.2 *Effect of mitochondrial uncoupling and mETC Inhibition on I_{Kv}*

Incubation of MASMCs with 2 μM CCCP caused a parallel leftward shift in both I_{Kv} activation (ΔV_a=-9.9±3 mV, n=8, $p<0.02$) and inactivation (ΔV_h=-5.9±1.4 mV, n=8, $p<0.004$) dependencies (Fig. 5.3). No effect was observed on k_a, but k_h decreased from 8.5±0.6 mV to 7.1±0.4 mV (n=8, $p<0.03$). A small but significant I_{Kv} peak inhibition was also observed at +50 mV (13.6±4.5 %, n=8, $p<0.02$, Fig. 5.3 C). No acceleration of the current decay (shown in traces in Fig. 5.3 A&D) and therefore no significant effects upon the non-inactivating component were observed. These results, despite some differences, show that generally mitochondrial uncoupling also affects I_{Kv} in MASMCs in a similar way to those in PASMCs. Therefore, to investigate if any specific differences are observed between the two cell types the effects of complex III and ATP synthase inhibition by antimycin and oligomycin were studied in MASMCs since their effects were most pronounced in PASMCs.

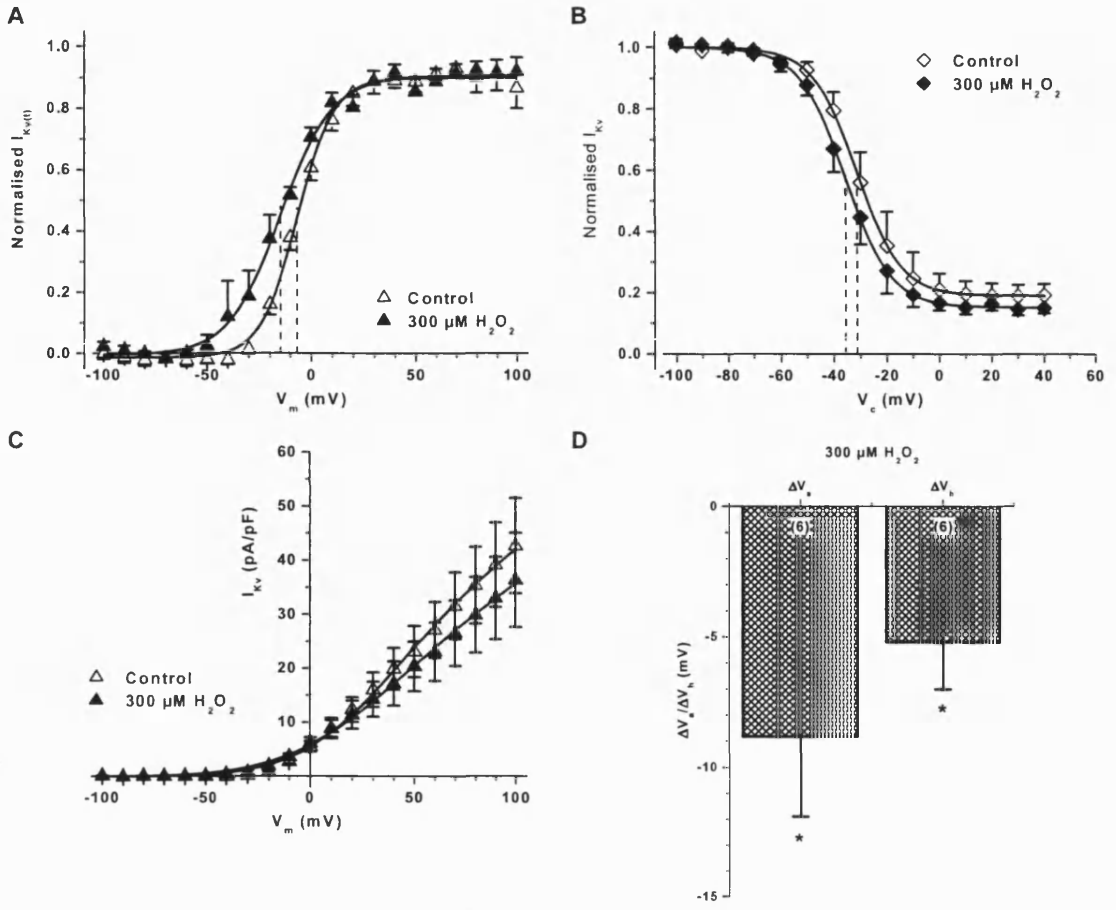

Figure 5.2. Effect of H_2O_2 on MASMCs. (A&B) Normalised average I_{Kv} activation and inactivation curves in the presence and absence of 300 μM H_2O_2. Cells were equilibrated for 5 minutes in H_2O_2 prior to recording. The dotted lines indicate V_a (A) and V_h (B). (C) Comparison of H_2O_2-induced changes in the peak I_{Kv} measured from a single exponential fit of the current activation at each V_m. (D) ΔV_a and ΔV_h for H_2O_2 in MASMCs.

As antimycin gave the most pronounced effects in PASMCs and was used for all subsequent studies, its effects were also compared in MASMCs. A significant effects on both activation and inactivation dependencies was still observed, with ΔV_a = -8±2.5 mV (n=12, p<0.008) and ΔV_h = -4.6±1.6 mV, (n=9, p<0.02); however the effect of inactivation was significantly smaller than that observed for the PASMCs (p<0.0007, see Fig. 5.4 A). An equivalent decrease in I_{Kv} block for antimycin to that in PASMCs was observed (32.9±5.3 %, n=12, p<0.002). Nevertheless, no effect

upon the slope of the steady state activation or inactivation dependencies nor the non-inactivating component was observed in MASMCs (Fig 5.4 C). In addition the non-inactivating component was significantly smaller under control conditions in MASMCs (Fig. 5.4 B) when compared to the larger non-inactivating component observed in PASMCs.

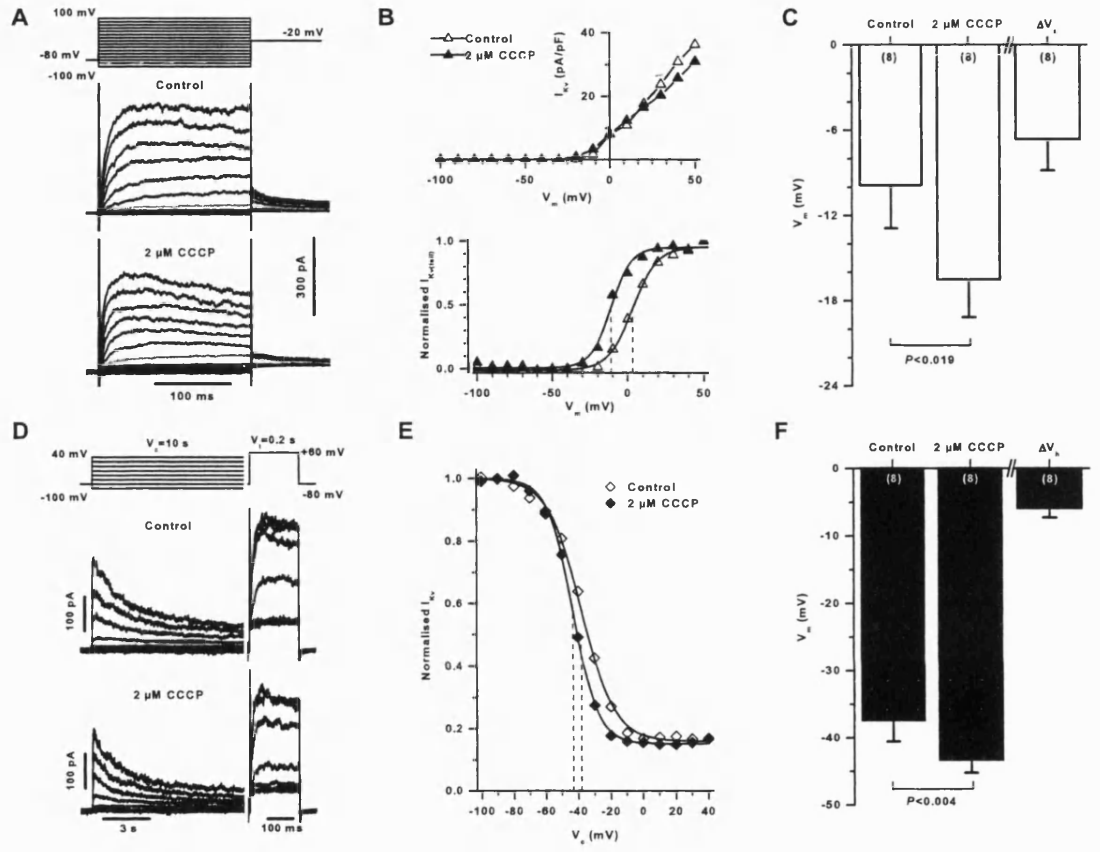

Figure 5.3. Effect of mitochondrial uncoupling with CCCP. A-C, Modulation of I_{Kv} activation. (A) Voltage protocol and original current traces recorded 5 min after pre-incubation of MASMCs with the mitochondrial uncoupler CCCP (2 μM). Note an enhancement of I_{Kv} amplitude at negative membrane potentials (compare the I_{Kv} traces at -30 mV shown in grey in panel A). (B) Comparison of CCCP-induced changes in the peak I_{Kv} measured from a single exponential fit of the current activation at each V_m, and normalised tail currents (upper and lower panel respectively). (C) The mean absolute (V_a) and relative (ΔV_a) changes in I_{Kv} activation (the latter was subsequently used for comparison). D-F, Effect on I_{Kv} inactivation. (D) Availability protocol and current traces recorded in the absence and presence of CCCP from a representative MASMC. (E) CCCP-induced changes in the normalised

I_{Kv} measured with the availability protocol. (F) The mean absolute (V_h) and relative (ΔV_h) changes in I_{Kv} inactivation. A and D were obtained from different cells with C_m=17.7 and 10.9 pF, respectively. Lines in B were drawn with V_a= 3.3 and -11.1 mV (dashed lines) and k_a=8.2 and 6.8 mV, for control and CCCP respectively. Lines in E were drawn with V_h=-37.6 and -43.2 mV (dashed lines) and k_h= 9.8 and 7.7 mV and the non-inactivating component equal to 0.16 and 0.15 in control and CCCP-containing solutions respectively.

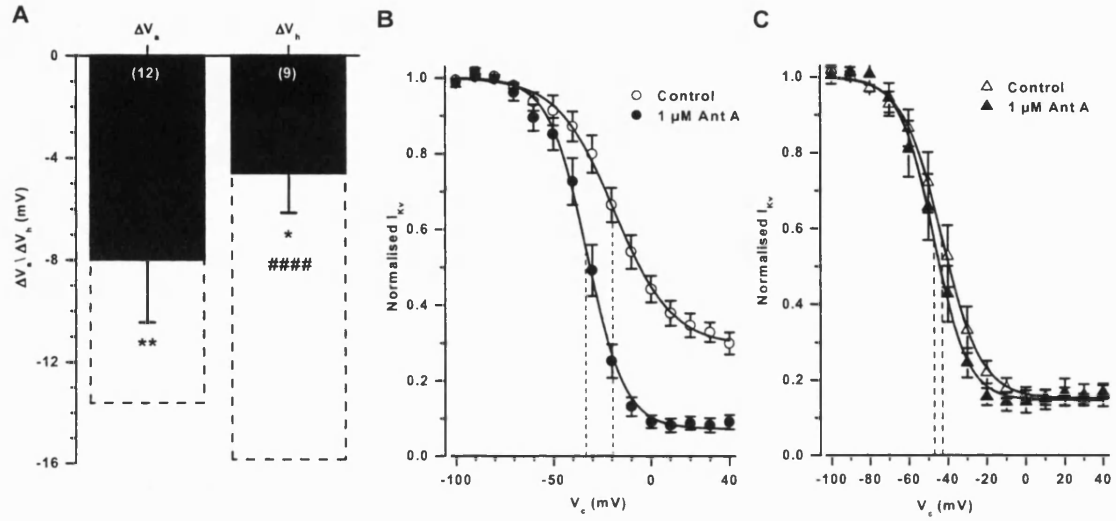

Figure 5.4. Comparison of the effects of antimycin on I_{Kv} in rat PA and MA SMCs. (A) Changes in activation and inactivation for MASMCs (black) and PASMCs (dotted). Normalised average I_{Kv} inactivation in PASMCs (B) and MASMCs (C). The dotted lines in (B) and (C) represent the absolute mean V_a and V_h values in the presence and absence of antimycin.

5.2.3 Effect of oligomycin on I_{Kv} in MASMCs

The inhibitor of ATP synthase oligomycin, which in PASMCs caused a shift comparable to that in antimycin, failed to significantly alter I_{Kv} activation in MASMCs. The effect in MASMC was significantly smaller than that in PASMCs ΔV_a = -3.6±3.6 mV (n=9, p<0.027, one tailed t-test to PASMC) (Fig 5.5 A&C). There was still, however, a significant reduction in I_{Kv} amplitude of 30.8±4.1 %, n=9,

$p<0.01$. Furthermore, this was significantly reduced in comparison to the PASMCs ($p<0.01$) (Fig. 5.5 C). Again, there was no effect upon the slope of the steady state inactivation dependency or the non-inactivating component (Fig. 5.5 B).

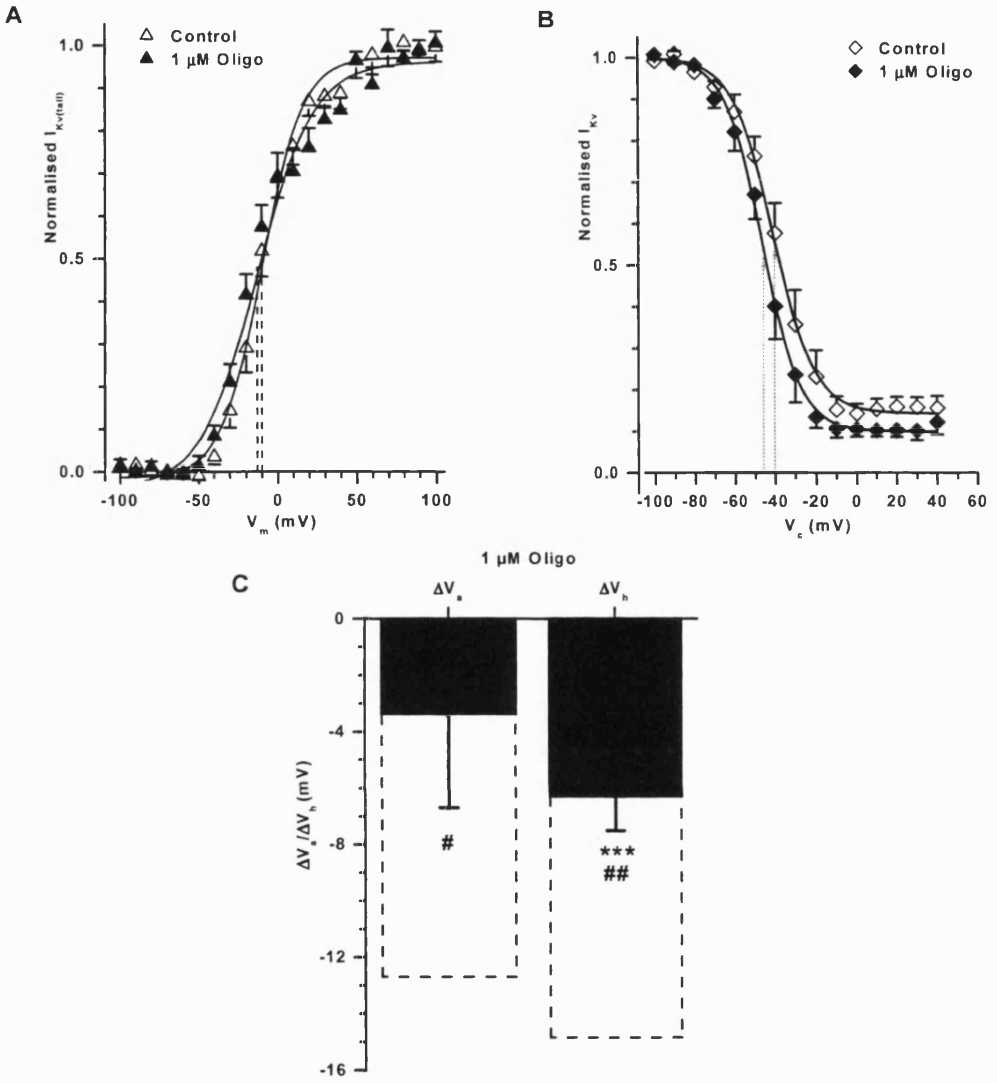

Figure 5.5. Effect of oligomycin on I_{Kv} in MASMCs. (A&B) mean normalised activation and inactivation dependencies fitted to the Boltzmann equation. The dotted lines indicate the V_a and V_h in the absence and presence of oligomycin (1 µM). (C) Relative changes in V_a and V_h for MASMCs (black bars) and PASMCs (shown as dotted bars for comparison).

TABLE 5.1. Effect of CCCP, antimycin, H_2O_2 and oligomycin on the voltage-dependent parameters of I_{Kv}.

	Steady-state I_{Kv} activation and $I_{Kv(50)}$ block					**I_{Kv} inactivation**				
	V_a (mV)	k_a (mV)	ΔV_a (mV)	$I_{Kv(50)}$ *block* (%)	n	V_h (mV)	k_h (mV)	A	ΔV_h (mV)	n
PSS	-9.9±3	9.5±0.7				-37.4±3.2	8.5±0.6	0.16±0.01		
CCCP (2 μM)	-16.5±2.7 (p<0.02)	11.2±0.9	-6.6±2.2	13.6±4.5 (p<0.02)	8	-43.3±1.9 (p<0.004)	7.1±0.4 (p<0.03)	0.15±0.00	-5.9±1.4	8
PSS	-11.2±2.9	4.6±2.7				-43.2±3.6	7.3±0.5	0.16±0.02		
Antimycin (1 μM)	-19.2±4.1 (p<0.008)	4.2±2.8	-8±2.5	32.9±15.3 (p<0.002)	12	-47.8±3.6 (p<0.02)	6.1±0.5	0.15±0.03	-4.6±1.6 (p<0.0007)[a]	9
PSS	-7.7±1.6	8.6±0.7				-29.6±4.1	6.7±0.2	0.19±0.04		
H_2O_2 (300 μM)	-17.8±5 (p<0.04)[b]	9.4±0.9	-10.1±4.6	8.9±14.4	6	-34.8±3.5 (p<0.04)	7.2±0.5	0.15±0.02	-5.2±1.8	6
PSS	-12.5±2.6	9.5±0.5				-39.4±3.4	8.7±0.5	0.13±0.02		
Oligomycin (1 μM)	-16.1±4	11.4±1.4	-3.6±3.6 (p<0.027)[a,b]	30.8±4.1 (p<0.01)	9	-45.7±3.2 (p<0.001)	7.6±0.5	0.1±0.02	-6.3±1.2 (p<0.01)[a]	9

Here and in subsequent Tables p values show significant differences between the values measured in control conditions and in the presence of the tested inhibitor obtained in the same MASMCs (paired two-tail t-test) unless indicated otherwise.

[a] represents significant difference in comparison to the same condition in PASMCs.

[b] represents significance with a paired one-tail t-test.

5.3 Discussion

Although there were similarities, particularly with CCCP, the data in this chapter serves to highlight substantial differences in the mETC mediated regulation of I_{Kv}. Such differences include: 1) H_2O_2 induced larger shifts in ΔV_a and caused a significant negative shift in ΔV_h in MASMCs (an effect not observed in PASMCs); 2) antimycin had a much smaller effect on both parameters, with ΔV_h being significantly reduced in comparison to PASMCs; 3) oligomycin had virtually no significant effect on the steady-state activation of I_{Kv} in MASMCs, although a small shift in ΔV_h, which was significantly smaller than that in PASMCs, was observed. Interestingly, the block of I_{Kv} at +50mV observed in all conditions, except H_2O_2 in MASMCs, mimicked that observed in the PASMCs (Fig. 5.2).

In conclusion, although mETC inhibition caused an effect on I_{Kv}, there are significant differences between the two preparations, indicating that either different mechanisms or a differential association between the mitochondria and Kv channels in MASMCs. In addition, there was a lack of the effect of hypoxia in MASMCs, described in chapter 4. Hypoxia has recently been shown to have little effect on I_{Kv} in MASMCs in a study which suggested that differential expression of the Kv1.5 channel could account for the hypoxia-sensitive mechanism essential for inhibition of channel activity exclusively in PASMCs (Platoshyn *et al.*, 2006).

Since a detailed investigation of the mechanism of mETC inhibitions has not been performed to the same degree as in PASMCs, it is difficult to comment on the mechanisms of the observed differences. Indeed, unpublished observations from our lab indicate that the effects of Mg^{2+}_i on I_{Kv2} in conduit PASMCs and on I_{Kv} in aortic SMCs (both assumed to be Kv2.1 mediated currents) (Tammaro *et al.*, 2005; Smirnov *et al.*, 2002) were also different, suggesting that possible variations in the channel structural organisation could be an important factor in determination of tissue specificity of Mg^{2+}_i-mediated effects. A possible involvement of other channel subtypes is supported, though indirectly, by the lack of non-inactivation component in MASMCs under control conditions.

The understanding of these differences between the Kv channel structure and Mg^{2+}_i represent an interesting and challenging task and remain to be fully elucidated using the approaches described in this thesis. Additionally, to assess the contribution of H_2O_2 to the mitochondrial dependent regulation of I_{Kv} in MASMCs further experiments, reflecting those characterising the effect in PASMCs in chapter 3, are essential to understand the precise mechanism of differences between the PA and MA.

Chapter 6

FUNCTIONAL RELEVANCE OF THE MITOCHONDRIAL DEPENDENT REGULATION OF I_{KV}.

6.1 Introduction

The processes of activation and inactivation of I_{Kv} can be used to describe the dependence of the whole cell open probability of Kv channels on membrane potential (Leblanc *et al.*, 1994). Data can be compared by deriving "whole cell open channel probability" (whole cell P_o) as a product of the average I_{Kv} activation and availability in each condition. The "window current" is represented by the area under the curves and defines the range of V_m where ion channels should always be open. Analysis of the "window currents" can be used to create predictive models illustrated in Fig. 6.1

Since mitochondrial inhibition affected I_{Kv} in both cell types, although to a different degree, it is important to evaluate whether changes in the I_{Kv} voltage dependent characteristics (with CCCP, antimycin, oligomycin or H_2O_2) observed in PASMCs would have the same impact on the theoretical window currents as in MASMCs.

In PASMCs the mitochondrial uncoupler, CCCP, had a dual effect on the predicted window currents. At membrane potentials negative to -20 mV there is a marked enhancement of the whole cell P_o, whereas above this potential the whole cell P_o decreases (Fig. 6.1 A). However, in MASMCs, in the physiological range of membrane potentials there is an only an increase in whole cell P_o in the presence of CCCP (Fig 6.1 B).

Antimycin and oligomycin mimicked the dual effects on whole cell P_o that were predicted for CCCP in PASMCs (Fig. 6.1 C&E) Again, in MASMCs the predicted whole cell P_o for CCCP was mimicked by antimycin (Fig 6.1 D). With oligomycin a small reduction in whole cell P_o was predicted at membrane potentials above -30mV (Fig 6.1 F).

Interestingly, H_2O_2 mimicked the effects of CCCP in both PA and MA SMCs. In PASMCs it had the most pronounced increase in P_o in the negative range of membrane potentials, at potentials above 0 mV there was some reduction in P_o. The predicted window current for H_2O_2 in MASMCs show a relatively small reduction in the P_o for Kv channels below -50 mV, above this there is a predicted increase in P_o (Fig. 6.2).

This theoretical consideration, despite some similarity in the action of mETC inhibitors in PA and MA SMCs nevertheless suggest that the overall impact on Kv channels should be different in the physiological range of membrane potentials. It is therefore important to consider if a mechanism involving a mitochondrial dependent regulation of I_{Kv} had effects upon the regulation of intact artery contractility, as would be predicted by the proposed theoretical window currents. From the predicted window currents it would be expected that that application of mETC inhibitors will increase the excitability of PAs when the cell membrane is depolarised above the resting potential of -30 mV. In MAs an increased excitability would be expected reflecting the predicted window currents.

Therefore, the effects of mETC inhibition with CCCP and antimycin and increased ROS were studied in intact small PAs with a particular focus on K^+ dependent mechanisms. All the data presented thus far is precisely focussed on the regulation of Kv channel currents, it must be remembered that the situation is a whole artery is much more complex as other channels/exchangers are known to be present (see Chapter 1) and involved in the regulation of pulmonary arterial tone.

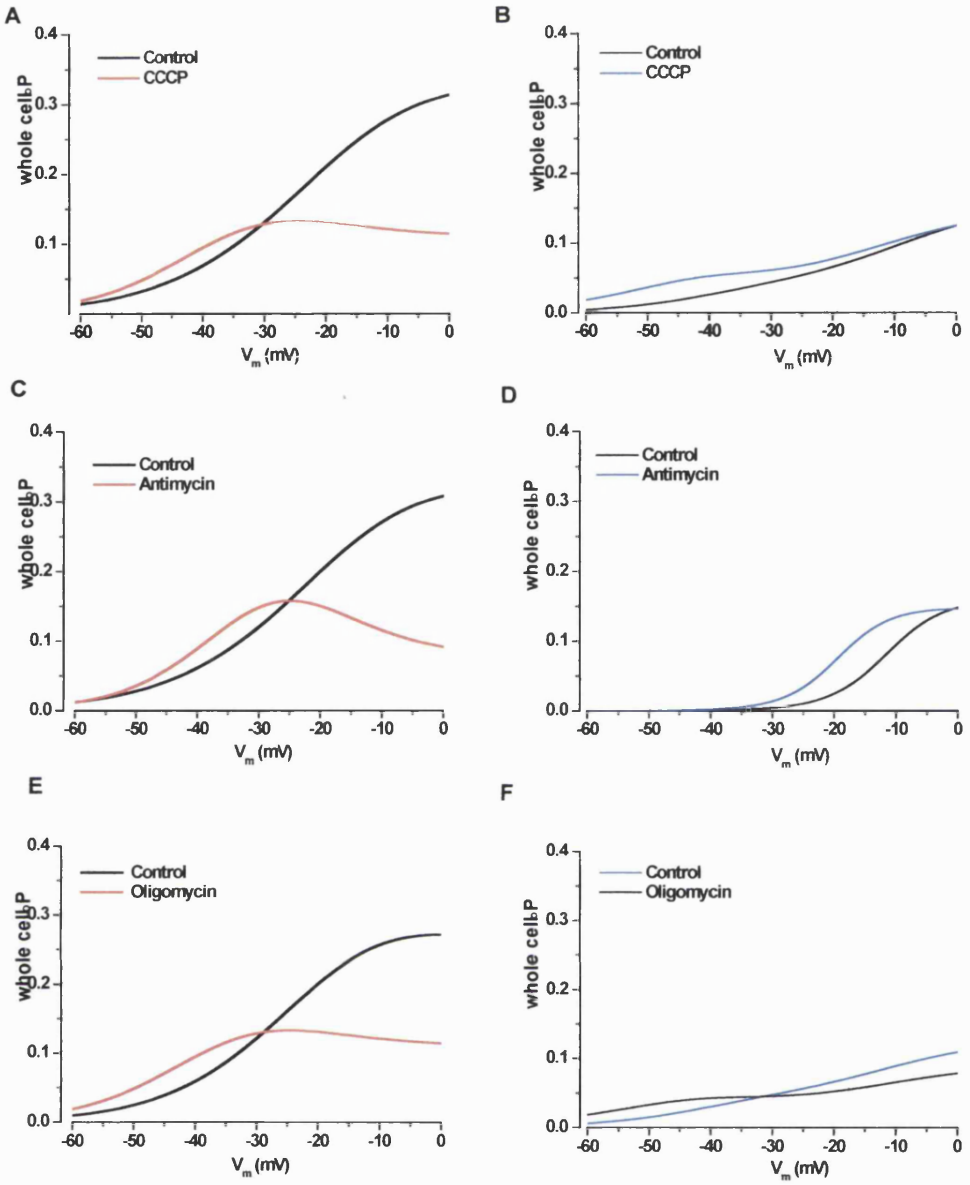

Figure 6.1. Effect of mETC inhibitors on Kv channel window currents in PA and MA SMCs. Theoretical window currents for CCCP, antimycin and oligomycin in PASMCs (A, C & E, respectively) and MASMCs (B, D and F, respectively).

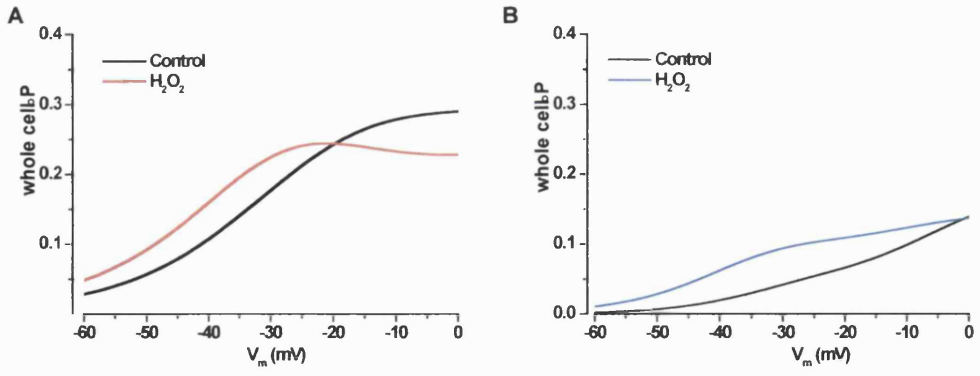

Figure 6.2. Effect of H_2O_2 on Kv channel window currents in PA and MA SMCs (A) and MASMCs (B). Theoretical window currents in the absence and presence of H_2O_2 (300 μM).

6.2 Results

It is important to note that all experiments were carried out in pairs in a two vessel myograph where for each experiment one PA and one MA from the same rat were mounted, ensuring consistency of the data. The vessel internal diameters were routinely estimated for all vessels used in myograph experiments; the average vessel size was 351.4±12 μm in PA (n=86) and 215.7±5.6 μm in MA (n=78). To assess the physiological significance of the mitochondrial dependent regulation of I_{Kv} in PAs preliminary data was acquired looking at the effects of 1) uncoupling mitochondrial membrane potential with CCCP, 2) blocking the mETC distally with antimycin, and 3) increasing ROS levels with H_2O_2, either directly on vessel tone or on a DR to increasing K^+ concentration (reflecting stepping changes in the membrane potential, predominantly via inhibition of K^+ channels causing depolarisation).

6.2.1 Effect of mitochondrial uncoupling on intact PA and MA

Uncoupling of the mitochondrial proton gradient using CCCP (2 μM, 10 minute exposure) caused an increase in vessel tone in only the PA, which was significantly larger then the effect in the MA (p<0.042) where there was no change in vessel tone observed (Fig. 6.3).

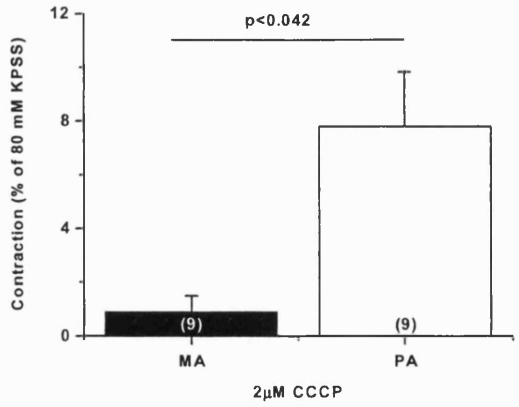

Figure 6.3. Effect of CCCP on intact PA and MA. Exposure of PA and MA to 2 μM CCCP for 10 minutes, peak contraction obtained in the 10 minute period is shown.

6.2.2 Effect of extracellular Ca^{2+} on CCCP response in MA and PA

The dependence of the CCCP induced contraction on extracellular Ca^{2+} was assessed in two experiments; one using 5 μM diltiazem to inhibit L-type VDCC and one in the presence of Ca^{2+} free Krebs supplemented with 1 μM EGTA. In the PA, where CCCP induced an increase in vessel tone, diltiazem (5 μM) reduced the contraction by approx 50% (Fig. 6.4 A&B) and removal of extracellular Ca^{2+} also reduced but did not prevent the contraction, supporting a component of depolarisation mediated contraction. Interestingly, in MA where CCCP itself did not cause contraction, removal of extracellular Ca^{2+} markedly increased the vessel tone; the addition of diltiazem had no obvious effects (Fig. 6.4 A).

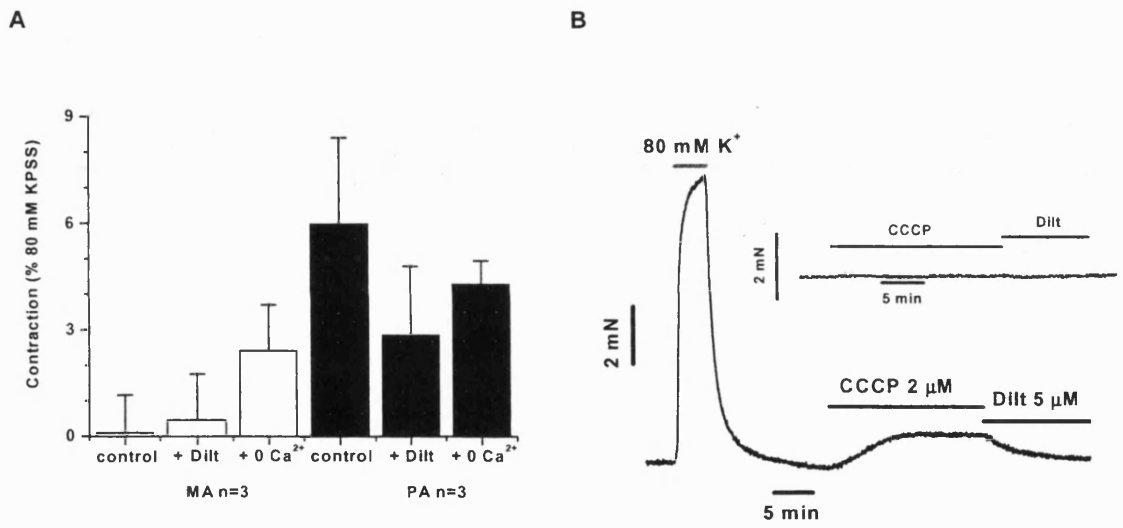

Figure 6.4. Effect of extracellular Ca^{2+} entry on the CCCP induced contraction in MA and PA. (A) Response to 5 min incubation in CCCP (2 μM). MA are clear bars and PA are black bars. Experiments were carried out in control, with 5 μM diltiazem applied after CCCP or pre-incubation for 10 minutes in Ca^{2+} free Krebs solution. (B) Representative trace in PAs showing contraction to CCCP with subsequent application of diltiazem, the vessel had an internal diameter of 170 μm. Insert shows a representative trace for the paired MA, internal diameter 152 μm.

6.2.3 Effect of CCCP on dose response curves to K^+ and U46619

To further investigate a possible relevance of the observed effects of CCCP on K^+ channels a cumulative DR to K^+ in the absence and presence of the agent was constructed (equimolar replacement of NaCl for KCl, with final [K^+] of 10, 20, 40. 80 and 100 mM K^+ applied at 5 minute intervals). Arteries were pre-incubated for 10 minutes with CCCP. Fig. 6.5 shows representative traces comparing K^+ DR curves, in the absence and presence of CCCP, in MA (A) and PA (B). Reflecting the decrease in maximal contraction, a significant leftward shift in the DR curve to K^+ was observed for CCCP in PA (EC_{50} = 37.7±1.6 mM, control and 19.9±1 mM, in CCCP, n=3, $p<0.009$) (highlighted in the normalised DR in Fig. 6.6 A&B), however in MA there was a complete inhibition of contraction (Fig 6.7). Additionally, CCCP almost entirely inhibited contraction in response to U46619 in the MA, a thromboxane A_2 analogue causing agonist mediated contraction. The contraction to U46619 was blocked to a lesser extent in the PA and, in contrast to the effects upon the DR to K^+, no effect was observed upon the EC_{50} in the absence (27.7 nM, n=1) and presence (28.7 nM, n=1) of CCCP (Fig 6.5 C&D).

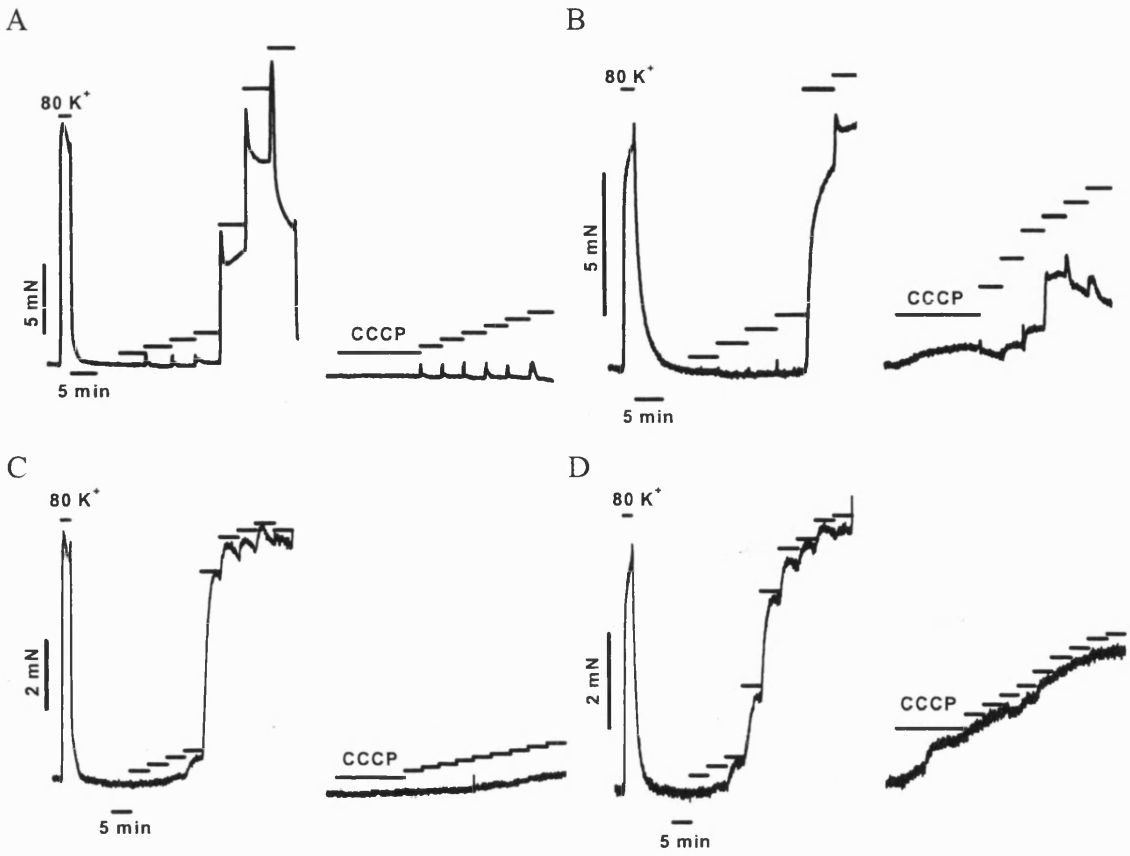

Figure 6.5. Effect of CCCP on dose response curves to K^+ and U46619. Pre-contraction was carried out before the control and test dose response (DR) to 80 mM K^+ (indicated at beginning of traces). Representative DR curves to K^+ (10, 20, 40, 80 and 100 mM K^+) in MA (A) and PA (B). The vessels have an internal diameter of 210 μm (mesenteric) and of 375 μm (pulmonary). Representative DR curves to U46619 (1, 5, 10, 15, 20, 50, 100, 200, 500 and 1000 nM U46619) in MA(C) and PA (D). The vessels have an internal diameter of 165 μm (mesenteric) and of 255 μm (pulmonary). Arteries were pre-incubated in CCCP for 20 minutes prior to commencing the test DR.

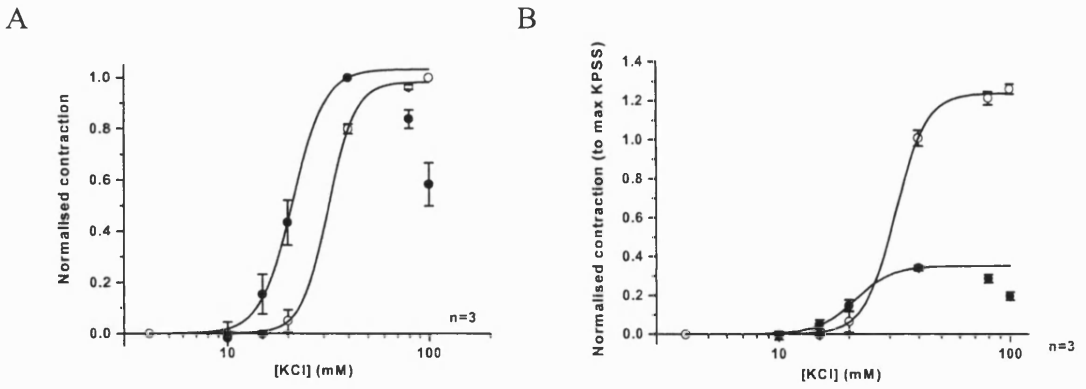

Figure 6.6. Effect of CCCP on K^+ induced contraction in PAs. DR curve normalised to the maximum contraction for that DR, in the absence (open circles) and presence (filled circles) of CCCP (2 μM) (A). (B) the same DR curves normalised to the maximal response to 80 mM K^+ (used to establish maximal contractility of the vessel). Lines represent a fit with the Hill equation [EQN 6.1].

[EQN 6.1] $$p = \frac{x^n}{(x^n + EC_{50}{}^n)},$$

where p is the proportion of ligand bound to a population of receptors, x is concentration, EC_{50} is the concentration for p= 0.5 and n estimates the number of molecules bound per site.

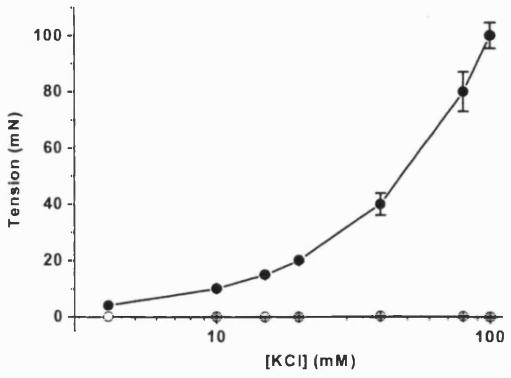

Figure 6.7. Effect of CCCP on K^+ induced contraction in MAs. DR curve in the absence (open circles) and presence (filled circles) of CCCP (2 μM) to K^+.

6.2.4 Effect of ROS and mETC complex III inhibition on contraction to K^+

Exposure of the vessels to 300 μM H_2O_2 for 10 minutes evoked a transient contraction in both vessels. The MA predominantly relaxed to baseline whereas the PA maintained a degree of increased tension (Fig. 6.8 A&B). There was, however, no significant difference on the maximum contraction (when expressed as a % of the averaged maximum contraction to 80 mM K^+ in either vessel) between the mesenteric and pulmonary arteries (Fig. 6.8 C).

Antimycin, whilst mimicking CCCP and ROS in MA did not have such a substantial effect of the K^+ induced increase in vessel tone. Interestingly, in contrast to previously reported observations, antimycin (data not shown) alone did not cause contraction of PA nor MA (Leach *et al.*, 2001).

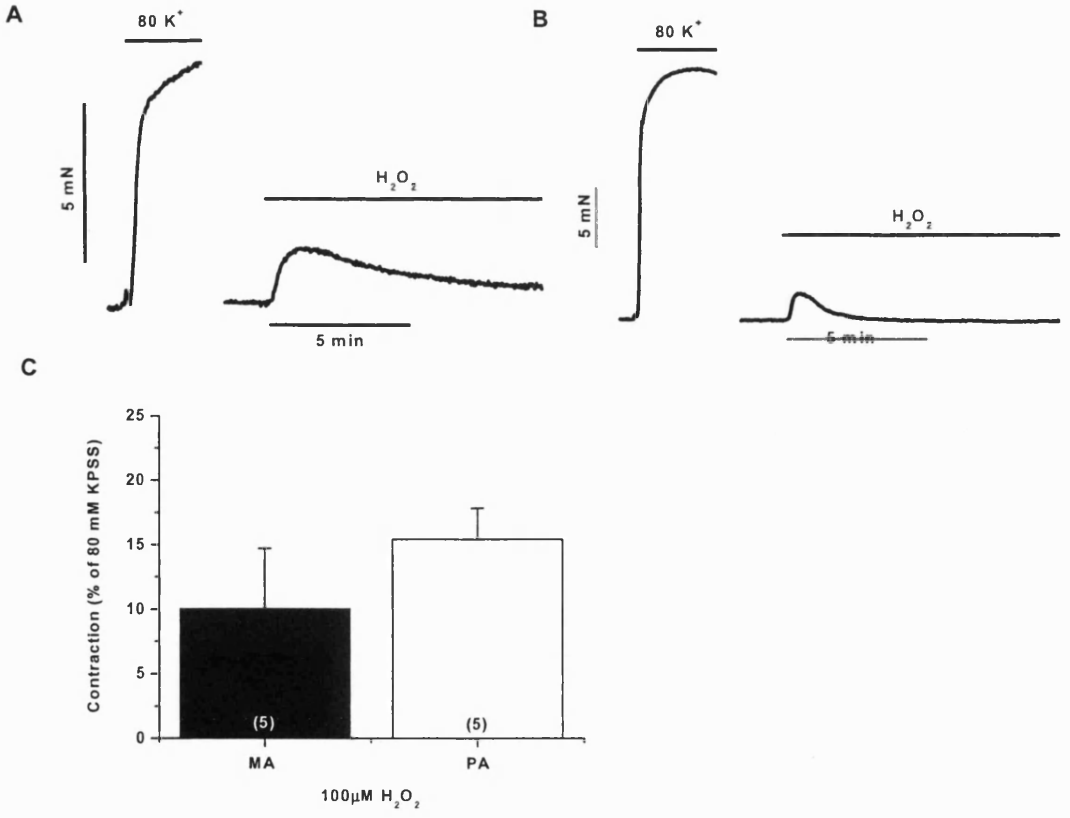

Figure 6.8. Effect of 300 μM H_2O_2 on intact PA and MA. Representative traces showing the application of 300 μM H_2O_2 in PA (A) and MA (B). The estimated

internal diameter of the vessels was 362 μm (pulmonary) and 302 μm (mesenteric). (C) Exposure of PA and MA to H_2O_2 for 10 minutes, peak contraction obtained in the 10 minute period is shown.

To additionally consider the effects of antimycin and H_2O_2 on K^+ channels in PAs they were each studied on a cumulative DR to K^+. As with CCCP, vessels were pre-incubated for 10 minutes prior to the DR and a significant leftward shift in the DR curve to K^+ was also observed for H_2O_2 (EC_{50} = 20.5±0.1 mM , control and 16.7±0.2 mM, in H_2O_2, n=2, p<0.005) (highlighted in the normalised DR in Fig. 6.9 C), reflecting the decrease in maximal contraction. The data aquired with antimycin was not able to be fitted at this stage due to the low number of experiments (Fig. 6.8 A).

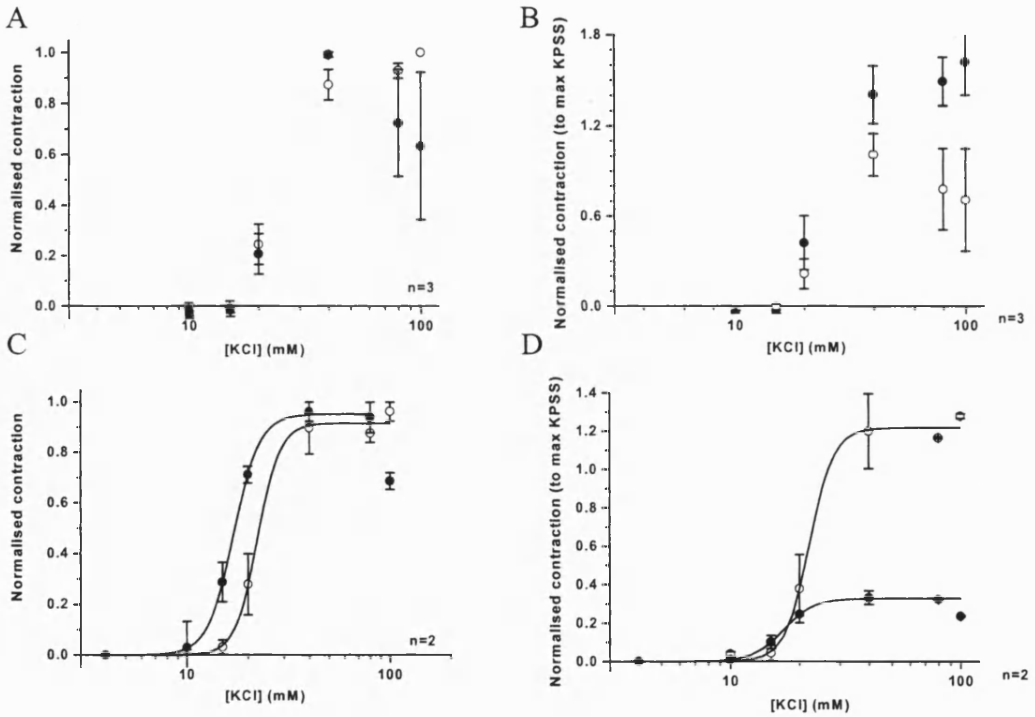

Figure 6.9. Effect of antimycin and H_2O_2 on K^+ induced contraction in PAs. DR curve normalised to the maximum contraction for that DR, in the absence (open circles) and presence (filled circles) of antimycin (1 μM) (A) and H_2O_2 (300 μM) (C). (B & D) are the same DR curves normalised to the maximal contraction to 80 mM K^+. Lines represent a fit with the Hill equation [EQN 6.1].

It is also worth noting that contraction in response to elevated extracellular K^+ was virtually completely inhibited in the presence of antimycin, contraction remaining was equal to 19.4±7.6 %, n=3, p<0.007, CCCP (0.38±0.6 %, n=2) and 100 μM H_2O_2 (4.3±4 %, n=3, p<0.012) in MA (Fig. 6.10). In the PA, despite not reaching significance (possibly due to the low experiment numbers) there was a substantial inhibition of the maximal contraction in response to CCCP (27.1±1.2 %, n=2), 100 μM H_2O_2 (35.7±13.9 %, n=3) and 300 μM H_2O_2 (26±3 %, n=2); antimycin, on the other hand, did not inhibit the K^+ dependent contraction (64.7±11 %, n=3) (Fig. 6.10). It is worth noting that the inhibition of contraction in the MA was significantly larger than that in the PA for antimycin (p<0.028) and CCCP (p<0.0007) (Fig. 6.10)

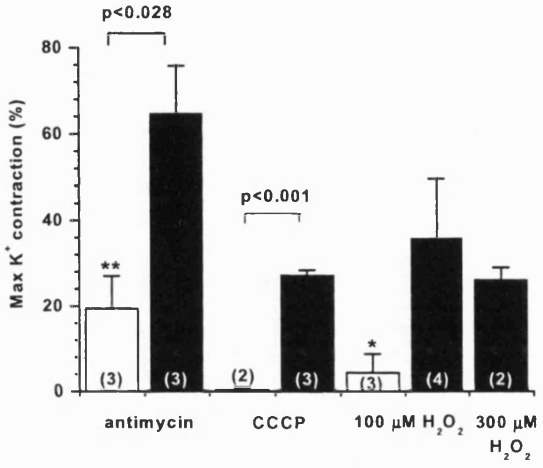

Fig 6.10. Effect of mETC inhibitors and H_2O_2 on maximal K^+ contraction in PA and MA PAs (black bars) and MAs (open bars) were pre-incubated fro 10 minutes in either antimycin (1μM), CCCP (2 μM) or H_2O_2, (100 and 300 μM) prior to recording a cumulative DR to K^+. The data is expressed as the % of the maximal contraction in the control DR.

6.3 Discussion

As predicted by the window current models application of CCCP uncoupling $\Delta\Psi_m$, increased the excitability of PAs when the cell membrane is depolarised using extracellular K^+. For instance, if the resting membrane potential on average is -55 mV (range between -52 and -58 mV from microelectrode studies (Gonczi *et al.,* 2006; Casteels *et al.,* 1977; Bonnet *et al.,* 2001; Suzuki & Twarog, 1982)), then 10 and 20 mM KCl should depolarise PAs by 17 and 37 mV respectively (calculated by the Nernst equation). According to the model this would result in I_{Kv} inhibiton and increased excitability of PAs as were observed with CCCP. When PAs were contracted using thromboxane analogue, U46619, such an increase in tissue excitability was not observed, suggesting the specificity of these effects to depolarising action of KCl.

Interestingly, the CCCP mediated contraction was partially inhibited by either block of Ca^{2+} entry via L-type VDCC or removal of extracellular Ca^{2+}, suggesting that the CCCP induced contraction, is mediated by other mechanisms in addition to Ca^{2+} entry in response to depolarisation caused by Kv channel. Indeed, Ca^{2+} release from the mitochondria can be stimulated by both CCCP (Komatsu *et al.,* 2004) and H_2O_2 (Roychoudhury *et al.*, 1996) and could represent an alternative mechanism for increased $Ca^{2+}{}_i$. Recent evidence also strongly supports an important role for CCE in response to hypoxia in the PA (Becker *et al.*, 2006).

Under my experimental conditions antimycin did not cause contraction in either PAs or MAs. Other researchers have shown antimycin to have a vasoconstrictor effect however, this was either in whole lung preparations (Rounds & McMurtry, 1981;Waypa *et al.*, 2001; Weissmann *et al.*, 2003) or in PASMCs ((Waypa *et al.*, 2001) and not in isolated PAs as was performed in this thesis. Additionally, 10 μM antimycin has been shown not to induce contraction in rat aorta (Zhou *et al.*, 1997).

In the MA complete inhibition of contraction in response to pre-incubation with CCCP, antimycin and H_2O_2 observed irrespective of the contractile stimulus. H_2O_2 did induce a similar level of contraction to that seen in PA, which was transient in duration. Such results do corroborate with the dilation of systemic circulation in response to hypoxia.

The transient contractile response to H_2O_2 in the MA, which has been also observed by others (Gao *et al.*, 2003a), is more difficult to explain based on the theoretical prediction of the behaviour of Kv channels which should favour relaxation. Overall data regarding the effects of H_2O_2 on mesenteric arteries is conflicting, with some arteries contracting and others dilating, in rabbit MASMCs H_2O_2 is proposed to increase vasodilator prostaglandins and cause hyperpolarisation via K_{ATP} channel activation (Hattori *et al.*, 2003) whereas in the rat, however, H_2O_2 caused constriction (Gao & Lee, 2001, Gao *et al.*, 2003b). It is possible that higher concentrations of ROS are necessary for activation of a vasodilatory pathway. Differential regulation of the smooth muscle contractility may be due to activation of other types of K^+ channels. Additionally, ROS have been previously shown to regulate BK_{Ca} channels relaxing systemic circulation (Brakemeier *et al.*, 2003; Liu & Folz, 2004) and K_{ATP} channels are proposed to be involved in rabbit mesenteric arteries (Hattori *et al.*, 2003).

In summary, mitochondrial dependent pathway(s) are possibly important in the regulation of both PA and MA contractility by differential mechanisms resulting in contraction of PA and relaxation in MA. Many more experiments are necessary to fully elucidate the precise mechanisms which are involved in this very complex modulation of vessel contractility. The results in this chapter serve to suggest the in the pulmonary circulation mitochondrial dependent signalling is involved in regulation depolarisation mediated contraction, not, however, necessarily via VDCC. Depolarisation may also be enhanced by Ca^{2+} activated Cl^- channels, known to be present and induce contraction in PA (Piper & Greenwood, 2003). In addition ROS (namely H_2O_2) displays a similar effect on PA contractility as in MAs, though combined with the electrophysiological data this is most probably independent of the effect on Kv channel currents.

Chapter 7

INVOLVEMENT OF THE NA^+ DEPENDENT EXCHANGERS IN THE REGULATION OF I_{KV}

7.1 Introduction

Differences in the WC and perforated patch data may be indicative that extrusion mechanisms, which may be more active in non-dialysed cells, could be involved. One of the main mechanisms for Mg^{2+} extrusion is through the Na^+ dependent Mg^{2+} antiporter (NME). Several additional pathways may be functionally linked to the NME, for example consequential changes in the Na^+ gradient after NME activation could regulate the other Na^+ dependent exchangers. Other exchangers currently identified in the pulmonary circulation include the Na^+-Ca^{2+} exchanger (NCE) and the Na^+-H^+ exchanger (NHE), with the Na^+-K^+ ATPase being the main mechanism for Na^+ extrusion. Such extrusion mechanisms are functionally important in ion homeostasis. The following sections will discuss the role of each of the above-mentioned Na^+ dependent mechanisms and their proposed role in the pulmonary circulation.

7.1.1 Sodium dependent exchangers

7.1.1.1 NME

Activation of the NHE has recently been shown to modulate Na^+-Mg^{2+} transport in VSMCs and, additionally, increased activity of NHE could influence the change in Na^+-dependent regulation of $[Mg^{2+}]_i$ observed in spontaneously hypertensive rats (SHR) (Touyz & Schiffrin, 1999). As with the other exchangers, the NME has been identified in a range of tissues including; human trophoblast cells (Standley & Standley, 2002), sheep ruminal epithelial cells (Schweigel *et al.*, 2006) and erythrocytes (Rivera *et al.*, 2005). There is also experimental evidence supporting the Na^+ dependence of Mg^{2+} extrusion in VSMCs. Romani *et al.*, (1993) demonstrated that the removal of extracellular Na^+ inhibits Mg^{2+} extrusion, while Gunther & Vormann, (1985) showed an inhibition of Mg^{2+} extrusion in Na^+ containing solution but in the presence of amiloride

or imipramine inhibiting the exchanger. Inhibitors of NME have been shown to attenuate development of hypertension in rats infused with Ang II (Touyz & Yao, 2003). However, the NME is yet to be cloned and has not been extensively studied in the pulmonary vasculature.

7.1.1.2 NCE

The NCE was first described in the 1960's when groups working in the UK, Germany and the USA all concluded from their work that there was a coupled transport system for Na^+ and Ca^{2+} exchange, an entity they termed the Na^+-Ca^{2+} exchanger. The importance of the NCE as a primary mechanism of calcium extrusion and the knowledge that small changes its activity lead to large effects on cell function has been recognised by four international conferences dedicated to NCE research (2001, 1996, 1991). The NCE operates in parallel with Ca^{2+} channels and pumps in the plasma membrane and can either move Ca^{2+} into or out of cells. Its activity is regulated by the electrochemical gradient across the membrane and operates using Na^+ gradients as a source of energy. The presence of the NCE in cardiac cells, for example atrial smooth muscle (Reuter *et al.*, 1973), has been extensively investigated and established to perform a "house-keeping" role to maintain low intracellular Ca^{2+} levels. Such mechanisms of Ca^{2+} overload have putative roles in myocardial ischemia, myocardial infarction, reperfusion and cardiac arrhythmias (reviewed by Hobai & O'Rourke, 2004). It is thus suggested that NCE inhibitors may have cardio-protective roles (Takahashi *et al.*, 2003). Indeed, the NCE is currently being investigated as a target for anti-arrhythmic therapy; there is strong evidence for arrhythmias related to Ca^{2+} overload caused by increased Na^+ load and activation of the NCE (Sipido *et al.*, 2006). Its functional presence in many other species and tissues has also been documented including guinea pig uretha (Aickin *et al.*, 1984), brain synaptosomes (Blaustein *et al.*, 1996), neurones, astrocytes (Juhaszova *et al.*, 1996) and pancreatic beta cells (Van Eylen *et al.*, 1997). Existence of Na^+-Ca^{2+} exchange was first documented in vascular smooth muscle by Bohr *et al.*, (1969). Since then its activity has been established in cultured VSMCs (Nabel *et al.*, 1988) and cultured bovine PAECs (Sage *et al.*, 1991), before Aaronson *et al.*, (1991) provided evidence for a role of Na^+-Ca^{2+} exchange in human resistance vasculature in the recovery from contraction. The NCE activity is

noticeably inhibited decreasing the rate of Ca^{2+} extrusion from the cytosol in PASMCs exposed to mild hypoxia (Wang *et al.*, 2000).

In 1990, the NCE was cloned from dog heart muscle (Nicoll *et al.*, 1990). The NCE has three currently identified isoforms the NCE1, 2 and 3, who have a similar overall structure (Blaustein & Lederer, 1999). An intracellular loop, thought to comprise the exchanger modulation by protein kinases and intracellular ions, connects to a 5TM domain at the N-terminal and a 6TM domain at the C-terminal. Most recently, mRNA for the NCE1 and NCKX3 (a potassium dependent Ca^{2+} exchanger) isoforms of the NCE has been isolated from cultured PASMC (Zhang *et al.*, 2005). This study also suggested that the NCE expressed in cultured PASMCs contributed to Ca^{2+} entry due to the reverse mode of the NCE, elevating cytosolic Ca^{2+} by store depletion. It was therefore predicted that blockade of the reverse mode NCE may be a possible therapeutic target in the treatment of PH (Zhang *et al.*, 2005). The most recent evidence, however, shows that a response resembling that observed in HPV in PAs induced by the removal of Na^+_o was not due to inhibition of the NCE but was inhibited by the inhibitors of CCE, and thus is not supportive of a role for NCE in HPV (Becker *et al.*, 2006).

7.1.1.3 NHE

The NHE exchanger is electrogenic exchanging Na^+ for H^+ and is primarily involved in pH homeostasis in many mammalian cell types acting alongside several other ion transport systems such as the Na^+ independent Cl^-/HCO_3 and Na^+ dependent Cl^-/HCO_3 transporters. The NHE is activated by an increase in intracellular H^+ concentration. Extracellular Na^+ is exchanged for intracellular H^+ in a 1:1 stoichiometry. Excessive stimulation of the exchanger will ultimately increase intracellular Na^+, which, in turn, can drive the Na^+-K^+ ATPase increasing the energy demands of the cell and/or activate the NCE driving Ca^{2+} into the cell. In cardiac tissue such Ca^{2+} overload can lead to ischemia/reperfusion injury or myocardial infarction (Piper *et al.*, 1996). Also, in patients with hypertension, abnormalities in NHE exchange have been noted in several cell types including red blood cells (Canessa *et al.*, 1991; Rosskopf *et al.*, 1992), cultured VSMCs (Berk *et al.*, 1989) and skeletal muscle (Dudley *et al.*, 1990).

The NHE has, more recently, been studied in PASMCs and significant roles in apoptosis, proliferation (Yao *et al.*, 2002) and in hypoxic mechanisms are evident (Rios *et al.*, 2005). In PASMCs from 3 week hypoxic rats it was found that pH_i and NHE-1 mRNA expression levels were significantly elevated and that DMA (an inhibitor of the NHE) also elevated the rate of apoptosis (Yao *et al.*, 2002). Additionally, exposure of mouse PASMCs to CH increased pH_i, NHE activity, and NHE1 expression; such changes are thought to contribute to the development of PH (Rios *et al.*, 2005). The NHE has additionally been shown to aid in recovery from acid loads during hypoxia (Madden *et al.*, 2000). Since the cloning of the first Na^+ H^+ exchanger (NHE1) by Pouyssegui's lab in 1989 nine isoforms of the exchanger have been identified (NHE 1-9) (Sardet *et al.*, 1989). NHE 2-9 are more restricted in their distribution, unlike NHE 1, which is ubiquitously expressed in the plasma membrane. The structure of the TM proteins are similar containing 12 helical hydrophobic membrane spanning domains, a ~500 amino acid N terminus functionally responsible for catalysing the amiloride sensitive NHE and a ~300 amino acid C terminal acting as a regulatory domain.

7.1.1.4 Na^+-K^+ ATPase

Na^+-K^+ ATPase or Na^+-K^+ pump is ubiquitously expressed and is the first enzyme to gain recognition as an ion pump. The Na^+-K^+ ATPase is electrogenic transporting three Na^+ in exchange for two K^+ and therefore induces changes in the membrane potential. Recently, small membrane proteins characterised by an FXYD motif have been shown to associate with the Na^+-K^+ ATPase and modulate its properties for the transport of Na^+ or K^+, possibly implicating a role in pathophysiological states (Geering, 2006). It has previously been proposed that the regulation of the Na^+-K^+ ATPase may have a crucial role in the regulation of the contractility of VSM (Aronson, 1984) and indeed in the canine pulmonary artery hypoxia inhibits the Na^+-K^+ ATPase (Tamaoki *et al.*, 1997). The basic function of the Na^+-K^+ ATPase is to maintain low $[Na^+]_i$ and high $[K^+]_i$. Located in the plasma membrane it is composed of α and β subunits. The α subunit, containing the binding sites for ATP and the cardiac glycoside ouabain, is also the active catalytic subunit. The β subunit acts as a chaperone that ensures correct

insertion of the α subunit in the plasma membrane and additionally modulates the affinity of the enzyme for cations.

7.1.2 Inhibitors of the exchangers

Amiloride was the first NHE inhibiting drug to be discovered. Its properties as a K^+ sparing diuretic and subsequently a Na^+ channel blocker were discovered back in the 1960's. Subsequently, in 1977 the first observations that external Na^+ and amiloride had effects upon pH_i were noticed (Aickin & Thomas, 1977). Inhibition of the NHE was noted initially in renal microvilli (Kinsella & Aronson, 1981), mouse neuroblastoma cells (Moolenaar *et al.*, 1981), cultured skeletal muscle (Vigne *et al.*, 1982) and in VSMCs (Little *et al.*, 1986). In animal models NHE inhibitors have been shown to offer substantial protection from myocardial infarction (Masereel *et al.*, 2003). Derivatives of amiloride were developed to create a higher specificity for the NHE. N-methyl-isobutyl amiloride (MIA) has a K_d of 2.3 nM for the NCE1 (Talor *et al.*, 1989), its higher selectivity towards the NHE is created by substitution of the nitrogen of the 5-amino group in the pyrazine structure, other improved derivatives include DMA, EIPA and HAM.

Amiloride also blocks the NME at concentrations 10-50 times lower (around 100 μM) than those at which it blocks the NHE. In addition, amiloride is known to block the Na^+-K^+ATPase (Soltoff & Mandel, 1983) and to decrease the open state conductivity of the epithelial sodium channel in a dose dependent manner (Sariban-Sohraby *et al.*, 1984). Amongst the blockers used to inhibit NME, imipramine and quinidine are considered to be relatively selective (Gunther, 1993b).

For the NCE initially di- and tri- valent cations such as Na^{2+} and La^{3+} were known to act as inhibitors; however they also blocked many other ion channels and transporters at low doses. KB-R7943 was the first "fairly specific" inhibitor of the NCE, blocking it in its reverse mode (IC_{50} = 2 μM, Iwamoto *et al.*, 1996) developed as a prototype in 1996 and at up to 10 μM is shown to exert little influence over other transport mechanisms. Above 10 μM, however, there are questions over its selectivity, there are reports that at this concentration there is inhibition of the Ca^{2+}-ATPase, the Na^+-K^+ ATPase (Iwamoto

et al., 1996), SOC (Arakawa *et al.*, 2000) and of voltage gated Na^+ channels (Watano *et al.*, 1999). Since KB-R7943 other benzyloxyphenyl derivatives have been formed exhibiting improved potency and specificity for the NCE1 isoform, SEA0400 (Matsuda *et al.*, 2001) and SN-6, which inhibits in the forward mode of the exchanger (Iwamoto, 2004, Iwamoto *et al.*, 2004). Additionally, benzamil (a benzyl substituted derivative of amiloride) is commonly used to inhibit the exchanger in its forward mode (Kleyman & Cragoe, Jr., 1988).

7.1.3 Putative link between I_{Kv} and Na^+-dependent transport mechanisms.

The exchangers are directly involved in regulating intracellular ion homeostasis. Mg^{2+}, Ca^{2+} and H^+ can all be regulated by activation of the respective exchangers, the NME, NCE and NHE, respectively. In the process of regulating these ions via the exchangers, Na^+_i is indirectly regulated.

7.1.3.1 Ion homeostasis

Na^+ dependent exchangers can regulate intracellular concentrations of Ca^{2+} and particularly Mg^{2+}. In support of this, Romani *et al.*, (1993) demonstrated that the removal of extracellular Na^+ inhibits Mg^{2+} extrusion, while Gunther & Vormann, (1985) showed an inhibition of Mg^{2+} extrusion in Na^+ containing solution but in the presence of amiloride inhibiting the NME. Inhibition of this exchanger by amiloride may thus cause an increase in intracellular Mg^{2+}. Removal of Na^+_o could also inhibit the NHE, which may be driven by the inward Na^+ gradient under our experimental conditions, resulting in an increased intracellular proton concentration.

7.1.3.2 Ion interactions with I_{Kv}

Reports exist suggesting that mono- and di- valent cations (such as Mg^{2+} and Ca^{2+}) can affect the activity of Kv channels in various tissues (Ludewig *et al.*, 1993; Lopatin & Nichols, 1994; Gomez-Hernandez *et al.*, 1997; Tammaro *et al.*, 2005). It has been previously demonstrated that increased concentrations of these intracellular divalent cations can inhibit I_{Kv} in VSMCs (Gelband *et al.*, 1993; Tammaro *et al.*, 2001;Tammaro *et al.*, 2005). It is also worth noting that neither of the above papers discriminated between the effects of Mg^{2+} and Ca^{2+} on Kv channels. Altura and Altura (1984) extensively reviewed the importance of Mg^{2+} and K^+ interactions in VSMCs highlighting the small changes in free [Mg^{2+}] near VSMC membranes could exert significant effects on both the mechanical and electrical properties of the cell (Altura & Altura, 1984). Furthermore, elevation of intracellular proton concentration can alter the activity of K^+ channels either 1) by blocking the channel (Starkus *et al.*, 2003a), 2) by altering the voltage sensitivity of the channel gating (Nimigean *et al.*, 2003) or 3) indirectly, for example via altering other ion homeostasis (Farrukh *et al.*, 1996).

As demonstrated in previous chapters $Mg^{2+}{}_i$ is important in mitochondrial dependent regulation of I_{Kv}, the current investigation therefore considered the activity of the NME and other Na^+ dependent exchangers and their effects upon Kv currents in rat small PASMCs. It is currently unknown whether Kv channels are functionally linked to the activity of Na^+ dependent exchangers. Although evidence in the pulmonary vasculature has shown that the transmembrane Na^+ gradient can be utilized to energize the exchange of Mg^{2+} (Touyz & Schiffrin, 1996), in addition to Ca^{2+} (Sage *et al.*, 1991; Yuan *et al.*, 1993) and H^+ (Silverman *et al.*, 1995; Madden *et al.*, 2001) via NME, NCE or the NHE, respectively.

7.2 Results

To initially consider whether the exchangers are involved in the modulation of I_{Kv} in PAMSCs, external Na^+ was removed blocking all Na^+ dependent exchangers in their forward direction.

7.2.1 Effect of Na^+_o removal on I_{Kv}

To effectively analyse and compare changes in key characteristics of I_{Kv} activation whilst maximising experimental productivity, under a variety of experimental conditions, data obtained with the ramping voltage protocol (described in chapter 2) was leak-subtracted offline and expressed as current density. Resulting *I-V*s were fitted to [EQN 2.7] to derive and compare the I_{Kv} steady state activation parameters of the half-activation potential (V_a), slope factor (k_a) and maximal conductance (G_{max}). To facilitate comparison the relative changes in V_a (referred to as ΔV_a) were calculated as the difference between absolute V_a parameters in control (PSS) and test external solutions in the same cell (as described in detail in Chapter 2). To evaluate the effects on I_{Kv} amplitude changes in G_{max} were considered.

7.2.2 Comparison of Na^+_o removal by ramp and tail current protocols

Removal of Na^+_o by equimolar replacement with NMDG caused a marked augmentation of the I_{Kv} amplitude in the negative voltage range. Notably, both representations of the *I-V* relationship (the tail current and ramping protocol) caused similar significant ΔV_a shifts (-17.3±2.4 and -16.9±3.4 mV, $0.00002<p<0.0006$, n=11, respectively) (Fig. 7.1). Changes in k_a were also comparable for tail and ramp protocols (10.3±1.3 to 9.1±1.2 mV and 14.5±1.7 to 11.2±2 mV, $0.02<p<0.05$, n=11, respectively). It is worth mentioning that direct comparison of G_{max} block and I_{Kv} block measured at +100mV in 11 cells showed a similar effect of Na^+ removal with a decreased current of 7.6±5.8 and 8.7±3.4 %, respectively; the percentage G_{max} block has therefore been considered for the remainder of this chapter. Furthermore, a Na^+_o-dependent decrease in the G_{max} measured at +100 mV using a 200ms voltage step protocol was similar to

the changes in G_{max} calculated from the ramp (14.2±8.3 %). Therefore, the voltage ramp protocol was subsequently used to compare the effect of Na^+ removal on I_{Kv}. The individual data is presented in Table 7.1.

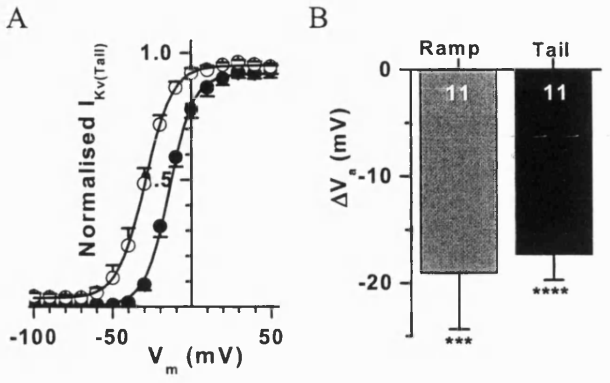

Figure 7.1. Effect of Na^+_o removal on I_{Kv} tail currents. (A) Normalised I_{Kv} tail currents in the presence (filled circles) and absence (open circles) of Na^+_o. (B) ΔV_a measured using a ramping protocol and with I_{Kv} tail currents.

To assess the possibility that whole cell dialysis may be interfering with the intracellular ionic activity experiments were additionally carried out in the non-dialysed cells using the perforated patch technique. In non-dialysed cells a significant shift of -15±1.9 mV (n=8, p<0.00009) was observed, with no effect upon G_{max} block, mimicking the effect of Na^+ free extracellular solution in dialysed cells (Table 7.1).

TABLE 7.1. Effect of different voltage protocols on changes in the voltage-dependent parameters of I_{Kv}.

	Steady-state $I_{Kv\ activation}$ and G_{max} block				
	V_a (mV)	k_a (mV)	ΔV_a (mV)	G_{max} *block* (%)	*n*
PSS	-2.6±3.2	14.5±1.7			
NMDG (Ramp)	-19.5±3.9 (p<0.00057)	11.2±2 (p<0.021)	-16.9±3.4	7.6±5.8	11
PSS	14.8±2.8	24.9±1.1			
NMDG (Step)	-2.8±4.3 (p<0.0043)	27.2±1	-17.7±4.8	14.2±8.3	11
PSS	-11.7±1.7	10.3±1.3	-17.3±2.4		11
NMDG (tail)	-29±2.6 (p<0.000027)	9.1±1.2 (p<0.042)			
Perforated Patch					
PSS	15±2.5	22.2±1	-15±1.9	22.3±11	8
NMDG (Ramp)	0±3.3 (p<0.00009)	23.1±3			

Here and in subsequent tables p values show significant difference between the values measured in control conditions and in test conditions obtained in the same PASMC (paired two-tail t-test) unless otherwise stated.

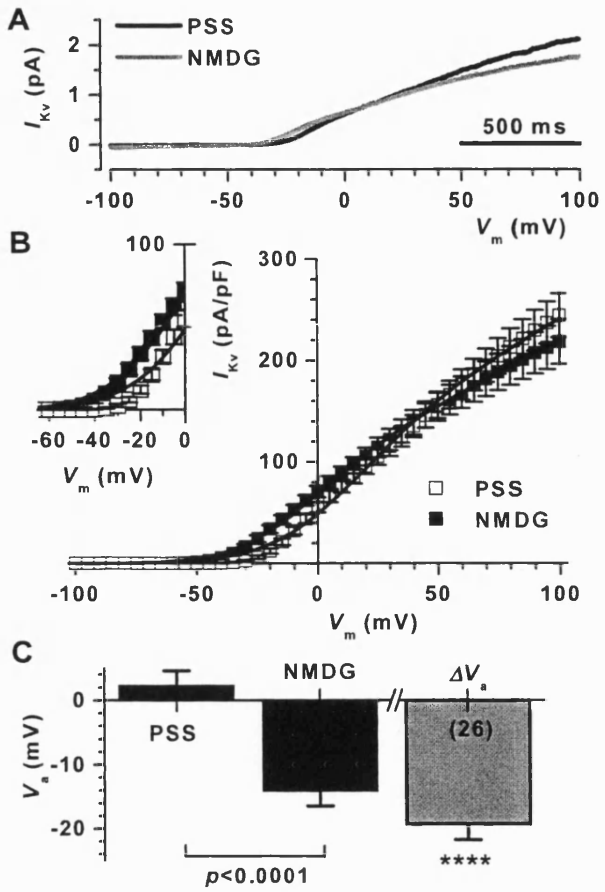

Figure 7.2. Effect of extracellular Na^+ removal on I_{Kv} activation. (A) I_{Kv} recordings using a 2 s ramp protocols between -100 and +100 mV, from the holding potential -80 mV from a representative PASMC, C_m = 10.8 pF. (B) Resulting *I-Vs* were fitted to the standard Boltzmann function to derive and compare half-activation potential (V_a), slope factor (k_a) and maximal conductance (G_{max}). The effect of removal of extracellular Na^+ (NMDG replacement) is highlighted in the insert showing the negative shift in I_{Kv} between 0 and -60 mV. (C) Shows absolute V_a values for PSS and NMDG and the relative change in V_a to which all subsequent data is compared to.

7.2.3 Involvement of the Na^+ dependent shifts in mitochondrial dependent regulation of I_{Kv}

For continuity with the previous chapters and to assess a potential contribution of the NME to the mitochondrial dependent regulation of I_{Kv} the effect of CCCP on the Na^+ dependent shift in tail currents (fitted to +100 mV) was considered. An interaction

between the mitochondrial regulated Mg^{2+} dependent effects on I_{Kv} and the Na^+ dependent exchangers was therefore considered by pre-incubation of cells for 5 minutes in CCCP prior to recording control *I-Vs* and removal of extracellular Na^+.

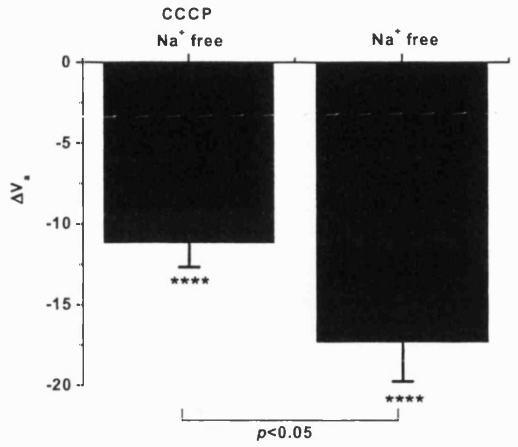

Figure 7.3. Effect of mitochondrial uncoupling on the Na^+ dependent modulation of I_{Kv}. Changes in the ΔV_a by removal of Na^+_o in the presence and absence of CCCP (2 μM).

The ΔV_a was significantly ($p<0.04$) inhibited in the presence of mitochondrial uncoupler CCCP (2 μM) from -17.1±2.3 mV (n=11, $p<0.00003$) to -10.5±1.8 mV (n=11, $p<0.0002$) (Fig. 7.3). The significant increase in the slope of the steady state activation dependencies induced by Na^+_o removal (from 9.5±1.1 mV to 7.8±0.7 mV (n=11, $p<0.05$)) was also inhibited in the presence of CCCP (Table 7.2). No significant G_{max} block at either +50 or +100 mV was observed.

7.2.4 Effect of Na^+_o removal on whole cell I_{Kv} in rat small PASMCs

Fig. 7.2 summarises the effect of the removal of Na^+_o studied in 26 PASMCs studied with the ramp protocol. As can be clearly seen in the figure, I_{Kv} amplitude was markedly increased in the negative voltage range of -50 to 10 mV (by >115%). For example, the mean I_{Kv} density was increased from 2.4±1 to 16.5±2.9 pA/pF, ($p<0.0001$) at -30 mV. This increase was associated with a significant reduction in the mean V_a from 3.8±2.1 mV (PSS) to -15.5±2.4 mV (NMDG) ($p<0.001$, Fig. 7.2 C), corresponding to a mean leftward shift of -19.3±2.5 mV in I_{Kv}. The insert in Fig. 7.2 B highlights the resulting marked enhancement of I_{Kv} at negative voltages and thus the leftward shift in

the steady state activation. Notably, the theoretical approximation of I_{Kv} was also improved in the negative voltage range of -30 mV in the Na^+_o-free solution. Accompanying the shift in V_a was a significant reduction in k_a from 17.9±0.9 (PSS) to 15.1±1.2 mV (NMDG) (p<0.0001). Also, a small decrease of 8.7±3.4 % in G_{max} was observed (n=26, p<0.02).

TABLE 7.2. Effect of CCCP on Na^+ dependent changes in I_{Kv} activation, studied using tail currents to +50mV.

	Steady-state $I_{Kv\ activation}$ and G_{max} block				
	V_a (mV)	k_a (mV)	ΔV_a (mV)	G_{max} *block* (%)	n
PSS	-12.5±1.7	9.5±1.1			
NMDG (Tail)	-29.6±2.6 (p<0.00003)	7.8±0.7 (p<0.05)	-17.1±2.3	13.5±8.2	11
CCCP (2 μM)	-15±2.3	10.8±0.7			
CCCP (2 μM) + NMDG (Tail)	-25.5±2.7 (p<0.0002)	10.5±1.8	-10.5±1.8 (p<0.04)[a]	15.6±7.5	11

[a] represents a non paired t-test to control Na^+ free shift (above)

G_{max} % was calculated from the fitted peak I_{Kv}

It is important to note that the shift in I_{Kv} activation was reversible and reproducible. Three applications of Na^+ free extracellular solution for 5 minutes with 5 minute recovery in PSS produced shifts of -26.4±6 mV, -18.7±2.6 mV and -19.1± 2.4 mV, respectively (n=5).

7.2.5 Na^+_o dependence of the effects on I_{Kv}

The effects of different Na^+_o replacement were also considered to verify the shift observed by buffering with NMDG. Na^+_o replacement with isotonic K^+ (ΔV_a = -21.9±0.9 mV, n=7, p<0.0001) or Tris-Cl (ΔV_a = -14±1.7 mV, n=5, p<0.01) also caused significant leftward shifts in I_{Kv} activation comparable to those observed in NMDG

(Fig. 7.4). Equally consistent were changes in k_a from 19.1±0.7 to 3.9±0.4 mV (KCl, n=7, $p<0.0001$) and from 18±1 to 14.3±1.7 mV (Tris-Cl, n=5, $p<0.05$). Na^+ replacement with LiCl, however, produced a significantly smaller shift than that in NMDG ($p<0.05$, Fig. 7.4), although the slope of I_{Kv} activation dependency was similarly increased from 17.6±2.6 (PSS) to 12.9±2.5 mV (LiCl), n=4, $p<0.0003$. The magnitude of G_{max} inhibition in Tris-Cl and LiCl was also comparable to that in NMDG (5.9±4.5% and 7.5±3.9%, respectively, $p>0.05$, whereas G_{max} was enhanced by 14.8±12.6% (n=7, $p<0.001$) in isotonic K^+, as expected due to changes in E_k.

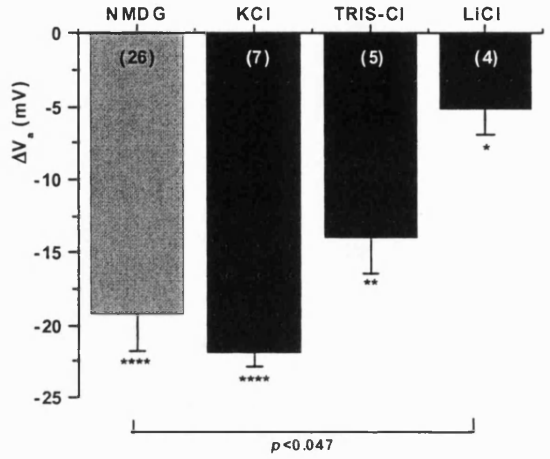

Figure 7.4. Comparison of different extracellular Na^+ replacement on I_{Kv} activation. Effects of Na^+ replacement by NMDG buffer, isotonic K^+, TRIS buffer and LiCl on ΔV_a. Grey control bars on the left represent the effect of NMDG replacement for extracellular Na^+ and are present for comparison.

Removal of Na^+_o would, in theory 1) inhibit the NME causing an increase in intracellular Mg^{2+}, 2) inhibit the NCE leading to a reduction in the extrusion of Ca^{2+} from the cell and 3) inhibit the NHE reducing H^+ extrusion from the cell. This would, in theory, cause intracellular accumulation of either Ca^{2+} and/or H^+ in addition to Mg^{2+}, or even a combination of these cations, each of which is capable of modulating K^+ conductance (Grissmer & Cahalan, 1989; Lopatin & Nichols, 1994). Therefore, all the Na^+ dependent exchangers need to be taken into consideration to explain the observed effects on I_{Kv} activation.

TABLE 7.3. Effect of different extracellular Na^+ replacements on the voltage-dependent parameters of I_{Kv}.

	Steady-state I_{Kv} activation and G_{max} block				
	V_a (mV)	k_a (mV)	ΔV_a (mV)	G_{max} *block* (%)	*n*
PSS	3.8±2.1	17.9±0.9			
NMDG	-15.5±2.4 (p<0.00000004)	15.1±1.2 (p<0.00007)	-19.3±2.5	8.7±3.4 (p<0.018)	26
PSS	0.4±2.6	19.1±0.7			
Isotonic K^+ (140 mM)	-21.5±1.9 (p<0.0000004)	3.9±0.4 (p<0.0000004)	-21.9±0.9	-14.8±12.6 (p<0.00052)	7
PSS	-7.1±1.9	18±1			
Tris-Cl	-21.2±3.5 (p<0.0039)	14.3±1.7 (p<0.05)	-14±1.7	5.9±4.5	5
PSS	-2.3±4.8	17.6±2.6			4
LiCl	-7.4±3.3 (p<0.03)	12.9±2.5 (p<0.0003)	-5.1±1.7 (p<0.047)[a]	7.5±3.9	

[a] represents p values compared to the control (NMDG) shift.

7.2.6 *Role of the NME*

The NME was initially assessed using a low concentration of amiloride (100μM), thought to preferentially block NME with a potency comparable to that of imipramine (Kleyman & Cragoe, Jr., 1988). Cell incubation with amiloride alone caused has no significant effect on ΔV_a, though notably the Na^+_o-dependent shift in I_{Kv} activation of -6.5±2.1 mV, n=11, was significantly reduced (p<0.015) (Fig. 7.5 A). Furthermore, no significant changes in the slope of I_{Kv} activation were observed (12.3± 2.1 to 13.4± 3.3 mV, n=11). A significant I_{Kv} block both in the presence of amiloride (17.6±2.7 %, p<0.004) and after the subsequent removal of Na^+_o (14.2±6.2 %, p<0.007) was also found (Fig. 7.5 B). It was not possible to use imipramine, an inhibitor of the NME, as it suppressed I_{Kv} by 83±3.7% (n=3) at 10 μM, a concentration which is 5-10 times smaller than that used to block the NME (Ebel *et al.*, 2004; Tashiro & Konishi, 2000).

Equimolar replacement of EGTA with a more potent Mg^{2+} buffer, EDTA, in the pipette solution substantially attenuated the Na^{+}_{o}- dependent shift in I_{Kv} activation (Fig. 7.4 A). A significant block in I_{Kv} amplitude, comparable to that in the control, was also observed (Fig. 7.5 B); however there was no effect on the slope factor (k_a = 17.6±0.8 mV in PSS vs. 16.8±1 mV in NMDG, n=18).

The relatively weak effect of EDTA may suggest a constant influx of Mg^{2+} from outside, hence causing extracellular Mg^{2+} removal. Therefore, the role of extracellular Mg^{2+} was investigated by i) removal of extracellular Mg^{2+} from the PSS ('Mg^{2+}-free' solution) and ii) equimolar replacement of 1.2 mM extracellular Mg^{2+} with Ca^{2+} ('Mg^{2+}-free+Ca^{2+}, solution). In Mg^{2+}-free PSS I_{Kv} activation dependency was significantly shifted leftward by -7.6±2.9, n=7, p<0.041, however this effect was not observed when Mg^{2+} was replaced with Ca^{2+} with ΔV_a = -0.9±1.9, n=10 (Fig. 7.5 C). This indicates that it is likely to be mediated by the interaction of divalent cations with fixed extracellular surface charges in the vicinity of the Kv channel. k_a was not significantly affected in either condition. Although the subsequent removal of Na^{+}_{o} caused a further leftward shift in I_{Kv} activation (ΔV_a =-8±0.8, n=7, p<0.0001), the effect was significantly reduced in both conditions compared to the control (p<0.03) (Fig. 7.5 C), suggesting that extracellular Mg^{2+}, but not Ca^{2+}, influx is likely to contribute to the Na^{+}_{o}-dependent shift of I_{Kv} activation. The slope of the activation dependency was significantly increased in both conditions with k_a = 16.3± 2 and 15.3± 2.2 mV (Mg^{2+}-free', n=7, p<0.03) and k_a = 15.8±1.4 and 13.1±1.5 mV (Mg^{2+}-free+ Ca^{2+}', n=10, p<0.018) in Na^{+}_{o}-containing and Na^{+}_{o}-free solutions, respectively. It should be noted that only the removal of Mg^{2+} alone had a significant effect on G_{max} blocking by 15.3± 4.5 % (n=7, p<0.011, Fig. 7.5 D), comparable to that in control. Any subsequent effect of Na^{+}_{o}-free solution was similarly not significant in both conditions (Fig. 7.5 D).

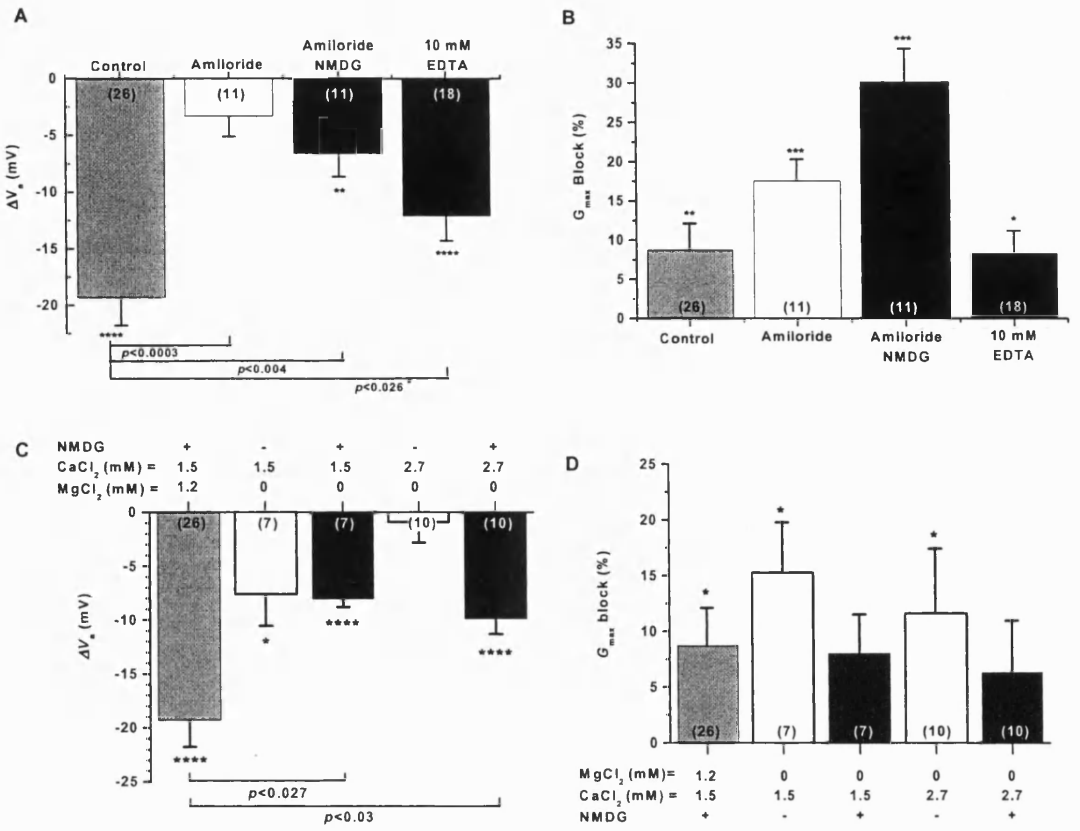

Figure 7.5. NME in the Na^+ dependent regulation of I_{Kv}. (A) & (B) Effects of selective inhibition of the NME with 100 μM amiloride (perfused for 6 minutes prior to recording) and (C) & (D) increasing Mg^{2+}_i to 10 mM and buffering Mg^{2+}_i with more potent Mg^{2+} buffer EDTA (10 mM) on ΔV_a and G_{max} block, respectively. Open bars represent the shift caused by the change in condition alone and black bars represent the shift due to Na^+ replacement with NMDG. Grey control bars are present for comparison. [a] denotes comparison with one tailed *t*-test.

TABLE 7.4. Effect of intracellular [Mg^{2+}] on the voltage-dependent parameters of I_{Kv}.

	Steady-state I_{Kv} activation and G_{max} block				
	V_a (mV)	k_a (mV)	ΔV_a (mV)	G_{max} *block* (%)	*n*
PSS	3.8±2.1	17.9±0.9			
NMDG	-5.5±2.4 (p<0.00000004)	15.1±1.2 (p<0.00007)	-19.3±2.5	8.7±3.4 (p<0.018)	26
PSS	-3.6±3.9	14.2±2.2			
PSS (100 μM Amiloride)	-6.9±3.8	12.3±2.1	-3.3±1.8 (p<0.0003)[a]	17.6±2.7 (p<0.0038)	11
NMDG (100 μM Amiloride)	-13.4±4.6 (p<0.013)	13.4±3.3	-6.5±2.1 (p<0.0034)[a]	14.2±6.2 (p<0.0011)	11
PSS (10 mM Mg^{2+})	-11.3±4.5 (p<0.0016)[a]	11.5±1.9 (p<0.0016)[a]			
NMDG (10 mM Mg^{2+})	-24.8±3.4 (p<0.000032)	9.8±1.8 (p<0.0031)	-13.5±1.9	16.9±3.5 (p<0.00045)	11
PSS (10 mM EDTA)	6.9±1.9	17.6±0.8			
NMDG (10 mM EDTA)	-5.4±2 (p<0.000016)	16.8±1	-12.1±2.2 (p<0.026)[a, b]	8.3±2.9 (p<0.031)	18

[a] represents p values compared to the control (NMDG) shift.

[b] denotes one tailed t-test.

If the effect of amiloride on the Na^+_o-dependent modulation of I_{Kv} activation is due to its inhibition of NME and removal of Mg^{2+}_o causes a decrease in Mg^{2+}_i, then increasing Mg^{2+}_i would also be expected to mimic these effects. Increased Mg^{2+}_i from 0.5 mM to 10 mM in the pipette solution with $MgCl_2$ alone caused a leftward shift in the I_{Kv} activation, with the difference between the two conditions being 10.1 mV, (p<0.002, unpaired t-test) (Fig. 7.6 A), mimicking the shift in the Na^+_o free in PASMCs dialysed with 0.5 mM $MgCl_2$. Additionally, in 10 mM Mg^{2+}, there is a significant increase in the slope of the steady state activation dependency from 17.9±0.9 mV (0.5 mM Mg^{2+}, n=26) to 14.7±1.2 mV (10 mM Mg^{2+}, n=19), p<0.035 (unpaired t-test). Notably, cell dialysis with 10 mM $MgCl_2$ alone resulted in significant inhibition of I_{Kv} amplitude; G_{max} block was decreased from 1.4±0.1 mV (0.5mM Mg^{2+}) to 0.56±0.1 mV (10 mM Mg^{2+}), p<0.000004 (unpaired t-test). The relative shift in the I_{Kv} steady-state activation in the NMDG buffer was diminished in 11 paired cells dialysed with 10 mM $MgCl_2$, though not significantly (ΔV_a = -13.5±1.9 mV, n=11) (Fig. 7.6 B).

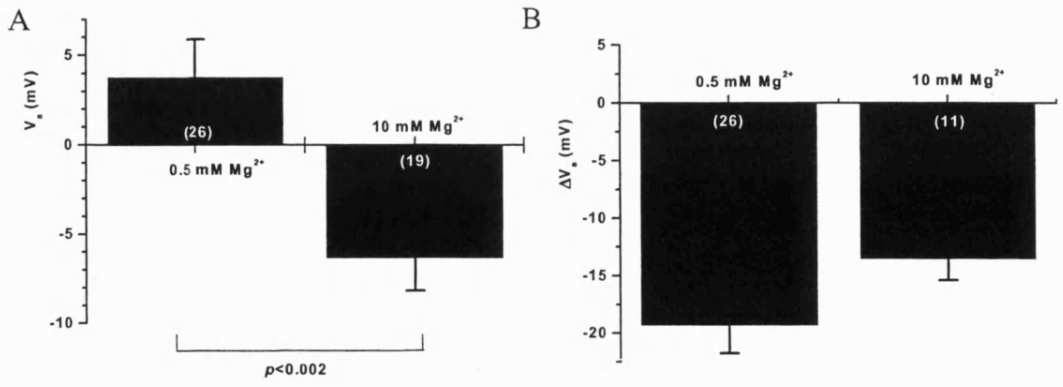

Figure 7.6. Effect of increased intracellular Mg^{2+}. (A) Comparison of 10 mM Mg^{2+} on V_a and (B) effect of increased Mg^{2+} on the Na^+-dependent shift in V_a.

7.2.7 Role of the NCE in the regulation of I_{Kv} in rat PASMCs

To investigate the involvement of the NCE, the effects of elevated (from 10 to 220 nM) free intracellular Ca^{2+} and increased buffering capacity for Ca^{2+} by equimolar BAPTA replacement of EGTA on I_{Kv} activation, were investigated. If the NCE is involved, it was expected that the effect of the Na^+ free solution would be attenuated. Neither of these conditions however significantly altered the effect of NMDG on ΔV_a compared to the control pipette solution (Fig. 7.7 A). A significant increase in I_{Kv} amplitude at -30 mV (4.2±1.2 pA/pF, n=5, 2.9±1.1 pA/pF, n=6, $0.02<p<0.05$, BAPTA and 220nM $[Ca^{2+}]_i$, respectively; data not shown) also support the changes in ΔV_a. Nevertheless, a significant decrease in k_a from 16±1.5 to 12.9±1.4 mV (n=5, $p<0.028$) and from 19.3±2.1 to 13.3±2.2 mV (n=5, $p<0.0002$) was observed for both elevated $Ca^{2+}{}_i$ and in the presence of BAPTA, respectively. Also, it is worth noting that in both these conditions, where $[Ca^{2+}]_i$ is increased or decreased, a significantly enhanced block of I_{Kv} is observed, (Fig. 7.7 B). Overall, these data suggest that the NCE activity could be at least partly responsible for some of the effects of $Na^+{}_o$ removal on I_{Kv} activation.

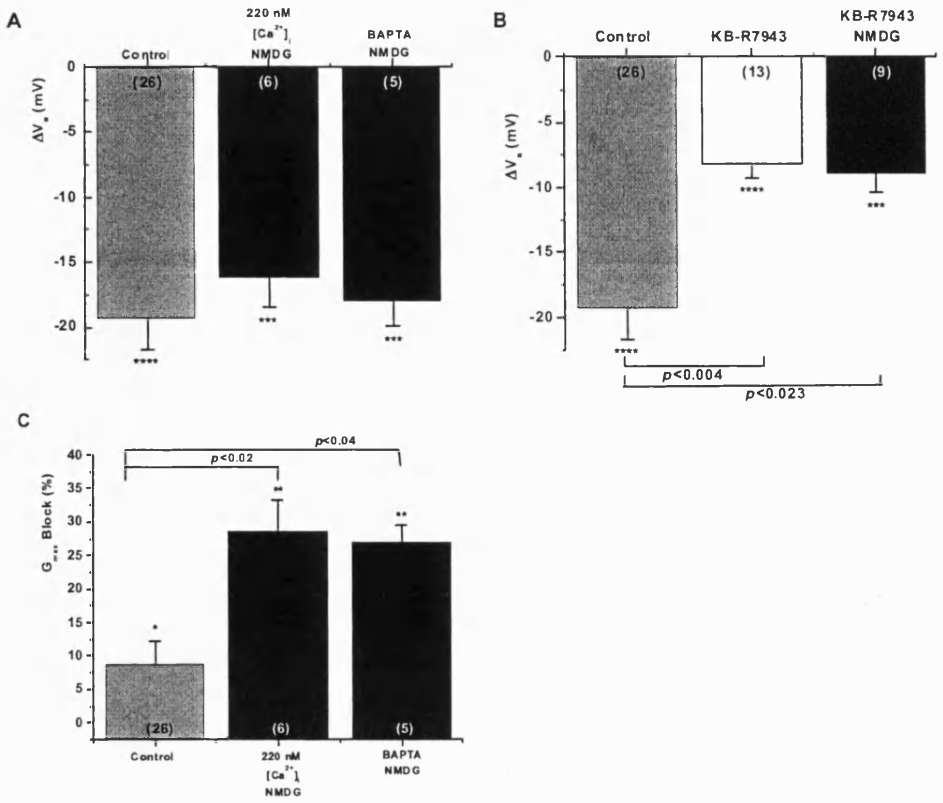

Figure 7.7. NCE in the Na^+ dependent regulation of I_{Kv}. (A) Effects of increasing Ca^{2+}_i to 220 nM and buffering Ca^{2+}_i with more potent Ca^{2+} buffer BAPTA (10 mM) on ΔV_a and (C) on G_{max} block. (B) Effect of NCE inhibitor KB-R7943 on ΔV_a. G_{max} block is measured as 1- the ratio of the G_{max} in control and test (NMDG) and is expressed as a percentage. Open bars represent the shift caused by the change in condition alone and black bars represent the shift due to Na^+ replacement with NMDG. Grey control bars are present for comparison.

Pre-treatment of PASMCs with 3 μM KB-R7943, an inhibitor of the reverse mode of the NCE has further confirmed this. KB-R7943 alone mimicked the effect of Na^+_o removal on both V_a (Fig. 7.7 B) (causing a leftward shift of -8.2±1.1 mV, n=13, p<0.0001) and the slope of I_{Kv} activation (reducing k_a from 15.3±1.4 mV (PSS) to 10.5±1 mV (KBR), (n=13, p<0.0001). Moreover, subsequent Na^+ removal caused a significantly smaller additional shift in the I_{Kv} activation (Fig. 7.6 B) with no significant effect on k_a (8.2±0.8 and 6.3±1 mV, n=9, before and after Na^+ removal respectively, n=9). The I_{Kv} block was also significantly increased both in KB-R7943 alone and after subsequent removal of Na^+_o (Fig. 7.7 C).

TABLE 7.5. Effect of intracellular [Ca^{2+}] on the voltage-dependent parameters of I_{Kv}.

	Steady-state I_{Kv} activation and G_{max} block				
	V_a (mV)	k_a (mV)	ΔV_a (mV)	G_{max} *block* (%)	*n*
PSS	3.8±2.1	17.9±0.9			
NMDG	-5.5±2.4 (p<0.00000004)	15.1±1.2 (p<0.00007)	-19.3±2.5	8.7±3.4 (p<0.018)	26
PSS (220nM $Ca^{2+}]_i$	4.1±4.2	16±1.5			
NMDG (220nM $Ca^{2+}]_i$	-12.1±4 (p<0.00091)	12.9±1.4 (p<0.028)	-16.2±2.3	28.6±4.7 (p<0.0014) (p<0.013)[a]	6
PSS (10mM BAPTA)	6±2.7	19.3±2.1			
NMDG (10mM BAPTA)	-11.9±3.1 (p<0.00074)	13.3±2.2 (p<0.00011)	-18±1.9	26.8±2.6 (p<0.0057) (p<0.031)[a]	5
PSS	1.1±2.7	15.3±1.4			
KBR (μM)	-7.1±2.5 (p<0.0000074)	10.5±1 (p<0.000016)	-8.2±1.1 (p<0.004)[a]	30.6±3 (p<0.000088) (p<0.0002)[a]	13
KBR (μM)	-12.1±2.8	8.2±0.8			
NMDG (KBR μM)	-21.1±2.8 (p<0.00033)	6.3±1	-8.9±1.5 (p<0.023)[a]	31.2±7 (p<0.0093) (p<0.0033)[a]	9

[a] represents p values compared to the control (NMDG) shift.

7.2.8 Role of the NHE

To investigate the possibility of a change in H^+ several approaches were used; 1) elevation of intracellular HEPES from 10 mM to 110 mM, 2) extracellular acidosis (pH 6.6), 3) alkalosis (pH 7.8) and 4) NHE inhibitor MIA.

The HEPES concentration was increased in order to increase intracellular proton buffering capacity. Removal of Na^+ under such conditions had an effect on ΔV_a similar to that under control conditions measured after 5 minutes exposure to Na^+_o-free solution (ΔV_a = -18.1± 2.1 mV, n=10) (Fig. 7.8 A). However, the analysis of the time-dependent changes in V_a showed a significant slow-down of the development of the effects of Na^+ removal in the presence of 110mM HEPES (τ = 2.5±0.7 s, n=6) compared to that in the

control conditions (τ =1.1±0.2 s, n=20, p<0.016). In addition, changes in the slope of I_{Kv} activation dependency were no longer significant (k_a = 15.8±2 mV vs k_a= 14.9±4.2 mV, in PSS and NMDG, respectively). Furthermore, the relative degree of I_{Kv} block caused by Na^+_o removal (19.2±2.9%, n=10, p<0.006) was significantly greater than that under control conditions (p<0.05, Fig. 7.8 C). The results indicate the potential involvement of intracellular protons could contribute to the observed effect of Na^+_o -free solution on I_{Kv} in PASMCs.

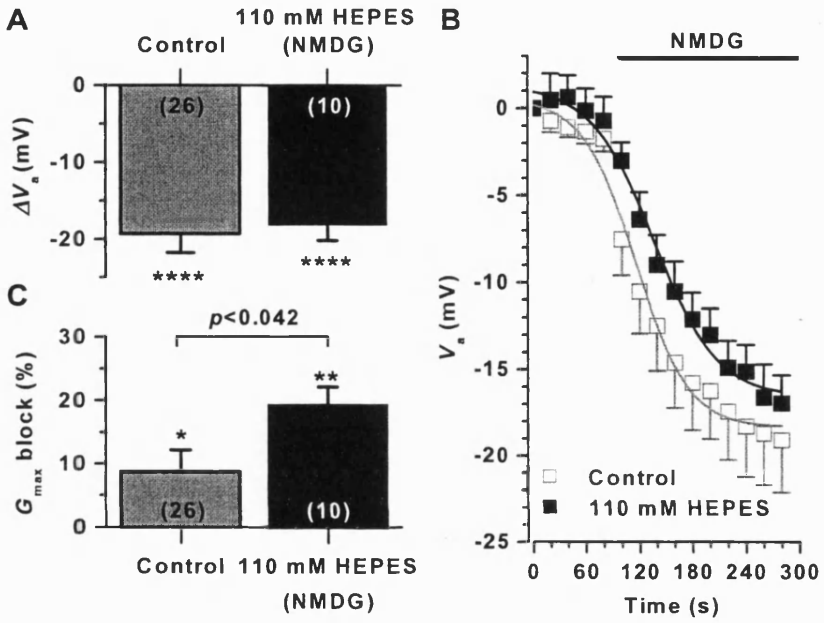

Figure 7.8. Effect of buffering H^+_i on Na^+ dependent regulation of I_{Kv}. Effects of buffering H^+_i with potent H^+ buffer HEPES (110 mM) on ΔV_a (A) and G_{max} block (C). (B) The time dependency of Na^+ removal compared in control and in the presence of H^+ buffer HEPES. Grey control bars on the left are present for comparison.

The role of the NHE was therefore further evaluated by investigating the effect of Na^+_o removal upon extracellular pH and in the presence of the NHE specific inhibitor MIA. Extracellular acidification to pH 6.6, favouring an influx of protons into the cell, had no effect upon steady state I_{Kv} activation alone, though did cause a significant decrease of the maximal Kv conductance (Fig. 7.9 A&B). Na^+_o dependent changes in V_a (Fig. 7.9 A) and k_a were preserved; ΔV_a =-15.8±1.2, n=4 and k_a 10.6±3.6 (PSS, pH 6.6) and k_a =

8.1±3.5 mV (NMDG, pH 6.6) (p<0.037). Interestingly, no further effect on the G_{max} was observed in Na^+_o-free solution at pH 6.6 (Fig. 7.9 B). Extracellular alkalosis (which should facilitate proton efflux from the cell) caused a significant shift in I_{Kv} activation; ΔV_a = -9.2±1.7 mV, n=5, p<0.01 (Fig. 7.9 A). Furthermore, unlike extracellular acidification, the extracellular alkalinisation caused a significant decrease in k_a from 17.9±2.1 mV (pH=7.2) to 12.7±2.3 mV (pH=7.8) (p<0.0015), thus mimicking the effects of Na^+_o -free solution under control conditions. Subsequent removal of Na^+_o caused a small, but no longer significant, additional shift in I_{Kv} activation dependency (ΔV_a = -6.8±4.8 mV, n=5) (Fig. 7.9 A). A further increase in the slope of activation dependency (k_a to 9.3±1.5 mV, p<0.02 when compared to pH = 7.8 alone) was also observed.

These results suggest that conditions facilitating the reduction of intracellular proton concentration attenuated the effect of Na^+_o removal on the steady-state activation, but not on the I_{Kv} block. In this case inhibition of the NHE, if it is constantly active under our experimental conditions, would be expected to mimic the effect of extracellular acidosis.

Blockade of the NHE with specific inhibitor 5-(N-methyl-N-isobutyl) amiloride (MIA) (25μM) alone had no significant effect upon I_{Kv} activation (Fig. 7.9 A). However, the slope of the dependencies was increased with k_a = 17.7±2.5 mV (PSS) and k_a = 14.4 ±2.1 mV (MIA, p<0.031), associated with a significant I_{Kv} block (Fig. 7.9 B), resembling the effect of extracellular acidosis. In the presence of MIA Na^+_o removal caused a reduced leftward shift in I_{Kv} activation, ΔV_a = -11.4±1.2 mV (n=5, Fig. 7.9 A), with no significant changes in k_a (14.4±2.1 vs 14±2.4 mV, n=5). The I_{Kv} block was also further increased (26.5±7 %, n=5, p<0.036). This suggests that overall the inhibition of NHE by removal of Na^+ contributes to the modulation of I_{Kv}, but is not the only mechanism involved in this process.

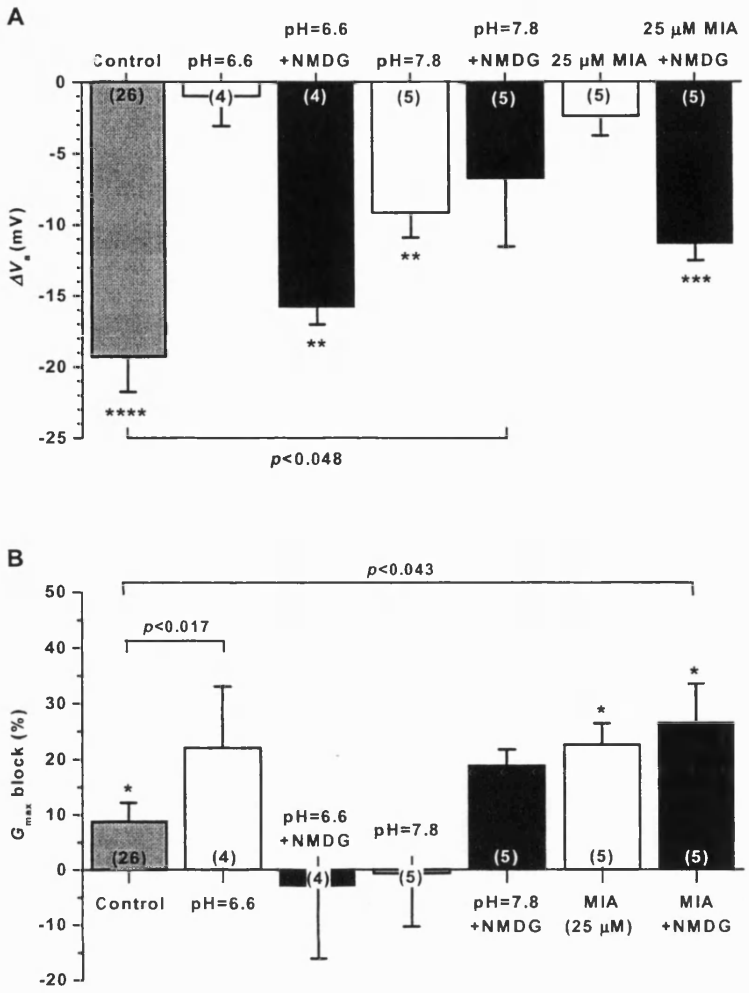

Figure 7.9. NHE in the Na^+ dependent regulation of I_{Kv}. Effects of extracellular pH and NHE specific inhibitor MIA (25 µM) on ΔV_a (a) and G_{max} block (b). Open bars represent the shift caused by the change in condition alone and black bars represent the shift due to Na^+ replacement with NMDG. Grey control bars are present for comparison.

7.2.9 Effect of Na^+ removal on I_{Kv} in MASMCs.

Specificity of the effect of Na^+_o removal on I_{Kv} in pulmonary circulation was evaluated by comparison to systemic circulation using MASMCs. When studied under the same experimental conditions, although Na^+_o removal caused a leftward shift in I_{Kv} activation (Fig. 7.10 A), the effect was 2.6 times smaller than that in PASMCs (Fig. 7.10 B). Furthermore, no significant effect on the slope factor was found (k_a = 15.2±0.7 mV in

PSS and 17.1±2.1 mV in NMDG). This evidence strongly suggests that the Na^+_o-dependent modulation of I_{Kv} activation is relatively specific for PASMCs. G_{max}, however, was similarly reduced by 10.4±3.9 % (n=11. $p<0.01$) upon removal of Na^+_o (Further details in Table 7.7).

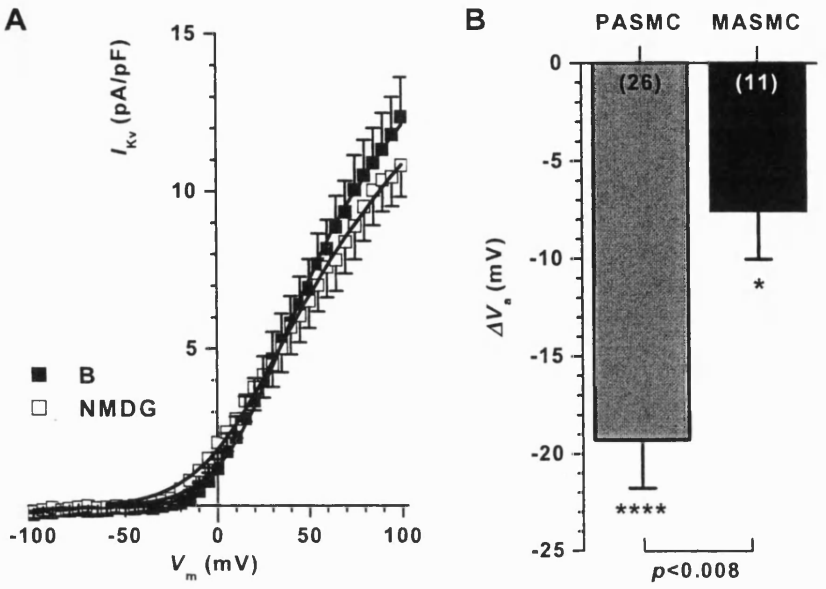

Figure 7.10. Effect of Na^+ removal in MASMCs. (A) *I-V* relationship in MASMCs in control and where extracellular Na^+ has been removed. (B) Shows the relative changes in V_a in MASMCs and PASMCs.

TABLE 7.6. Effect of intracellular [H^+] on the voltage-dependent parameters of I_{Kv}.

	Steady-state I_{Kv} activation and G_{max} block				
	V_a (mV)	k_a (mV)	ΔV_a (mV)	G_{max} *block* (%)	*n*
PSS	3.8±2.1	17.9±0.9			
NMDG	-5.5±2.4 (p<0.00000004)	15.1±1.2 (p<0.00007)	-19.3±2.5	8.7±3.4 (p<0.018)	26
PSS (110 mM HEPES)	2.8±2.1	15.8±2			
NMDG (110 mM HEPES)	-15.3±1.4 (p<0.000012)	14.9±4.2	-18.1±2.1	19.2±2.9 (p<0.0053) (p<0.041)[a]	6
PSS	-4.4±7.1	13.2±4.8			
pH 6.6	-5.4±8.4	10.6±3.6	-1±2.1 (p<0.0084)[a]	33.3±11 (p<0.017)[a]	4
NMDG pH 6.6	-19±6.5 (p<0.0063)	8.1±3.5 (p<0.037)	-15.8±1.2	-3±13	4
PSS	3.1±7.4	17.9±2.1			
pH 7.8	-6.1±5.8 (p<0.0063)	12.7±2.3 (p<0.0015)	-9.2±1.7	-0.7±9.7	5
NMDG pH 7.8	-12.9±4.5	9.3±1.5 (p<0.02)	-6.8±4.8 (p<0.048)[a]	18.8±2.9	5
PSS	2.7±2.1	17.7±2.5			
MIA (25 μM)	0.3±1.4	14.4±2.1 (p<0.031)	-2.4±1.4 (p<0.065)[a]	22.6±3.7 (p<0.012)	5
NMDG MIA (25 μM)	-11.1±0.9 (p<0.00074)	1.4±2.4	-11.4±1.7	26.5±7 (p<0.036) (p<0.043)[a]	5

[a] represents p values compared to the control (NMDG) shift.

TABLE 7.7. The effects of Na^+ removal in MASMC on the voltage-dependent parameters of I_{Kv}.

	Steady-state $I_{Kv\ activation}$ and G_{max} block				
	V_a (mV)	k_a (mV)	ΔV_a (mV)	G_{max} *block* (%)	n
PSS	15±5.1 (p<0.021)[a]	15.2±0.7			
NMDG	7.5±6 (p<0.014)	17.1±2.1	-7.5±2.5 (p<0.0078)[a]	10.4±3.9	11

[a] represents p values compared to the control (NMDG) shift

7.3 Discussion

In this part of the study changes in the voltage-dependent parameters of I_{Kv} activation induced by the removal of Na^+_o were used to investigate an involvement of the Na^+-dependent exchangers in the regulation of I_{Kv} in rat small PASMCs. The main observations include: i) removal of Na^+_o, which is expected to block the activity of the Na^+-dependent exchangers caused a significant leftward shift and an increase in slope of the activation dependency of I_{Kv} activation and a significant reduction in the whole cell maximal conductance, ii) this effect was significantly attenuated by the mitochondrial uncoupler CCCP, suggesting a possible cross talk between the mitochondrial inhibition (described in previous chapters) and Na^+ dependent extrusion mechanisms, iii) a putative involvement of the NME and a complex interaction with the NCE and NHE was shown to be involved in regulation of I_{Kv} iv) Na^+_o-dependent effects on I_{Kv} activation were significantly greater in pulmonary as opposed to systemic (mesenteric) SMCs, suggesting that the observed effects are more specific for PASMCs. The investigation then focused on identifying a possible underlying mechanism and focussed on a role for the three there sodium dependent exchangers present in vascular SMCs, the NHE, NCE and NME, which should all be blocked in the forward direction by Na^+_o removal.

7.3.1 Validation of the ramp voltage protocol

Since the voltage ramp protocol was used throughout this study, the validity of the data was initially confirmed by comparison to the tail protocol, which was routinely used in previous chapters. Comparable shifts in I_{Kv} activation were observed with both voltage protocols when Na^+_o was removed.

It is worth noting that a better theoretical approximation of the experimental values in the physiological range of V_m in the absence than in the presence of Na^+_o was evident (Fig. 7.2 B). Discrepancy between the theory and experimental data were not observed in *I-V*s derived from tail current, suggesting that the reduced I_{Kv} amplitude in the negative voltage range is Na^+ dependent. It has been observed that Kv channels, particularly the Kv1 sub-type expressed in this cell type (Smirnov & Beck, 2002), can be permeable for other monovalent cations such as Na^+, Cs^+, Li^+ (Korn & Ikeda, 1995;

Fedida *et al.*, 1999). It is therefore possible that inward Na^+ flux may interfere with K^+ efflux at negative potentials due to a greater electro-chemical driving force for sodium in this voltage range (Gomez-Lagunas, 2001). However, more complex interactions between Na^+-dependent transport processes influencing the Kv current activation in rat PASMCs cannot be entirely excluded, for example intracellular cations, Na^+ and Mg^{2+}, could be responsible.

7.3.2 Na^+_o specificity

Removal of Na^+_o has a considerable effect upon whole cell steady state I_{Kv} activation shifting it by almost 20 mV to more negative potentials. The effect of the Na^+_o-free solution on I_{Kv} was independent of the type of Na^+_o substitution. All substitutions (except the LiCl-based buffer has a significantly smaller effect (Fig. 7.3)) caused significant and comparable negative shifts in I_{Kv} activation, suggesting the involvement of active Na^+-dependent membrane transport mechanisms under our experimental conditions. Further investigation was therefore focussed on the identification of whether the NCE, NHE and/or NME (all known to be present in PASMCs (Wang *et al.*, 2000; Ziegler *et al.*, 1992; Rios *et al.*, 2005) are involved in the observed effects. These three exchangers were primarily focussed on due to their involvement of cellular homeostasis of Ca^{2+}, H^+, Mg^{2+} and Na^+, which are known to affect I_{Kv} (Gelband *et al.*, 1993; Berger *et al.*, 1998). The lesser effect of the LiCl substitution, which can activate the NHE (Kobayashi *et al.*, 2000), but not the NCE (Wang *et al.*, 2000), on I_{Kv} activation indirectly suggested a possible involvement of the NHE.

A potential effect of each ion and contribution of the exchangers to the Na^+ dependent exchange mechanism was assessed using various pipette buffers (cells were dialysed for 5 min prior to recording), different extracellular solutions and inhibitors of the Na^+-dependent transport systems.

7.3.3 Role of the NME

The NME, has not been so extensively studied particularly in vascular smooth muscle In this chapter experiments carried out with different solutions and inhibitors provides evidence favouring a functional link between the NME and I_{Kv}. In chapter 3 evidence

for a putative link between mitochondrial dependent increased Mg^{2+}_i and the regulation of I_{Kv}. In this chapter CCCP, which was shown to increase Mg^{2+}_i in chapter 3, significantly attenuate the effect of Na^+ free extracellular solution. To summarise the findings presented in this chapter the evidence in favour of an active NME under my experimental conditions includes:

1) Replacement of EGTA with EDTA, a more potent buffer of Mg^{2+} (Fig. 7.5 C&D) in the pipette solution showed a marked attenuation of the Na^+-dependent shift in the I_{Kv} activation.

2) Application of a low concentration of amiloride (100 μM) alone, which has been shown to be relatively selective for blocking NME (Gunther & Vormann, 1985) significantly inhibited the Na^+-dependent shift in I_{Kv}. It is worth mentioning that the effects of amiloride were more potent than those of MIA, however an additional effect of amiloride on the NHE cannot be entirely excluded (Masereel *et al.*, 2003). Any effect on the NCE may be regarded as unlikely since its selectivity for amiloride is 10-50 times higher than that for the NME (Blaustein & Lederer, 1999). Imipramine, a putative NME inhibitor (Gunther & Vormann, 1985), due to its potent I_{Kv} inhibitory property, was deemed an unsuitable pharmacological tool for this study.

3) Inhibition of this exchanger by amiloride may cause an increase in Mg^{2+}_i by restricting its extrusion in exchange for Na^+_o. The removal of extracellular Mg^{2+} represents the most important evidence in favour of the involvement of the NME and Mg^{2+}_i in the observed Na^+_o-dependent I_{Kv} modulation. Importantly, the overall effect of the removal of Na^+ on the I_{Kv} activation was significantly reduced in both reduced extracellular Mg^{2+} (0 mM $MgCl_2$) and increased intracellular Mg^{2+} (10 mM $MgCl_2$), but unaffected by Ca^{2+}_o. Furthermore these experiments suggest the presence of a continuous influx of Mg^{2+} into PASMCs, which is balanced by the activity of the NME as the main mechanism of Mg^{2+} extrusion.

Movement of Mg^{2+} across the cell membrane has been extensively studied using Mg^{2+} sensitive dyes, for example mag-fura-2, indicating a free $[Mg^{2+}]_i$ in the range of 0.6-0.8mM (Gunther, 1993). A fluctuation around this physiological range has also been shown to block the outward currents of potassium channels, interfering directly with the

passage of K^+ ions. This can induce inward rectification of the channel current-voltage relationship at positive potentials or a complete block of the channel pore (Harris & Isacoff, 1996). Gelband *et al.*, (1993) showed that an increase in intracellular divalent cation concentration significantly suppressed I_{Kv} in isolated SMCs. The possibility of a direct effect of $Mg^{2+}{}_i$ on I_{Kv} was also investigated and it was found that an increase to 10 mM $MgCl_2$ in the pipette solution, produced further shifts in I_{Kv} availability.

7.3.3 Effect of Na^+ removal on I_{Kv} block

If Na^+ is mainly acting via inhibition of the NME leading to increased $Mg^{2+}{}_i$, the I_{Kv} block may be similar to the effects observed with the mitochondrial inhibitors. $Mg^{2+}{}_i$ has been shown to block the outward currents of potassium channels, interfering directly with the passage of K^+ ions. This can induce inward rectification of the channel current-voltage relationship at positive potentials or a complete block of the channel pore (Harris & Isacoff, 1996). In support of this Gelband *et al.*, (1993) showed an increase in the intracellular divalent cation concentration significantly suppressed I_{Kv} in isolated SMCs and Tammaro *et al.* (2001) have demonstrated an analogous dependence of $Mg^{2+}{}_i$ on $Mg^{2+}{}_o$ in rat aortic SMCs. Additionally, an increase in $Na^+{}_i$ in KB-R7943 and in pH_o=7.8 may be responsible for driving the shifts in $Na^+{}_o$-free solution. Extracellular protons are known to decrease whole cell I_{Kv} (Fedida *et al.*, 2005; Starkus *et al.*, 2003b). A direct effect of the inhibitors (KB-R7943 and MIA) on the Kv channels also cannot be excluded. Neither this data nor the proposed model can explain the enhanced effect of BAPTA and HEPES on G_{max}, therefore further investigation of this is necessary to gain full understanding.

7.3.4 Involvement of the NCE and NHE

The ability of KB-R7943, a reverse mode NCE inhibitor i) to mimic and ii) significantly attenuate the effect of $Na^+{}_o$-free solution, suggests that the reverse mode of the NCE could be important for the $Na^+{}_o$-dependent modulation of I_{Kv}. However, the presence of 10 mM EGTA in the control conditions makes a direct effect of increased $Ca^{2+}{}_i$ on I_{Kv} activation unlikely. Since the reverse mode of the NCE is generally activated by elevated $Na^+{}_i$ (Blaustein & Lederer, 1999), it is possible that sub-membrane $Na^+{}_i$ accumulation represents the main driving force for reverse NCE activity under our

experimental conditions and also suggests that under our conditions the forward mode of the exchanger is inoperative. Notably, operation of the NCE in the reverse mode under resting Ca^{2+}_i was demonstrated in PASMCs (Wang *et al.*, 2000). This study demonstrated that the removal of Na^+_o during normoxic conditions increased the peak Ca^{2+}_i and slowed the decay rate of the Ca^{2+} peak. Additionally, the NCE current was inhibited during mild hypoxia. The reverse mode has also been shown to be the predominant NCE activity contributing to basal Ca^{2+}_i in the umbilical vein SMCs (Rebolledo *et al.*, 2006); KB-R7943 decreased $[Ca^{2+}]_i$, caused a relaxation of the artery rings and lowered Na^+_o increased $[Ca^{2+}]_i$ proportionally. Removal of extracellular Ca^{2+} should therefore inhibit the NCE in its forward mode and subsequently reduce Ca^{2+} extrusion from the cytosol and increase $[Ca^{2+}]_i$. However, no extracellular Ca^{2+}-dependence of the effects were found under the experimental conditions used in this work (Fig. 7.5), also, neither elevation of $[Ca^{2+}]_i$ from 10 to 220 nM nor buffering of $[Ca^{2+}]_i$ with 10mM BAPTA (Fig. 7.5) had any effect upon the Na^+ dependent shift in steady state I_{Kv} that we observed. Interestingly, there was a significant reduction in I_{Kv} density, which may be due to a direct block of the Kv channel by Ca^{2+}. Thus NCE activity, if involved, is likely to affect the Kv channels indirectly, perhaps via changes in intracellular Na^+ concentration.

The NHE is considered to be one of the main sources for Na^+ influx under physiological conditions (Rebolledo *et al.*, 2006). Despite the lack of proton gradient under our conditions, which should prevent the NHE activity, some Na^+ influx could not be entirely ruled out. The existence of a relatively low activity of the NHE, under my experimental conditions, is further supported by the following experimental observations; 1) cell dialysis with 110 mM HEPES was unable to attenuate the Na^+_o-dependent modulation of I_{Kv} activation after 5 mins, however it did significantly reduce the time-dependence of the effect, and 2) MIA, a selective inhibitor of the NHE, was unable to significantly affect the activation, although did reduce the effect of the Na^+_o-free solution. The effect of extracellular acidification had no significant effect upon I_{Kv} activation, as was expected since the activity of the NHE is generally inhibited under decreased pH_o (Ahn & Hume, 1997). Conversely, an increase in the outward directed proton gradient with pH_o=7.8, which should increase the NHE activity and lead to an increased Na^+ influx, significantly attenuated the effect of Na^+-free solution on I_{Kv}, thus resembling the effect of KB-R7943. The common feature of both processes is that they

result in accumulation of Na^+_i. This may inhibit the NME and increase Mg^{2+}_i, reducing the overall Na^+ dependent shift in I_{Kv} activation. During HPV pH_i decreases and the NHE is then driven by inwardly directed Na^+ and outwardly directed H^+ gradients, facilitating the recovery from intracellular acidity (Madden *et al.*, 2000).

The observed effects of Na^+_o removal on I_{Kv} activation in PAMSCs is explained in the simplified diagram in Fig 7.11. A continuous flux of Mg^{2+}_o activated the NME, which leads to an increase in Na^+. In turn this activates the reverse mode of the NCE to remove some of the Na^+ and thus maintain a low Na^+_i. Removal of Na^+_o will inhibit the NME, resulting in accumulation of Mg^{2+}_i which will subsequently alter I_{Kv} activation (Zhang & Melvin, 1995). Since the NME activity is also dependent upon the Na^+ gradient (Nakayama *et al.*, 2003; Tashiro & Konishi, 1997), then, for example inhibition of the NME with amiloride or activation of the NHE by extracellular acidosis, which should lead to increased local Na^+_i, would mimic the effects of the Na^+_o-free solution, this was not the case. Despite not currently having a plausible explanation of this effect it is entirely possible that amiloride also suppresses Mg^{2+}_o influx. Mechanisms of Mg^{2+} entry into VSMCs are yet to be identified and recently He and colleagues (2005) have reported that TRPM7 could be responsible for Mg^{2+}_i entry into VSMC. Further investigation is necessary to fully address this question.

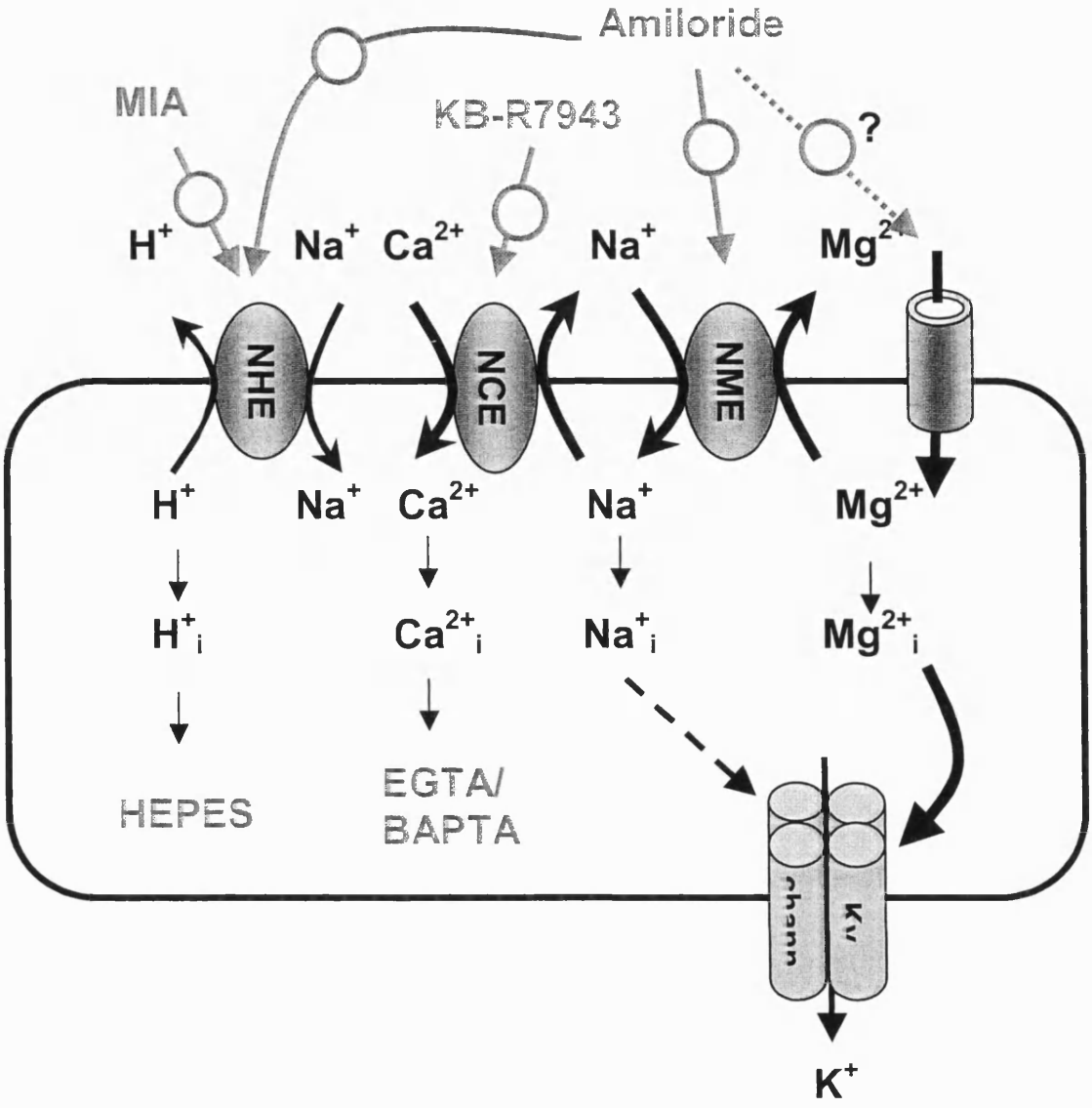

Figure 7.11. Schematic diagram describing a proposed interaction between the Na^+-dependent transport mechanisms and Kv channels in PASMCs.

To conclude, this data suggests that Kv channel activity at physiological membrane potentials is chiefly dependent upon Mg^{2+}_i, whose concentration is determined by the balance between Mg^{2+}_o influx and its extrusion by the NME. This therefore represents a novel regulatory mechanism for I_{Kv} in PASMCs. The results are also consistent with NME activity being dependent upon Na^+_i, which is, in turn, regulated by the NHE and perhaps the NCE, which are the main regulators of Na^+ influx. Under physiological conditions it its therefore the NHE which is most likely to have the greatest influence in the regulation of Na^+_i, the forward mode of the NCE would become more important during periods of agonist induced stimulation. The Na^+-K^+ ATPase, which has not been

considered in this study, is also likely to contribute to this process by removing intracellular Na^+ in exchange for extracellular K^+. The relationships between the components of the proposed mechanism are multifaceted and their interdependence makes the prediction for the changes in intact preparations difficult. In addition the complexity of the regulation of Kv channels in PASMCs may partly be responsible for controversies surrounding K channel roles in HPV. It is worth mentioning that hypoxia is known to modify the activity of the NHE (Rios *et al.*, 2005), and $Mg^{2+}{}_i$ is deemed important for the regulation of the mitochondria. Altogether, the proposed mitochondrial regulated Mg^{2+} dependent modulation of I_{Kv} proposed in Chapter 3, may also alter the activity of the NME (and subsequently the other Na^+ dependent exchangers), enhancing the effects on I_{Kv} activation. This also suggests that modulation of I_{Kv} via the proposed mechanism may be employed in HPV and further consideration of this is necessary.

Chapter 8

CONCLUDING REMARKS

8.1 Summary

A similarity between the effect of hypoxia on I_{Kv} activation in PASMCs (but not in MASMCs) and those of mitochondrial inhibitors and hypoxia-induced increases in $Mg^{2+}{}_i$ suggest, albeit indirectly, that the mitochondrial induced Mg^{2+} dependent mechanism of I_{Kv} modulation could be involved in HPV. The predicted dual effect of mETC inhibition by CCCP and antimycin on the whole cell Kv channel open probability could explain both hypoxia mediated effects on I_{Kv} in PASMCs; enhancement of the current and its subsequent inhibition at more positive potentials. Both observations have been observed in PASMCs previously. Also the model prediction partly agreed with the functional studies

Notably, although it is difficult to evaluate the level of hypoxia-induced increases in $Mg^{2+}{}_i$ from our experiments, local changes in $Mg^{2+}{}_i$ close to the Kv channels may be substantial providing that ion diffusion is restricted. The existence of a restricted diffusion space has been previously demonstrated by measuring the changes in the K^+ gradient during the development of I_{Kv} in rat intra-PASMCs and was thought to be caused by extracellular K^+ accumulation (Smirnov & Aaronson, 1994). It is however possible that intracellular compartmentalisation can also contribute to this process. This phenomenon (not observed in other VSMCs) might potentially be responsible for greater local changes in $Mg^{2+}{}_i$ in PASMCs than in systemic SMCs.

The observation that reduced antimycin-induced effects and the absence of rotenone- and oligomycin-mediated effects in non-dialysed compared to dialysed PASMCs suggests the involvement of other mechanisms attenuating the effect of mitochondrial inhibitors in intact cells. The experimental evidence shows that an increased cellular redox state and/or lower local $Mg^{2+}{}_i$ (due to a higher levels of intracellular ATP, Mg^{2+} uptake by mitochondria or Mg^{2+} extrusion) could be responsible. A similarity between the mean V_a values measured in intact PASMCs and cells dialysed with Na_2ATP or

EDTA in the absence of inhibitors may indirectly support the latter possibility. However, little is known about Mg^{2+}_i homeostasis and mechanisms of its regulation in the pulmonary circulation, and further experimentation is necessary to better understand the role of Mg^{2+} in such a complex phenomenon as HPV.

The findings additionally suggest that I_{Kv} activity at physiological membrane potentials chiefly depends on Mg^{2+}_i, whose concentration is determined by the balance between the extracellular Mg^{2+} influx and its extrusion by the NME, thus representing a novel regulatory mechanism for I_{Kv} in PASMCs. NME activity which depends on Na^+_i is implicated and is consecutively regulated by the NCE and particularly the NHE, as the main regulator of Na^+ influx. Therefore, the NHE is likely to play a greater role in the regulation of Na^+_i under physiological conditions, whilst the forward mode of the NCE should become more important during agonist-induced stimulation. Notably, the Na^+-K^+-ATPase, whose role has not been evaluated in this study, is likely to contribute to this process. Possible complexity of the relationship between various components and their reciprocal dependence make difficult the prediction of the changes in I_{Kv} in intact preparations. The complexity of the regulation of Kv channels in PASMCs might partly be responsible for the controversies surrounding the role of Kv channels in HPV (Ward *et al.*, 2006). It is noteworthy that hypoxia alters both NCE and NHE activity (Madden *et al.*, 2001; Wang *et al.*, 2000), whereas Mg^{2+}_i is important for the regulation of mitochondria, a putative oxygen sensor for HPV, suggesting that modulation of I_{Kv} via this mechanism could also be engaged in HPV.

It is important to also consider that this study, selectively investigating Kv channels, does not, however, exclude the likely contribution of *heteromultimeric* Kv1 channels which might be expressed in PASMCs in different proportions and contribute to variability of parameters. This possibility can be indirectly supported by the evidence shown in chapter 7 whereby cell dialysis with increased [$MgCl_2$] caused a significantly greater effect on I_{Kv} inactivation than activation in PASMCs, whereas similar changes in Mg^{2+}_i caused virtually identical shifts in both dependencies for the current mediated by expressed Kv1.5 α-subunit (Tammaro *et al.*, 2005), which are thought to be one of the channel components in these cells.

Figure 8.1 summarises the data discussed in this thesis and proposes a mechanism by which Mg^{2+}_i is changed by a, yet unidentified, mitochondrial dependent mechanism affecting Kv channel activity.

(1) Hypoxia (P_{O2} < 40mmHg) has two proposed effects relating to the regulation of Kv channels in the pulmonary circulation. The mechanism postulated from evidence in this thesis suggests an inhibitory effect of hypoxia on the mETC causing a decrease in $\Delta\Psi_m$ and alters the rate of Mg^{2+} uptake and release from the mitochondria. The proposed increase in Mg^{2+}_i activates Kv channels.

(2) Simultaneously, hypoxia has been shown to inhibit TASK channels causing membrane depolarisation and activation of L-Type VDCC and entry of Ca^{2+} into the cell (Gurney & Joshi, 2006). In succession CICR from the SR occurs further elevating intracellular Ca^{2+}, additionally a role for CCE has been proposed to occur in response to hypoxia (Becker *et al.*, 2006), SOC are postulated to be the molecular correlates for CCE in PASMCs (Kunichika *et al.*, 2004). Increased sensitivity of the contractile apparatus to Ca^{2+} may be responsible for the sustained phase of HPV (Robertson *et al.*, 2003).

(3) Inhibition of I_{Kv} occurs at more depolarised membrane potentials. Decreased I_{Kv} has also been widely established to occur in response to hypoxia (Post *et al.*, 1992; Yuan *et al.*, 1993).

Additionally changes Mg^{2+} may subsequently change the ATP-to-ADP ratio which may alter Kv channel phosphorylation (Perozo & Bezanilla, 1991; Perozo & Bezanilla, 1990). This thesis also postulates a role for ROS in the regulation of I_{Kv}, however in intact cells and arteries this seems to be a less prominent effect. ROS, predominantly via mETC complex III, may be involved in the regulation of vessel contractility involving more prominent mechanisms to regulation of I_{Kv}.

(4) A continuous flux of Mg^{2+}_o and increased Mg^{2+} from mitochondria activates the NME, which leads to an increase in Na^+. In turn this activates the reverse mode of the NCE to remove some of the Na^+ and thus maintain a low Na^+_i. Removal of Na^+_o will

inhibit the NME, resulting in accumulation of Mg^{2+}_i which will subsequently alter I_{Kv} activation.

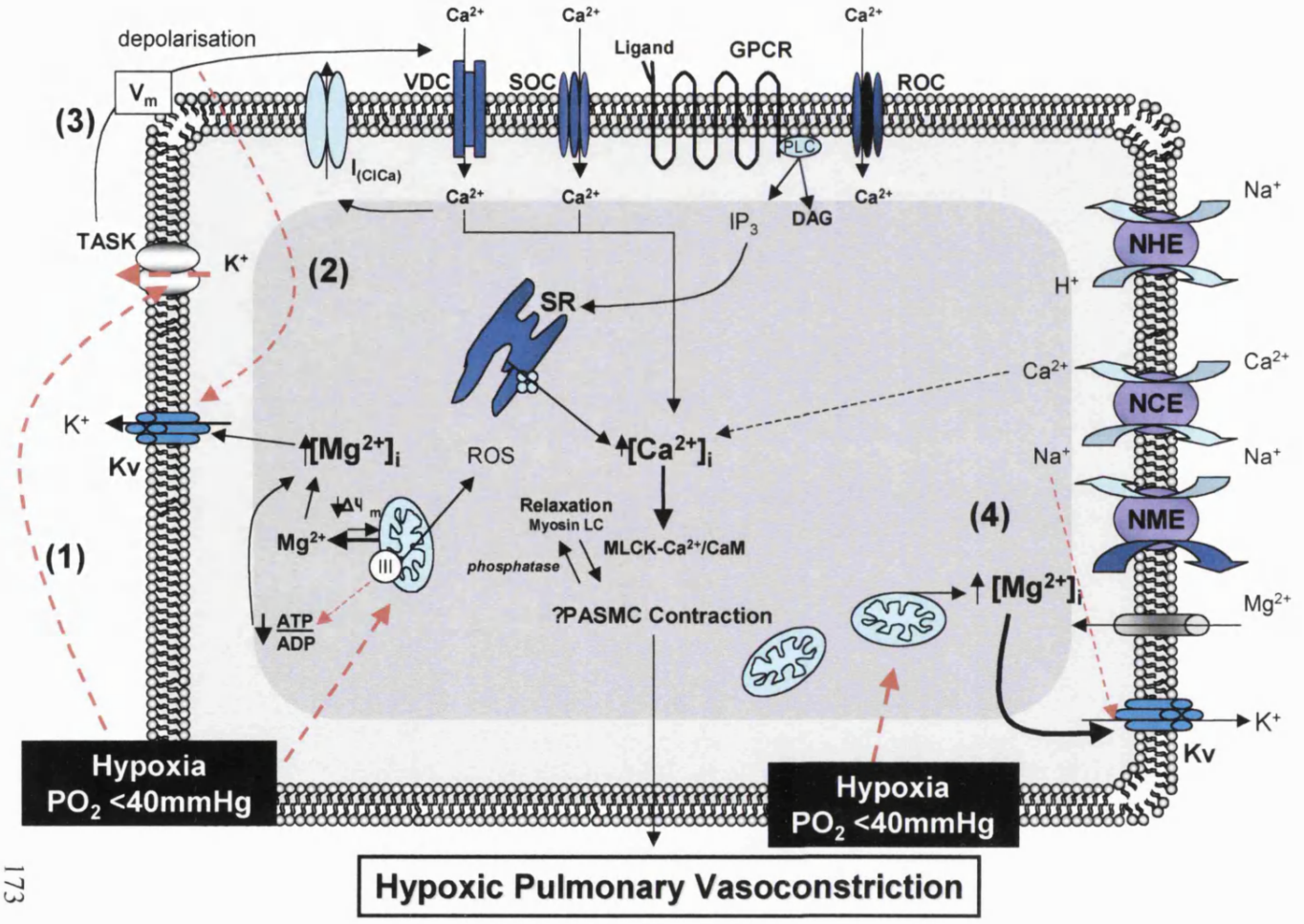

Figure 8.1. A hypothetical diagram demonstrating the proposed involvement of Kv channels in HPV.

8.2 Future Directions

Several questions have arisen from this thesis which requires further experimental investigation to answer.

1) What is the exact involvement of the mitochondrial Mg^{2+} dependent pathway in HPV and how does it differ from the mesenteric circulation?

2) What is the exact mechanism of mitochondrial mediated Kv channel regulation in the mesenteric circulation?

A more comprehensive investigation of the involvement of the mETC and intracellular Mg^{2+}, as was carried out for the PASMCs, will be necessary to answer this question and elucidate the differences in the mechanisms between the two tissues.

3) Importance of Kv channel structural organisation?

4) To what extent are phosphorylation mediated processes involved in this mechanism?

5) Is the Na^{+}-K^{+} ATPase involved in this mitochondrial dependent regulation of I_{Kv} in PASMCs?

6) The involvement of cellular redox state.

7) To understand the relationship between the activity of the exchange mechanisms, particularly those of the NCE and NME.

Importantly, simultaneous patch clamp and fluorescence measurements of pH, Ca^{2+} and Mg^{2+} need to be carried out.

Chapter 9

REFERENCES

(1991). Sodium-Calcium Exchange. Proceedings of the Second International Conference. April 7-11, 1991, Baltimore, Maryland. *Ann. N. Y. Acad. Sci.*, **639**, 1-667.

(1996). 3rd International Conference on Sodium-Calcium Exchange. Woods Hole, Massachusetts, April 23-26, 1995. Proceedings. *Ann. N. Y. Acad. Sci.*, **779**, 1-589.

(2001). Abstracts of the American Physiological Society Conferences. Cellular and Molecular Physiology of Sodium-Calcium Exchange, Banff, Alberta, Canada, October 10-14, 2001. Genome and Hormones: An Integrative Approach to Gender Differences in Physiology, Pittsburgh, Pennsylvania, USA, October 17-20, 2001. *Physiologist.*, **44**, 219-286.

AARONSON, P. I., POSTON, L., WOOLFSON, R. G. & SMIRNOV, S. V. (1991). Evidence for Na-Ca exchange in human resistance arteries. *Ann. N. Y. Acad. Sci.*, **639**, 521-530.

ARONSON, J. K. (1984). The role of the Na^+, K^+-ATPase in the regulation of vascular smooth-muscle contractility, and its relationship to essential hypertension. *Biochem. Soc. Trans.*, **12**, 943-945.

AARONSON, P. I., ROBERTSON, T. P., KNOCK, G. A., BECKER, S., LEWIS, T. H., SNETKOV, V. & WARD, J. P. (2006). Hypoxic pulmonary vasoconstriction: mechanisms and controversies. *J. Physiol.*, **570**, 1-8.

AARONSON, P. I., ROBERTSON, T. P. & WARD, J. P. (2002). Endothelium-derived mediators and hypoxic pulmonary vasoconstriction. *Respiratory Physiology & Neurobiology*, **132**, 107-120.

ACCILI, E. A., KIEHN, J., YANG, Q., WANG, Z., BROWN, A. M. & WIBLE, B. A. (1997). Separable Kvβ subunit domains alter expression and gating of potassium channels. *J. Biol. Chem.*, **272**, 25824-25831.

AGGARWAL, S. K. & MACKINNON, R. (1996). Contribution of the S4 segment to gating charge in the Shaker K^+ channel. *Neuron.*, **16**, 1169-1177.

AGUILAR-BRYAN, L. & BRYAN, J. (1999). Molecular biology of adenosine triphosphate-sensitive potassium channels. *Endocrine Reviews*, **20**, 101-135.

AHN, D. S. & HUME, J. R. (1997). pH regulation of voltage-dependent K^+ channels in canine pulmonary arterial smooth muscle cells. *Pflügers Arch.*, **433**, 758-765.

AICKIN, C. C., BRADING, A. F. & BURDYGA, T. V. (1984). Evidence for sodium-calcium exchange in the guinea-pig ureter. *J. Physiol.*, **347**, 411-430.

AICKIN, C. C. & THOMAS, R. C. (1977). The effect of external Na and amiloride on pH_i recovery in mouse soleus muscle [proceedings]. *J. Physiol.*, **269**, 80P-81P.

AIELLO, E. A., CLÉMENT-CHOMIENNE, O., SONTAG, D. P., WALSH, M. P. & COLE, W. C. (1996). Protein kinase C inhibits delayed rectifier K^+ current in rabbit vascular smooth muscle cells. *Am. J. Physiol.*, **271**, H109-H119.

AIELLO, E. A., WALSH, M. P. & COLE, W. C. (1995). Phosphorylation by protein kinase A enhances delayed rectifier K^+ current in rabbit vascular smooth muscle cells. *Am. J. Physiol.*, **268**, H926-H934.

ALIOUA, A., MAHAJAN, A., NISHIMARU, K., ZAREI, M. M., STEFANI, E. & TORO, L. (2002). Coupling of c-Src to large conductance voltage- and Ca^{2+}-activated K^+ channels as a new mechanism of agonist-induced vasoconstriction. *Proc. Natl. Acad. Sci. USA*, **99**, 14560-14565.

ALTURA, B. M. & ALTURA, B. T. (1984). Magnesium, electrolyte transport and coronary vascular tone. *Drugs*, **28**, 120-142.

ANDERSSON, B. S., AW, T. Y. & JONES, D. P. (1987). Mitochondrial transmembrane potential and pH gradient during anoxia. *Am. J. Physiol.*, **252**, t-55.

ARAKAWA, N., SAKAUE, M., YOKOYAMA, I., HASHIMOTO, H., KOYAMA, Y., BABA, A. & MATSUDA, T. (2000). KB-R7943 inhibits store-operated Ca^{2+} entry in cultured neurons and astrocytes. *Biochem. Biophys. Res. Commun.*, **20;279**, 354-357.

ARCHER, S. L., GRAGASIN, F. S., WU, X., WANG, S., MCMURTRY, S., KIM, D. H., PLATONOV, M., KOSHAL, A., HASHIMOTO, K., CAMPBELL, W. B., FALCK, J. R. & MICHELAKIS, E. D. (2003). Endothelium-derived hyperpolarizing factor in human internal mammary artery is 11,12-epoxyeicosatrienoic acid and causes relaxation by activating smooth muscle BK_{Ca} channels. *Circulation.*, **107**, 769-776.

ARCHER, S. L., HUANG, J., HENRY, T., PETERSON, D. & WEIR, E. K. (1993). A redox-based O_2 sensor in rat pulmonary vasculature. *Circ. Res.*, **73**, 1100-1112.

ARCHER, S. L., HUANG, J. M. C., REEVE, H. L., HAMPL, V., TOLAROVA, S., MICHELAKIS, E., WEIR, E. K. & HUANG, J. M. (1996). Differential distribution of electrophysiologically distinct myocytes in conduit and resistance arteries determines their response to nitric oxide and hypoxia. *Circ. Res.*, **78**, 431-442.

ARCHER, S. L., LONDON, B., HAMPL, V., WU, X., NSAIR, A., PUTTAGUNTA, L., HASHIMOTO, K., WAITE, R. E. & MICHELAKIS, E. D. (2001). Impairment of hypoxic pulmonary vasoconstriction in mice lacking the voltage-gated potassium channel Kv1.5. *FASEB J.*, **15**, 1801-1803.

ARCHER, S. & MICHELAKIS, E. (2002). The mechanism(s) of hypoxic pulmonary vasoconstriction: potassium channels, redox O_2 sensors, and controversies. *News Physiol. Sci.*, **17**, 131-137.

ARCHER, S. L., REEVE, H. L., MICHELAKIS, E., PUTTAGUNTA, L., WAITE, R., NELSON, D. P., DINAUER, M. C. & WEIR, E. K. (1999). O_2 sensing is preserved in mice lacking the gp91 phox subunit of NADPH oxidase. *Proc. Natl. Acad. Sci. U. S. A.*, **96**, 7944-7949.

ARCHER, S. L., SOUIL, E., DINH-XUAN, A. T., SCHREMMER, B., MERCURE, J. V., EL YAAGOUBI, A., NGUYEN-HUU, L., REEVE, H. L. & HAMPL, V. (1998). Molecular identification of the role of voltage-gated K^+ channels, Kv1.5 and Kv2.1, in hypoxic pulmonary vasoconstriction and control of resting membrane potential in rat pulmonary artery myocytes. *J. Clin. Invest.*, **101**, 2319-2330.

ARCHER, S. L., WILL, J. A. & WEIR, E. K. (1986). Redox status in the control of pulmonary vascular tone. *Herz*, **11**, 127-141.

ARCHER, S. L., WU, X. C., THEBAUD, B., NSAIR, A., BONNET, S., TYRRELL, B., MCMURTRY, M. S., HASHIMOTO, K., HARRY, G. & MICHELAKIS, E. D. (2004). Preferential expression and function of voltage-gated, O_2-sensitive K^+ channels in resistance pulmonary arteries explains regional heterogeneity in hypoxic pulmonary vasoconstriction: ionic diversity in smooth muscle cells. *Circ. Res.*, **95**, 308-318.

BAE, M., KIM, S., KO, E., LEE, S. H., HO, W. K. & EARM, Y. E. (2002). Intracellular Mg^{2+} hyperpolarizes rabbit coronary artery smooth muscle cells by differential modulation of $Ca^{2+}{}_i$-dependent ion channels. *Pflügers Arch.*, **444**, 523-531.

BARLOW, R. S., EL-MOWAFY, A. M. & WHITE, R. E. (2000). H_2O_2 opens BK_{Ca} channels via the PLA_2-arachidonic acid signaling cascade in coronary artery smooth muscle. *Am. J. Physiol.*, **279**, H475-H483.

BARMAN, S. A., ZHU, S., HAN, G. & WHITE, R. E. (2003). cAMP activates BK_{Ca} channels in pulmonary arterial smooth muscle via cGMP-dependent protein kinase. *Am. J. Physiol Lung Cell Mol. Physiol.*, **284**, L1004-L1011.

BARMAN, S. A., ZHU, S. & WHITE, R. E. (2004). Protein kinase C inhibits BK_{Ca} channel activity in pulmonary arterial smooth muscle. *Am. J. Physiol.*, **286**, L149-L155.

BARMAN, S. A., ZHU, S. & WHITE, R. E. (2005). Hypoxia modulates cyclic AMP activation of BK_{Ca} channels in rat pulmonary arterial smooth muscle. *Lung.*, **183**, 353-361.

BAUER, A. J. & SANDERS, K. M. (1985). Gradient in excitation-contraction coupling in canine gastric antral circular muscle. *J. Physiol.*, **369**, 283-294.

BECKER, S., KNOCK, G. A., SNETKOV, V., WARD, J. P. & AARONSON, P. I. (2006). Role of capacitative Ca^{2+} entry but not Na^+/Ca^{2+} exchange in hypoxic pulmonary vasoconstriction in rat intrapulmonary arteries. *Novartis. Found. Symp.*, **272**, 259-268.

BEECH, D. J. (2005). Emerging functions of 10 types of TRP cationic channel in vascular smooth muscle. *Clin. Exp. Pharmacol. Physiol.*, **32**, 597-603.

BEECH, D. J. & BOLTON, T. B. (1989). Two components of potassium current activated by depolarization of single smooth muscle cells from the rabbit portal vein. *J. Physiol.*, **418**, 293-309.

BEECH, D. J., ZHANG, H., NAKAO, K. & BOLTON, T. B. (1993). K channel activation by nucleotide diphosphates and its inhibition by glibenclamide in vascular smooth muscle cells. *Br. J. Pharmacol.*, **110**, 573-582.

BELAIBA, R. S., DJORDJEVIC, T., BONELLO, S., FLUGEL, D., HESS, J., KIETZMANN, T. & GORLACH, A. (2004). Redox-sensitive regulation of the HIF pathway under non-hypoxic conditions in pulmonary artery smooth muscle cells. *Biol. Chem.*, **385**, 249-257.

BELEVICH, I., VERKHOVSKY, M. I. & WIKSTROM, M. (2006). Proton-coupled electron transfer drives the proton pump of cytochrome c oxidase. *Nature.*, **440**, 829-832.

BERGDAHL, A., GOMEZ, M. F., WIHLBORG, A. K., ERLINGE, D., EYJOLFSON, A., XU, S. Z., BEECH, D. J., DREJA, K. & HELLSTRAND, P. (2005). Plasticity of TRPC expression in arterial smooth muscle: correlation with store-operated Ca^{2+} entry. *Am. J. Physiol Cell Physiol.*, **288**, C872-C880.

BERGER, M. G., VANDIER, C., BONNET, P., JACKSON, W. F. & RUSCH, N. J. (1998). Intracellular acidosis differentially regulates K_V channels in coronary and pulmonary vascular muscle. *Am. J. Physiol.*, **275**, H1351-H1359.

BERK, B. C., VALLEGA, G., MUSLIN, A. J., GORDON, H. M., CANESSA, M. & ALEXANDER, R. W. (1989). Spontaneously hypertensive rat vascular smooth muscle cells in culture exhibit increased growth and Na^+/H^+ exchange. *J. Clin. Invest.*, **83**, 822-829.

BERRA-ROMANI, R., BLAUSTEIN, M. P. & MATTESON, D. R. (2005). TTX-sensitive voltage-gated Na^+ channels are expressed in mesenteric artery smooth muscle cells. *Am. J. Physiol Heart Circ. Physiol.*, **289**, H137-H145.

BLANCO, G., SANCHEZ, G. & MERCER, R. W. (1998). Differential regulation of Na,K-ATPase isozymes by protein kinases and arachidonic acid. *Arch. Biochem. Biophys.*, **359**, 139-150.

BLAUSTEIN, M. P., FONTANA, G. & ROGOWSKI, R. S. (1996). The Na^{+}-Ca^{2+} exchanger in rat brain synaptosomes. Kinetics and regulation. *Ann. N. Y. Acad. Sci.*, **779**, 300-317.

BLAUSTEIN, M. P. & LEDERER, W. J. (1999). Sodium/calcium exchange: its physiological implications. *Physiol. Rev.*, **79**, 763-854.

BOHR, D. F., SEIDEL, C. & SOBIESKI, J. (1969). Possible role of sodium-calcium pumps in tension development of vascular smooth muscle. *Microvasc. Res.*, **1**, 335-343.

BOLGUNAS, S., CLARK, D. A., HANNA, W. S., MAUVAIS, P. A. & PEMBER, S. O. (2006). Potent inhibitors of the Q_i site of the mitochondrial respiration complex III. *J. Med. Chem.*, **49**, 4762-4766.

BOLOTINA, V., GERICKE, M. & BREGESTOVSKI, P. (1991). Kinetic differences between Ca^{2+}-dependent K^{+} channels in smooth muscle cells isolated from normal and atherosclerotic human aorta. *Pros. R. Soc. London Ser. B*, **244 (1309)**, 51-55.

BOLOTINA, V. M., NAJIBI, S., PALACINO, J. J., PAGANO, P. J. & COHEN, R. A. (1994). Nitric oxide directly activates calcium-dependent potassium channels in vascular smooth muscle. *Nature*, **368**, 850-853.

BOLTON, T. B. (1979). Mechanisms of action of transmitters and other substances on smooth muscle. *Physiol. Rev.*, **59**, 606-718.

BRANDOLIN, G., LE SAUX, A., TREZEGUET, V., LAUQUIN, G. J. & VIGNAIS, P. V. (1993). Chemical, immunological, enzymatic, and genetic approaches to studying the arrangement of the peptide chain of the ADP/ATP carrier in the mitochondrial membrane. *J. Bioenerg. Biomembr.*, **25**, 459-472.

BRAKEMEIER, S., EICHLER, I., KNORR, A., FASSHEBER, T., KOHLER, R. & HOYER, J. (2003). Modulation of Ca^{2+}-activated K^{+} channel in renal artery endothelium in situ by nitric oxide and reactive oxygen species. *Kidney Int.*, **64**, 199

BRAYDEN, J. E. (1996). Potassium channels in vascular smooth muscle. *Clin. Exp. Pharmacol. Physiol.*, **23**, 1069-1076.

BRAYDEN, J. E. & NELSON, M. T. (1992). Regulation of arterial tone by activation of calcium-dependent potassium channels. *Science*, **256**, 532-535.

BRECHT, M. & DE GROOT, H. (1994). [Changes in cytosol Ca^{2+}-, Mg^{2+}-, H^{+}-, N^{+}-, and K^{+}-concentrations in cultivated hepatocytes in hypoxic conditions]. *Zentralbl. Chir.*, **119**, 341-346.

BRENNER, R., PEREZ, G. J., BONEV, A. D., ECKMAN, D. M., KOSEK, J. C., WILER, S. W., PATTERSON, A. J., NELSON, M. T. & ALDRICH, R. W. (2000). Vasoregulation by the beta1 subunit of the calcium-activated potassium channel. *Nature.*, **19;407**, 870-876.

BRUEGGEMANN, L. I., MARKUN, D. R., BARAKAT, J. A., CHEN, H. & BYRON, K. L. (2005). Evidence against reciprocal regulation of Ca^{2+} entry by vasopressin in A7r5 rat aortic smooth-muscle cells. *Biochem. J.*, **388**, 1-44.

BRUEGGEMANN, L. I., MARKUN, D. R., HENDERSON, K. K., CRIBBS, L. L. & BYRON, K. L. (2006). Pharmacological and electrophysiological characterization of store-operated currents and capacitative Ca^{2+} entry in vascular smooth muscle cells. *J. Pharmacol. Exp. Ther.*, **317**, 488-499.

CACHERO, T. G., MORIELLI, A. D. & PERALTA, E. G. (1998). The small GTP-binding protein RhoA regulates a delayed rectifier potassium channel. *Cell*, **93**, 1077-1085.

CARL, A., KENYON, J. L., UEMURA, D., FUSETANI, N. & SANDERS, K. M. (1991). Regulation of Ca^{2+}-activated K^{+} channels by protein kinase A and phosphatase inhibitors. *Am. J. Physiol.*, **261**, C387-C392.

CANESSA, M., MORGAN, K., GOLDSZER, R., MOORE, T. J. & SPALVINS, A. (1991). Kinetic abnormalities of the red blood cell sodium-proton exchange in hypertensive patients. *Hypertension.*, **17**, 340-348.

CHANDEL, N. S., MCCLINTOCK, D. S., FELICIANO, C. E., WOOD, T. M., MELENDEZ, J. A., RODRIGUEZ, A. M. & SCHUMACKER, P. T. (2000). Reactive oxygen species generated at mitochondrial complex III stabilize hypoxia-inducible factor-1alpha during hypoxia: a mechanism of O_2 sensing. *J. Biol. Chem.*, **275**, 25130-25138.

CHEN, C., SAXENA, A. K., SIMCOKE, W. N., GARBOCZI, D. N., PEDERSEN, P. L. & KO, Y. H. (2006). Mitochondrial ATP synthase. Crystal structure of the catalytic F1 unit in a vanadate-induced transition-like state and implications for mechanism. *J. Biol. Chem.*, **281**, 13777-13783.

CHEN, Q., VAZQUEZ, E. J., MOGHADDAS, S., HOPPEL, C. L. & LESNEFSKY, E. J. (2003). Production of reactive oxygen species by mitochondria: central role of complex III. *J. Biol. Chem.*, **278**, 36027-36031.

CHEONG, A., DEDMAN, A. M. & BEECH, D. J. (2001). Expression and function of native potassium channel [K(V)alpha1] subunits in terminal arterioles of rabbit. *J. Physiol.*, **534**, 3-700.

CHERANOV, S. Y. & JAGGAR, J. H. (2004). Mitochondrial modulation of Ca^{2+} sparks and transient K_{Ca} currents in smooth muscle cells of rat cerebral arteries. *J. Physiol.*, **556**, 3-71.

CHOBY, C., MANGONI, M. E., BOCCARA, G., NARGEOT, J. & RICHARD, S. (2000). Evidence for tetrodotoxin-sensitive sodium currents in primary cultured myocytes from human, pig and rabbit arteries. *Pflugers Arch.*, **440**, 149-152.

CHOI, B. H., CHOI, J. S., JEONG, S. W., HAHN, S. J., YOON, S. H., JO, Y. H. & KIM, M. S. (2000). Direct block by bisindolylmaleimide of rat Kv1.5 expressed in Chinese hamster ovary cells. *J. Pharmacol. Exp. Ther.*, **293**, 634-640.

CHRISSOBOLIS, S. & SOBEY, C. G. (2002). Inhibitory effects of protein kinase C on inwardly rectifying K^+- and ATP-sensitive K^+ channel-mediated responses of the basilar artery. *Stroke.*, **33**, 1692-1697.

CLAPHAM, D. E., RUNNELS, L. W. & STRUBING, C. (2001). The TRP ion channel family. *Nat. Rev. Neurosci.*, **2**, 387-396.

CLAPP, L. H. & GURNEY, A. M. (1992). ATP-sensitive K^+ channels regulate resting potential of pulmonary arterial smooth muscle cells. *Am. J. Physiol.*, **262**, H916-H920.

CLAPP, L. H. & GURNEY, A. M. (1993). ATP-sensitive K^+ channels in the pulmonary vasculature. In *Ion Flux in Pulmonary Vascular Control*, eds. Weir, E. K., Hume, J. R. & Reeves, J. T., pp. 129-139.New York and London: Plenum Press.

CLAPP, L. H. & GURNEY, A. M. (1992). ATP-sensitive K^+ channels regulate resting potential of pulmonary arterial smooth muscle cells. *Am. J. Physiol.*, **262**, H916-H920.

COPPOCK, E. A. & TAMKUN, M. M. (2001). Differential expression of K_V channel α- and β-subunits in the bovine pulmonary arterial circulation. *Am. J. Physiol.*, **281**, L1350-L1360.

COX, D. H. & ALDRICH, R. W. (2000). Role of the β1 subunit in large-conductance Ca^{2+}-activated K^+ channel gating energetics. Mechanisms of enhanced Ca^{2+} sensitivity. *J. Gen. Physiol.*, **116**, 411-432.

COX, R. H. & PETROU, S. (1999). Ca^{2+} influx inhibits voltage-dependent and augments Ca^{2+}-dependent K^+ currents in arterial myocytes. *Am. J. Physiol.*, **277**, C51-C63.

COX, R. H. & RUSCH, N. J. (2002). New expression profiles of voltage-gated ion channels in arteries exposed to high blood pressure. *Microcirculation*, **9**, 243-257.

COX, R. H., ZHOU, Z. & TULENKO, T. N. (1998). Voltage-gated sodium channels in human aortic smooth muscle cells. *J. Vasc. Res.*, **35**, 310-317.

CUI, Y., GIBLIN, J. P., CLAPP, L. H. & TINKER, A. (2001). A mechanism for ATP-sensitive potassium channel diversity: Functional coassembly of two pore-forming subunits. *Proc. Natl. Acad. Sci. U. S. A.*, **98**, 729-734.

CUI, Y., TRAN, S., TINKER, A. & CLAPP, L. H. (2002). The molecular composition of K_{ATP} channels in human pulmonary artery smooth muscle cells and their modulation by growth. *Am. J. Respir. Cell Mol. Biol.*, **26**, 135-143.

DAVIES, A. R. & KOZLOWSKI, R. Z. (2001). Kv channel subunit expression in rat pulmonary arteries. *Lung*, **179**, 147-161.

DEMIN, O. V., KHOLODENKO, B. N. & SKULACHEV, V. P. (1998). A model of O2.-generation in the complex III of the electron transport chain. *Mol. Cell Biochem.*, **184**, 21-33.

DIETRICH, A., CHUBANOV, V., KALWA, H., ROST, B. R. & GUDERMANN, T. (2006). Cation channels of the transient receptor potential superfamily: Their role in physiological and pathophysiological processes of smooth muscle cells. *Pharmacol. Ther.*, ..

DEFARIAS, F. P., CARVALHO, M. F., LEE, S. H., KACZOROWSKI, G. J. & SUAREZ-KURTZ, G. (1996). Effects of the K^+ channel blockers paspalitrem-C and paxilline on mammalian smooth muscle. *Eur. J. Pharmacol.*, **314**, 123-128.

DORNER, A., OLESCH, M., GIESSEN, S., PAUSCHINGER, M. & SCHULTHEISS, H. P. (1999). Transcription of the adenine nucleotide translocase isoforms in various types of tissues in the rat. *Biochim. Biophys. Acta.*, **1417**, 16-24.

DRUMMOND, R. M. & TUFT, R. A. (1999). Release of Ca^{2+} from the sarcoplasmic reticulum increases mitochondrial [Ca^{2+}] in rat pulmonary artery smooth muscle cells. *J. Physiol.*, **516**, 139-147.

DU, W., FRAZIER, M., MCMAHON, T. J. & EU, J. P. (2005). Redox activation of intracellular calcium release channels (ryanodine receptors) in the sustained phase of hypoxia-induced pulmonary vasoconstriction. *Chest.*, **128**, Suppl-558S.

DUDLEY, C. R., TAYLOR, D. J., NG, L. L., KEMP, G. J., RATCLIFFE, P. J., RADDA, G. K. & LEDINGHAM, J. G. (1990). Evidence for abnormal Na^+/H^+ antiport activity detected by phosphorus nuclear magnetic resonance spectroscopy in exercising skeletal muscle of patients with essential hypertension. *Clin. Sci. (Lond).*, **79**, 491-497.

DUMAS, J. P., BARDOU, M., GOIRAND, F. & DUMAS, M. (1999). Hypoxic pulmonary vasoconstriction. *Gen. Pharmacol.*, **33**, 289-297.

EBEL, H., HOLLSTEIN, M. & GUNTHER, T. (2004). Differential effect of imipramine and related compounds on Mg^{2+} efflux from rat erythrocytes. *Biochim. Biophys. Acta.*, **1667**, 132-140.

EDWARDS, G., IBBOTSON, T. & WESTON, A. H. (1993). Levcromakalim may induce a voltage-independent K-current in rat portal veins by modifying the gating properties of the delayed rectifier. *Br. J. Pharmacol.*, **110**, 1037-1048.

EVANS, A. M., MUSTARD, K. J., WYATT, C. N., PEERS, C., DIPP, M., KUMAR, P., KINNEAR, N. P. & HARDIE, D. G. (2005). Does AMP-activated protein kinase couple inhibition of mitochondrial oxidative phosphorylation by hypoxia to calcium signaling in O_2-sensing cells? *J. Biol. Chem.*, **280**, 41504-41511.

EVANS, A. M., OSIPENKO, O. N. & GURNEY, A. M. (1996). Properties of a novel K^+ current that is active at resting potential in rabbit pulmonary artery smooth muscle cells. *J. Physiol.*, **496**, 407-420.

FAGAN, K. A., OKA, M., BAUER, N. R., GEBB, S. A., IVY, D. D., MORRIS, K. G. & MCMURTRY, I. F. (2004). Attenuation of acute hypoxic pulmonary vasoconstriction and hypoxic pulmonary hypertension in mice by inhibition of Rho-kinase. *Am. J. Physiol Lung Cell Mol. Physiol.*, **287**, L656-L664.

FARRUKH, I. S., HOIDAL, J. R. & BARRY, W. H. (1996). Effect of intracellular pH on ferret pulmonary arterial smooth muscle cell calcium homeostasis and pressure. *J. Appl. Physiol.*, **80**, 496-505.

FAXEN, K., GILDERSON, G., ADELROTH, P. & BRZEZINSKI, P. (2005). A mechanistic principle for proton pumping by cytochrome c oxidase. *Nature.*, **437**, 286-289.

FEDIDA, D., MARUOKA, N. D. & LIN, S. (1999). Modulation of slow inactivation in human cardiac Kv1.5 channels by extra- and intracellular permeant cations. *J. Physiol.*, **515**, 315-329.

FEDIDA, D., ZHANG, S., KWAN, D. C., EDULJEE, C. & KEHL, S. J. (2005). Synergistic inhibition of the maximum conductance of Kv1.5 channels by extracellular K+ reduction and acidification. *Cell Biochem. Biophys.*, **43**, 231-242.

FRANCO-OBREGÓN, A. & LÓPEZ-BARNEO, J. (1996). Differential oxygen sensitivity of calcium channels in rabbit smooth muscle cells of conduit and resistance pulmonary arteries. *J. Physiol.*, **491**, 511-518.

GAO, Y. D. & GARCIA, M. L. (2003). Interaction of agitoxin2, charybdotoxin, and iberiotoxin with potassium channels: selectivity between voltage-gated and Maxi-K channels. *Proteins*, **52**, 146-154.

GAO, Y. J., HIROTA, S., ZHANG, D. W., JANSSEN, L. J. & LEE, R. M. (2003). Mechanisms of hydrogen-peroxide-induced biphasic response in rat mesenteric artery. *Br. J. Pharmacol.*, **138**, 1085-1092.

GAO, Y. J. & LEE, R. M. (2001). Hydrogen peroxide induces a greater contraction in mesenteric arteries of spontaneously hypertensive rats through thromboxane A_2 production. *Br. J. Pharmacol.*, **134**, 1639-1646.

GAO, Y. Q., YANG, W. & KARPLUS, M. (2005). A structure-based model for the synthesis and hydrolysis of ATP by F1-ATPase. *Cell.*, **123**, 195-205.

GARDENER, M. J., JOHNSON, I. T., BURNHAM, M. P., EDWARDS, G., HEAGERTY, A. M. & WESTON, A. H. (2004). Functional evidence of a role for two-pore domain potassium channels in rat mesenteric and pulmonary arteries. *Br. J. Pharmacol.*, **142**, 192-202.

GARDENER, M. J., JOHNSON, I. T., BURNHAM, M. P., EDWARDS, G., HEAGERTY, A. M. & WESTON, A. H. (2004). Functional evidence of a role for two-pore domain potassium channels in rat mesenteric and pulmonary arteries. *Br. J. Pharmacol.*, **142**, 192-202.

GASBARRINI, A., BORLE, A. B., FARGHALI, H., BENDER, C., FRANCAVILLA, A. & VAN THIEL, D. (1992). Effect of anoxia on intracellular ATP, Na^+_i, Ca^{2+}_i, Mg^{2+}_i, and cytotoxicity in rat hepatocytes. *J. Biol. Chem.*, **267**, 6654-6663.

GEERING, K. (2006). FXYD proteins: new regulators of Na-K-ATPase. *Am. J. Physiol Renal Physiol.*, **290**, F241-F250.

GELBAND, C. H., ISHIKAWA, T., POST, J. M., KEEF, K. D. & HUME, J. R. (1993). Intracellular divalent cations block smooth muscle K^+ channels. *Circ. Res.*, **73**, 24-34.

GENOVA, M. L., VENTURA, B., GIULIANO, G., BOVINA, C., FORMIGGINI, G., PARENTI, C. G. & LENAZ, G. (2001). The site of production of superoxide radical in mitochondrial Complex I is not a bound ubisemiquinone but presumably iron-sulfur cluster N2. *FEBS Lett.*, **505**, 364-368.

GHERGHICEANU, M. & POPESCU, L. M. (2006). Caveolar nanospaces in smooth muscle cells. *J. Cell Mol. Med.*, **10**, 519-528.

GIANGIACOMO, K. M., GARCIA, M. L. & MCMANUS, O. B. (1992). Mechanism of iberiotoxin block of the large-conductance calcium-activated potassium channel from bovine aortic smooth muscle. *Biochemistry.*, **31**, 6719-6727.

GIBOR, G., YAKUBOVICH, D., PERETZ, A. & ATTALI, B. (2004). External barium affects the gating of KCNQ1 potassium channels and produces a pore block via two discrete sites. *J. Gen. Physiol.*, **124**, 83-102.

GLAVIND-KRISTENSEN, M., MATCHKOV, V., HANSEN, V. B., FORMAN, A., NILSSON, H. & AALKJAER, C. (2004). KATP-channel-induced vasodilation is modulated by the Na,K-pump activity in rabbit coronary small arteries. *Br. J. Pharmacol.*, **143**, 872-880.

GOLOVINA, V. A., PLATOSHYN, O., BAILEY, C. L., WANG, J., LIMSUWAN, A., SWEENEY, M., RUBIN, L. J. & YUAN, J. X. (2001). Upregulated *TRP* and enhanced capacitative Ca^{2+} entry in human pulmonary artery myocytes during proliferation. *Am. J. Physiol.*, **280**, H746-H755.

GOMEZ-HERNANDEZ, J. M., LORRA, C., PARDO, L. A., STUHMER, W., PONGS, O., HEINEMANN, S. H. & ELLIOTT, A. A. (1997). Molecular basis for different pore properties of potassium channels from the rat brain Kv1 gene family. *Pflugers Arch.*, **434**, 661-668.

GOMEZ-LAGUNAS, F. (2001). Na^+ interaction with the pore of Shaker B K(+) channels: zero and low K(+) conditions. *J. Gen. Physiol.*, **118**, 639-648.

GOMEZ-VIQUEZ, L., GUERRERO-SERNA, G., GARCIA, U. & GUERRERO-HERNANDEZ, A. (2003). SERCA pump optimizes Ca^{2+} release by a mechanism independent of store filling in smooth muscle cells. *Biophys. J.*, **85**, 370-380.

GROPP, T., BRUSTOVETSKY, N., KLINGENBERG, M., MULLER, V., FENDLER, K. & BAMBERG, E. (1999). Kinetics of electrogenic transport by the ADP/ATP carrier. *Biophys. J.*, **77**, 714-726.

GUERINI, D., COLETTO, L. & CARAFOLI, E. (2005). Exporting calcium from cells. *Cell Calcium.*, **38**, 281-289.

GUNTHER, T. (1993). Mechanisms and regulation of Mg^{2+} efflux and Mg^{2+} influx. *Miner. Electrolyte Metab.*, **19**, 259-265.

GRISSMER, S. & CAHALAN, M. D. (1989). Divalent ion trapping inside potassium channels of human T lymphocytes. *J. Gen. Physiol.*, **93**, 609-630.

GUNTHER, T. & VORMANN, J. (1985). Mg^{2+} efflux is accomplished by an amiloride-sensitive Na^{+}/Mg^{2+} antiport. *Biochem. Biophys. Res. Commun.*, **130**, 540-545.

GURNEY, A. M. & JOSHI, S. (2006). The role of twin pore domain and other K^{+} channels in hypoxic pulmonary vasoconstriction. *Novartis. Found. Symp.*, **272**, 218-228.

GURNEY, A. M., OSIPENKO, O. N., MACMILLAN, D., MCFARLANE, K. M., TATE, R. J. & KEMPSILL, F. E. (2003). Two-pore domain K channel, TASK-1, in pulmonary artery smooth muscle cells. *Circ. Res.*, **93**, 957-964.

GUTTERMAN, D. D., MIURA, H. & LIU, Y. (2005). Redox modulation of vascular tone: focus of potassium channel mechanisms of dilation. *Arterioscler. Thromb. Vasc. Biol.*, **25**, 671-678.

GUZY, R. D., HOYOS, B., ROBIN, E., CHEN, H., LIU, L., MANSFIELD, K. D., SIMON, M. C., HAMMERLING, U. & SCHUMACKER, P. T. (2005). Mitochondrial complex III is required for hypoxia-induced ROS production and cellular oxygen sensing. *Cell Metab.*, **1**, 401-408.

HAMILL, O. P., MARTY, A., NEHER, E., SAKMANN, B. & SIGWORTH, F. J. (1981). Improved patch-clamp techniques for high-resolution current recording from cells and cell-free membrane patches. *Pflügers Arch.*, **391**, 85-100.

HASUNUMA, K., RODMAN, D. M. & MCMURTRY, I. F. (1991). Effects of K^+ channel blockers on vascular tone in the perfused rat lung. *Am. Rev. Respir. Dis.*, **144**, 884-887.

HATTORI, T., KAJIKURI, J., KATSUYA, H. & ITOH, T. (2003). Effects of H2O2 on membrane potential of smooth muscle cells in rabbit mesenteric resistance artery. *Eur. J. Pharmacol.*, **%19;464**, 101-109.

HARRIS, R. E. & ISACOFF, E. Y. (1996). Hydrophobic mutations alter the movement of Mg^{2+} in the pore of voltage-gated potassium channels. *Biophys. J.*, **71**, 209-219.

HILLE, B. (2001). *Ionic Channels of Excitable Membranes*, 3rd ed., pp. 1-814.Sunderland, Massachusetts: Sinauer Associates Inc.

HIMPENS, B., DE SMEDT, H., DROOGMANS, G. & CASTEELS, R. (1992). Differences in regulation between nuclear and cytoplasmic Ca^{2+} in cultured smooth muscle cells. *Am. J. Physiol.*, **263**, C95-C105.

HISLOP, A. & REID, L. (1978). Normal structure and dimensions of the pulmonary arteries in the rat. *J. Anat.*, **125**, 1-83.

HOBAI, I. A. & O'ROURKE, B. (2004). The potential of Na^+/Ca^{2+} exchange blockers in the treatment of cardiac disease. *Expert. Opin. Investig. Drugs.*, **13**, 653-664.

HOFMANN, T., SCHAEFER, M., SCHULTZ, G. & GUDERMANN, T. (2002). Subunit composition of mammalian transient receptor potential channels in living cells. *Proc. Natl. Acad. Sci. U. S. A.*, **99**, 7461-7466.

HOGG, D. S., DAVIES, A. R., MCMURRAY, G. & KOZLOWSKI, R. Z. (2002). $K_V2.1$ channels mediate hypoxic inhibition of I_{KV} in native pulmonary arterial smooth muscle cells of the rat. *Cardiovasc. Res.*, **55**, 349-360.

HONG, S. J. & CHANG, C. C. (1998). Novel inhibition of contractility by wortmannin in skeletal muscle. *Br. J. Pharmacol.*, **124**, 849-856.

HONG, Z., WEIR, E. K., NELSON, D. P. & OLSCHEWSKI, A. (2004). Subacute hypoxia decreases voltage-activated potassium channel expression and function in pulmonary artery myocytes. *Am. J. Respir. Cell Mol. Biol.*, **31**, 337-343.

HOROWITZ, A., MENICE, C. B., LAPORTE, R. & MORGAN, K. G. (1996). Mechanisms of smooth muscle contraction. *Physiol Rev.*, **76**, 967-1003.

HUANG, W., YEN, R. T., MCLAURINE, M. & BLEDSOE, G. (1996). Morphometry of the human pulmonary vasculature. *J. Appl. Physiol.*, **81**, 2123-2133.

HUDMAN, D., RAINBOW, R. D., LAWRENCE, C. L. & STANDEN, N. B. (2002). The origin of calcium overload in rat cardiac myocytes following metabolic inhibition with 2,4-dinitrophenol. *J. Mol. Cell Cardiol.*, **34**, 859-871.

HUNTE, C., PALSDOTTIR, H. & TRUMPOWER, B. L. (2003). Protonmotive pathways and mechanisms in the cytochrome bc1 complex. *FEBS Lett.*, **545**, 39-46.

HULME, J. T., COPPOCK, E. A., FELIPE, A., MARTENS, J. R. & TAMKUN, M. M. (1999). Oxygen sensitivity of cloned voltage-gated K^+ channels expressed in the pulmonary vasculature. *Circ. Res.*, **85**, 489-497.

INOUE, R., JENSEN, L. J., SHI, J., MORITA, H., NISHIDA, M., HONDA, A. & ITO, Y. (2006). Transient receptor potential channels in cardiovascular function and disease. *Circ. Res.*, **99**, 119-131.

ISHIGURO, M., WELLMAN, T. L., HONDA, A., RUSSELL, S. R., TRANMER, B. I. & WELLMAN, G. C. (2005). Emergence of a R-type Ca^{2+} channel (CaV 2.3) contributes to cerebral artery constriction after subarachnoid hemorrhage. *Circ. Res.*, **96**, 419-426.

ISOMOTO, S., KONDO, C., YAMADA, M., MATSUMOTO, S., HIGASHIGUCHI, O., HORIO, Y., MATSUZAWA, Y. & KURACHI, Y. (1996). A novel sulfonylurea receptor forms with BIR (Kir6.2) a smooth muscle type ATP-sensitive K^+ channel. *J. Biol. Chem.*, **271**, 24321-24324.

ITOH, H., TAKAHASHI, A., ADACHI, K., NOJI, H., YASUDA, R., YOSHIDA, M. & KINOSITA, K. (2004). Mechanically driven ATP synthesis by F1-ATPase. *Nature.*, **427**, 465-468.

IWAMOTO, T. (2004). Forefront of Na^+/Ca^{2+} exchanger studies: molecular pharmacology of Na^+/Ca^{2+} exchange inhibitors. *J. Pharmacol. Sci.*, **96**, 27-32.

IWAMOTO, T., INOUE, Y., ITO, K., SAKAUE, T., KITA, S. & KATSURAGI, T. (2004). The exchanger inhibitory peptide region-dependent inhibition of Na^+/Ca^{2+} exchange by SN-6 [2-[4-(4-nitrobenzyloxy)benzyl]thiazolidine-4-carboxylic acid ethyl ester], a novel benzyloxyphenyl derivative. *Mol. Pharmacol.*, **66**, 45-55.

IWAMOTO, T., WATANO, T. & SHIGEKAWA, M. (1996). A novel isothiourea derivative selectively inhibits the reverse mode of Na^+/Ca^{2+} exchange in cells expressing NCX1. *J. Biol. Chem.*, **271**, 22391-22397.

JACKSON, W. F. (1993). Arteriolar tone is determined by activity of ATP-sensitive potassium channels. *Am. J. Physiol.*, **265**, t-803.

JACKSON, W. F. (2000a). Hypoxia does not activate ATP-sensitive K^+ channels in arteriolar muscle cells. *Microcirculation*, **7**, 137-145.

JACKSON, W. F. (2000b). Ion channels and vascular tone. *Hypertension*, **35**, 173-178.

JACKSON, W. F., HUEBNER, J. M. & RUSCH, N. J. (1997). Enzymatic isolation and characterization of single vascular smooth muscle cells from cremasteric arterioles. *Microcirculation*, **4**, 35-50.

JIANG, Z. L., KASSAB, G. S. & FUNG, Y. C. (1994). Diameter-defined Strahler system and connectivity matrix of the pulmonary arterial tree. *J. Appl. Physiol.*, **76**, 882-892.

JOSHI, S., BALAN, P. & GURNEY, A. M. (2006). Pulmonary vasoconstrictor action of KCNQ potassium channel blockers. *Respir. Res.*, **20;7**, 31.

JUHASZOVA, M. & BLAUSTEIN, M. P. (1997). Na^+ pump low and high ouabain affinity α subunit isoforms are differently distributed in cells. *Proc. Natl. Acad. Sci. USA*, **94**, 1800-1805.

JUHASZOVA, M., SHIMIZU, H., BORIN, M. L., YIP, R. K., SANTIAGO, E. M., LINDENMAYER, G. E. & BLAUSTEIN, M. P. (1996). Localization of the Na^+-Ca^{2+} exchanger in vascular smooth muscle, and in neurons and astrocytes. *Ann. N. Y. Acad. Sci.*, **779**, 318-335.

KADENBACH, B. (2003). Intrinsic and extrinsic uncoupling of oxidative phosphorylation. *Biochim. Biophys. Acta*, **1604**, 77-94.

KANG, T. M., PARK, M. K. & UHM, D. Y. (2002). Characterization of hypoxia-induced $[Ca^{2+}]_i$ rise in rabbit pulmonary arterial smooth muscle cells. *Life Sci.*, **70**, 2321-2333.

KHARKHUN, M. I., BELEVICH, A. E., POVSTIAN, O. V. & SHUBA, M. F. (2000). The role of voltage-gated potassium channels in the formation of a resting membrane potential in the myocytes of rat resistive arteries. *Fiziologichnyi Zhurnal*, **46**, 91-97.

KINSELLA, J. L. & ARONSON, P. S. (1981). Amiloride inhibition of the Na^+-H^+ exchanger in renal microvillus membrane vesicles. *Am. J. Physiol.*, **241**, F374-F379.

KLEYMAN, T. R. & CRAGOE, E. J., JR. (1988). Amiloride and its analogs as tools in the study of ion transport. *J. Membr. Biol.*, **105**, 1-21.

KNOT, H. J. & NELSON, M. T. (1995). Regulation of membrane potential and diameter by voltage-dependent K^+ channels in rabbit myogenic cerebral arteries. *Am. J. Physiol.*, **269**, H348-H355.

KOBAYASHI, S., KANAIDE, H. & NAKAMURA, M. (1986). Complete overlap of caffeine- and K^+ depolarization-sensitive intracellular calcium storage site in cultured rat arterial smooth muscle cells. *J. Biol. Chem.*, **261**, 15709-15713.

KOBAYASHI, Y., PANG, T., IWAMOTO, T., WAKABAYASHI, S. & SHIGEKAWA, M. (2000). Lithium activates mammalian Na^+/H^+ exchangers: isoform specificity and inhibition by genistein. *Pflugers Arch.*, **439**, 455-462.

KORN, S. J. & IKEDA, S. R. (1995). Permeation selectivity by competition in a delayed rectifier potassium channel. *Science.*, **269**, 410-412.

KOROVKINA, V. P. & ENGLAND, S. K. (2002). Molecular diversity of vascular potassium channel isoforms. *Clin. Exp. Pharmacol. Physiol.*, **29**, 317-323.

KOSTER, J. C., BLANCO, G. & MERCER, R. W. (1995). A cytoplasmic region of the Na,K-ATPase alpha-subunit is necessary for specific alpha/alpha association. *J. Biol. Chem.*, **270**, 14332-14339.

KUBOTA, T., SHINDO, Y., TOKUNO, K., KOMATSU, H., OGAWA, H., KUDO, S., KITAMURA, Y., SUZUKI, K. & OKA, K. (2005). Mitochondria are intracellular magnesium stores: investigation by simultaneous fluorescent imagings in PC12 cells. *Biochim. Biophys. Acta.*, **1744**, 19-28.

KUN, E. (1976). Kinetics of ATP-dependent Mg^{2+} flux in mitochondria. *Biochemistry.*, **15**, 2328-2336.

KUNICHIKA, N., YU, Y., REMILLARD, C. V., PLATOSHYN, O., ZHANG, S. & YUAN, J. X. (2004). Overexpression of TRPC1 enhances pulmonary vasoconstriction induced by capacitative Ca2+ entry. *Am. J. Physiol Lung Cell Mol. Physiol.*, **287**, L962-L969.

KUSHNAREVA, Y., MURPHY, A. N. & ANDREYEV, A. (2002). Complex I-mediated reactive oxygen species generation: modulation by cytochrome c and NAD(P)+ oxidation-reduction state. *Biochem. J.*, **368**, 2-53.

LAMBERT, A. J. & BRAND, M. D. (2004). Inhibitors of the quinone-binding site allow rapid superoxide production from mitochondrial NADH:ubiquinone oxidoreductase (complex I). *J. Biol. Chem.*, **279**, 39414-39420.

LANGDOWN, A. J. & MARSHALL, J. M. (1995). Analysis of responses observed in mesenteric microcirculation of the rat during systemic hypoxia. *J. Physiol.*, **482**, 669-677.

LEACH, R. M., HILL, H. M., SNETKOV, V. A., ROBERTSON, T. P. & WARD, J. P. (2001). Divergent roles of glycolysis and the mitochondrial electron transport chain in hypoxic pulmonary vasoconstriction of the rat: identity of the hypoxic sensor. *J. Physiol.*, **536**, 211-224.

LEACH, R.M., HILL, H.S., SNETKOV, V.A., & WARD, J.P. (2002). Hypoxia, energy state and pulmonary vasomotor tone. *Respiratory Physiology & Neurobiology.*,**132**, 55-67.

LEACH, R. M., ROBERTSON, T. P., TWORT, C. H. & WARD, J. P. T. (1994). Hypoxic vasoconstriction in rat pulmonary and mesenteric arteries. *Am. J. Physiol.*, **266**, L223-L231.

LEBLANC, N., WAN, X. & LEUNG, P. M. (1994). Physiological role of Ca^{2+}-activated and voltage-dependent K^+ currents in rabbit coronary myocytes. *Am. J. Physiol.*, **266**, C1523-C1537.

LENAZ, G., FATO, R., GENOVA, M. L., BERGAMINI, C., BIANCHI, C. & BIONDI, A. (2006). Mitochondrial Complex I: Structural and functional aspects. *Biochim. Biophys. Acta.*, 1757(9-10), 1406.

LESAGE, F. & LAZDUNSKI, M. (2000). Molecular and functional properties of two-pore-domain potassium channels. *Am. J. Physiol Renal Physiol.*, **279**, F793-F801.

LESH, R. E., NIXON, G. F., FLEISCHER, S., AIREY, J. A., SOMLYO, A. P. & SOMLYO, A. V. (1998). Localization of ryanodine receptors in smooth muscle. *Circ. Res.*, **82**, 175-185.

LEYSSENS, A., NOWICKY, A. V., PATTERSON, L., CROMPTON, M. & DUCHEN, M. R. (1996). The relationship between mitochondrial state, ATP hydrolysis, $[Mg^{2+}]_i$ and $[Ca^{2+}]_i$ studied in isolated rat cardiomyocytes. *J. Physiol.*, **496**, 111-128.

LI, W. & ALDRICH, R. W. (2004). Unique inner pore properties of BK channels revealed by quaternary ammonium block. *J. Gen. Physiol.*, **124**, 43-57.

LITTLE, P. J., CRAGOE, E. J., JR. & BOBIK, A. (1986). Na-H exchange is a major pathway for Na influx in rat vascular smooth muscle. *Am. J. Physiol.*, **251**, t-12.

LIU, J. Q. & FOLZ, R. J. (2004). Extracellular superoxide enhances 5-HT-induced murine pulmonary artery vasoconstriction. *Am. J. Physiol.*, **287**, L111-L118.

LIU, J. Q., SHAM, J. S., SHIMODA, L. A., KUPPUSAMY, P. & SYLVESTER, J. T. (2003). Hypoxic constriction and reactive oxygen species in porcine distal pulmonary arteries. *Am. J. Physiol Lung Cell Mol. Physiol.*, **285**, L322-L333.

LIU, Y. & GUTTERMAN, D. D. (2002a). Oxidative stress and potassium channel function. *Clin. Exp. Pharmacol. Physiol.*, **29**, 305-311.

LIU, Y. & GUTTERMAN, D. D. (2002b). The coronary circulation in diabetes: influence of reactive oxygen species on K^+ channel-mediated vasodilation. *Vascular Pharmacology*, **38**, 43-49.

LIU, Y., TERATA, K., RUSCH, N. J. & GUTTERMAN, D. D. (2001). High glucose impairs voltage-gated K^+ channel current in rat small coronary arteries. *Circ. Res.*, **89**, 146-152.

LOPATIN, A. N. & NICHOLS, C. G. (1994). Internal Na^+ and Mg^{2+} blockade of DRK1 (Kv2.1) potassium channels expressed in *Xenopus* oocytes. Inward rectification of a delayed rectifier. *J. Gen. Physiol.*, **103**, 203-216.

LÓPEZ-BARNEO, J. (1994). Oxygen-sensitive ion channels: how ubiquitous are they? *Trends Neurosci.*, **17**, 133-135.

LOPEZ-BARNEO, J., PARDAL, R.,& ORTEGA-SAENZ, P. (2001). Cellular mechanism of oxygen sensing. *Annu Rev Physiol.*, **63**, 259-287.

LU, T., WANG, X. L., HE, T., ZHOU, W., KADUCE, T. L., KATUSIC, Z. S., SPECTOR, A. A. & LEE, H. C. (2005). Impaired arachidonic acid-mediated activation of large-conductance Ca^{2+}-activated K^+ channels in coronary arterial smooth muscle cells in Zucker Diabetic Fatty rats. *Diabetes.*, **54**, 2155-2163.

LUDEWIG, U., LORRA, C., PONGS, O. & HEINEMANN, S. H. (1993). A site accessible to extracellular TEA^+ and K^+ influences intracellular Mg^{2+} block of cloned potassium channels. *European Biophysics Journal*, **22**, 237-247.

MACKINNON, R. (1991a). Determination of the subunit stoichiometry of a voltage-activated potassium channel. *Nature.*, **350**, 232-235.

MACKINNON, R. (1991b). New insights into the structure and function of potassium channels. *Current Opinion in Neurobiology*, **1**, 14-19.

MADDEN, J. A., KELLER, P. A. & KLEINMAN, J. G. (2000). Changes in smooth muscle cell pH during hypoxic pulmonary vasoconstriction: a possible role for ion transporters. *Physiol. Res.*, **49**, 561-566.

MADDEN, J. A., RAY, D. E., KELLER, P. A. & KLEINMAN, J. G. (2001). Ion exchange activity in pulmonary artery smooth muscle cells: the response to hypoxia. *Am. J. Physiol.*, **280**, L264-L271.

MALLI, R., FRIEDEN, M., OSIBOW, K., ZORATTI, C., MAYER, M., DEMAUREX, N. & GRAIER, W. F. (2003). Sustained Ca^{2+} transfer across mitochondria is Essential for mitochondrial Ca2+ buffering, sore-operated Ca^{2+} entry, and Ca^{2+} store refilling. *J. Biol. Chem.*, **278**, 44769-44779.

MANDAL, M., DAS, S., CHAKRABORTI, T., MANDAL, A. & CHAKRABORTI, S. (2003). Role of matrix metalloprotease-2 in oxidant activation of Ca^{2+} ATPase by hydrogen peroxide in pulmonary vascular smooth muscle plasma membrane. *J. Biosci.*, **28**, 205-213.

MANDEGAR, M., FUNG, Y. C., HUANG, W., REMILLARD, C. V., RUBIN, L. J. & YUAN, J. X. (2004). Cellular and molecular mechanisms of pulmonary vascular remodeling: role in the development of pulmonary hypertension. *Microvasc. Res.*, **68**, 75-103.

MANDEGAR, M., REMILLARD, C. V. & YUAN, J. X. (2002). Ion channels in pulmonary arterial hypertension. *Prog. Cardiovasc. Dis.*, **45**, 81-114.

MANDEGAR, M. & YUAN, J. X. (2002). Role of K^+ channels in pulmonary hypertension. *Vascular Pharmacology*, **38**, 25-33.

MANSFIELD, K. D., GUZY, R. D., PAN, Y., YOUNG, R. M., CASH, T. P., SCHUMACKER, P. T. & SIMON, M. C. (2005). Mitochondrial dysfunction resulting from loss of cytochrome c impairs cellular oxygen sensing and hypoxic HIF-alpha activation. *Cell Metab.*, **1**, 393-399.

MARBAN, E., YAMAGISHI, T. & TOMASELLI, G. F. (1998). Structure and function of voltage-gated sodium channels. *J. Physiol.*, **508**, 647-657.

MARSHALL, C., MAMARY, A. J., VERHOEVEN, A. J. & MARSHALL, B. E. (1996). Pulmonary artery NADPH-oxidase is activated in hypoxic pulmonary vasoconstriction. *Am. J. Respir. Cell Mol. Biol.*, **15**, 633-644.

MASEREEL, B., POCHET, L. & LAECKMANN, D. (2003). An overview of inhibitors of Na(+)/H(+) exchanger. *Eur. J. Med. Chem.*, **38**, 547-554.

MASON, H.S., BOURKE, S. & KEMP. P.J. (2004). Selective modulation of ligand-gated P2X purinoceptor channels by acute hypoxia is mediated by reactive oxygen species. *Mol Pharmacol.*, **66**(6),1525-35.

MASON, H. S., LATTEN, M. J., GODOY, L. D., HOROWITZ, B. & KENYON, J. L. (2002). Modulation of Kv1.5 currents by protein kinase A, tyrosine kinase, and protein tyrosine phosphatase requires an intact cytoskeleton. *Mol. Pharmacol.*, **61**, 285-293.

MATSUDA, T., ARAKAWA, N., TAKUMA, K., KISHIDA, Y., KAWASAKI, Y., SAKAUE, M., TAKAHASHI, K., TAKAHASHI, T., SUZUKI, T., OTA, T., HAMANO-TAKAHASHI, A., ONISHI, M., TANAKA, Y., KAMEO, K. & BABA, A. (2001). SEA0400, a novel and selective inhibitor of the Na^{+}-Ca^{2+} exchanger, attenuates reperfusion injury in the in vitro and in vivo cerebral ischemic models. *J. Pharmacol. Exp. Ther.*, **298**, 249-256.

MATSUNO-YAGI, A. & HATEFI, Y. (1993). Studies on the mechanism of oxidative phosphorylation. ATP synthesis by submitochondrial particles inhibited at F0 by venturicidin and organotin compounds. *J. Biol. Chem.*, **268**, 6168-6173.

MCMURTRY, I. F., BAUER, N. R., FAGAN, K. A., NAGAOKA, T., GEBB, S. A. & OKA, M. (2003). Hypoxia and Rho/Rho-kinase signaling. Lung development versus hypoxic pulmonary hypertension. *Adv. Exp. Med. Biol.*, **543**, 127-137.

MCMURTRY, I. F., DAVIDSON, A. B., REEVES, J. T. & GROVER, R. F. (1976). Inhibition of hypoxic pulmonary vasoconstriction by calcium antagonists in isolated rat lungs. *Circ. Res.*, **38**, 99-104.

MICHELAKIS, E. D., HAMPL, V., NSAIR, A., WU, X., HARRY, G., HAROMY, A., GURTU, R. & ARCHER, S. L. (2002). Diversity in mitochondrial function explains differences in vascular oxygen sensing. *Circ. Res.*, **90**, 1307-1315.

MICHELAKIS, E. D., THEBAUD, B., WEIR, E. K. & ARCHER, S. L. (2004). Hypoxic pulmonary vasoconstriction: redox regulation of O_2-sensitive K^+ channels by a mitochondrial O_2-sensor in resistance artery smooth muscle cells. *J. Mol. Cell Cardiol.*, **37**, 1119-1136.

MINAMI, K., FUKUZAWA, K. & NAKAYA, Y. (1993). Protein kinase C inhibits the Ca^{2+}-activated K^+ channel of cultured porcine coronary artery smooth muscle cells. *Biochem. Biophys. Res. Commun.*, **190**, 263-269.

MITCHELL, P. (1961). Coupling of phosphorylation to electron and hydrogen transfer by a chemi-osmotic type of mechanism. *Nature.*, **191**, 144-148.

MOOLENAAR, W. H., BOONSTRA, J., VAN DER SAAG, P. T. & DE LAAT, S. W. (1981). Sodium/proton exchange in mouse neuroblastoma cells. *J. Biol. Chem.*, **256**, 12883-12887.

MOUDGIL, R., MICHELAKIS, E. D. & ARCHER, S. L. (2005). Hypoxic pulmonary vasoconstriction. *J. Appl. Physiol.*, **98**, 390-403.

NABEL, E. G., BERK, B. C., BROCK, T. A. & SMITH, T. W. (1988). Na^+-Ca^{2+} exchange in cultured vascular smooth muscle cells. *Circ. Res.*, **62**, 486-493.

NAGAOKA, T., FAGAN, K. A., GEBB, S. A., MORRIS, K. G., SUZUKI, T., SHIMOKAWA, H., MCMURTRY, I. F. & OKA, M. (2005). Inhaled Rho kinase inhibitors are potent and selective vasodilators in rat pulmonary hypertension. *Am. J. Respir. Crit Care Med.*, **171**, 494-499.

NAKAYAMA, S., NOMURA, H., SMITH, L. M., CLARK, J. F., UETANI, T. & MATSUBARA, T. (2003). Mechanisms for monovalent cation-dependent depletion of intracellular Mg^{2+}:Na^+-independent Mg^{2+} pathways in guinea-pig smooth muscle. *J. Physiol.*, **551**, 843-853.

NEHER, E. (1992). Correction for liquid junction potentials in patch clamp experiments. *Methods Enzymol.*, **207**, 123-131.

NEHER, E. & SAKMANN, B. (1976). Single-channel currents recorded from membrane of denervated frog muscle fibres. *Nature.*, **260**, 799-802.

NELSON, M. T., PATLAK, J. B., WORLEY, J. F. & STANDEN, N. B. (1990). Calcium channels, potassium channels, and voltage dependence of arterial smooth muscle tone. *Am. J. Physiol.*, **259**, C3-C18.

NELSON, M. T. & QUAYLE, J. M. (1995). Physiological roles and properties of potassium channels in arterial smooth muscle. *Am. J. Physiol.*, **268**, C799-C822.

NICOLL, D. A., LONGONI, S. & PHILIPSON, K. D. (1990). Molecular cloning and functional expression of the cardiac sarcolemmal Na^{+}-Ca^{2+} exchanger. *Science.*, **250**, 562-565.

NICHOLLS, D. G. (2004). Mitochondrial membrane potential and aging. *Aging Cell.*, **3**, 35-40.

NING, X. H., XU, C. S., SONG, Y. C., XIAO, Y., HU, Y. J., LUPINETTI, F. M. & PORTMAN, M. A. (1998). Hypothermia preserves function and signaling for mitochondrial biogenesis during subsequent ischemia. *Am. J. Physiol.*, **274**, t-93.

NIMIGEAN, C. M., CHAPPIE, J. S. & MILLER, C. (2003). Electrostatic tuning of ion conductance in potassium channels. *Biochemistry.*, **42**, 9263-9268.

NOSKOV, S. Y., BERNECHE, S. & ROUX, B. (2004). Control of ion selectivity in potassium channels by electrostatic and dynamic properties of carbonyl ligands. *Nature.*, **431**, 830-834.

NOSKOV, S. Y. & ROUX, B. (2006). Ion selectivity in potassium channels. *Biophys. Chem.*, **124**(3):279-91.

OHYA, S., SERGEANT, G. P., GREENWOOD, I. A. & HOROWITZ, B. (2003). Molecular variants of KCNQ channels expressed in murine portal vein myocytes: a role in delayed rectifier current. *Circ. Res.*, **92**, 1016-1023.

OHYA, S., HOROWITZ, B. & GREENWOOD, I. A. (2002). Functional and molecular identification of ERG channels in murine portal vein myocytes. *Am. J. Physiol Cell Physiol.*, **283**, C866-C877.

OLSCHEWSKI, A., HONG, Z., NELSON, D. P. & WEIR, E. K. (2002). Graded response of K^+ current, membrane potential, and $[Ca^{2+}]_i$ to hypoxia in pulmonary arterial smooth muscle. *Am. J. Physiol.*, **283**, L1143-L1150.

OLSCHEWSKI, A., LI, Y., TANG, B., HANZE, J., EUL, B., BOHLE, R. M., WILHELM, J., MORTY, R. E., BRAU, M. E., WEIR, E. K., KWAPISZEWSKA, G., KLEPETKO, W., SEEGER, W. & OLSCHEWSKI, H. (2006). Impact of TASK-1 in human pulmonary artery smooth muscle cells. *Circ. Res.*, **98**, 1072-1080.

ORIO, P., ROJAS, P., FERREIRA, G. & LATORRE, R. (2002). New disguises for an old channel: MaxiK channel beta-subunits. *News Physiol Sci.*, **17**, 156-161.

OSIPENKO, O. N., EVANS, A. M. & GURNEY, A. M. (1997). Regulation of the resting potential of rabbit pulmonary artery myocytes by a low threshold, O_2-sensing potassium current. *Br. J. Pharmacol.*, **120**, 1461-1470.

OSIPENKO, O. N., ALEXANDER, D., MACLEAN, M. R. & GURNEY, A. M. (1998). Influence of chronic hypoxia on the contributions of non-inactivating and delayed rectifier K currents to the resting potential and tone of rat pulmonary artery smooth muscle. *Br. J. Pharmacol.*, **124**, 1335-1337.

PACAUD, P., LOIRAND, G., LAVIE, J. L., MIRONNEAU, C. & MIRONNEAU, J. (1989). Calcium-activated chloride current in rat vascular smooth muscle cells in short-term primary culture. *Pflügers Arch.*, **413**, 629-636.

PADDENBERG, R., ISHAQ, B., GOLDENBERG, A., FAULHAMMER, P., ROSE, F., WEISSMANN, N., BRAUN-DULLAEUS, R. C. & KUMMER, W. (2003). Essential role of complex II of the respiratory chain in hypoxia-induced ROS generation in the pulmonary vasculature. *Am. J. Physiol Lung Cell Mol. Physiol.*, **284**, L710-L719.

PANDE, J., MALLHI, K. K., SAWH, A., SZEWCZYK, M. M., SIMPSON, F. & GROVER, A. K. (2006). Aortic smooth muscle and endothelial plasma membrane Ca^{2+}

pump isoforms are inhibited differently by the extracellular inhibitor caloxin 1b1. *Am. J. Physiol Cell Physiol.*, **290**, C1341-C1349.

PAREKH, A. B. (2003). Mitochondrial regulation of intracellular Ca^{2+} signalling: more than just simple Ca2+ buffers. *News Physiol Sci.*, **18**, 252-256.

PARK, W. S., SON, Y. K., HAN, J., KIM, N., KO, J. H., BAE, Y. M. & EARM, Y. E. (2005). Staurosporine inhibits voltage-dependent K^+ current through a PKC-independent mechanism in isolated coronary arterial smooth muscle cells. *J. Cardiovasc. Pharmacol.*, **45**, 260-269.

PATEL, A. J. & HONORE, E. (2001). Properties and modulation of mammalian 2P domain K+ channels. *Trends Neurosci.*, **24**, 339-346.

PATEL, A. J., LAZDUNSKI, M. & HONORÉ, E. (1997). Kv2.1/Kv9.3, a novel ATP-dependent delayed-rectifier K^+ channel in oxygen-sensitive pulmonary artery myocytes. *EMBO J.*, **16**, 6615-6625.

PENG, W., KARWANDE, S. V., HOIDAL, J. R. & FARRUKH, I. S. (1996). Potassium currents in cultured human pulmonary arterial smooth muscle cells. *J. Appl. Physiol.*, **80**, 1187-1196.

PEROZO, E. & BEZANILLA, F. (1990). Phosphorylation affects voltage gating of the delayed rectifier K^+ channel by electrostatic interactions. *Neuron*, **5**, 685-690.

PIPER, H. M., BALSER, C., LADILOV, Y. V., SCHAFER, M., SIEGMUND, B., RUIZ-MEANA, M. & GARCIA-DORADO, D. (1996). The role of Na^+/H^+ exchange in ischemia-reperfusion. *Basic Res. Cardiol.*, **91**, 191-202.

PIPER, A. S. & GREENWOOD, I. A. (2003). Anomalous effect of anthracene-9-carboxylic acid on calcium-activated chloride currents in rabbit pulmonary artery smooth muscle cells. *Br. J. Pharmacol.*, **138**, 31-38.

PLATOSHYN, O., BREVNOVA, E. E., BURG, E. D., YU, Y., REMILLARD, C. V. & YUAN, J. X. (2006). Acute hypoxia selectively inhibits KCNA5 channels in pulmonary artery smooth muscle cells. *Am. J. Physiol Cell Physiol.*, **290**, C907-C916.

PLATOSHYN, O., GOLOVINA, V. A., BAILEY, C. L., LIMSUWAN, A., KRICK, S., JUHASZOVA, M., SEIDEN, J. E., RUBIN, L. J. & YUAN, J. X. (2000). Sustained membrane depolarization and pulmonary artery smooth muscle cell proliferation. *Am. J. Physiol.*, **279**, C1540-C1549.

PLATOSHYN, O., REMILLARD, C. V., FANTOZZI, I., MANDEGAR, M., SISON, T. T., ZHANG, S., BURG, E. & YUAN, J. X. (2004). Diversity of voltage-dependent K+ channels in human pulmonary artery smooth muscle cells. *Am. J. Physiol Lung Cell Mol. Physiol.*, **287**, L226-L238.

PLATOSHYN, O., REMILLARD, C. V., FANTOZZI, I., SISON, T. & YUAN, J. X. (2005). Identification of functional voltage-gated Na^+ channels in cultured human pulmonary artery smooth muscle cells. *Pflugers Arch.*, **451**, 380-387.

PLATOSHYN, O., YU, Y., GOLOVINA, V. A., MCDANIEL, S. S., KRICK, S., LI, L., WANG, J. Y., RUBIN, L. J. & YUAN, X.-J. (2001). Chronic hypoxia decreases K_V channel expression and function in pulmonary artery myocytes. *Am. J. Physiol.*, **280**, L801-L812.

POST, J. M., HUME, J. R., ARCHER, S. L. & WEIR, E. K. (1992). Direct role for potassium channel inhibition in hypoxic pulmonary vasoconstriction. *Am. J. Physiol.*, **262**, C882-C890.

POZEG, Z. I., MICHELAKIS, E. D., MCMURTRY, M. S., THÉBAUD, B., WU, X. C., DYCK, J. R., HASHIMOTO, K., WANG, S., MOUDGIL, R., HARRY, G., SULTANIAN, R., KOSHAL, A. & ARCHER, S. L. (2003). In vivo gene transfer of the O_2-sensitive potassium channel Kv1.5 reduces pulmonary hypertension and restores hypoxic pulmonary vasoconstriction in chronically hypoxic rats. *Circulation*, **107**, 2037-2044.

PUGSLEY, M. K. & TABRIZCHI, R. (2000). The vascular system. An overview of structure and function. *J. Pharmacol. Toxicol. Methods.*, **44**, 333-340.

QUAYLE, J. M., NELSON, M. T. & STANDEN, N. B. (1997). ATP-sensitive and inwardly rectifying potassium channels in smooth muscle. *Physiol. Rev.*, **77**, 1165-1232.

QUINTERO, M., COLOMBO, S. L., GODFREY, A. & MONCADA, S. (2006). Mitochondria as signalling organelles in the vascular endothelium. *Proc. Natl. Acad. Sci. U. S. A.*, **103**, 5379-5384.

REBOLLEDO, A., SPERONI, F., RAINGO, J., SALEMME, S. V., TANZI, F., MUNIN, V., ANON, M. C. & MILESI, V. (2006). The Na^+/Ca^{2+} exchanger is active and working in the reverse mode in human umbilical artery smooth muscle cells. *Biochem. Biophys. Res. Commun.*, **20;339**, 840-845.

REEVE, H. L., WEIR, E. K., NELSON, D. P., PETERSON, D. A. & ARCHER, S. L. (1995). Opposing effects of oxidants and antioxidants on K^+ channel activity and tone in rat vascular tissue. *Exp. Physiol.*, **80**, 825-834.

REID, R. A., MOYLE, J. & MITCHELL, P. (1966). Synthesis of adenosine triphosphate by a protonmotive force in rat liver mitochondria. *Nature.*, **212**, 257-258.

REMILLARD, C. V. & YUAN, J. X. (2004). Activation of K^+ channels: an essential pathway in programmed cell death. *Am. J. Physiol.*, **286**, L49-L67.

REMILLARD, C. V. & YUAN, J. X. (2005). High altitude pulmonary hypertension: role of K+ and Ca2+ channels. *High Alt. Med. Biol.*, **6**, 133-146.

REUTER, H., BLAUSTEIN, M. P. & HAEUSLER, G. (1973). Na-Ca exchange and tension development in arterial smooth muscle. *Phil. Trans. R. Soc. Lond. (B)*, **265**, 87-94.

RIOS, E. J., FALLON, M., WANG, J. & SHIMODA, L. A. (2005). Chronic hypoxia elevates intracellular pH and activates Na^+/H^+ exchange in pulmonary arterial smooth muscle cells. *Am. J. Physiol Lung Cell Mol. Physiol.*, **289**, L867-L874.

RIVERA, A., FERREIRA, A., BERTONI, D., ROMERO, J. R. & BRUGNARA, C. (2005). Abnormal regulation of Mg2+ transport via Na/Mg exchanger in sickle erythrocytes. *Blood.*, **105**, 382-386.

ROBBINS, J. (2001). KCNQ potassium channels: physiology, pathophysiology, and pharmacology. *Pharmacol. Ther.*, **90**, 1-19.

ROBERTSON, T. P., AARONSON, P. I. & WARD, J. P. (2003). Ca^{2+} sensitization during sustained hypoxic pulmonary vasoconstriction is endothelium dependent. *Am. J. Physiol.*, **284**, L1121-L1126.

ROBERTSON, T. P., AARONSON, P. I. & WARD, J. P. T. (1995). Hypoxic vasoconstriction and intracellular Ca^{2+} in pulmonary arteries: evidence for PKC-independent Ca^{2+} sensitization. *Am. J. Physiol.*, **268**, H301-H307.

ROBERTSON, T. P., DIPP, M., WARD, J. P., AARONSON, P. I. & EVANS, A. M. (2000a). Inhibition of sustained hypoxic vasoconstriction by Y-27632 in isolated intrapulmonary arteries and perfused lung of the rat. *Br. J. Pharmacol.*, **131**, 5-9.

ROBERTSON, T. P., HAGUE, D., AARONSON, P. I. & WARD, J. P. (2000b). Voltage-independent calcium entry in hypoxic pulmonary vasoconstriction of intrapulmonary arteries of the rat. *J. Physiol.*, **525**, 669-680.

RODMAN, D. M., REESE, K., HARRAL, J., FOUTY, B., WU, S., WEST, J., HOEDT-MILLER, M., TADA, Y., LI, K. X., COOL, C., FAGAN, K. & CRIBBS, L. (2005). Low-voltage-activated (T-type) calcium channels control proliferation of human pulmonary artery myocytes. *Circ. Res.*, **96**, 864-872.

ROMANI, A., MARFELLA, C. & SCARPA, A. (1993). Cell magnesium transport and homeostasis: role of intracellular compartments. *Miner. Electrolyte Metab.*, **19**, 282-289.

ROSSKOPF, D., SIFFERT, G., OSSWALD, U., WITTE, K., DUSING, R., AKKERMAN, J. W. & SIFFERT, W. (1992). Platelet Na^{+}-H^{+} exchanger activity in normotensive and hypertensive subjects: effect of enalapril therapy upon antiport activity. *J. Hypertens.*, **10**, 839-847.

ROUNDS, S. & MCMURTRY, I. F. (1981). Inhibitors of oxidative ATP production cause transient vasoconstriction and block subsequent pressor responses in rat lungs. *Circ. Res.*, **48**, 393-400.

ROYCHOUDHURY, S., GHOSH, S. K., CHAKRABORTI, T. & CHAKRABORTI, S. (1996). Role of hydroxyl radical in the oxidant H2O2-mediated Ca^{2+} release from pulmonary smooth muscle mitochondria. *Mol. Cell Biochem.*, **159**, 95-103.

RUEDA, A., GARCIA, L. & GUERRERO-HERNANDEZ, A. (2002). Luminal Ca^{2+} and the activity of sarcoplasmic reticulum Ca^{2+} pumps modulate histamine-induced all-or-none Ca^{2+} release in smooth muscle cells. *Cell Signal.*, **14**, 517-527.

SAGE, S. O., VAN BREEMEN, C. & CANNELL, M. B. (1991). Sodium-calcium exchange in cultured bovine pulmonary artery endothelial cells. *J. Physiol.*, **440**, 569-580.

SAKURADA, S., TAKUWA, N., SUGIMOTO, N., WANG, Y., SETO, M., SASAKI, Y. & TAKUWA, Y. (2003). Ca^{2+}-dependent activation of Rho and Rho kinase in membrane depolarization-induced and receptor stimulation-induced vascular smooth muscle contraction. *Circ. Res.*, **19;93**, 548-556.

SARDET, C., FRANCHI, A. & POUYSSEGUR, J. (1989). Molecular cloning, primary structure, and expression of the human growth factor-activatable Na^+/H^+ antiporter. *Cell.*, **56**, 271-280.

SARIBAN-SOHRABY, S., LATORRE, R., BURG, M., OLANS, L. & BENOS, D. (1984). Amiloride-sensitive epithelial Na^+ channels reconstituted into planar lipid bilayer membranes. *Nature.*, **308**, 80-82.

SAUZEAU, V., LE JEUNE, H., CARIO-TOUMANIANTZ, C., SMOLENSKI, A., LOHMANN, S. M., BERTOGLIO, J., CHARDIN, P., PACAUD, P. & LOIRAND, G. (2000). Cyclic GMP-dependent protein kinase signalling pathway inhibits RhoA-induced Ca^{2+} sensitization of contraction in vascular smooth muscle. *J. Biol. Chem.*, **275**, 21722-21729.

SCHUBERT, R., KRIEN, U. & GAGOV, H. (2001). Protons inhibit the BK_{Ca} channel of rat small artery smooth muscle cells. *J. Vasc. Res.*, **38**, 30-38.

SCHWEIGEL, M., PARK, H. S., ETSCHMANN, B. & MARTENS, H. (2006). Characterization of the Na^+-dependent Mg^{2+} transport in sheep ruminal epithelial cells. *Am. J. Physiol Gastrointest. Liver Physiol.*, **290**, G56-G65.

SEARLE, G. J., HARTNESS, M. E., HOAREAU, R., PEERS, C. & KEMP, P. J. (2002). Lack of contribution of mitochondrial electron transport to acute O_2 sensing in model airway chemoreceptors. *Biochem. Biophys. Res. Commun.*, **291**, 332-337.

SHI, J. & CUI, J. (2001). Intracellular Mg^{2+} enhances the function of BK-type Ca^{2+}-activated K^+ channels. *J. Gen. Physiol.*, **118**, 589-606.

SILVERMAN, H. S., DI LISA, F., HUI, R. C., MIYATA, H., SOLLOTT, S. J., HANFORD, R. G., LAKATTA, E. G. & STERN, M. D. (1994). Regulation of intracellular free Mg^{2+} and contraction in single adult mammalian cardiac myocytes. *Am. J. Physiol.*, **266**, t-33.

SILVERMAN, E. S., THOMPSON, B. T., QUINN, D. A., KINANE, T. B., BONVENTRE, J. V. & HALES, C. A. (1995). Na^+/H^+ exchange in pulmonary artery smooth muscle from spontaneously hypertensive and Wistar-Kyoto rats. *Am. J. Physiol.*, **269**, L673-L680.

SINGHAL, S., HENDERSON, R., HORSFIELD, K., HARDING, K. & CUMMING, G. (1973). Morphometry of the human pulmonary arterial tree. *Circ. Res.*, **33**, 190-197.

SIPIDO, K. R., VARRO, A. & EISNER, D. (2006). Sodium calcium exchange as a target for antiarrhythmic therapy. *Handb. Exp. Pharmacol.* 159-199.

SKOU, J. C. (2004). The identification of the sodium pump. *Biosci. Rep.*, **24**, 436-451.

SKOU, J. C. & ESMANN, M. (1992). The Na,K-ATPase. *J. Bioenerg. Biomembr.*, **24**, 249-261.

SMIRNOV, S. V. & AARONSON, P. I. (1994). Alteration of the transmembrane K^+ gradient during development of delayed rectifier in isolated rat pulmonary arterial cells. *J. Gen. Physiol.*, **104**, 241-264.

SMIRNOV, S. V. & AARONSON, P. I. (1996). Modulatory effects of arachidonic acid on the delayed rectifier K^+ current in rat pulmonary arterial myocytes. Structural aspects and involvement of protein kinase C. *Circ. Res.*, **79**, 20-31.

SMIRNOV, S. V. & BECK,R. Modulation of cell membrane capacitance by arachidonic acid in rat aortic myocytes. Biophysical Journal 82[1 Pt 2(2)], 285A. 2002.

SMIRNOV, S. V., BECK, R., TAMMARO, P., ISHII, T. & AARONSON, P. I. (2002). Electrophysiologically distinct smooth muscle cell subtypes in rat conduit and resistance pulmonary arteries. *J. Physiol.*, **538**, 867-878.

SMIRNOV, S. V., ROBERTSON, T. P., WARD, J. P. T. & AARONSON, P. I. (1994). Chronic hypoxia is associated with reduced delayed rectifier K^+ current in rat pulmonary artery muscle cells. *Am. J. Physiol.*, **266**, H365-H370.

SMIRNOV, S. V., TAMMARO, P., HUTCHINGS, S. R. & SMITH, A. L. (2003). Role of voltage-gated K^+ (K_V) channels in vascular function. *Neurophysiology*, **35**, 262-275.

SMITH, A. L., YUILL, K. H. & SMIRNOV, S. V. (2005). Effects of hydrogen peroxide (H_2O_2) on voltage-dependent K^+ (Kv) currents in rat small pulmonary arterial myocytes (PAMs): the role of intracellular redox state. From the University of Cambridge, Summer 2005 Meeting: Proceedings of the British Pharmacological Society at http://www.pa2online.org/abstracts/Vol3Issue2abst125P.pdf

SOBEY, C. G. (2001). Potassium channel function in vascular disease. *Arterioscler. Thromb. Vasc. Biol.*, **21**, 28-38.

SOLTOFF, S. P. & MANDEL, L. J. (1983). Amiloride directly inhibits the Na,K-ATPase activity of rabbit kidney proximal tubules. *Science.*, **220**, 957-958.

SOMLYO, A. V. & SOMLYO, A. P. (1968). Electromechanical and pharmacomechanical coupling in vascular smooth muscle. *J. Pharmacol. Exp. Ther.*, **159**, 129-145.

SON, Y. K., PARK, W. S., KIM, S. J., EARM, Y. E., KIM, N., YOUM, J. B., WARDA, M., KIM, E. & HAN, J. (2006). Direct inhibition of a PKA inhibitor, H-89 on KV channels in rabbit coronary arterial smooth muscle cells. *Biochem. Biophys. Res. Commun.*, **341**, 931-937.

STANDLEY, P. R. & STANDLEY, C. A. (2002). Identification of a functional Na^+/Mg^{2+} exchanger in human trophoblast cells. *Am. J. Hypertens.*, **15**, 565-570.

STARKUS, J. G., VARGA, Z., SCHONHERR, R. & HEINEMANN, S. H. (2003). Mechanisms of the inhibition of Shaker potassium channels by protons. *Pflügers Arch.*

STOCK, D., GIBBONS, C., ARECHAGA, I., LESLIE, A. G. & WALKER, J. E. (2000). The rotary mechanism of ATP synthase. *Curr. Opin. Struct. Biol.*, **10**, 672-679.

SUN, P. W., KYOUNG, S. Y., KIM, N., BOUM, Y. J., JOO, H., WARDA, M., KO, J. H., EARM, Y. E. & HAN, J. (2006). The protein kinase A inhibitor, H-89, directly inhibits KATP and Kir channels in rabbit coronary arterial smooth muscle cells. *Biochem. Biophys. Res. Commun.*, **340**, 1104-1110.

SWARD, K., DREJA, K., LINDQVIST, A., PERSSON, E. & HELLSTRAND, P. (2002). Influence of mitochondrial inhibition on global and local [Ca(2+)](I) in rat tail artery. *Circ. Res.*, **19;90**, 792-799.

SWÄRD, K., DREJA, K., SUSNJAR, M., HELLSTRAND, P., HARTSHORNE, D. J. & WALSH, M. P. (2000). Inhibition of Rho-associated kinase blocks agonist-induced Ca^{2+} sensitization of myosin phosphorylation and force in guinea-pig ileum. *J. Physiol.*, **522**, 33-49.

SWEENEY, M., YU, Y., PLATOSHYN, O., ZHANG, S., MCDANIEL, S. S. & YUAN, J. X. (2002). Inhibition of endogenous TRP1 decreases capacitative Ca^{2+} entry and attenuates pulmonary artery smooth muscle cell proliferation. *Am. J. Physiol Lung Cell Mol. Physiol.*, **283**, L144-L155.

TAKAHASHI, K., TAKAHASHI, T., SUZUKI, T., ONISHI, M., TANAKA, Y., HAMANO-TAKAHASHI, A., OTA, T., KAMEO, K., MATSUDA, T. & BABA, A. (2003). Protective effects of SEA0400, a novel and selective inhibitor of the Na^+/Ca^{2+} exchanger, on myocardial ischemia-reperfusion injuries. *Eur. J. Pharmacol.*, **458**, 155-162.

TALOR, Z., NG, S. C., CRAGOE, E. J. & ARRUDA, J. A. (1989). Methyl isobutyl amiloride: a new probe to assess the number of Na-H antiporters. *Life Sci.*, **45**, 517-523.

TAMAOKI, J., TAGAYA, E., NISHIMURA, K., ISONO, K. & NAGAI, A. (1997). Role of Na^+-K^+ ATPase in cyclic GMP-mediated relaxation of canine pulmonary artery smooth muscle cells. *Br. J. Pharmacol.*, **122**, 112-116.

TAMMARO, P., AARONSON,P.I. & SMIRNOV,S.V. Modulation of the native Kv2.1 channel by phosphorylation in rat aortic myocytes. Biophysical Journal 80[1 Pt 2], 440a. 2001.

TAMMARO, P., SMIRNOV, S. V. & MORAN, O. (2004). Effects of intracellular magnesium on Kv1.5 and Kv2.1 potassium channels. *Eur. Biophys. J.*

TAMMARO, P., SMITH, A. L., CROWLEY, B. L. & SMIRNOV, S. V. (2005). Modulation of the voltage-dependent K^+ current by intracellular Mg^{2+} in rat aortic smooth muscle cells. *Cardiovasc. Res.*, **65**, 387-396.

TAMMARO, P., SMITH, A. L., HUTCHINGS, S. R. & SMIRNOV, S. V. (2004). Pharmacological evidence for a key role of voltage-gated K^+ channels in the function of rat aortic smooth muscle cells. *Br. J. Pharmacol.*, **143**, 303-317.

TANG, X. D., GARCIA, M. L., HEINEMANN, S. H. & HOSHI, T. (2004). Reactive oxygen species impair Slo1 BK channel function by altering cysteine-mediated calcium sensing. *Nat. Struct. Mol. Biol.*, **11**, 171-178.

TASHIRO, M. & KONISHI, M. (1997). Na^+ gradient-dependent Mg^{2+} transport in smooth muscle cells of guinea pig tenia cecum. *Biophys. J.*, **73**, 3371-3384.

TASHIRO, M. & KONISHI, M. (2000). Sodium gradient-dependent transport of magnesium in rat ventricular myocytes. *Am. J. Physiol.*, **279**, C1955-C1962.

TASKER, P. N., MICHELANGELI, F. & NIXON, G. F. (1999). Expression and distribution of the type 1 and type 3 inositol 1, 4, 5-trisphosphate receptor in developing vascular smooth muscle. *Circ. Res.*, **84**, 536-542.

TERAMOTO, N. (2006). Physiological roles of ATP-sensitive K+ channels in smooth muscle. *J. Physiol.*, **572**, 3-24.

TINEL, N., DIOCHOT, S., LAURITZEN, I., BARHANIN, J., LAZDUNSKI, M. & BORSOTTO, M. (2000). M-type KCNQ2-KCNQ3 potassium channels are modulated by the KCNE2 subunit. *FEBS Lett.*, **480**, 137-141.

TOUYZ, R. M. & SCHIFFRIN, E. L. (1996). Angiotensin II and vasopressin modulate intracellular free magnesium in vascular smooth muscle cells through Na+-dependent protein kinase C pathways. *J. Biol. Chem.*, **271**, 24353-24358.

TOUYZ, R. M. & SCHIFFRIN, E. L. (1999). Activation of the Na^+-H^+ exchanger modulates angiotensin II-stimulated Na^+-dependent Mg^{2+} transport in vascular smooth muscle cells in genetic hypertension. *Hypertension.*, **34**, 442-449.

TOUYZ, R. M. & YAO, G. (2003). Inhibitors of Na^+/Mg^{2+} exchange activity attenuate the development of hypertension in angiotensin II-induced hypertensive rats. *J. Hypertens.*, **21**, 337-344.

TREIMAN, M., CASPERSEN, C. & CHRISTENSEN, S. B. (1998). A tool coming of age: thapsigargin as an inhibitor of sarco-endoplasmic reticulum Ca^{2+}-ATPases. *Trends Pharmacol. Sci.*, **19**, 131-135.

TURNER, J. L. & KOZLOWSKI, R. Z. (1997). Relationship between membrane potential, delayed rectifier K^+ currents and hypoxia in rat pulmonary arterial myocytes. *Exp. Physiol.*, **82**, 629-645.

TURRENS, J. F. (1997). Superoxide production by the mitochondrial respiratory chain. *Biosci. Rep.*, **17**, 3-8.

TURRENS, J. F., ALEXANDRE, A. & LEHNINGER, A. L. (1985). Ubisemiquinone is the electron donor for superoxide formation by complex III of heart mitochondria. *Arch. Biochem. Biophys.*, **237**, 408-414.

VAN BREEMEN, C. & SAIDA, K. (1989). Cellular mechanisms regulating $[Ca^{2+}]_i$ smooth muscle. *Annu. Rev. Physiol.*, **51**, 315-329.

VAN EYLEN, F., SVOBODA, M. & HERCHUELZ, A. (1997). Identification, expression pattern and potential activity of Na/Ca exchanger isoforms in rat pancreatic B-cells. *Cell Calcium.*, **21**, 185-193.

VIGNE, P., FRELIN, C. & LAZDUNSKI, M. (1982). The amiloride-sensitive Na^+/H^+ exchange system in skeletal muscle cells in culture. *J. Biol. Chem.*, **257**, 9394-9400.

WADSWORTH, R. M. (1994). Vasoconstrictor and vasodilator effects of hypoxia. *Trends Pharmacol. Sci.*, **15**, 47-53.

WALLNER, M., MEERA, P. & TORO, L. (1996). Determinant for β-subunit regulation in high-conductance voltage-activated and Ca^{2+}-sensitive K^+ channels: an additional transmembrane region at the N terminus. *Proc. Natl. Acad. Sci. USA*, **93**, 14922-14927.

WANG, J., WEIGAND, L., WANG, W., SYLVESTER, J. T. & SHIMODA, L. A. (2005). Chronic hypoxia inhibits Kv channel gene expression in rat distal pulmonary artery. *Am. J. Physiol Lung Cell Mol. Physiol.*, **288**, L1049-L1058.

WANG, Q., CURRAN, M. E., SPLAWSKI, I., BURN, T. C., MILLHOLLAND, J. M., VANRAAY, T. J., SHEN, J., TIMOTHY, K. W., VINCENT, G. M., DE JAGER, T., SCHWARTZ, P. J., TOUBIN, J. A., MOSS, A. J., ATKINSON, D. L., LANDES, G. M., CONNORS, T. D. & KEATING, M. T. (1996). Positional cloning of a novel potassium channel gene: KVLQT1 mutations cause cardiac arrhythmias. *Nat. Genet.*, **12**, 17-23.

WANG, X., TONG, M., CHINTA, S., RAJ, J. U. & GAO, Y. (2006). Hypoxia-induced reactive oxygen species downregulate ETB receptor-mediated contraction of rat pulmonary arteries. *Am. J. Physiol Lung Cell Mol. Physiol.*, **290**, L570-L578.

WANG, Y. X., DHULIPALA, P. K. & KOTLIKOFF, M. I. (2000). Hypoxia inhibits the Na^+/Ca^{2+} exchanger in pulmonary artery smooth muscle cells. *FASEB J.*, **14**, 1731-1740.

WANG, Z., JIN, N., GANGULI, S., SWARTZ, D. R., LI, L. & RHOADES, R. A. (2001). Rho-kinase activation is involved in hypoxia-induced pulmonary vasoconstriction. *Am. J. Respir. Cell Mol. Biol.*, **25**, 628-635.

WANG, Z., LANNER, M. C., JIN, N., SWARTZ, D., LI, L. & RHOADES, R. A. (2003). Hypoxia inhibits myosin phosphatase in pulmonary arterial smooth muscle cells: role of Rho-kinase. *Am. J Respir. Cell Mol. Biol.*, **29**, 465-471.

WANG, R., WU, L. & WANG, Z. (1997). The direct effect of carbon monoxide on KCa channels in vascular smooth muscle cells. *Pflugers Arch.*, **434**, 285-291.

WELLMAN, G. C., QUAYLE, J. M. & STANDEN, N. B. (1998). ATP-sensitive K^+ channel activation by calcitonin gene-related peptide and protein kinase A in pig coronary arterial smooth muscle. *J. Physiol.*, **507**, 117-129.

WILSON, A. J., JABR, R. I. & CLAPP, L. H. (2000). Calcium modulation of vascular smooth muscle ATP-sensitive K^+ channels: role of protein phosphatase-2B. *Circ. Res.*, **87**, 1019-1025.

WARD, J.P.T. (2003). Mitochondria and oxygen sensing: fuelling the controversy. *J Physiol*, **548.3**, 164.

WARD, J. P., SNETKOV, V. A. & AARONSON, P. I. (2004). Calcium, mitochondria and oxygen sensing in the pulmonary circulation. *Cell Calcium.*, **36**, 209-220.

WARD, J. P., WEIR, E. K. & ARCHER, S. L. (2006). Hypoxic Pulmonary Vasoconstriction is /is not mediated by increased production of reactive oxygen species. *J. Appl. Physiol.*, ..

WATANO, T., HARADA, Y., HARADA, K. & NISHIMURA, N. (1999). Effect of Na^+/Ca^{2+} exchange inhibitor, KB-R7943 on ouabain-induced arrhythmias in guinea-pigs. *Br. J. Pharmacol.*, **127**, 1846-1850.

WAYPA, G. B., CHANDEL, N. S. & SCHUMACKER, P. T. (2001). Model for hypoxic pulmonary vasoconstriction involving mitochondrial oxygen sensing. *Circ. Res.*, **88**, 1259-1266.

WAYPA, G. B., MARKS, J. D., MACK, M. M., BORIBOUN, C., MUNGAI, P. T. & SCHUMACKER, P. T. (2002). Mitochondrial reactive oxygen species trigger calcium increases during hypoxia in pulmonary arterial myocytes. *Circ. Res.*, **91**, 719-726.

WAYPA, G. B. & SCHUMACKER, P. T. (2002). O_2 sensing in hypoxic pulmonary vasoconstriction: the mitochondrial door re-opens. *Respiratory Physiology & Neurobiology*, **132**, 81-91.

WAYPA, G. B. & SCHUMACKER, P. T. (2005). Hypoxic pulmonary vasoconstriction: redox events in oxygen sensing. *J. Appl. Physiol.*, **98**, 404-414.

WAYPA, G. B. & SCHUMACKER, P. T. (2006). Role for mitochondrial reactive oxygen species in hypoxic pulmonary vasoconstriction. *Novartis. Found. Symp.*, **272**, 176-192.

WEIBEL, E. R. (1963). Principles and methods for the morphometric study of the lung and other organs. *Lab Invest.*, **12**, 131-155.

WEIR, E. K. & ARCHER, S. L. (1995). The mechanism of acute hypoxic pulmonary vasoconstriction: the tale of two channels. *FASEB J.*, **9**, 183-189.

WEIR, E. K. & ARCHER, S. L. (2006a). Counterpoint: Hypoxic pulmonary vasoconstriction is not mediated by increased production of reactive oxygen species. *J. Appl. Physiol.*, **101**, 995-998.

WEIR, E. K. & ARCHER, S. L. (2006b). Last Word: Point:Counterpoint authors respond to commentaries on "Hypoxic pulmonary vasoconstriction is/is not mediated by increased production of reactive oxygen species". *J. Appl. Physiol.*, **101**, 1005.

WEIR, E. K., EATON, J. W. & CHESLER, E. (1985). Redox status and pulmonary vascular reactivity. *Chest*, **88**, 249S-252S.

WEISSMANN, N., EBERT, N., AHRENS, M., GHOFRANI, H. A., SCHERMULY, R. T., HÄNZE, J., FINK, L., ROSE, F., CONZEN, J., SEEGER, W. & GRIMMINGER, F. (2003). Effects of mitochondrial inhibitors and uncouplers on hypoxic vasoconstriction in rabbit lungs. *Am. J. Respir. Cell Mol. Biol.*, **29**, 721-732.

WEISSMANN, N., SCHERMULY, R. T., GHOFRANI, H. A., HANZE, J., GOYAL, P., GRIMMINGER, F. & SEEGER, W. (2006a). Hypoxic pulmonary vasoconstriction--triggered by an increase in reactive oxygen species? *Novartis. Found. Symp.*, **272**, 196-208.

WEISSMANN, N., SOMMER, N., SCHERMULY, R. T., GHOFRANI, H. A., SEEGER, W. & GRIMMINGER, F. (2006b). Oxygen sensors in hypoxic pulmonary vasoconstriction. *Cardiovasc. Res.*, **71**, 620-629.

WEISSMANN, N., ZELLER, S., SCHAFER, R. U., TUROWSKI, C., AY, M., QUANZ, K., GHOFRANI, H. A., SCHERMULY, R. T., FINK, L., SEEGER, W. & GRIMMINGER, F. (2006c). Impact of mitochondria and NADPH oxidases on acute and sustained hypoxic pulmonary vasoconstriction. *Am. J. Respir. Cell Mol. Biol.*, **34**, 505-513.

WANG, R., WU, L. & WANG, Z. (1997). The direct effect of carbon monoxide on KCa channels in vascular smooth muscle cells. *Pflugers Arch.*, **434**, 285-291.

WELLMAN, G. C., QUAYLE, J. M. & STANDEN, N. B. (1998). ATP-sensitive K+ channel activation by calcitonin gene-related peptide and protein kinase A in pig coronary arterial smooth muscle. *J. Physiol.*, **507**, 117-129.

WIKSTROM, M. K. & SAARI, H. T. (1977). The mechanism of energy conservation and transduction by mitochondrial cytochrome c oxidase. *Biochim. Biophys. Acta.*, **462**, 347-361.

WILSON, A. J., JABR, R. I. & CLAPP, L. H. (2000). Calcium modulation of vascular smooth muscle ATP-sensitive K^+ channels: role of protein phosphatase-2B. *Circ. Res.*, **87**, 1019-1025.

WOLIN, M. S., AHMAD, M. & GUPTE, S. A. (2005). Oxidant and redox signaling in vascular oxygen sensing mechanisms: basic concepts, current controversies, and potential importance of cytosolic NADPH. *Am. J. Physiol Lung Cell Mol. Physiol.*, **289**, L159-L173.

WYATT, C. N. & BUCKLER, K. J. (2004). The effect of mitochondrial inhibitors on membrane currents in isolated neonatal rat carotid body type I cells. *J. Physiol.*, **556**, 1-91

XIA, X. M., ZENG, X. & LINGLE, C. J. (2002). Multiple regulatory sites in large-conductance calcium-activated potassium channels. *Nature*, **418**, 880-884.

XI, Q., TCHERANOVA, D., PARFENOVA, H., HOROWITZ, B., LEFFLER, C. W. & JAGGAR, J. H. (2004). Carbon monoxide activates K_{Ca} channels in newborn arteriole smooth muscle cells by increasing apparent Ca^{2+} sensitivity of alpha-subunits. *Am. J. Physiol Heart Circ. Physiol.*, **286**, H610-H618.

XI, Q., CHERANOV, S. Y. & JAGGAR, J. H. (2005). Mitochondria-derived reactive oxygen species dilate cerebral arteries by activating Ca^{2+} sparks. *Circ. Res.*, **19;97**, 354-362.

YAO, W., QIAN, G. & YANG, X. (2002). Roles of NHE-1 in the proliferation and apoptosis of pulmonary artery smooth muscle cells in rats. *Chin Med. J. (Engl.).*, **115**, 107-109.

YEN, R. T., ZHUANG, F. Y., FUNG, Y. C., HO, H. H., TREMER, H. & SOBIN, S. S. (1984). Morphometry of cat's pulmonary arterial tree. *J. Biomech. Eng.*, **106**, 131-136.

YEUNG, S. Y. & GREENWOOD, I. A. (2005). Electrophysiological and functional effects of the KCNQ channel blocker XE991 on murine portal vein smooth muscle cells. *Br. J. Pharmacol.*, **146**, 585-595.

YU, C. A., XIA, D., KIM, H., DEISENHOFER, J., ZHANG, L., KACHURIN, A. M. & YU, L. (1998). Structural basis of functions of the mitochondrial cytochrome bc1 complex. *Biochim. Biophys. Acta.*, **1365**, 151-158.

YUAN, J. X. (2001). Oxygen-sensitive K^+ channel(s): where and what? *Am. J. Physiol.*, **281**, L1345-L1349.

YUAN, X.-J. (1995). Voltage-gated K^+ currents regulate resting membrane potential and $[Ca^{2+}]_i$ in pulmonary arterial myocytes. *Circ. Res.*, **77**, 370-378.

YUAN, X.-J., GOLDMAN, W. F., TOD, M. L., RUBIN, L. J. & BLAUSTEIN, M. P. (1993). Hypoxia reduces potassium currents in cultured rat pulmonary but not mesenteric arterial myocytes. *Am. J. Physiol.*, **264**, L116-L123.

YUAN, X.-J., SALVATERRA, C. G., TOD, M. L., JUHASZOVA, M., GOLDMAN, W. F., RUBIN, L. J. & BLAUSTEIN, M. P. (1993). The sodium gradient, potassium channels, and regulation of calcium in pulmonary and mesenteric arterial smooth muscles: effects of hypoxia. In *Ion Flux in Pulmonary Vascular Control*, eds. Weir, E. K., Hume, J. R. & Reeves, J. T., pp. 205-222.New York and London: Plenum Press.

YUAN, X.-J., SUGIYAMA, T., GOLDMAN, W. F., RUBIN, L. J. & BLAUSTEIN, M. P. (1996). A mitochondrial uncoupler increases K_{Ca} currents but decreases K_V currents in pulmonary artery myocytes. *Am. J. Physiol.*, **270**, C321-C331.

YUAN, X.-J., TOD, M. L., RUBIN, L. J. & BLAUSTEIN, M. P. (1990). Contrasting effects of hypoxia on tension in rat pulmonary and mesenteric arteries. *Am. J. Physiol.*, **259**, H281-H289.

YUAN, X.-J., TOD, M. L., RUBIN, L. J. & BLAUSTEIN, M. P. (1994). Deoxyglucose and reduced glutathione mimic effects of hypoxia on K^+ and Ca^{2+} conductances in pulmonary artery cells. *Am. J. Physiol.*, **267**, L52-L63.

YUAN, X.-J., TOD, M. L., RUBIN, L. J. & BLAUSTEIN, M. P. (1995). Inhibition of cytochrome P-450 reduces voltage-gated K^+ currents in pulmonary arterial myocytes. *Am. J. Physiol.*, **268**, C259-C270.

YUAN, X.-J., TOD, M. L., RUBIN, L. J. & BLAUSTEIN, M. P. (1995). Hypoxic and metabolic regulation of voltage-gated K^+ channels in rat pulmonary artery smooth muscle cells. *Exp. Physiol.*, **80**, 803-813.

YUN, C. H., TSE, C. M., NATH, S. K., LEVINE, S. A., BRANT, S. R. & DONOWITZ, M. (1995). Mammalian Na^+/H^+ exchanger gene family: structure and function studies. *Am. J. Physiol.*, **269**, G1-11.

ZHANG, G. H. & MELVIN, J. E. (1995). Regulation by extracellular Na^+ of cytosolic Mg^{2+} concentration in Mg^{2+}-loaded rat sublingual acini. *FEBS Lett.*, **371**, 52-56.

ZHANG, S., YUAN, J. X., BARRETT, K. E. & DONG, H. (2005). Role of Na^+/Ca^{2+} exchange in regulating cytosolic Ca^{2+} in cultured human pulmonary artery smooth muscle cells. *Am. J. Physiol Cell Physiol.*, **288**, C245-C252.

ZHANG, Y., OLTMAN, C. L., LU, T., LEE, H. C., DELLSPERGER, K. C. & VANROLLINS, M. (2001). EET homologs potently dilate coronary microvessels and activate BK_{Ca} channels. *Am. J. Physiol Heart Circ. Physiol.*, **280**, H2430-H2440.

ZHOU, Q., SATAKE, N. & SHIBATA, S. (1997). The contractile mechanism of sodium metavanadate in isolated rat aortae. *J. Cardiovasc. Pharmacol.*, **30**, 84-89.

ZIEGLER, A., SOMLYO, A. V. & SOMLYO, A. P. (1992). β-adrenergic effects on cellular Na, Mg, Ca, K and Cl in vascular smooth muscle: electron probe analysis of rabbit pulmonary artery. *Cell Calcium*, **13**, 593-602.

Chapter 10

PUBLICATIONS

TAMMARO, P., **SMITH, A. L.,**, CROWLEY, B. & SMIRNOV, S. V. (2004). Modulation of the voltage-dependent K^+ current by intracellular magnesium in rat aortic smooth muscle cells. *Cardiovasc. Res.* **65**, 387-396

TAMMARO, P., **SMITH, A. L.,**, HUTCHINGS, S. R., & SMIRNOV, S. V. (2004). Pharmacological evidence for a key role of voltage-gated K^+ channels in the function of rat aortic smooth muscle cells. *B.J.P.* **143**, 303-317

SMIRNOV, S. V., TAMMARO, P., HUTCHINGS, S. R., & **SMITH, A. L**. (2003). Role of voltage gated K^+ (K_v) channels in vascular function. *Neurophysiology.* **35**, 262-274

Publications (in preparation)

FIRTH, A. L.,, YUILL, K. H., & SMIRNOV, S. V. Investigation of the mechanisms of interaction between voltage-gated potassium channels and mitochondria in rat small pulmonary arterial myocytes.

FIRTH, A. L.,, YUILL, K. H., & SMIRNOV, S. V. Involvement of the NME in the regulation of voltage-gated potassium channel currents in rat resistance arteries.

Conference abstracts

SMITH,, A. L.,, YUILL, K. H., & SMIRNOV, S. V. (2005). The effect of mitochondrial electron transport chain (ETC) inhibitors on voltage-dependent K^+ (Kv) currents in rat small pulmonary arterial myocytes (PAMs). *Proc. J Physiol* **.567P**:PC159

SMITH, A. L.,, YUILL, K. H., & SMIRNOV, S. V. (2005). Effects of hydrogen peroxide (H_2O_2) on voltage-dependent K^+ (Kv) currents in rat small pulmonary arterial myocytes (PAMs): the role of intracellular redox state. From the University of Cambridge, Summer 2005 Meeting: Proceedings of the British Pharmacological Society at http://www.pa2online.org/abstracts/Vol3Issue2abst125P.pdf

SMITH, A. L.,, YUILL, K. H., & SMIRNOV, S. V. (2005). Effect of extracellular Na^+ removal and amiloride on voltage-gated K^+ channel currents (I_{Kv}) in rat small (resistance) pulmonary arterial myocytes (PAMs). *Biophysical Journal*, **88(1),** 305a, 1492-pos

SMIRNOV, S. V., & **SMITH, A. L.**. (2005). Voltage-gated K^+ (Kv) channel currents in mouse intrapulmonary and mesenteric arteries. *Biophysical Journal,* **88(1),** 304a, 1490-pos.

SMITH, A. L., & SMIRNOV, S. V. (2004). K^+ channel currents in rat small pulmonary arterial myocytes (PAMs). *Proc. J. Physiol*, **560P**, C41

SMITH, A. L., & SMIRNOV, S. V. (2004). The effect of organ culture and endothelin-1 treatment on Kv currents in rat small pulmonary arterial myocytes. From the University of Bath, Summer 2004 Meeting: Proceedings of the British Pharmacological Society at http://www.pa2online.org/abstracts/Vol2Issue2abst012P.pdf

SMIRNOV, S. V., TAMMARO, P., **SMITH, A. L.,** & HUTCHINGS, S. R. (2004). Pharmacological evidence for a key role of voltage-gated K^+ channels in the function of rat aortic smooth muscle cells. From the University of Bath, Summer 2004 Meeting: Proceedings of the British Pharmacological Society at http://www.pa2online.org/abstracts/Vol2Issue2abst010P.pdf

TAMMARO, P., HUTCHINGS, S., **SMITH, A. L.**, SMIRNOV, S. V. (2003). Mechanism of induced rhythmic activity in rat aortic smooth muscle cells (SMCs). *FEPS*, P20-08